Modelling Aquatic Ecosystems

Course 701-0426-00 ETH Zürich
Spring Semester 2025

Peter Reichert, Johanna Mieleitner and Nele Schuwirth

Eawag: Swiss Federal Institute of Aquatic Science and Technology
Department of Systems Analysis, Integrated Assessment and Modeling
8600 Dübendorf, Switzerland

and

ETH Zürich
Department of Environmental Systems Science
8092 Zürich, Switzerland

January 27, 2025

Contents

Preface

It is the goal of this course to give an introduction to modelling of aquatic ecosystems with a focus on model formulation and use of model simulations to improve our understanding of processes that characterize the behaviour of aquatic ecosystems. A very brief introduction is also provided to the estimation of prediction uncertainty, considering demographic and environmental stochasticity and parameter uncertainty, and of the estimation of model parameters from observed data. Particular emphasis is on the linkage between ecological and biogeochemical processes through elemental mass balances expressed by stoichoimetric relationships.

It is assumed that the reader of this manuscript has a basic knowledge of physical, chemical and biological processes in aquatic ecosystems. We concentrate on the mathematical formulation of these processes and on their integration to a model of the ecosystem that provides insight into biogeochemical cycles and function of the ecosystem. The course is accompanied by a series of didactical examples of biogeochemical-ecological models of aquatic ecosystems of increasing degree of complexity (chapter 11). These models are implemented based on a toolbox of functions for performing stoichiometric calculations and dynamic simulations, respectively. These tools are implemented as two packages for the freely available statistics and graphics software R (`http://www.r-project.org`). These packages, stoichcalc and ecosim, are also briefly described in the appendix to this manuscript (chapters 15 and 16). The implementations of all the didactical models described in chapter 11 can be downloaded from `http://www.eawag.ch/forschung/siam/lehre/modaqecosys`.

After a short introduction motivating the need for aquatic ecosystems models and overviews of important processes in aquatic ecosystems and of model structures for describing aquatic populations and communities, this manuscript is divided into the following six parts:

- **Part I: Basic Concepts**
  Formulation of mass balance equations and transformation processes with differential equations models and possible behavior of their solutions. This type of models is particularly relevant for describing the coupling between biogeochemical and ecological models and builds the basis of a large part of the manuscript.

- **Part II: Formulation of Ecosystem Processes**
  Based on the notation introduced in part I, this part gives short descriptions of all processes that will be used to build the example ecosystem models. The processes are divided into physical processes, chemical processes, and biological processes.

- **Part III: Stochasticity, Uncertainty and Parameter Estimation**
  A brief introduction is provided into causes, description, and propagation of demo-

graphic and environmental stochasticity and uncertainty due to incomplete knowledge of driving forces and structure and function of the ecosystem. This is followed by a brief overview of techniques used to estimate model parameters and ecosystem states from observed data.

- **Part IV: Simple Models of Aquatic Ecosystems**
  Starting with a very simple lake phytoplankton model, lake and river ecosystem models of increasing complexity are built-up and discussed. All the models described in part IV are implemented in R to provide the opportunity to learn about the effects of changes in driving forces and model parameters.

- **Part V: Advanced Aquatic Ecosystem Modelling**
  Although the simple models discussed in part IV already reflect many important pattern of real aquatic ecosystems, models for application in research and practice usually need additional elements. In this part, important additional processes, refinements of processes described in a simpler way in the previous part of the manuscript, modifications to or alternative model structures are discussed. The part ends with a brief description of some models that are frequently used in practice and research, and with a few examples of case studies of model application.

- **Part VI: Appendix**
  In the appendix, the notation used in the manuscript is listed, an introduction is given to the most important univariate probability distributions, and short introductions to the R packages used for stoichiometric calculations and for dynamic model simulations are given.

The structure of the manuscript outlined above is based on the concept of building up the relevant constituents before combining them to an aquatic ecosystem model. This makes it easy to find a description of the relevant structures or processes needed to build-up such a model. While it is possible to read the manuscript in this order, it is certainly more stimulating to organize a course based on the didactic models. For this reason, for teaching or reading the manuscript, it is recommended to start with the introduction and read as much of the basics chapter as required to understand the first didactic example. Then, the didactic examples can be studied, while continuing reading the necessary sections of the basics and process formulation chapters as required for the examples. To support this process, at the beginning of each didactic example it is listed which sections are required to understand the example. In parallel to studying the sections on the didactic models, practical modelling experience can be gained by performing the calculations with the software described in the appendix. This implementation allows the reader to check effects of modifications to model assumptions or parameter values through numerical simulation. After having read the didactic examples (this implies then also all basic and process formulation sections), it should be easy to proceed to the advanced modelling elements in part V.

We tried to do our best in presenting the topics and eliminating errors. But still there are opportunities for improvement and there may be remaining errors. Any hints for improving this manuscript are very welcome. Please send your error reports or suggestions for improvement to nele.schuwirth@eawag.ch. We thank Anne Dietzel, Simon-Lukas Rinderknecht, Martin Frey, Irene Wittmer, Colombe Siegenthaler - Le Drian, David

Machac, Lorenz Ammann, Catalina Chaparro Pedraza, Emma Chollet Ramampiandra, Chuxinyao Wang and students of our courses for their hints for improving this manuscript.

Peter Reichert and Nele Schuwirth, January 27, 2025

Chapter 1

Introduction

We start this chapter by briefly discussing the motivation for developing models of aquatic ecosystems in section 1.1. Then, in section 1.2, we give an overview of the most important transformation and transport processes in lakes and rivers before providing an overview of possible structures of the biological part of ecological models in section 1.3.

1.1 Motivation for Modelling Aquatic Ecosystems

There are three main objectives for constructing and using ecosystem models:

1. **Improving our understanding of ecosystem function**:
   Comparing results of simulations of a model with measured data provides a test of the hypotheses formulated in the model. Thus, ecosystem models are ideal tools for quantitative testing of hypotheses about ecosystem function. Due to linking concentrations with fluxes and transformation rates they provide a deeper insight into ecosystem mechanisms than can be gained by data analysis without the use of models. In addition, model setup, simulations and tests stimulate creative thinking about important mechanisms in ecosystems.

2. **Summarizing and communicating knowledge about ecosystems**:
   Ecosystem models are perfect communication tools for exchanging quantitatively formulated knowledge of processes in the ecosystem. A systematic notation of transformation processes that separates process stoichiometry from rates can help to give a transparent overview of processes represented in the model and their formulation.

3. **Supporting ecosystem management**:
   Ecosystem models can support ecosystem management by predicting the consequences of suggested management alternatives. As both, our knowledge and its representation in the models, are incomplete, a considerable effort must be made in quantifying prediction uncertainty if the models are applied for management purposes.

The ecosystem model to be used depends on the objective of the study. Models for improving the understanding and communicating knowledge usually have a higher structural resolution of model components and processes than models for ecosystem management. For management purposes, getting the important mass fluxes correct is usually more important than gaining a complete insight into the substructures at all trophical levels of the food web. However, knowledge gained from more detailed research models often stimulates the development of simpler management models. In some cases, the same model can even be used for different application fields.

1.2 Overview of Processes in Aquatic Ecosystems

Aquatic ecosystems can be divided into different zones: The main water body that is not close to the sediment or the shore or river bank is called the **pelagic zone**. Close to the surface of the water body, the pelagic zone is surrounded by the **littoral zone** that consists of the water body close to the shore or river bank and of the adjacent periodically inundated area. The pelagic zone is bounded below by the **benthic zone** that consists of the water body above the sediment and the top sediment layers. The pore space in the sediment below the benthic zone is called the **interstitial zone** which often connects to the groundwater.

Figure 1.1 gives an overview of the most **important transformation processes in a pelagic food web**. Most transformation process models of the pelagic zone of surface wa-

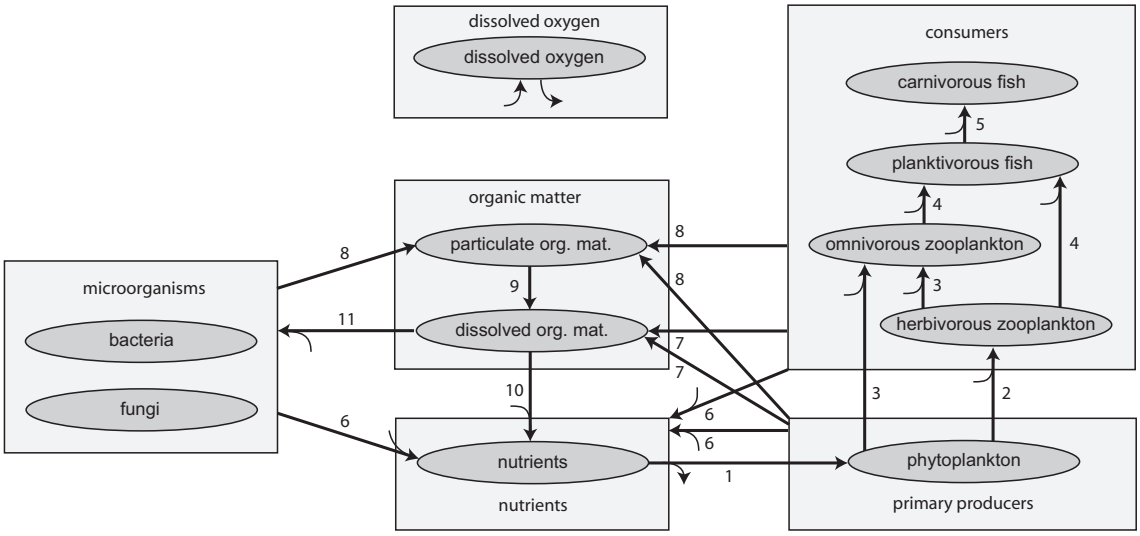

Figure 1.1: Overview of important processes in the food web of the pelagic zone of surface waters. The following processes are considered: 1 = growth of algae (primary production); 2 = growth of herbivorous zooplankton (grazing); 3 = predation of omni- or carnivorous zooplankton; 4 = predation of planktivorous fish; 5 = predation of carnivorous fish; 6 = respiration; 7 = release of dissolved organic matter during death and sloppy feeding; 8 = death; 9 = hydrolysis (typically mediated by microorganims); 10 = mineralization (mediated by microorganisms that may or may not be explicitly included); 11 = growth of bacteria, fungi or other (heterotrophic) microorganisms. Thin arrows indicate oxygen consumption or production. Note that more biological processes may be relevant, in particular anoxic and anaerobic mineralization and nitrification (see chapter 8).

ters are based on a simplification or refinement of the process scheme shown in this figure. By primary production, nutrients discharged into the lake are converted into phytoplankton biomass. This process requires light and produces dissolved oxygen. Herbivorous zooplankton grazes on phytoplankton as its food source. Omnivorous zooplankton grazes on herbivorous zooplankton and phytoplankton, carnivorous zooplankton on herbivorous zooplankton. Zooplankton serves as food for planktivorous fish which again are the food source for carnivorous fish. All these grazing activities require dissolved oxygen and lead to release of particulate organic material (fecal pellets and remainings from sloppy feeding),

dissolved organic matter (released from broken cells), and nutrients. Furthermore, respiration of these organisms also transforms biomass into nutrients. Death of all organisms transfers them to particulate organic matter. Particulate organic matter is hydrolyzed to dissolved organic substances which is mineralized into nutrients. These last two processes are of particular importance in the sediment of the lake. In the presence of dissolved oxygen, mineralization is accompanied by dissolved oxygen consumption. In deeper sediment layers, after all dissolved oxygen diffusing into the sediment from the water column is used up, mineralization requires reducing nitrate, manganese oxide, iron hydroxide, or sulfate. Finally, mineralization is also possible by methanogenesis.

Figure 1.2 shows a similar diagram as Figure 1.1 for the **transformation processes in a benthic food web**. Periphyton (sessile algae) grows on nutrients provided in the

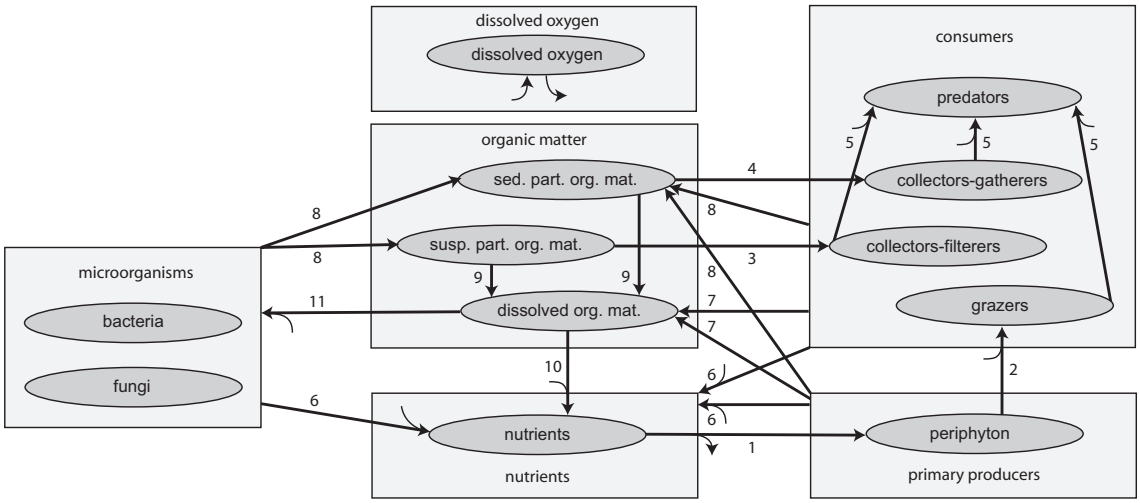

Figure 1.2: Overview of important processes in the food web of the benthic zone of surface waters. The following processes are considered: 1 = growth of periphyton (primary production); 2 = growth of grazers (grazing of periphyton); 3 = growth of collectors-filterers; 4 = growth of collectors-gatherers; 5 = predation; 6 = respiration; 7 = release of dissolved organic matter during death and sloppy feeding; 8 = death/detachment; 9 = hydrolysis (typically mediated by microorganisms); 10 = mineralization (mediated by microorganisms that may or may not be explicitly included); 11 = growth of bacteria, fungi or other (heterotrophic) microorganisms. Thin arrows indicate oxygen consumption or production. Note that more biological processes may be relevant, in particular anoxic and anaerobic mineralization and nitrification (see chapter 8).

water column. Grazers grow on these periphyton mats. Filterers grow on particulate organic matter suspended in the water column, whereas gatherers grow on sedimented particulate organic matter at the river bed. All three groups of benthic invertebrates are predated by predators (invertebrates or fish). Similarly to the pelagic food web shown in Figure 1.1 all classes of invertebrates and fish are subject to respiration, release of dissolved organic matter (through broken cells), excretion, and death. Particulate organic matter is hydrolyzed to dissolved organic matter which is subsequently mineralized to nutrients.

Despite the importance of the interaction of pelagic (Figure 1.1) with benthic (Figure 1.2) food webs in many systems (especially small or shallow lakes and large streams), for

the didactic examples in this manuscript we use deep lakes as a model system dominated by pelagic processes and rivers of small or intermediate size as model systems dominated by benthic processes. We discuss in the following two paragraphs, how the transport processes in these two systems interact with the food webs discussed above.

Figure 1.3 shows the most important **transport processes in a lake**. These transport

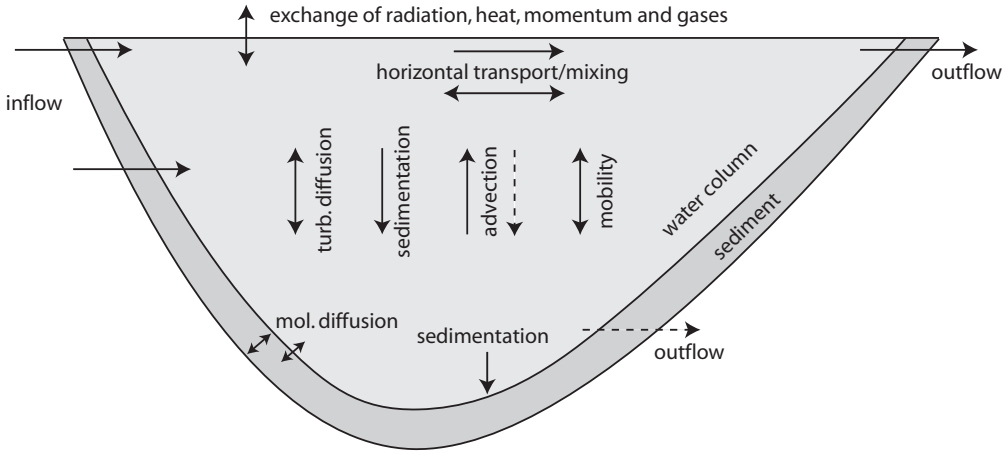

Figure 1.3: Overview of important transport processes in a lake.

processes lead to partial spatial separation of the transformation processes discussed in Figure 1.1. The density of the inflow to the lake is mainly determined by its temperature and suspended solid concentration. Depending on this density and on stratification of the lake, the inflow enters the lake in a certain depth (with some entrainment of water from the layers above). As the outflow is not at the same level (at the surface for natural lakes and close to the bottom for many reservoirs), this leads to vertical advection of (part of) the water column. In addition, the water column is mixed by turbulent diffusion, again depending on the stratification of the water column. During periods of stratification (usually caused by warm and less dense water layers laying above colder and denser layers), horizontal mixing is usually much faster than vertical mixing. Radiation, heat, momentum, dissolved oxygen, carbon dioxide, and molecular nitrogen are exchanged over the lake surface. Due to its mobility, zooplankton and some phytoplankton species move actively through the water column. Particulate substances are deposited at the surface of the sediment due to sedimentation. Dissolved substances are transported within the sediment pore water and between pore water and lake water by molecular diffusion. The interaction of transformation and transport processes discussed separately in the previous paragraphs (Figures 1.1 and 1.3) leads to the following typical spatial separation of processes in a lake: Primary production of phytoplankton takes place in the upper mixed layer of the lake, the epilimnion, where sufficient light is available. This process is based on and consumes nutrients delivered by the inflow and nutrients diffusing to the surface layer from the depth of the lake where they are produced by mineralization of organic material. Zooplankton can actively move through the water column. Herbivorous zooplankton feeds on phytoplankton in the surface layer of the lake. Also fish predominantly feed in the surface layer on plankton as the light allows them to catch their food. Particulate organic material produced by the organisms is usually sedimenting through the water column much quicker than mineralization takes place. For this reason a large fraction of this material reaches the sediment where mineralization processes consume dissolved oxygen,

nitrate and other compounds that can be used for the oxidation of organic substances. In the sediments and often also in the hypolimnion diffusivities are small. This leads to large gradients of dissolved oxygen, nitrate and mineralization products in the sediment and the hypolimnion of the lake.

Figure 1.4 shows the most important **transport processes in a river** required to understand benthic populations and substance turnover. The most important processes are here sedimentation of organic material and resuspension and detachment of organic particles and periphyton. Despite the smaller number of important transport processes in this case compared to the example for the lake shown in Figure 1.3, it is not easier to model such a system as particularly the resuspension and detachment processes depend sensitively on the morphology of the river bed.

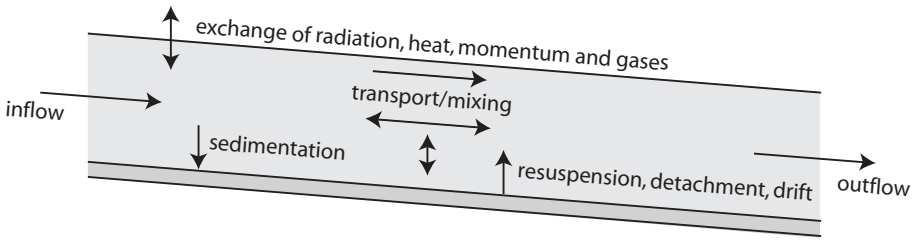

Figure 1.4: Overview of important transport processes in a river.

Aquatic ecosystem models have to represent the main physical, chemical and biological processes of the most important chemical elements in the system and represent the biological communities building the ecosystem. The overview of these processes given in this section demonstrates that building such a model is a demanding task. In this manuscript we will start in chapter 11 with building very simple didactic ecosystem models, we will then increase the complexity of these models and end in chapter 13 with a brief outline of structure and application of research models of aquatic ecosystems.

1.3 Overview of Biological Model Structures

As outlined in the previous section, ecosystem models have to represent the main physical, chemical and biological processes in an ecosystem. Figure 1.5 shows the interactions between the abiotic (called 'physical') and the biological sub-models and the interaction across the system boundaries with the 'rest of the world. In this section, we discuss

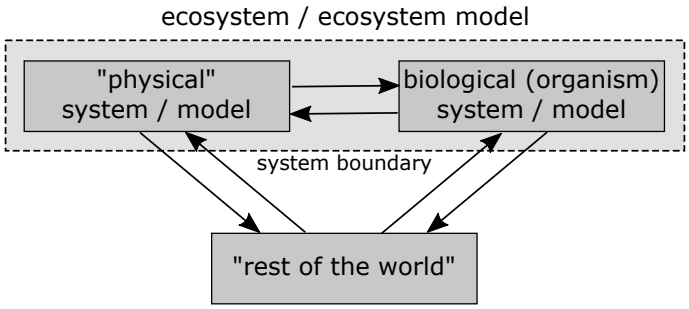

Figure 1.5: Division of an ecosystem model into an abiotic (called 'physical') and a biotic model component, both of which interact across the system boundary with teh 'rest of the world'.

possible model structures of the biological sub-model.

Depending on the research task, we may want to describe a single population (the organisms of a single species) or a community consisting of mutiple species. Often, instead of modelling species, functional groups (e.g. algae, zooplankton, etc.) are modelled without distincting the species within each functional group. Depending on the spatial resolution required to describe the system, we may describe a single population or community or multiple, interacting populations or communities in meta-population or meta-community models. Fig. 1.6 gives an overview of these model types.

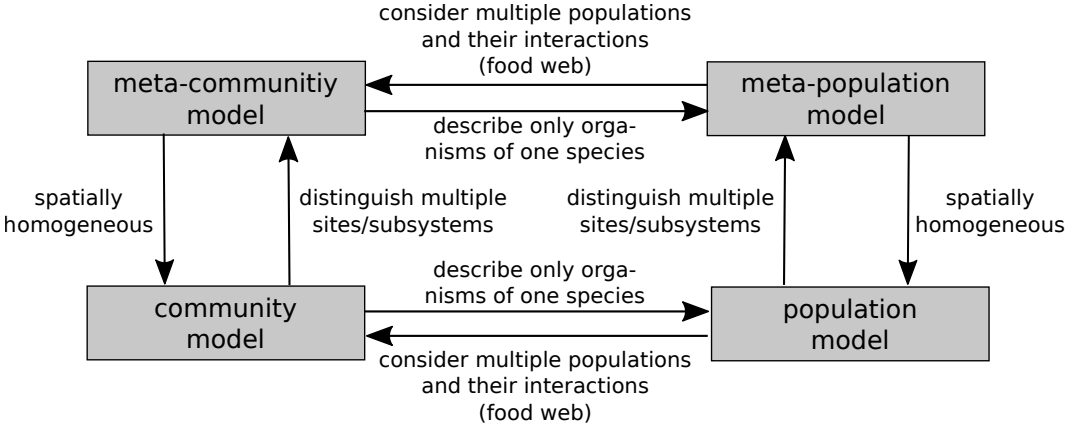

Figure 1.6: Classification of biological (sub-)models into population, community, meta-population and meta-community models and the distincting aspects between these classes.

Fig. 1.7 gives an overview of possible structures of population or community models. As a biological community consists if individual organism that each differ from each other and which are affected by death, birth or cell division, and food uptake processes that can usually only be described stochastically (we cannot predict the time of death of an

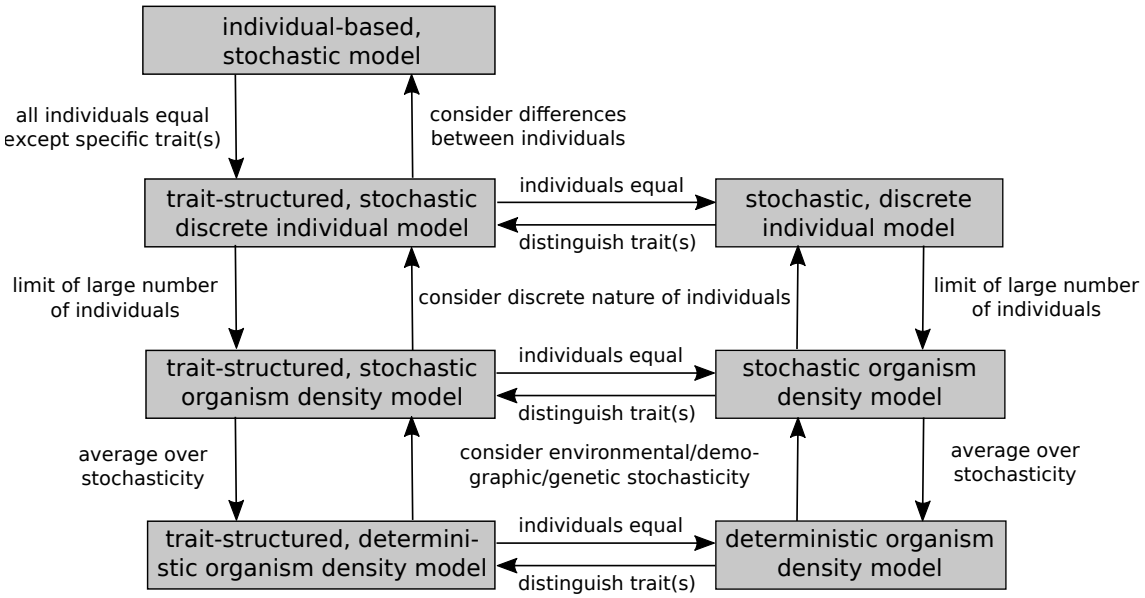

Figure 1.7: Possible structures of population or community models and the distincting aspects between the different model structures.

individual organism), an individual-based, stochastic model is the most natural description of the biological part of an ecosystem model (or of a laboratory population or community model). Using this model structure, the state of the system is described by all individuals with all their properties (e.g. age, life stage, mass, size, etc.). This is shown at the top level in Fig. 1.7. When assuming all individuals are equal except specific traits (e.g. age, life stage, mass, size), we get a trait-structured, stochastic, discree individual models. In this model structure, the state of the system is described by the number of individuals of each species (or functional group) for each trait value (e.g. for each age or size class). This model structure is shown directly below the individual-based model. We can further simplify the model structure by moving to the right in Fig. 1.7 and assuming all individuals of a population to be equal without resolving any of their traits (stochastic, discrete individuals model) or by moving down and assuming that we can approximate the discrete population or community by population or community densities because there are large numbers of individuals for each of the distinguished species or functional group and trait value (trait-structured, stochastic organism density model). Combining both assumptions leads to the stochastic organism density model shown in the middle of the right column of model structures in Fig. 1.7. A final simplification is to average over stochasticity and describing only the means of the numbers of individuals or organism densities. This leads to the model structures in the bottom row of Fig. 1.7. In these models, the time-evolution of populations or communities are described by deterministic difference or differential equations.

Final choices in model structure selection are the spatial and temporal resolutions of the model. All possible choices for the combinations of these resolutions are illustrated in Fig. 1.8. Regarding the temporal resolution, it has first to be decided whether the model should be static or dynamic. For dynamic models a discrete or continuous time resolution is possible. Regarding the spatial resolution, a system can either be described by discrete spatial elements ('mixed boxes') or a continuous spatial description is possible.

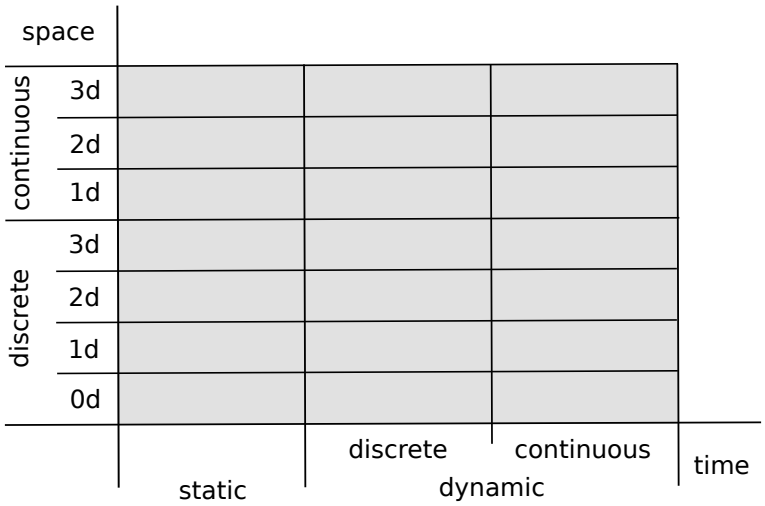

Figure 1.8: Possible combinations of spatial and temporal resolution of an ecosystem model.

If the spatial dimension is resolved, the dimensionality of the description has to be chosen. It may be possible to not resolve all spatial dimensions as mixing may be quite different across different dimensions. The choice of the spatial dimension depends on the system and on the processes and spatial and time scales of interest. As an example, for the description of transport in rivers over very long distances, a one-dimensional model may be sufficient. However, for the etimation of the spread of a pollutant plume from an outlet into the river over its depth and width, a two- or even three-dimensional description may be required. We will provide mixing distance estimates for rivers and lakes to support the selection of the adequate dimensionality of a model in chapter 6.

In the parts I to IV of the manuscript we will mainly focus on determinstc organism density models (lower right model structure in Fig. 1.7) and in part IV exclusively on zero-dimensional example models. This class of models is ideally suited to link biogeochemical processes to ecological processes and it is simple enough to allow for efficient model implementation. We will come back to other kinds of models in part V.

Part I

Basic Concepts

Chapter 2

Principles of Modelling Environmental Systems

This manuscript focuses on the formulation of mathematical models of aquatic ecosystems and on their use to improve our understanding of processes characterizing the behaviour of aquatic ecosystems. In this chapter we briefly explain how these elements are embedded in a more general framework of model application for improving scientific knowledge and and supporting societal decision making.

2.1 Meaning of Models

Scientific research aims at improving our understanding of the mechanisms responsible for the observed behaviour of a system. A **system** is an assemblage of objects comprising a whole with each component related to other components. An environmental system is a part of the environment bounded by well-defined **system boundaries**. We use the notion "environmental system" in a wide sense. A system denoted as "environmental system" in this manuscript can be a part of the natural environment, but it could also be a part of a laboratory or a technical system. The system behaves according to its **internal mechanisms** and it is affected by **external influence factors** that are not part of the system. Ideas about the structure and function of a system build a **conceptual model** of the system. Often, such ideas are quantitatively formulated using the language of mathematics. They form then a **mathematical model**. As environmental systems are overwhelmingly complex, for building a model, choices must be made on aspects of the system to focus on and on the level of detail of its description. For his reason, there is no single, "true" model of an environmental system. Instead, the model to be used depends on the planned purpose of application.

A model is constructed by a process of abstraction of observed behaviour to suggested underlying mechanisms. Once the model is formulated mathematically, it can be used to calculate future (model) behaviour, particularly under changed external influence factors. This future model behaviour then represents a prediction of future system behaviour under the specified boundary conditions. This mutual relationship between system and model is illustrated in Figure 2.1.

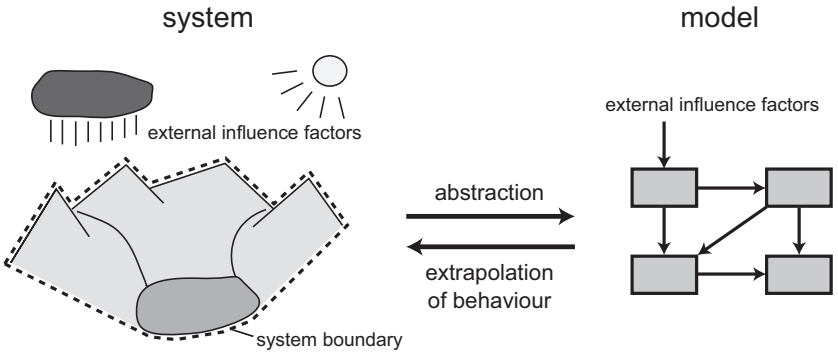

Figure 2.1: Mutual relationship between a system and its representation by a model.

2.2 Formulation of Models

The most important techniques for building mathematical models of environmental systems are the formulation of empirical relationships based on measured data and the formulation of mass-balance equations. The application of both techniques is based on a simplified representation of important structural characteristics of the system. In typical aquatic ecosystem models, the dependence of rates of growth, death, respiration and other conversion processes on nutrients, light, food, temperature and other influence factors is usually formulated empirically. Once these expressions are given, mass-balance equations are solved for organisms and compounds to build a mechanistic process model of the system. Building such models and interpreting their behaviour is the main focus of this manuscript.

Empirical formulation of sub-models relies on unknown coefficients, so-called model **parameters**. Such parameters can have a physical, chemical or biological meaning that makes it possible to measure them without running the model. However, many empirical model formulations also have parameters that must be estimated by searching for values that lead to the best fit of model results with corresponding measurements.

The development of mechanistic models usually starts with the formulation of a deterministic model, i.e. a model that leads to a unique prediction for given initial conditions, parameter values and external influence factors. To account for simplifications of the model description, uncertainty in external influence factors, random processes, and measurement error, stochastic elements are added. The simplest such error model consist of an additive random error added to the output of the deterministic model. Stochastic models lead to probabilistic predictions even in the case that initial conditions, parameter values and external influence factors are specified precisely. The propagation of uncertainty in these input variables through the model increases the uncertainty of model predictions.

2.3 Learning with Models

Once a model of an environmental system is formulated, it can be used to predict future behaviour under modified external influence factors. Such predictions have to be tested against measurements. The analysis of failed tests can lead to ideas for model improvements. In order to thoroughly test models of environmental systems, one has usually to rely on historical time series of changes in external influence factors and observed effects

on the system. For laboratory or technical systems, one usually has the additional degree of freedom to manipulate external influence factors in order to optimize the possible gain of information. Figure 2.2 illustrates this cycle of model (re-)formulation, experiment or measurement planning, testing the model with new data, and using the gained information to update the model structure.

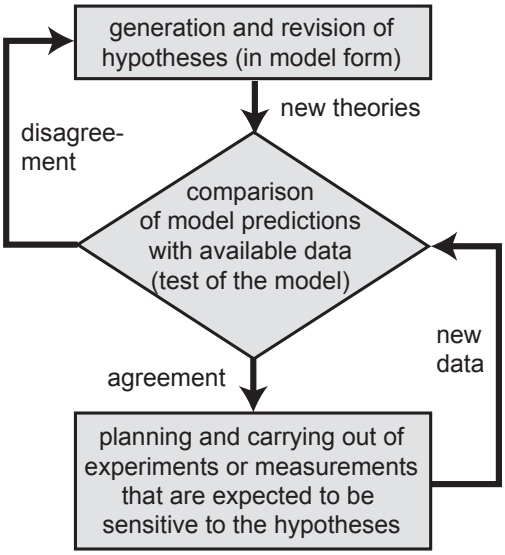

Figure 2.2: Flow diagram of the model-based learning process.

The procedure of learning about ecosystem function with the aid of models according to Figure 2.2 requires the formulation of a stochastic model. Such a model is often an extension of a deterministic core model. Statistical inference is then used to estimate model parameters and their uncertainty and statistical tests are carried out to check the fulfillment of the statistical assumptions.

2.4 Model-Based Decision Support

Decision sciences provide a general framework for rational decision making (Clemen, 1996; Eisenführ and Weber, 1999). Building on this framework, environmental (or more generally societal) decisions can be structured into the steps shown in Fig. 2.3 (Reichert et al., 2015). Step 7 of this procedure requires the prediction of the consequences of all decision alternatives. This can only be done by an adequately built model of the investigated system that considers the external influence factors characterizing the decision alternatives and quantifies the prediction uncertainty. Such a model can be a mental model of an expert who provides her or his knowledge, a simple statistical extrapolation model, or a sophisitcated mechanistic model of the relevant systems.

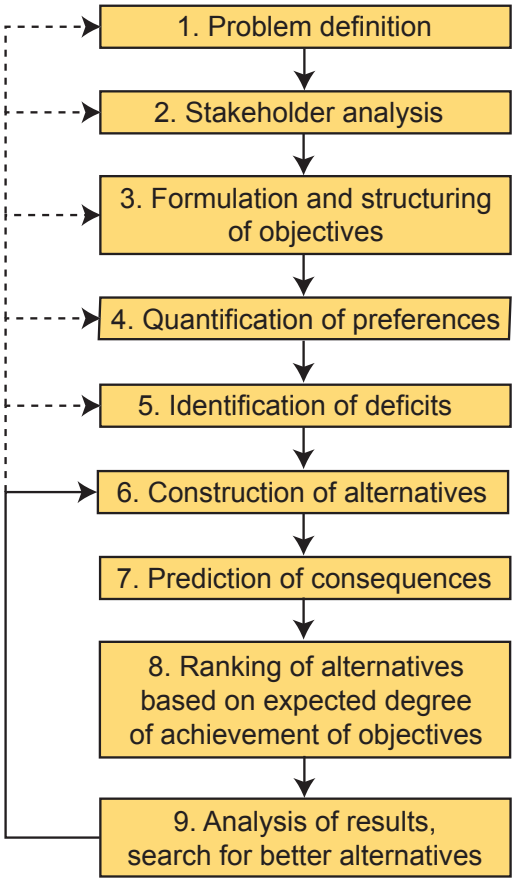

Figure 2.3: Structured decision making process according to (Reichert et al., 2015).

Chapter 3

Formulation of Mass Balance Equations

Aquatic ecosystem models are based on mass balances of substances and organisms in the investigated system. The general idea of the mathematical formulation of mass balances is outlined in section 3.1. This concept is then applied to get more detailed formulations of mass balance equations for a single mixed reactor in section 3.2, for a system of mixed reactors in section 3.3, and for a continuously described system in section 3.4.

3.1 General Concept of Mass Balance Equations

The basic idea of the formulation of conservation laws or mass balances is very simple. We formulate a set of such balances for "masses" that may have a more general meaning than a physical mass. It could be volume, momentum, energy, etc. instead. It is a quantity for which we want to formulate balance equations. We use the following notation:

- **m**: Vector of "masses" (quantities of substances, physical variables or properties) in a given region for which balance equations are to be formulated ([**m**]).
- **J**: Vector of total (net) input of the masses, **m**, to the given region per unit of time ([**m**]T^{-1}).
- **R**: Vector of total (net) production of the masses, **m**, in the given region per unit of time ([**m**]T^{-1}).

For each variable, the dimensions are given in parentheses. [**m**] refers to the vector of dimensions of the "masses" for which balance equations are formulated. This can be mass, volume, momentum, energy, etc. T refers to the dimension of time. Figure 3.1 visualizes these definitions. From the definitions given above it is evident, that the "masses" at time

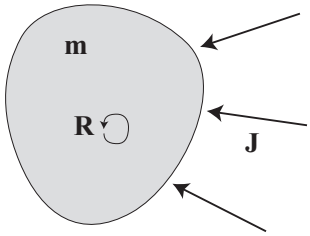

Figure 3.1: Illustration of the notation for "masses", **m**, input, **J**, and sources **R** of substances, physical variables, or other properties within a given region.

t_{end} can be calculated from the "masses" at the earlier time t_{ini} by adding the integral of net input plus net production over this time interval

$$\boxed{\mathbf{m}(t_{\mathrm{end}}) = \mathbf{m}(t_{\mathrm{ini}}) + \int_{t_{\mathrm{ini}}}^{t_{\mathrm{end}}} \mathbf{J}(t)\,\mathrm{d}t + \int_{t_{\mathrm{ini}}}^{t_{\mathrm{end}}} \mathbf{R}(t)\,\mathrm{d}t} \tag{3.1}$$

This is the **integral form of the balance equations**. If we assume that the solution to this equation is differentiable with respect to t_{end} we get after replacing t_{end} by t and doing this differentiation

$$\boxed{\frac{\mathrm{d}\mathbf{m}}{\mathrm{d}t}(t) = \mathbf{J}(t) + \mathbf{R}(t)} \tag{3.2}$$

This is the **differential form of the balance equations**.

The equations 3.1 and 3.2 seem to be trivial. Nevertheless, depending on the expressions used for **J** and **R**, these equations can have solutions with complex behaviour that are difficult to calculate. In the next three sections, we derive applied versions of these equations for the cases of (i) a single mixed reactor, (ii) a system of mixed rectors, and (iii) a spatially continuous system.

3.2 Mass Balance in a Mixed Reactor

As we can assume water to be incompressible (constant density, ρ), we can formulate balance equations for volume instead of mass of water. If we combine water volume with masses of dissolved or suspended substances or organisms in water and with masses of substances or organisms attached to a surface in the reactor to a "mass" vector as defined in the previous section, we get the following expressions for "masses", net input, and total production rates

$$\mathbf{m} = \begin{pmatrix} V \\ VC_1 \\ VC_2 \\ \vdots \\ VC_{n_\mathrm{v}} \\ AD_1 \\ AD_2 \\ \vdots \\ AD_{n_a} \end{pmatrix}, \mathbf{J} = \begin{pmatrix} Q_\mathrm{in} - Q_\mathrm{out} \\ Q_\mathrm{in}C_{\mathrm{in},1} - Q_\mathrm{out}C_1 + J_{\mathrm{int},1} \\ Q_\mathrm{in}C_{\mathrm{in},2} - Q_\mathrm{out}C_2 + J_{\mathrm{int},2} \\ \vdots \\ Q_\mathrm{in}C_{\mathrm{in},n_\mathrm{v}} - Q_\mathrm{out}C_{n_\mathrm{v}} + J_{\mathrm{int},n_\mathrm{v}} \\ 0 \\ 0 \\ \vdots \\ 0 \end{pmatrix}, \mathbf{R} = \begin{pmatrix} 0 \\ Vr_{C_1} \\ Vr_{C_2} \\ \vdots \\ Vr_{C_{n_\mathrm{v}}} \\ Ar_{D_1} \\ Ar_{D_2} \\ \vdots \\ Ar_{D_{n_\mathrm{a}}} \end{pmatrix} \tag{3.3}$$

Here, the variables have the following meaning:

- V: Current reactor volume (L^3).
- A: Surface area in the reactor available for colonization or adsorption (L^2).
- Q_in: Inflow to the reactor ($\mathrm{L}^3\mathrm{T}^{-1}$). Q_in must fulfill the condition $Q_\mathrm{in} \geq 0$.
- Q_out: Outflow of the reactor ($\mathrm{L}^3\mathrm{T}^{-1}$). Q_out must fulfill the condition $Q_\mathrm{out} \geq 0$.
- C_j: Concentration of dissolved or suspended substance or organism j (ML^{-3}).
- $C_{\mathrm{in},j}$: Concentration of dissolved or suspended substance or organism j in the inflow (ML^{-3}).
- $J_{\mathrm{int},j}$: Flux of dissolved or suspended substance or organism j across the interface (MT^{-1}).
- D_j: Surface density of attached substance or organism j (ML^{-2}).
- r_{C_j}: Production rate of dissolved or suspended substance or organism j per unit volume ($\mathrm{ML}^{-3}\mathrm{T}^{-1}$).
- r_{D_j}: Production rate of attached substance or organism j per unit surface area ($\mathrm{ML}^{-2}\mathrm{T}^{-1}$).
- n_v: Number of dissolved or suspended substances.
- n_a: Number of substances attached to a surface.

Substances and organisms are assumed to be well mixed within the reactor. If we aggregate the concentrations, interface fluxes and production rates into vectors

$$\mathbf{C} = \begin{pmatrix} C_1 \\ C_2 \\ \vdots \\ C_{n_\mathrm{v}} \end{pmatrix}, \quad \mathbf{J}_\mathrm{int} = \begin{pmatrix} J_{\mathrm{int},1} \\ J_{\mathrm{int},2} \\ \vdots \\ J_{\mathrm{int},n_\mathrm{v}} \end{pmatrix}, \quad \mathbf{r_C} = \begin{pmatrix} r_{C_1} \\ r_{C_2} \\ \vdots \\ r_{C_{n_\mathrm{v}}} \end{pmatrix} \tag{3.4}$$

and

$$\mathbf{D} = \begin{pmatrix} D_1 \\ D_2 \\ \vdots \\ D_{n_\mathrm{a}} \end{pmatrix} \quad , \quad \mathbf{r_D} = \begin{pmatrix} r_{D_1} \\ r_{D_2} \\ \vdots \\ r_{D_{n_\mathrm{a}}} \end{pmatrix} \tag{3.5}$$

and substitute these expressions first into (3.3) and then into (3.2) we get the following differential equations

$$\boxed{\frac{\mathrm{d}V}{\mathrm{d}t} = Q_\mathrm{in} - Q_\mathrm{out}} \tag{3.6}$$

$$\boxed{\frac{\mathrm{d}}{\mathrm{d}t}\Big(V\mathbf{C}\Big) = Q_\mathrm{in}\mathbf{C}_\mathrm{in} - Q_\mathrm{out}\mathbf{C} + \mathbf{J}_\mathrm{int} + V\mathbf{r_C}} \tag{3.7}$$

$$\boxed{\frac{\mathrm{d}}{\mathrm{d}t}\Big(A\mathbf{D}\Big) = A\mathbf{r_D}} \tag{3.8}$$

The "mass" fluxes underlying this equation are visualized in Figure 3.2.

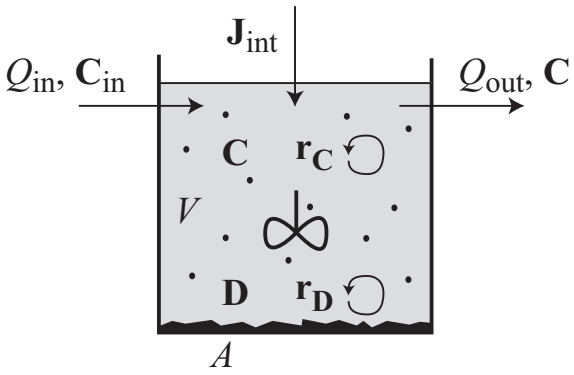

Figure 3.2: Illustration of the notation for a single mixed reactor.

By differentiation of equation (3.7) and substitution of equation (3.6) for $\mathrm{d}V/\mathrm{d}t$, we get a differential equation for substance or organism concentrations

$$\boxed{\frac{\mathrm{d}\mathbf{C}}{\mathrm{d}t} = \frac{Q_\mathrm{in}}{V}\Big(\mathbf{C}_\mathrm{in} - \mathbf{C}\Big) + \frac{\mathbf{J}_\mathrm{int}}{V} + \mathbf{r_C}} \tag{3.9}$$

Changes in concentration are caused by inflow, outflow, flux across the interface, and by transformation processes. We will assume that the surface area available for colonization and adsorption is constant. Equation (3.8) simplifies then to

$$\boxed{\frac{\mathrm{d}\mathbf{D}}{\mathrm{d}t} = \mathbf{r_D}} \tag{3.10}$$

3.3 Mass Balance in a Multi-Reactor System

A multi-reactor system consists of a set of linked single reactors. We label the reactors by the upper index k and introduce links labelled with the lower index l and characterized by

- k_l^{from}: Index of reactor at which the link l starts.
- k_l^{to}: Index of reactor at which the link l ends.
- Q_l: Water flow of link l. This water flow leads to associated substance fluxes of all dissolved and suspended substances.
- $\mathbf{J}_l$: Vector of mass fluxes of link l that are not associated with water flow.

Note that the indices k_l^{from} and k_l^{to} determine the logical direction of the link. The direction of water flow and substance fluxes depends on the signs of Q_l and $\mathbf{J}_l$, with positive values indicating flow in the logical direction, negative values in the reverse direction. The set of the three equations (3.6), (3.7) and (3.8) of a single mixed reactor must then be reproduced for each reactor k and additional terms for water and substance exchange must be added. This leads to the following set of differential equations for each reactor k in the multi-reactor system:

$$\begin{aligned}\frac{\mathrm{d}V^k}{\mathrm{d}t} = \; & Q^k_{\text{in}} - Q^k_{\text{out}} \\ & - \sum_{l \text{ with } k_l^{\text{from}}=k} Q_l + \sum_{l \text{ with } k_l^{\text{to}}=k} Q_l\end{aligned} \tag{3.11}$$

$$\begin{aligned}\frac{\mathrm{d}}{\mathrm{d}t}\left(V^k\mathbf{C}^k\right) = \; & Q^k_{\text{in}}\mathbf{C}^k_{\text{in}} - Q^k_{\text{out}}\mathbf{C}^k + \mathbf{J}^k_{\text{int}} + V^k\mathbf{r}^k_{\mathbf{C}} \\ & - \sum_{l \text{ with } k_l^{\text{from}}=k} \left(Q_l\mathbf{C}^{\text{if}(Q_l,k_l^{\text{from}},k_l^{\text{to}})} + \mathbf{J}_l\right) \\ & + \sum_{l \text{ with } k_l^{\text{to}}=k} \left(Q_l\mathbf{C}^{\text{if}(Q_l,k_l^{\text{from}},k_l^{\text{to}})} + \mathbf{J}_l\right)\end{aligned} \tag{3.12}$$

$$\frac{\mathrm{d}}{\mathrm{d}t}\left(A^k\mathbf{D}^k\right) = A^k\mathbf{r}^k_{\mathbf{D}} \tag{3.13}$$

The first row in each of these equations reproduces the corresponding equation (3.6), (3.7) and (3.8) of the single reactor system. The subsequent rows describe exchange between the reactors. In the above equations

$$\text{if}(Q,k_1,k_2) = \begin{cases} k_1 & \text{if } Q \geq 0 \\ k_2 & \text{if } Q < 0 \end{cases} \tag{3.14}$$

returns the index from which the flow originates physically. This function is required as the link direction is defined logically, but advective transport is determined by the concentrations in the reactor from which the flow in the link originates physically (a positive discharge represents a physical flow aligned with the logical direction, a negative discharge a flow opposite to the logical link definition). The other symbols in the equations above have the following meaning:

V^k: Current volume of reactor k (L^3).

A^k: Surface area in reactor k available for colonization or adsorption (L^2).

Q^k_{in}: Inflow to reactor k across the system boundary (L^3T^{-1}). Q^k_{in} must fulfill the condition $Q^k_{\text{in}} \geq 0$.

Q^k_{out}: Outflow of reactor k across the system boundary (L^3T^{-1}). Q^k_{out} must fulfill the condition $Q^k_{\text{out}} \geq 0$.

$\mathbf{C}^k_{\text{in}}$: Vector of concentrations of dissolved or suspended substances or organisms in the inflow to reactor k (ML^{-3}).

$\mathbf{J}^k_{\text{int}}$: Vector of fluxes of dissolved or suspended substances or organisms across the interface to reactor k (MT^{-1}).

$\mathbf{D}^k$: Vector of surface densities of attached substances or organisms in reactor k (ML^{-2}).

$\mathbf{r}^k_{\mathbf{C}}$: Vector of production rates of dissolved or suspended substances or organisms per unit volume in reactor k ($ML^{-3}T^{-1}$).

$\mathbf{r}^k_{\mathbf{D}}$: Vector of production rates of attached substances or organisms per unit surface area in reactor k ($ML^{-2}T^{-1}$).

There are two special forms of substance fluxes that are of particular importance: advective and diffusive fluxes.

For an advective flux, the mass flux is proportional to the substance concentration in the reactor from which the flow originates physically:

$$\boxed{J^{\text{adv}}_{l,j} = q^{\text{adv}}_{l,j} \cdot C_j^{\text{if}(q^{\text{adv}}_{l,j}, k^{\text{from}}_l, k^{\text{to}}_l)}} \tag{3.15}$$

The advective transfer coefficients of link l, $q^{\text{adv}}_{l,j}$, can be universal (apply to all dissolved or suspended substances, this is physically advection with the water flow) or they can be substance-specific. An example needing a substance-specific "advective" flux is a "directed" transport not associated with water flow, such as sedimentation. This transport follows also the advection equation, but the sedimentation velocity replaces the flow velocity:

$$q^{\text{adv}}_{l,j} = A\, v_{\text{sed},j} \tag{3.16}$$

where the reactor k^{from}_l is assumed to lay on top of the reactor k^{to}_l, A is the horizontal contact area of the reactors, and $v_{\text{sed},j}$ is the sedimentation velocity of substance j. As such directed transport follows the advection equation (with a substance-specific instead of a universal transport velocity), we still call it an advective flux throughout this manuscript.

For a diffusive flux, the mass flux is proportional to the difference in substance concentration between the reactors and the direction of the flux is from the higher to the lower concentration:

$$\boxed{J^{\text{diff}}_{l,j} = q^{\text{diff}}_{l,j} \cdot (C_j^{k^{\text{from}}_l} - C_j^{k^{\text{to}}_l})} \tag{3.17}$$

A typical example of a diffusive flux is a discretized description of a diffusion process. In this case the diffusive exchange coefficients of the link, $q^{\text{diff}}_{l,j}$ are given by

$$q^{\text{diff}}_{l,j} = A\, \frac{D_j}{L_{\text{diff}}} \tag{3.18}$$

where A is the area across which the exchange takes place, D_j is the diffusion coefficient of substance j, and L_{diff} is a typical diffusion distance. The diffusion distance can be the box size in exchange direction, if the boxes discretize a region of nearly uniform diffusivity, or the thickness of a low-diffusivity interface between the two boxes. If the link represents turbulent diffusion, the exchange coefficient is universal and applies to all dissolved or suspended substances in the reactor. For molecular diffusion, the exchange coefficient is substance-specific.

3.4 Mass Balance in a Continuous System

3.4.1 One-Dimensional Case

If the substance for which balance equations should be formulated spreads continuously in space it is meaningful to introduce densities. In a one-dimensional system, a density is a "mass" per unit length of the system. As in section 3.1, "mass" is written in quotation marks to indicate that it has the meaning of any quantity for which it is meaningful to write a balance equation. In the following, we use a hat "ˆ" to distinguish the one-dimensional densities from three-dimensional densities. We use the following notation:

- $\hat{\boldsymbol{\rho}}$: Vector of one-dimensional densities ("mass" per unit length) of the quantities for which balance equations should be formulated ($[\mathbf{m}]L^{-1}$).
- $\hat{\mathbf{j}}$: Vector of total fluxes ("mass" per unit of time) of the quantities for which balance equations should be formulated ($[\mathbf{m}]T^{-1}$).
- $\hat{\mathbf{r}}$: Vector of "mass" per unit length and time of net production of the quantities for which balance equations should be formulated ($[\mathbf{m}]L^{-1}T^{-1}$).

This notation allows us to make the terms in the equations (3.1) and (3.2) concrete. If we look at an interval $[x_A,x_E]$ of the x-axis, as shown in Figure 3.3, we get

$$\mathbf{m}(t) = \int_{x_A}^{x_E} \hat{\boldsymbol{\rho}}(x,t)\,\mathrm{d}x \quad , \tag{3.19}$$

$$\mathbf{J}(t) = \hat{\mathbf{j}}(x_A,t) - \hat{\mathbf{j}}(x_E,t) \tag{3.20}$$

and

$$\mathbf{R}(t) = \int_{x_A}^{x_E} \hat{\mathbf{r}}(x,t)\,\mathrm{d}x \quad . \tag{3.21}$$

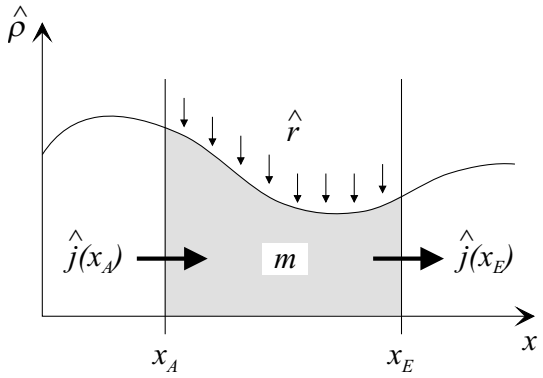

Figure 3.3: Illustration of the notation for the derivation of the one-dimensional mass balance equations.

With these expressions, equation (3.1) becomes

$$\boxed{\begin{aligned}\int_{x_A}^{x_E} \hat{\boldsymbol{\rho}}(x,t_{\text{end}})\,\mathrm{d}x = & \int_{x_A}^{x_E} \hat{\boldsymbol{\rho}}(x,t_{\text{ini}})\,\mathrm{d}x \\ & - \int_{t_{\text{ini}}}^{t_{\text{end}}} \left(\hat{\mathbf{j}}(x_E,t) - \hat{\mathbf{j}}(x_A,t)\right)\mathrm{d}t \\ & + \int_{t_{\text{ini}}}^{t_{\text{end}}}\int_{x_A}^{x_E} \hat{\mathbf{r}}(x,t)\,\mathrm{d}x\,\mathrm{d}t\end{aligned}} \tag{3.22}$$

for all $x_E > x_A$ and $t_{\text{end}} > t_{\text{ini}}$. This is the integral form of the one-dimensional mass balance equations.

If $\hat{\boldsymbol{\rho}}$ can be differentiated piecewise continuously with respect to t and $\hat{\mathbf{j}}$ with respect to x, we get

$$\hat{\boldsymbol{\rho}}(x,t_{\text{end}}) - \hat{\boldsymbol{\rho}}(x,t_{\text{ini}}) = \int_{t_{\text{ini}}}^{t_{\text{end}}} \frac{\partial}{\partial t}\,\hat{\boldsymbol{\rho}}(x,t)\,\mathrm{d}t \tag{3.23}$$

and

$$\hat{\mathbf{j}}(x_E,t) - \hat{\mathbf{j}}(x_A,t) = \int_{x_A}^{x_E} \frac{\partial}{\partial x}\,\hat{\mathbf{j}}(x,t)\,\mathrm{d}x \qquad . \tag{3.24}$$

Substituting equations (3.23) and (3.24) into equation (3.22) leads to

$$\int_{t_{\text{ini}}}^{t_{\text{end}}}\int_{x_A}^{x_E} \left(\frac{\partial}{\partial t}\,\hat{\boldsymbol{\rho}}(x,t) + \frac{\partial}{\partial x}\,\hat{\mathbf{j}}(x,t) - \hat{\mathbf{r}}(x,t)\right)\mathrm{d}x\,\mathrm{d}t = 0 \qquad . \tag{3.25}$$

As the integral is zero for all integration domains, also the integrand must be zero:

$$\boxed{\frac{\partial \hat{\boldsymbol{\rho}}}{\partial t} + \frac{\partial}{\partial x}\left(\hat{\mathbf{j}}\right) = \hat{\mathbf{r}}} \tag{3.26}$$

This is the differential form of the one-dimensional mass balance equations. Note that the bracket around $\hat{\mathbf{j}}$ indicates that the partial derivative should be taken by formulating $\hat{\mathbf{j}}$ as a function of x and t and not only of the explicit x-dependence, when $\hat{\mathbf{j}}$ is formulated as a function of substance concentrations in the system.

For aquatic ecosystem models, the most important application of one-dimensional mass balance equations are equations for cross-sectionally averaged substance transport. In this case

$$\hat{\rho} = AC \tag{3.27}$$

where A is the cross-sectional area and C is the cross-sectionally averaged substance concentration. The two important contributions to fluxes are usually advective and diffusive fluxes:

$$\hat{j} = AvC - AD\frac{\partial C}{\partial x} \tag{3.28}$$

where A is the cross-sectional area, v is the advective velocity (either due to water flow or due to movement of particles in the water column, such as sedimentation), and D is the diffusion coefficient (either molecular or turbulent diffusion). Finally, the net production rate, $\hat{r}$, can be expressed as A times the volumetric production rate, r:

$$\hat{r} = Ar \tag{3.29}$$

Substituting the expressions (3.27) to (3.29) into equation (3.26) yields

$$\boxed{\frac{\partial(AC)}{\partial t} + \frac{\partial(AvC)}{\partial x} = \frac{\partial}{\partial x}\left(AD\frac{\partial C}{\partial x}\right) + Ar} \tag{3.30}$$

This is the one-dimensional advection-diffusion equation that is the basis for one-dimensional biogeochemical and ecological models of aquatic systems. If the cross-sectional area, the advective velocity and the diffusion coefficient are constant in space and time, we get a special case of equation (3.30) in the form

$$\frac{\partial C}{\partial t} + v\frac{\partial C}{\partial x} = D\frac{\partial^2 C}{\partial x^2} + r \tag{3.31}$$

3.4.2 Three-Dimensional Case

The derivation of the three-dimensional mass balance equations is analogous to the derivation in the one-dimensional case discussed in the preceding section. In this section, we use arrows to indicate vectors in the three dimensional physical space, whereas bold symbols still mean vectors over different quantities for which balance equations should be formulated. We use the following notation:

- $\boldsymbol{\rho}$: Vector of densities ("mass" per unit volume) of the quantities for which balance equations should be formulated ($[\mathbf{m}]L^{-3}$).
- $\vec{\mathbf{j}}$: Vector of fluxes ("mass" per unit of time and cross-sectional area) of the quantities for which balance equations should be formulated ($[\mathbf{m}]L^{-2}T^{-1}$).
- $\mathbf{r}$: Vector of net production rates ("mass" per unit volume and time) of the quantities for which balance equations should be formulated ($[\mathbf{m}]L^{-3}T^{-1}$).

If we look at a piecewise smoothly bounded volume V in three-dimensional space we get

$$\mathbf{m}(t) = \int_V \boldsymbol{\rho}(\vec{x}, t)\,\mathrm{d}V \qquad , \tag{3.32}$$

$$\mathbf{J}(t) = -\int_A \vec{\mathbf{j}}(\vec{x}, t) \cdot \mathrm{d}\vec{A} \tag{3.33}$$

and

$$\mathbf{R}(t) = \int_V \mathbf{r}(\vec{x}, t)\,\mathrm{d}V \qquad . \tag{3.34}$$

Here, the variables have the following meaning:

$\vec{x}$: Three dimensional location vector in space (L),
A: Surface area of the volume V (L^2),
$\mathrm{d}\vec{A}$: Surface element multiplied by a outward directed vector of unit length (L^2).

These quantities are illustrated in Figure 3.4.

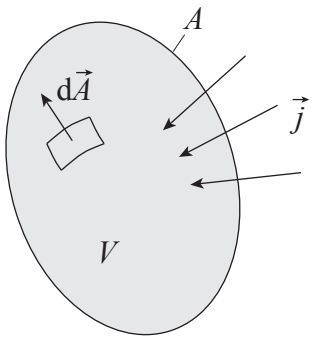

Figure 3.4: Illustration of the notation for the derivation of the three-dimensional mass balance equations.

If we substitute the equations (3.32) to (3.34) into equation (3.1) we get

$$\boxed{\begin{aligned}\int_V \boldsymbol{\rho}(\vec{x}, t_{\mathrm{end}})\,\mathrm{d}V = & \int_V \boldsymbol{\rho}(\vec{x}, t_{\mathrm{ini}})\,\mathrm{d}V \\ & - \int_{t_{\mathrm{ini}}}^{t_{\mathrm{end}}} \int_A \vec{\mathbf{j}}(\vec{x}, t) \cdot \mathrm{d}\vec{A}\,\mathrm{d}t \\ & + \int_{t_{\mathrm{ini}}}^{t_{\mathrm{end}}} \int_V \mathbf{r}(\vec{x}, t)\mathrm{d}V\,\mathrm{d}t\end{aligned}} \tag{3.35}$$

for all volumes V and all $t_{\mathrm{end}} > t_{\mathrm{ini}}$. This is the integral form of the three-dimensional mass balance equations.

If the function $\boldsymbol{\rho}$ is piecewise continuously differentiable with respect to t and $\vec{\mathbf{j}}$ with respect to $\vec{x}$, we get:

$$\boldsymbol{\rho}(\vec{x}, t_{\mathrm{end}}) - \boldsymbol{\rho}(\vec{x}, t_{\mathrm{ini}}) = \int_{t_{\mathrm{ini}}}^{t_{\mathrm{end}}} \frac{\partial}{\partial t}\,\boldsymbol{\rho}(\vec{x}, t)\,\mathrm{d}t \qquad . \tag{3.36}$$

According to the theorem of Gauss we can replace the intergral of the flux across the surface bounding a certain volume in space by the integral of the divergence of the flux

over this volume (the divergence of a vector field $\vec{v}$, represented by div, is a scalar field that quantifies the volume density of the outward flux of a vector field at each point in space; in cartesian coordinates, it is given by $\operatorname{div}\vec{v} = \partial v_x/\partial x + \partial v_y/\partial y + \partial v_z/\partial z$):

$$\int_A \vec{\mathbf{j}}(\vec{x},t)\cdot \mathrm{d}\vec{A} = \int_V \operatorname{div}\vec{\mathbf{j}}(\vec{x},t)\,\mathrm{d}V \tag{3.37}$$

Using these expressions, we can rewrite equation (3.35) in the form

$$\int_{t_{\mathrm{ini}}}^{t_{\mathrm{end}}} \int_V \left(\frac{\partial}{\partial t}\boldsymbol{\rho}(\vec{x},t) + \operatorname{div}\vec{\mathbf{j}}(x,t) - \mathbf{r}(\vec{x},t) \right) \mathrm{d}V\,\mathrm{d}t = 0 \tag{3.38}$$

for all V and all $t_{\mathrm{end}} > t_{\mathrm{ini}}$. As the integral is zero for all integration domains, also the integrand must be zero:

$$\boxed{\frac{\partial \boldsymbol{\rho}}{\partial t} + \operatorname{div}\vec{\mathbf{j}} = \mathbf{r}} \tag{3.39a}$$

or in components

$$\boxed{\frac{\partial \boldsymbol{\rho}}{\partial t} + \frac{\partial \mathbf{j}_x}{\partial x} + \frac{\partial \mathbf{j}_y}{\partial y} + \frac{\partial \mathbf{j}_z}{\partial z} = \mathbf{r}} \tag{3.39b}$$

This is the differential form of the three-dimensional mass balance equations.

For aquatic ecosystem models, the most important application of three-dimensional mass balance equations are equations for substance transport. In this case

$$\rho = C \qquad , \tag{3.40}$$

where C is the substance concentration. The two important contributions to fluxes are usually advective and diffusive fluxes. Advective fluxes are proportional to substance concentration and advective transport velocity (either the velocity of the transporting fluid or superimposed "directed" transport of the substance, e.g. by sedimentation) and diffusive flux proportional to the gradient of the concentration field and in opposed direction. This leads to the following equation for the flux vector (formulated for a single substance):

$$\vec{j} = \vec{v}\,C - \begin{pmatrix} D_x & & \\ & D_y & \\ & & D_z \end{pmatrix} \cdot \overrightarrow{\operatorname{grad}}(C) = \begin{pmatrix} v_x C - D_x \dfrac{\partial C}{\partial x} \\ v_y C - D_y \dfrac{\partial C}{\partial y} \\ v_z C - D_z \dfrac{\partial C}{\partial z} \end{pmatrix} \qquad , \tag{3.41}$$

where $\vec{v}$ is the vector of advective velocities (either due to water flow or due to movement of particles in the water column, such as sedimentation), D_x, D_y and D_z are the diffusion coefficients in x-, y- and z-direction (either molecular or turbulent diffusion), and $\overrightarrow{\operatorname{grad}}$ represents the gradient of the concentration field (the gradient of a scalar field s is a vector field that represents its steepest ascent direction and magnitude (slope); in cartesiann coordinates, it is given by $\overrightarrow{\operatorname{grad}}(s) = (\partial s/\partial x, \partial s/\partial y, \partial s/\partial z)^{\mathrm{T}}$ [T transposes the row vector

to a column vector]). Finally, we need the net production rate, r. Substituting the expressions (3.40) and (3.41) into equation (3.39) yields

$$\boxed{\begin{aligned}\frac{\partial C}{\partial t} + \frac{\partial (v_x C)}{\partial x} + \frac{\partial (v_y C)}{\partial y} + \frac{\partial (v_z C)}{\partial z} \\ = \frac{\partial}{\partial x}\left(D_x \frac{\partial C}{\partial x}\right) + \frac{\partial}{\partial y}\left(D_y \frac{\partial C}{\partial y}\right) + \frac{\partial}{\partial z}\left(D_z \frac{\partial C}{\partial z}\right) + r\end{aligned}} \tag{3.42}$$

This is the three-dimensional advection-diffusion equation that is the basis for three-dimensional biogeochemical and ecological models of aquatic systems.

Chapter 4

Formulation of Transformation Processes

In section 4.1 we introduce a process table notation for representing the transformation processes in the aquatic ecosystem. This process table notation is extremely convenient for getting an overview of the system of transformation processes used in a model. This notation is very popular in waste water engineering, but, despite its advantages, is rarely used in ecological modelling. We will consequently use this notation for the discussion of transformation processes in chapters 7 and 8, of didactical models in chapter 11, and of research models in chapter 13.

In section 4.2 we discuss the typical structure and typical terms of process rates used to quantify the effect of influence factors.

Finally, in section 4.3, we demonstrate how stoichiometric coefficients can be derived from the elemental composition of involved substances and organisms and from additional stoichiometric constraints.

4.1 Process Table Notation

We assume that a transformation process transforms different substances with proportional rates. These constants of proportionality are called "stoichiometric coefficients". For this reason, each process can be characterized by a set of such stoichiometric coefficients for all substances involved in the process and a unique process rate. It is common practice to set the stoichiometric coefficient of one of the substances to plus or minus unity. The process rate is then the rate of transformation of this substance and the other stoichiometric coefficients specify transformation rates of other substances relative to the transformation rate of this substance.

Table 4.1 outlines the elements of the process table notation introduced for a clear and consistent representation of a set of biogeochemical transformation processes used in an activated sludge model (Henze et al., 1986). The table has a row for each transformation process and a column for each of the modelled substances. An additional column contains the formulations of the process rates as functions of substance concentrations and external influence factors. The stoichiometric coefficients contained in each row of the main part of the table specify relative transformation rates of different substances for the process.

Process	Substances					Rate
	s_1	s_2	s_3	$\cdots$	$\mathrm{s}_{n_\mathrm{s}}$	
p_1	ν_{11}	ν_{12}	ν_{13}	$\cdots$	ν_{1n_s}	ρ_1
p_2	ν_{21}	ν_{22}	ν_{23}	$\cdots$	ν_{2n_s}	ρ_2
$\vdots$	$\vdots$	$\vdots$	$\vdots$	$\ddots$	$\vdots$	$\vdots$
$\mathrm{p}_{n_\mathrm{p}}$	$\nu_{n_\mathrm{p}1}$	$\nu_{n_\mathrm{p}2}$	$\nu_{n_\mathrm{p}3}$	$\cdots$	$\nu_{n_\mathrm{p}n_\mathrm{s}}$	ρ_{n_p}

Table 4.1: The process table summarizes process stoichiometry and process rates (see text for explanations).

In a homogeneous environment in which all process rates are expressed in the same units of changes, either mass per volume or mass per surface, and all concentrations are also expressed as mass per volume or mass per surface, the total (net) transformation rate of each substance can be calculated by a sum of the contributions of all processes as follows

$$r_j = \sum_{i=1}^{n_\mathrm{p}} \nu_{ij}\ \rho_i \tag{4.1}$$

In this equation, r_j is the total (net) transformation rate of substance j, ν_{ij} is the stoichiometric coefficient of process i for the substance j, ρ_i is the process rate of process i, and n_p is the number of processes used in the model. Note that the "distribution" of rate factors between stoichiometric coefficients and process rate is not unique. The remaining degree of freedom is usually eliminated by setting one of the stoichiometric coefficients to plus or minus unity. This leads to the interpretation of the process rate as the contribution of the process to the transformation of the substance with stoichiometric coefficient equal to plus or minus unity.

If some of the rates are expressed as rates of change of (suspended or dissolved) mass

per volume and others as rates of change of (attached or absorbed) mass per area and some of the substances are expressed as mass per volume and others as mass per area, we have to include geometric conversions in addition to stoichiometric coefficients into the rate calculation. We do this by specifying a vector of unit volumes and areas, $\boldsymbol{\xi}_\mathrm{p}$, for all processes and a vector of inverse unit volumes and areas, $\boldsymbol{\xi}_\mathrm{s}$, for all substances and generalizing equation (4.1) to

$$r_j = \xi_{\mathrm{s},j} \sum_{i=1}^{n_\mathrm{p}} \nu_{ij}\ \xi_{\mathrm{p},i}\ \rho_i \tag{4.2}$$

The factor $\xi_{\mathrm{p},i}$ converts the process rates per volume or per area into total transformation rates within the area or volume, the factor $\xi_{\mathrm{s},j}$ converts the total transformation rate of a substance within the volume or area back into a transformation rate per unit of volume or area.

By introducing the matrix of stoichiometric coefficients

$$\boldsymbol{\nu} = \overbrace{\left.\begin{pmatrix} \nu_{11} & \nu_{12} & \nu_{13} & \cdots & \nu_{1n_\mathrm{s}} \\ \nu_{21} & \nu_{22} & \nu_{23} & \cdots & \nu_{2n_\mathrm{s}} \\ \vdots & \vdots & \vdots & \ddots & \vdots \\ \nu_{n_\mathrm{p}1} & \nu_{n_\mathrm{p}2} & \nu_{n_\mathrm{p}3} & \cdots & \nu_{n_\mathrm{p}n_\mathrm{s}} \end{pmatrix}\right\}}^{\text{substances } \mathrm{s}_1, ..., \mathrm{s}_{n_\mathrm{s}}} \begin{matrix} \\ \\ \\ \\ \end{matrix} \left.\begin{matrix} \\ \\ \\ \\ \end{matrix}\right\} \begin{matrix} \text{processes} \\ \mathrm{p}_1, ..., \mathrm{p}_{n_\mathrm{p}} \end{matrix} \tag{4.3}$$

and the vector of process rates

$$\boldsymbol{\rho} = \left.\begin{pmatrix} \rho_1 \\ \rho_2 \\ \vdots \\ \rho_{n_\mathrm{p}} \end{pmatrix}\right\} \begin{matrix} \text{processes} \\ \mathrm{p}_1, ..., \mathrm{p}_{n_\mathrm{p}} \end{matrix} \tag{4.4}$$

equation (4.1) can be transformed into matrix notation. The column vector of total (net) transformation rates of all substances, $\mathbf{r}$, is then given as

$$\mathbf{r} = \boldsymbol{\nu}^\mathrm{T} \cdot \boldsymbol{\rho} \tag{4.5}$$

Similarly, equation (4.2) generalizes to

$$\begin{aligned} \mathbf{r} &= \mathrm{diag}\big(\boldsymbol{\xi}_\mathrm{s}\big) \cdot \boldsymbol{\nu}^\mathrm{T} \cdot \mathrm{diag}\big(\boldsymbol{\xi}_\mathrm{p}\big) \cdot \boldsymbol{\rho} \\ &= \begin{pmatrix} \xi_{\mathrm{s},1} & & & \\ & \xi_{\mathrm{s},2} & & \\ & & \ddots & \\ & & & \xi_{\mathrm{s},n_\mathrm{s}} \end{pmatrix} \cdot \boldsymbol{\nu}^\mathrm{T} \cdot \begin{pmatrix} \xi_{\mathrm{p},1} & & & \\ & \xi_{\mathrm{p},1} & & \\ & & \ddots & \\ & & & \xi_{\mathrm{p},n_\mathrm{p}} \end{pmatrix} \cdot \boldsymbol{\rho} \end{aligned} \tag{4.6}$$

Example 4.1: Growth of Suspended and Benthic Algae

Growth of algae with phosphate as the single, rate-limiting nutrient can be described by a simple stoichiometry in which phosphate satisfies the phosphorus need of algae.

If we denote the phosphorus content of algae by $\alpha_{\mathrm{P,ALG}}$ (gP/gDM) and measure algae as dry mass and phosphate in phosphorus units, we get the following process table for growth of suspended algae (ALG):

Process	Substances / Organisms		Rate
	HPO_4^{2-}	ALG	
	gP	gDM	
Growth of ALG	$-\alpha_{\mathrm{P,ALG}}$	1	$\rho_{\mathrm{gro,ALG}}$

In this table, $\rho_{\mathrm{gro,ALG}}$ is the process rate given in gDM per volume and time unit. In a spatially homogeneous environment, according to equation (4.1), this leads to transformation rate contributions for phosphate and suspended algae of

$$r_{C_{\mathrm{HPO}_4^{2-}}} = -\alpha_{\mathrm{P,ALG}} \cdot \rho_{\mathrm{gro,ALG}}$$

and

$$r_{C_{\mathrm{ALG}}} = 1 \cdot \rho_{\mathrm{gro,ALG}} = \rho_{\mathrm{gro,ALG}}$$

respectively. If we apply the more general equation (4.2), we need the conversion factor for the process rate from per volume to total

$$\xi_{\mathrm{p,gro,ALG}} = V$$

and for phosphate and algae from total to per volume

$$\xi_{\mathrm{s},\{\mathrm{HPO}_4^{2-},\mathrm{ALG}\}} = \begin{pmatrix} \frac{1}{V} \\ \frac{1}{V} \end{pmatrix}$$

where V is a typical volume within which the process is active (the value is not relevant, only the correct ratio of this volume to the area introduced below). This leads to the same equations as above:

$$r_{C_{\mathrm{HPO}_4^{2-}}} = \frac{1}{V} \cdot (-\alpha_{\mathrm{P,ALG}}) \cdot V \cdot \rho_{\mathrm{gro,ALG}} = -\alpha_{\mathrm{P,ALG}} \cdot \rho_{\mathrm{gro,ALG}}$$

and

$$r_{C_{\mathrm{ALG}}} = \frac{1}{V} \cdot 1 \cdot V \cdot \rho_{\mathrm{gro,ALG}} = \rho_{\mathrm{gro,ALG}}$$

Benthic algae are usually quantified as gDM per area available for colonization. Growth of benthic algae (SALG) has the same stoichiometry as given above

Process	Substances / Organisms		Rate
	HPO_4^{2-}	SALG	
	gP	gDM	
Growth of SALG	$-\alpha_{\mathrm{P,ALG}}$	1	$\rho_{\mathrm{gro,SALG}}$

(we assume the phosphorus content of SALG to be the same as that of ALG). However, as benthic algae are usually measured as surface densities, also the process rate $\rho_{\mathrm{gro,SALG}}$ is typically given in gDM per surface area and time unit. To convert this rate into a total rate we have to multiply it with the surface area

$$\xi_{\mathrm{p,gro,SALG}} = A$$

Conversion to a rate contribution of phosphate in the water overlaying the benthic algae needs then a division by the volume, V, whereas conversion to a rate contribution of benthic algae requires a division by the colonized surface area, A:

$$\xi_{\mathrm{s},\{\mathrm{HPO}_4^{2-},\mathrm{SALG}\}} = \begin{pmatrix} \frac{1}{V} \\ \frac{1}{A} \end{pmatrix}$$

This leads to:

$$r_{C_{\mathrm{HPO}_4^{2-}}} = \frac{1}{V} \cdot (-\alpha_{\mathrm{P,ALG}}) \cdot A \cdot \rho_{\mathrm{gro,SALG}} = -\frac{A}{V}\, \alpha_{\mathrm{P,ALG}}\, \rho_{\mathrm{gro,SALG}}$$

and

$$r_{D_{\mathrm{ALG}}} = \frac{1}{A} \cdot 1 \cdot A \cdot \rho_{\mathrm{gro,SALG}} = \rho_{\mathrm{gro,SALG}}$$

All possible conversion factors are thus V/V, V/A, A/V, and A/A. This demonstrates that we only need relative volumes and areas.

4.2 Typical Elements of Process Rates

The dependence of rates of chemical or biological processes on external influence factors is often formulated in product form. The rate is then the product of a rate under reference conditions of influence factors with modification factors that describe the effect of deviations of influence factors from their reference value. Often there are separate modification factors for all influence factors, but sometimes there are interactions which require the formulation of a modification factor that accounts for multiple influence factors.

Examples of this type of rates are the formulation of the growth rate of algae on ammonium as nitrogen source in the form

$$\rho_{\mathrm{gro,ALG,NH_4^+}} = k_{\mathrm{gro,ALG},T_0} \cdot f_{\mathrm{temp}}(T) \cdot f_{\mathrm{rad}}(I) \cdot f_{\mathrm{lim}}(C_{\mathrm{HPO_4^{2-}}}, C_{\mathrm{NH_4^+}}, C_{\mathrm{NO_3^-}}) \cdot f_{\mathrm{pref}}^{\mathrm{NH_4^+}}(C_{\mathrm{NH_4^+}}, C_{\mathrm{NO_3^-}}) \cdot C_{\mathrm{ALG}} \quad (4.7)$$

or the anoxic mineralization rate of organic particles in the form

$$\rho_{\mathrm{miner,anox,POM}}{+}{+} = k_{\mathrm{miner,anox,POM},T_0} \cdot f_{\mathrm{temp}}(T) \cdot f_{\mathrm{inh}}(C_{\mathrm{O_2}}) \cdot f_{\mathrm{lim}}(C_{\mathrm{NO_3^-}}) \cdot C_{\mathrm{POM}} \quad . \quad (4.8)$$

In these equations, $k_{\mathrm{gro,ALG},T_0}$ refers to the specific (per unit of algal biomass) growth rate of algae under non-limited conditions with respect to light and nutrients and at the standard temperature, T_0; $k_{\mathrm{miner,anox,POM},T_0}$ refers to the specific anoxic mineralization rate of organic particles under non-limited (with respect to nitrate) and non-inhibited (with respect to dissolved oxygen) conditions and at the standard temperature, T_0; T refers to temperature; I refers to incoming radiation; $C_{\mathrm{HPO_4^{2-}}}$ refers to the concentration of soluble reactive phosphorus assumed to be orthophosphate in stoichiometric calculations; $C_{\mathrm{NH_4^+}}$ refers to the concentration of ammonium ($\mathrm{NH_4^+}$); $C_{\mathrm{NO_3^-}}$ refers to the concentration of nitrate ($\mathrm{NO_3^-}$); $C_{\mathrm{O_2}}$ refers to the concentration of dissolved oxygen ($\mathrm{O_2}$); f_{temp} is the modification factor that accounts for temperature dependence; f_{rad} is the modification factor that describes the limiting effect of light intensity (radiation); f_{lim} are modification factors that describe limiting effects of substances required for the process (in these cases nutrients and dissolved oxygen); f_{pref} is a preference factor for the nitrogen source (in this case for $\mathrm{NH_4^+}$ instead of $\mathrm{NO_3^-}$), and f_{inh} is an inhibition factor of the process by a substance (in this case of anoxic mineralization by dissolved oxygen). The modification factors, f, describe the relative effects of the influence factors on the process rate. They are equal to unity at standard, non-limiting or non-inhibiting conditions. Although there are no indices showing this in the equations (4.7) and (4.8), the modification factors, f, and/or their parameter values may be different from process to process (e.g. the mineralization rate may have a different temperature dependence than the growth rate of algae). We will discuss typical formulations of such modification factors in the following subsections. The process rates given as examples in the equations (4.7) and (4.8) will be discussed in more detail in the sections 8.1 and 8.5.2, respectively.

Although the equations (4.7) and (4.8) are written for growth of algae and anoxic mineralization, the same structure of process rates is often used for other biological processes as well. This structure applies for all process formulations discussed in this manuscript.

4.2.1 Temperature Dependence of Process Rates

Figure 4.1 shows typical examples of temperature dependence of bacterial growth (Heitzer et al., 1991).

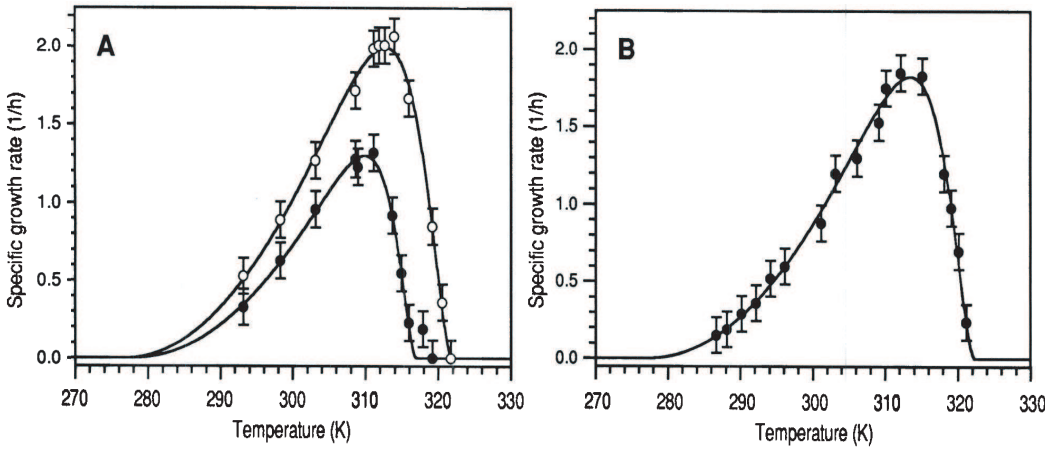

Figure 4.1: Examples of phenomenological modelling of temperature dependence of bacterial growth (Heitzer et al., 1991).

This kind of behaviour is typical for most biological reactions. It is characterized by an increasing branch from a minimum to an optimal temperature of growth followed by a decreasing branch to the maximum temperature of growth. The phenomenological model applied in Figure 4.1 is given by the following expression for the specific growth rate, μ (Ratkowsky et al., 1982):

$$\mu = \begin{cases} b^2 \, (T - T_{\min})^2 \left(1 - \exp\big(c(T - T_{\max})\big)\right)^2 & \text{for } T_{\min} \leq T \leq T_{\max} \\ 0 & \text{else} \end{cases} \tag{4.9}$$

As the temperature range in natural systems is quite limited, ecological models usually describe only the increasing branch. The most commonly used parameterization of this increasing branch is by an exponential function

$$f_{\text{temp}}^{\exp}(T) = \exp\Big(\beta(T - T_0)\Big) \tag{4.10}$$

Here, T_0 is the reference temperature at which the factor f_{temp} is unity, and β is the coefficient of temperature dependence, as illustrated in figure 4.2. This parameterization is reasonable, as long as the model is not applied to a water body in which the optimum temperature for a process is approached or even exceeded.

An extensive review of potential formulations for temperature dependence terms as well as of empirical data these models were fitted to can be found in (Kontopoulos et al., 2024).

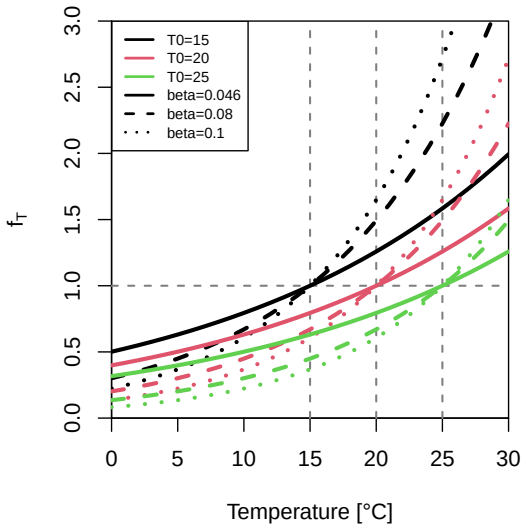

Figure 4.2: Illustration of the exponential temperature dependence function according to equation (4.10) for different parameter values (see legend).

4.2.2 Limitation of Process Rates by Substance Concentrations

The most important formulations of limitation of rates by substance concentrations are the Monod equation

$$f_{\text{lim}}^{\text{Monod}}(C) = \frac{C}{K + C} \tag{4.11}$$

the exponential equation

$$f_{\text{lim}}^{\text{exp}}(C) = 1 - \exp\left(-\frac{C}{K}\right) \tag{4.12}$$

the Blackman equation (Dabes et al., 1973)

$$f_{\text{lim}}^{\text{Blackman}}(C) = \begin{cases} \dfrac{C}{K} & \text{for } C < K \\ 1 & \text{for } C \geq K \end{cases} \tag{4.13}$$

and the Monod equation with a quadratic dependence on substance concentrations

$$f_{\text{lim}}^{\text{MonodQuadratic}}(C) = \frac{C^2}{K^2 + C^2} \tag{4.14}$$

In all of these equations, C is the substance concentration and K is a parameter with the same units as the concentration. In the Monod (4.11) and the quadratic Monod (4.14) equation, K is the half-saturation concentration at which the expression evaluates to 1/2. In the exponential equation (4.12), K is the concentration, at which the limitation is equal to $1 - e^{-1}$. Finally, in the Blackman equation (4.13), the limitation term reaches unity at $C = K$. Note that the Blackman equation is similar to the so called Holling-type I functional response, the Monod equation to the Holling-type II functional response, and the Monod equation with quadratic dependence on substance concentrations to the Holling-type III functional response (Holling, 1959). Figure 4.3 (a) shows the behaviour

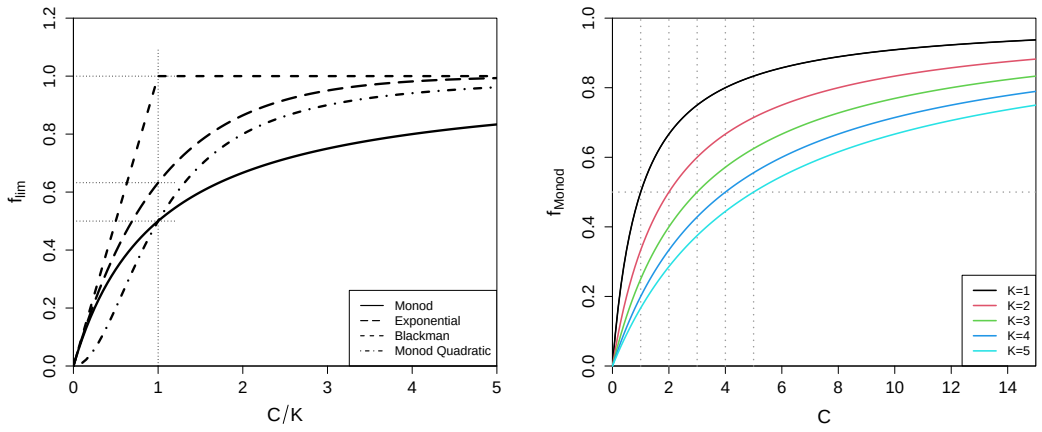

(a) (b)

Figure 4.3: (a) Behaviour of limitation factors according to the equations (4.11), (4.12), (4.13), and (4.14). (b) Illustration of the Monod limitation function according to equation (4.11) for different parameter values (see legend).

of these limitation functions and (b) the behaviour of the Monod function for different parameter values.

With increasing values of the concentrations, the factors asymptotically reach unity (i.e. saturation), for small concentrations, they approach zero. The approach to zero is linear for the Monod, the exponential and the Black equations and it is quadratic for the Monod with quadratic dependence on substrance concentrations. The Monod expression was originally derived by Michaelis and Menten for enzyme kinetics (Michaelis and Menten, 1913), but is here used as an empirical description of the saturation behaviour of a process rate with respect to nutrients (Monod, 1942).

In the example of algal growth (4.7), the limiting effect is due to multiple nutrients. This can be considered by multiplying the limiting factors or, according to "Liebig's law of the minimum", to consider only the most limiting nutrient. When using the Monod formulation (4.11) for describing limitation by a single nutrient, this leads to

$$f_{\text{lim}}^{\text{Monod,mult}}(C_{\text{HPO}_4^{2-}}, C_{\text{NH}_4^+}, C_{\text{NO}_3^-}) = \frac{C_{\text{HPO}_4^{2-}}}{K_{\text{HPO}_4^{2-}} + C_{\text{HPO}_4^{2-}}} \cdot \frac{C_{\text{NH}_4^+} + C_{\text{NO}_3^-}}{K_{\text{N}} + C_{\text{NH}_4^+} + C_{\text{NO}_3^-}} \quad (4.15)$$

or

$$f_{\text{lim}}^{\text{Monod,Liebig}}(C_{\text{HPO}_4^{2-}}, C_{\text{NH}_4^+}, C_{\text{NO}_3^-}) = \min\left(\frac{C_{\text{HPO}_4^{2-}}}{K_{\text{HPO}_4^{2-}} + C_{\text{HPO}_4^{2-}}}, \frac{C_{\text{NH}_4^+} + C_{\text{NO}_3^-}}{K_{\text{N}} + C_{\text{NH}_4^+} + C_{\text{NO}_3^-}}\right) \quad (4.16)$$

These expressions quantify limitation by phosphate and by inorganic nitrogen, taking into account that nitrogen can either be taken up in the form of ammonium or nitrate.

4.2.3 Inhibition of Process Rates by Substance Concentrations

We can use the same formulations for formulating inhibitions as we used for formulating limitations of process rates in section 4.2.2. To formulate inhibition we use unity minus

the expression for limitation:

$$f_{\text{inh}}(C) = 1 - f_{\text{lim}}(C) \tag{4.17}$$

This leads to the following options for limitation factors:

$$f_{\text{inh}}^{\text{Monod}}(C) = \frac{K}{K + C} \tag{4.18}$$

$$f_{\text{inh}}^{\text{exp}}(C) = \exp\left(-\frac{C}{K}\right) \tag{4.19}$$

$$f_{\text{inh}}^{\text{Blackman}}(C) = \begin{cases} 1 - \dfrac{C}{K} & \text{for } C < K \\ 0 & \text{for } C \geq K \end{cases} \tag{4.20}$$

$$f_{\text{inh}}^{\text{MonodQuadratic}}(C) = \frac{K^2}{K^2 + C^2} \tag{4.21}$$

Figure 4.4 (a) shows the behaviour of these modification factors and (b) the Monod inhibition function for different parameter values. At small concentrations, there is no inhibition, whereas the factors tend to zero for large concentrations.

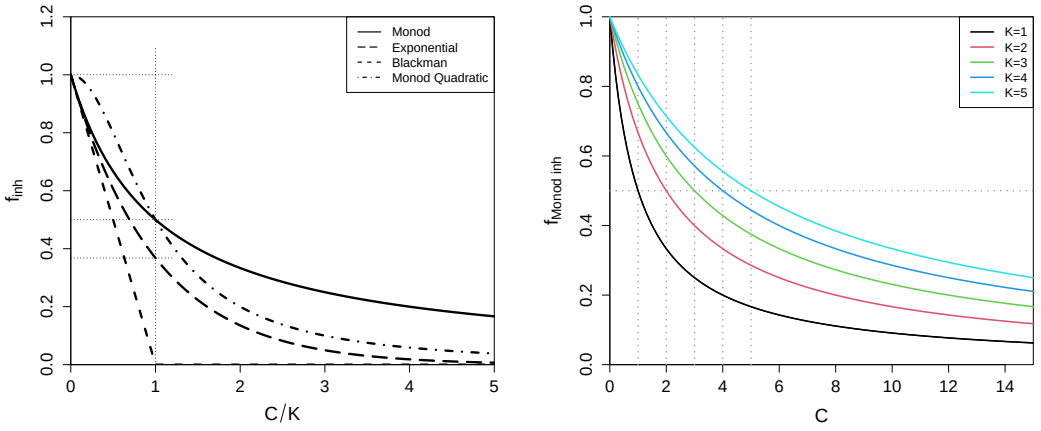

(a) (b)

Figure 4.4: (a) Behaviour of inhibition factors according to the equations (4.18), (4.19), (4.20), and (4.21). (b) Illustration of the Monod inhibition function according to equation (4.18) for different parameter values (see legend).

In the example of anoxic mineralization (4.8), the inhibition effect is due to dissolved oxygen and could thus be written as

$$f_{\text{inh}}^{\text{Monod}}(C_{\text{O}_2}) = \frac{K_{\text{O}_2}}{K_{\text{O}_2} + C_{\text{O}_2}} \tag{4.22}$$

4.2.4 Light Dependence of Primary Production

Primary production depends strongly on its energy source, light. Light dependence of the rate of primary production is expressed as a function of global or photosynthetically active radiation.

The three most often used light dependency functions are the Monod function (see also subsection 4.2.2 where the use of this function for other limitations is described)

$$f_{\text{rad}}^{\text{Monod}}(I) = \frac{I}{K_I + I} \ , \tag{4.23}$$

the Smith function (Smith, 1936)

$$f_{\text{rad}}^{\text{Smith}}(I) = \frac{I}{\sqrt{K_I^2 + I^2}} \ , \tag{4.24}$$

and the Steele function (Steele, 1962)

$$f_{\text{rad}}^{\text{Steele}}(I) = \frac{I}{I_{\text{opt}}} \exp\left(1 - \frac{I}{I_{\text{opt}}}\right) \ . \tag{4.25}$$

Figure 4.5 shows the behaviour of these three light dependence functions. The first two approaches show saturation of the production rate as a function of increasing light intensities, the last approach leads to inhibition at high intensities. In some applications in which inhibition at high light intensities is relevant, one may want to use an approach that parameterizes limitation at low intensities separately from inhibition at high intensities. This is not the case for the Steele function.

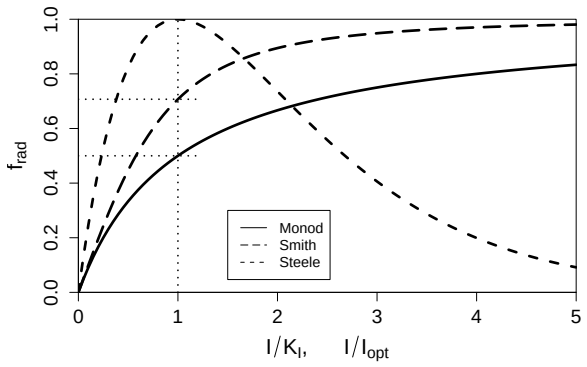

Figure 4.5: Behaviour of the light dependence functions according to the equations (4.23), (4.24), and (4.25).

As light penetrates a water body, it is attenuated. As long as concentration gradients of absorbing substances are not too strong, we can assume that the light extinction coefficient, λ, does not depend on water depth, z. Decreasing light intensity with increasing depth then follows the Beer-Lambert law (see Figure 4.6)

$$I = I_0 \exp\left(-\lambda z\right) \ , \tag{4.26}$$

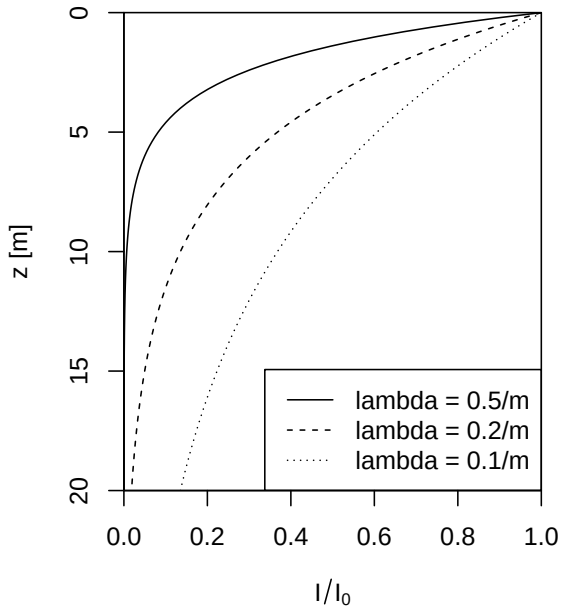

Figure 4.6: Relative light intensity, I/I_0 as a function of water depth, z, according to the Beer-Lambert law (4.26).

where I_0 is the light intensity at the water surface, λ is a light extinction coefficient, and z is water depth below the surface. The light extinction coefficient depends on the concentration of substances dissolved or suspended in the water, in particular on the concentration of algae. This implies that the assumption underlying equation (4.26), of a constant light extinction coefficient, will only be approximately fulfilled within a well-mixed surface layer. Within such a surface layer, the light extinction coefficient is often approximated by

$$\lambda = \lambda_1 + \lambda_2 \cdot C_{\mathrm{ALG}} \qquad , \tag{4.27}$$

where C_{ALG} is the concentration of algae. Usually, light intensities below such a surface layer are too small to sustain algal growth so that the approximation (4.26) can be reasonable for describing algal growth.

To describe decreasing algal growth rates with depth in such a surface layer, equation (4.26) has to be substituted into the light limitation factor of the growth rate (e.g. one of the factors 4.23 to 4.25). If we use a simplified model that describes the surface layer with primary production by a mixed box, we have to use depth-averaged rates. Because the light limitation factor is the only factor in the growth rate of algae that depends on the depth, we can use a depth-averaged light limitation factor. Note, that due to the nonlinear dependence of this factor on the light intensity, it would be incorrect to just use the averaged light in the limitation factor. Such an average factor, $\bar{f}_{\mathrm{rad}}(I_0, \lambda, h)$, is

calculated as

$$\bar{f}_{\text{rad}}(I_0, \lambda, h) = \frac{1}{h} \int_0^h f_{\text{rad}}\Big(I_0 \exp(-\lambda z)\Big) \mathrm{d}z \ , \tag{4.28}$$

where I_0 is the light intensity at the water surface, λ the light extinction coefficient, and h the thickness of the surface layer that is approximated by a mixed box.

For the factors (4.23) to (4.25), the integral (4.28) can be solved analytically leading to

$$\bar{f}_{\text{rad}}^{\text{Monod}}(I_0, \lambda, h) = \frac{1}{\lambda h} \log \left(\frac{K_I + I_0}{K_I + I_0 \exp(-\lambda h)} \right) \ , \tag{4.29}$$

$$\bar{f}_{\text{rad}}^{\text{Smith}}(I_0, \lambda, h) = \frac{1}{\lambda h} \log \left(\frac{\frac{I_0}{K_I} + \sqrt{1 + \left(\frac{I_0}{K_I}\right)^2}}{\frac{I_0 \exp(-\lambda h)}{K_I} + \sqrt{1 + \left(\frac{I_0 \exp(-\lambda h)}{K_I}\right)^2}} \right) \ , \tag{4.30}$$

and

$$\bar{f}_{\text{rad}}^{\text{Steele}}(I_0, \lambda, h) = \frac{\mathrm{e}}{\lambda h} \left[\exp\left(-\frac{I_0 \exp(-\lambda h)}{I_{\text{opt}}} \right) - \exp\left(-\frac{I_0}{I_{\text{opt}}} \right) \right] \ . \tag{4.31}$$

4.2.5 Preference Among Different Food Sources

Many organisms can grow on different food sources. This is evident from the simplified food web structures shown in Figures 1.1 and 1.2. It is important to note that the degree to which multiple food sources occur in a model food web, depends on the aggregation level of the model. As an example, growth of herbivorous zooplankton depends on only one food source, if phytoplankton is aggregated to one state variable in the model. If several groups of phytoplankton are distinguished in the model, we have to distinguish several food sources for growth of herbivorous zooplankton.

As the stoichiometry and kinetics of growth on one food source may be different from that on another, it is best to represent growth on different food sources by different processes. The process rates of these processes can still have many terms in common. But they also need a preference factor that depends on the concentrations of all food sources. The simplest conceptually satisfying expression for such a preference factor among n food sources with concentrations $C_1, ..., C_n$ is given as

$$f_{\text{pref}}^i(C_1, ..., C_n) = \frac{p_i C_i}{\sum_{j=1}^{n} p_j C_j} \tag{4.32}$$

where p_j is the preference coefficient for food source j. All preference coefficients p_j can be multiplied with the same arbitrary factor without changing the resulting value of the expression (4.32). Therefore, such a factor can be used to either normalize the

preference coefficients to unity, $\sum p_j = 1$, or to set one of the preference coefficients to unity and choose the other preference coefficients relative to this food source. If there is no preference between the different food sources, all preference coefficients p_j are set to unity. In this case, the consumption of the different food sources depends only on their relative concentration.

The preference factor (4.32) should not be misinterpreted as a limitation factor. The preference factor does not change its value if all concentrations go to zero while keeping their ratios. All preference factors sum to unity. This makes them relative factors associated with different food sources that still need combination with a limitation factor.

The simplest model would combine the preference factors with a limitation factor based on the sum of all food concentrations: $f_{\text{lim}}(C_1 + ... + C_n)$. If all the other factors in the rate expressions of the growth processes on the different food sources are the same, total growth then becomes independent on the ratios of the concentrations of the different food sources and only depends on the sum of the concentrations. However, other expressions are required if total growth depends on the food composition regarding different sources.

4.2.6 Example of a Process Table

Example 4.2: Growth of Algae and Zooplankton

A very simple ecological model for describing the most important transformation processes for plankton in a lake requires the three state variables phosphate (HPO_4^{2-}) as a growth-limiting nutrient, algae (ALG) as primary producers, and zooplankton (ZOO) as grazers of algae. We consider growth and death of both plankton groups. In this simple example, we do not consider dead organic particles and their mineralization. When denoting the phosphorus content of algae by $\alpha_{\text{P,ALG}}$ and the yield of grazing by zooplankton by Y_{ZOO}, which determines the produced zooplankton biomass per unit of consumed algal biomass, and formulating simple process rates according to the principles described above, we get the following process table:

Process	Substances / Organisms			Rate
	HPO_4^{2-}	ALG	ZOO	
	gP	gDM	gDM	
Growth of ALG	$-\alpha_{\text{P,ALG}}$	1		$k_{\text{gro,ALG,max}} \dfrac{C_{HPO_4^{2-}}}{K_{HPO_4^{2-},\text{ALG}} + C_{HPO_4^{2-}}} C_{\text{ALG}}$
Death of ALG		-1		$k_{\text{death,ALG}}\, C_{\text{ALG}}$
Growth of ZOO		$-\dfrac{1}{Y_{\text{ZOO}}}$	1	$k_{\text{gro,ZOO}}\, C_{\text{ALG}}\, C_{\text{ZOO}}$
Death of ZOO			-1	$k_{\text{death,ZOO}}\, C_{\text{ZOO}}$

The process rate of algal growth considers a growth limitation by phosphate that reaches saturation at high phosphate concentrations. The process rate of zooplankton growth is proportional to algae as well as zooplankton concentrations. This considers the dependence of zooplankton growth on algae as their food. Finally, death rates are described as first order decay processes.
Note that, according to equation (4.1), the process table given above is an abbreviated

notation for the following rate expressions for $C_{\mathrm{HPO}_4^{2-}}$, C_{ALG} and C_{ZOO}:

$$r_{\mathrm{HPO}_4^{2-}} = -\alpha_{\mathrm{P,ALG}} \cdot k_{\mathrm{gro,ALG,max}} \frac{C_{\mathrm{HPO}_4^{2-}}}{K_{\mathrm{HPO}_4^{2-},\mathrm{ALG}} + C_{\mathrm{HPO}_4^{2-}}} C_{\mathrm{ALG}}$$

$$r_{\mathrm{ALG}} = k_{\mathrm{gro,ALG,max}} \frac{C_{\mathrm{HPO}_4^{2-}}}{K_{\mathrm{HPO}_4^{2-},\mathrm{ALG}} + C_{\mathrm{HPO}_4^{2-}}} C_{\mathrm{ALG}} - k_{\mathrm{death,ALG}}\, C_{\mathrm{ALG}} - \frac{1}{Y_{\mathrm{ZOO}}} \cdot k_{\mathrm{gro,ZOO}}\, C_{\mathrm{ALG}}\, C_{\mathrm{ZOO}}$$

$$r_{\mathrm{ZOO}} = k_{\mathrm{gro,ZOO}}\, C_{\mathrm{ALG}}\, C_{\mathrm{ZOO}} - k_{\mathrm{death,ZOO}}\, C_{\mathrm{ZOO}}$$

This comparison makes it evident that the process table notation gives the much clearer overview of which process affects which substances (rows of the matrix) and which substances are affected by which processes (columns of the matrix). In the process rate notation, each process is spread to as many equations as there are affected substances. This makes the expressions much more complicated.

4.3 Derivation of Stoichiometry from Composition

It has been recognised since at least the 1950s that the stoichiometry of biological processes, or the composition of organic substances which constrain the stoichiometry, have a strong effect on biogeochemical mass fluxes and nutrient and oxygen concentrations in the environment (Redfield, 1958; McCarty, 1975; Andersen, 1997; Lenton and Watson, 2000a; Lenton and Watson, 2000b). Elemental mass conservation makes it also evident, that variation in nutrient content of food must have an effect on the yield and metabolism of consumer growth if the elemental composition of the consumer is less variable than that of the food (DeMott et al., 1998; Hessen et al., 2002; Anderson et al., 2005). This leads to a strong link between ecological and biogeochemical properties of ecosystems. It has, however, only recently been realized, that the stoichiometry of biological processes may also constitute a bridge between evolutionary biology and ecosystems ecology (Elser et al., 2000; Sterner and Elser, 2002; Kay et al., 2005; Elser, 2006). An important example for such a link between molecular biology, elemental composition of organisms and process kinetics is the "growth rate hypothesis" that states that rapidly growing cells have a particularly high demand for phosphorus-rich ribosomal RNA (Elser et al., 2000). Such links led to an increasing attention to stoichiometry in ecological studies.

In section 4.1 we introduced stoichiometric coefficients as relative transformation rates of different substances in a given process (see Table 4.1 and equation 4.1). The process i is defined by a joint process rate, ρ_i, and stoichiometric coefficients, ν_{ij}, that modify the process rate to the transformation rate of substance j. The contribution of the process i to the transformation rate of substance j is equal to $\nu_{ij}\rho_i$. Process kinetics are formulated by the process rate, ρ_i. Obviously, these relative process rates are connected to the "recipe" according to which a substance is built of constituents or how constituents are released when a substance is degraded or transformed or an organism grows or is decomposed. In this section, we start from the composition of all substances and organisms and analyze to which degree these compositions constrain the stoichiometric coefficients.

We will illustrate the concepts of stoichiometric calculations with the examples of growth, respiration, and death of algae and zooplankton. We start by introducing the derivation of stoichiometric coefficients from chemical substance notation in section 4.3.1. This approach is based on a given elemental composition of all substances and organisms involved. As the elemental composition may depend on the type of organisms and the environmental conditions to which they are exposed, we extend this approach to a parameterization of elemental mass fractions in section 4.3.2. The use of such a parameterization is illustrated with a very simple process model for growth and respiration of algae and subsequently generalized to a more complex model of growth, respiration and death of algae and zooplankton considering the elements C, H, O, N and P. This second model demonstrates both, the conceptual flexibility and feasibility of the approach as well as its practical limitation due to the increasing number of equations that are tedious to solve. These equations have to be solved again whenever new processes, substances or elements are considered in the model. This obviously calls for a general solution of this type of stoichiometric equations. Such a procedure, based on principles of linear algebra, is derived in section 4.3.3. This approach delivers the general solution of stoichiometric equations for specified processes. Furthermore, for a process characterized by the involved substances, the number of stoichiometric constraints can be derived that are required in addition to elemental mass and charge conservation to make the process definition unique.

This framework extends the flexibility of the parameterized mass fractions approach to modifications in processes and consideration of elements and substances.

4.3.1 Derivation of Stoichiometry from Chemical Substance Notation (given elemental mass fractions)

It is a straightforward concept to extend the commonly used chemical notation of molecules to organic material. As organic material consists of many different molecules, that cannot be separately addressed in the present context, the use of this concept requires its application to an "average" composition of organic material. We therefore introduce a chemical formula for a "molecule" that does not exist in this form, but represents average composition of organic material. This is sufficient for using established techniques of mass conservation of elements (counting atoms or moles) to derive stoichiometric coefficients as if this formula would represent an actual molecule or mole of organic matter.

This procedure for deriving stoichiometric coefficients is illustrated in this section using a universal composition of organic material. Different compositions of different classes of organic material will be introduced in the more general approach of parameterized elemental mass fractions in section 4.3.2. We will derive the stoichiometric coefficients for growth of algae with ammonium or nitrate as nitrogen source, respiration of algae and zooplankton, death of algae and zooplankton, and growth of zooplankton.

The five most important elements present in organic material are carbon (C), hydrogen (H), oxygen (O), nitrogen (N), and phosphorus (P). With consideration of these elements, primary production of algae consumes bicarbonate (HCO_3^-) (we refer here to the species that is most abundant at typical pH values; most algae will take up CO_2 which will then be replaced by $HCO_3^- + H^+ \rightarrow H_2O + CO_2$), ammonium ($NH_4^+$) or nitrate ($NO_3^-$), phosphate ($HPO_4^{2-}$), hydrogen ions ($H^+$) and water ($H_2O$) to produce organic material and dissolved oxygen (O_2). We will limit our discussion to these five elements in this section as this is sufficient to demonstrate the concept of stoichiometric calculations. The essential point for deriving stoichiometric coefficients for primary production by algae is the (average) composition of algal biomass. It has been shown that marine algal biomass can quite accurately be described by a composition according to the following chemical formula

$$\boxed{(CH_2O)_{106}(NH_3)_{16}(H_3PO_4)_1 = C_{106}H_{263}O_{110}N_{16}P} \tag{4.33}$$

(Redfield, 1958; Stumm and Morgan, 1981). This expression specifies typical elemental mass fractions of carbon, oxygen, hydrogen, nitrogen and phosphorus in organic matter, but should not be interpreted as describing a "molecule" of organic matter. Nevertheless, for conversion to dry mass of organic material, we need the total weight of a "mol" of the virtual organic substance (4.33). This mass is given as

$$\begin{aligned} m &= 106 \cdot 12 \ \frac{\text{gC}}{\text{“mol”}} + 263 \ \frac{\text{gH}}{\text{“mol”}} + 110 \cdot 16 \ \frac{\text{gO}}{\text{“mol”}} \\ &\quad +16 \cdot 14 \ \frac{\text{gN}}{\text{“mol”}} + 31 \ \frac{\text{gP}}{\text{“mol”}} \\ &= 3550 \ \frac{\text{gDM}}{\text{“mol”}} \quad . \end{aligned} \tag{4.34}$$

When considering all substances and organisms involved in a process, the stoichiometric coefficients can be derived from (i) the list of involved substances, (ii) the composition of

these substances, (iii) additional stoichiometric constraints, such as yields, if necessary. The derivation applies mass conservation of all elements and conservation of charge to provide the required equations to be solved for the unknown coefficients. A stringent discussion of how many additional constraints are required for a given process and given composition of involved substances will be given in section 4.3.3.

As an example, we demonstrate how to derive the stoichiometric coefficients for growth of algae with nitrate as nitrogen source. We start by writing this process in chemical notation with unknown stoichiometric coefficients a, b, c, d, e, and f as follows:

$$a\,\mathrm{HCO_3^-} + b\,\mathrm{NO_3^-} + c\,\mathrm{HPO_4^{2-}} + d\,\mathrm{H^+} + e\,\mathrm{H_2O} \rightarrow \mathrm{C_{106}H_{263}O_{110}N_{16}P} + f\,\mathrm{O_2} \quad .$$

The six constraints of conservation of C, O, H, N, P and charge lead to six constraining equations to determine these six parameters uniquely. First, conservation of C leads to

$$a \cdot 1 = 1 \cdot 106 \quad \rightarrow \quad a = 106 \quad ,$$

conservation of N to

$$b \cdot 1 = 1 \cdot 16 \quad \rightarrow \quad b = 16 \quad ,$$

and conservation of P to

$$c \cdot 1 = 1 \cdot 1 \quad \rightarrow \quad c = 1 \quad .$$

Using these solutions, conservation of H, O and charge lead to

$$\begin{aligned} &106 \cdot 1 + 1 \cdot 1 + d \cdot 1 + e \cdot 2 = 1 \cdot 263 \quad , \\ &106 \cdot 3 + 16 \cdot 3 + 1 \cdot 4 + e \cdot 1 = 1 \cdot 110 + f \cdot 2 \quad , \\ &106 \cdot (-1) + 16 \cdot (-1) + 1 \cdot (-2) + d \cdot (+1) = 0 \quad . \end{aligned}$$

The last equation then leads to

$$d = 124 \quad ,$$

the first then to

$$e = 16 \quad ,$$

and finally the second

$$f = 138 \quad .$$

This then results in the following equation for growth of algae with nitrate as the nitrogen source

$$\boxed{106\,\mathrm{HCO_3^-} + 16\,\mathrm{NO_3^-} + \mathrm{HPO_4^{2-}} + 124\,\mathrm{H^+} + 16\,\mathrm{H_2O} \rightarrow \mathrm{C_{106}H_{263}O_{110}N_{16}P} + 138\,\mathrm{O_2}} \tag{4.35}$$

Considering the "molar mass" according to equation (4.34), this implies the following stoichiometric coefficients for growth of algae with nitrate:

$$\begin{aligned}
\nu_{\mathrm{gro,ALG,NO_3^-\ HCO_3^-}} &= -\frac{106}{3550}\ \frac{\mathrm{molHCO_3^-}}{\mathrm{gDM}} \\
\nu_{\mathrm{gro,ALG,NO_3^-\ NO_3^-}} &= -\frac{16}{3550}\ \frac{\mathrm{molNO_3^-}}{\mathrm{gDM}} \\
\nu_{\mathrm{gro,ALG,NO_3^-\ HPO_4^{2-}}} &= -\frac{1}{3550}\ \frac{\mathrm{molHPO_4^{2-}}}{\mathrm{gDM}} \\
\nu_{\mathrm{gro,ALG,NO_3^-\ H^+}} &= -\frac{124}{3550}\ \frac{\mathrm{molH^+}}{\mathrm{gDM}} \\
\nu_{\mathrm{gro,ALG,NO_3^-\ H_2O}} &= -\frac{16}{3550}\ \frac{\mathrm{molH_2O}}{\mathrm{gDM}} \\
\nu_{\mathrm{gro,ALG,NO_3^-\ ALG}} &= 1\ \frac{\mathrm{gDM}}{\mathrm{gDM}} \\
\nu_{\mathrm{gro,ALG,NO_3^-\ O_2}} &= \frac{138}{3550}\ \frac{\mathrm{molO_2}}{\mathrm{gDM}} \quad .
\end{aligned} \tag{4.36}$$

Similarly, we obtain for growth of algae with ammonium as the nitrogen source

$$\boxed{106\,\mathrm{HCO_3^-} + 16\,\mathrm{NH_4^+} + \mathrm{HPO_4^{2-}} + 92\,\mathrm{H^+} \rightarrow \mathrm{C_{106}H_{263}O_{110}N_{16}P} + 106\,\mathrm{O_2}} \tag{4.37}$$

This implies the following stoichiometric coefficients for growth of algae with ammonium:

$$\begin{aligned}
\nu_{\mathrm{gro,ALG,NH_4^+\ HCO_3^-}} &= -\frac{106}{3550}\ \frac{\mathrm{molHCO_3^-}}{\mathrm{gDM}} \\
\nu_{\mathrm{gro,ALG,NH_4^+\ NH_4^+}} &= -\frac{16}{3550}\ \frac{\mathrm{molNH_4^+}}{\mathrm{gDM}} \\
\nu_{\mathrm{gro,ALG,NH_4^+\ HPO_4^{2-}}} &= -\frac{1}{3550}\ \frac{\mathrm{molHPO_4^{2-}}}{\mathrm{gDM}} \\
\nu_{\mathrm{gro,ALG,NH_4^+\ H^+}} &= -\frac{92}{3550}\ \frac{\mathrm{molH^+}}{\mathrm{gDM}} \\
\nu_{\mathrm{gro,ALG,NH_4^+\ H_2O}} &= 0 \\
\nu_{\mathrm{gro,ALG,NH_4^+\ ALG}} &= 1\ \frac{\mathrm{gDM}}{\mathrm{gDM}} \\
\nu_{\mathrm{gro,ALG,NH_4^+\ O_2}} &= \frac{106}{3550}\ \frac{\mathrm{molO_2}}{\mathrm{gDM}} \quad .
\end{aligned} \tag{4.38}$$

More details on primary production will be given in section 8.1.

Respiration is just the reverse process of this last process (4.37). This leads to the following expression for respiration of algal biomass

$$\boxed{\mathrm{C_{106}H_{263}O_{110}N_{16}P} + 106\,\mathrm{O_2} \rightarrow 106\,\mathrm{HCO_3^-} + 16\,\mathrm{NH_4^+} + \mathrm{HPO_4^{2-}} + 92\,\mathrm{H^+}} \tag{4.39}$$

The stoichiometric coefficients are then the negative values of those given by equation (4.38) for growth of algae with ammonium as the nitrogen source. The same equation applies to respiration of zooplankton.

As we assume in this section that all organisms and organic particles have the same composition, the death process is trivial from a stoichiometric point of view

$$\boxed{\mathrm{C_{106}H_{263}O_{110}N_{16}P} \rightarrow \mathrm{C_{106}H_{263}O_{110}N_{16}P}} \tag{4.40}$$

In this equation, the left hand side represents living algae, the right hand side dead organic particles (POM). The same equation applies to death of zooplankton.

We introduce two stoichiometric parameters for describing growth of zooplankton. The yield, Y_{ZOO}, defines the fraction of zooplankton dry mass built per dry mass of algae consumed, and the parameter f_{e} describes the fraction of dry mass of algae converted into dead organic particles due to sloppy feeding and excretion. We assume the remaining fraction of algal biomass f_{r} to be respired:

$$f_{\mathrm{r}} = 1 - Y_{\mathrm{ZOO}} - f_{\mathrm{e}} \tag{4.41}$$

When combining the negative stoichiometric coefficients for growth of algae from equation (4.38) with the fraction of algal biomass that is respired, renormalize it to the units of zooplankton by division by Y_{ZOO}, and add the mass balance of zooplankton and dead organic particles (POM) according to the stoichiometric parameters introduced above, we get the following stoichiometric coefficients for growth of zooplankton

$$\begin{aligned}
\nu_{\mathrm{gro,ZOO\ HCO_3^-}} &= \frac{f_{\mathrm{r}}}{Y_{\mathrm{ZOO}}}\,\frac{106}{3550}\,\frac{\mathrm{molHCO_3^-}}{\mathrm{gDM}} \\
\nu_{\mathrm{gro,ZOO\ NH_4^+}} &= \frac{f_{\mathrm{r}}}{Y_{\mathrm{ZOO}}}\,\frac{16}{3550}\,\frac{\mathrm{molNH_4^+}}{\mathrm{gDM}} \\
\nu_{\mathrm{gro,ZOO\ HPO_4^{2-}}} &= \frac{f_{\mathrm{r}}}{Y_{\mathrm{ZOO}}}\,\frac{1}{3550}\,\frac{\mathrm{molHPO_4^{2-}}}{\mathrm{gDM}} \\
\nu_{\mathrm{gro,ZOO\ O_2}} &= -\frac{f_{\mathrm{r}}}{Y_{\mathrm{ZOO}}}\,\frac{106}{3550}\,\frac{\mathrm{molO_2}}{\mathrm{gDM}} \\
\nu_{\mathrm{gro,ZOO\ H^+}} &= \frac{f_{\mathrm{r}}}{Y_{\mathrm{ZOO}}}\,\frac{92}{3550}\,\frac{\mathrm{molH^+}}{\mathrm{gDM}} \\
\nu_{\mathrm{gro,ZOO\ H_2O}} &= 0 \\
\nu_{\mathrm{gro,ZOO\ ALG}} &= -\frac{1}{Y_{\mathrm{ZOO}}}\,\frac{\mathrm{gDM}}{\mathrm{gDM}} \\
\nu_{\mathrm{gro,ZOO\ ZOO}} &= 1\,\frac{\mathrm{gDM}}{\mathrm{gDM}} \\
\nu_{\mathrm{gro,ZOO\ POM}} &= \frac{f_{\mathrm{e}}}{Y_{\mathrm{ZOO}}}\,\frac{\mathrm{gDM}}{\mathrm{gDM}} \quad .
\end{aligned} \tag{4.42}$$

Table 4.2 summarizes the stoichiometry of all of these processes in the form of a stoichiometric matrix that is part of the process table notation introduced in section 4.1.

Process	Substances / Organisms									
	NH_4^+	NO_3^-	HPO_4^{2-}	HCO_3^-	O_2	H^+	H_2O	ALG	ZOO	POM
	mol	mol	mol	mol	mol	mol	mol	gDM	gDM	gDM
Growth of ALG,NH_4^+	$-\frac{16}{3550}$		$-\frac{1}{3550}$	$-\frac{106}{3550}$	$\frac{106}{3550}$	$-\frac{92}{3550}$		1		
Growth of ALG,NO_3^-		$-\frac{16}{3550}$	$-\frac{1}{3550}$	$-\frac{106}{3550}$	$\frac{138}{3550}$	$-\frac{124}{3550}$	$-\frac{16}{3550}$	1		
Respiration of ALG	$\frac{16}{3550}$		$\frac{1}{3550}$	$\frac{106}{3550}$	$-\frac{106}{3550}$	$\frac{92}{3550}$		-1		
Death of ALG								-1		1
Growth of ZOO	$\frac{f_r}{Y_{ZOO}}\frac{16}{3550}$		$\frac{f_r}{Y_{ZOO}}\frac{1}{3550}$	$\frac{f_r}{Y_{ZOO}}\frac{106}{3550}$	$-\frac{f_r}{Y_{ZOO}}\frac{106}{3550}$	$\frac{f_r}{Y_{ZOO}}\frac{92}{3550}$		$-\frac{1}{Y_{ZOO}}$	1	$\frac{f_e}{Y_{ZOO}}$
Respiration of ZOO	$\frac{16}{3550}$		$\frac{1}{3550}$	$\frac{106}{3550}$	$-\frac{106}{3550}$	$\frac{92}{3550}$			-1	
Death of ZOO									-1	1

Table 4.2: Stoichiometry of growth of algae with ammonium or nitrate, growth of zooplankton, respiration of algae and zooplankton and death of algae and zooplankton. Note that the units of mol/gDM of all ratios of numbers are omitted to save space. They can be reconstructed by dividing the unit given in the third row of the column header by the unit of the substance or organism with a stoichiometric coefficient of unity.

4.3.2 Derivation of Stoichiometry from Parameterized Elemental Mass Fractions

The approach of deriving stoichiometric coefficients introduced in section 4.3.1 has the disadvantage that it depends on a fixed composition of organic material. As the composition of organic material depends on its type and on environmental conditions, it is useful to introduce composition parameters and derive stoichiometric coefficients as functions of these parameters. This makes it much easier to calculate stoichiometric coefficients for modified composition if necessary. In this section, we will derive such an approach. It is based on using elemental mass fractions of organic matter as model parameters.

We now introduce "elementary constituents" of which all substances or organisms are "composed". We write the expressions "constituents" and "composed" in quotation marks as they may represent chemical elements but, alternatively, any other conserved quantities, such as charge or chemical oxygen demand. We denote the "mass fraction" with which elementary constituent k contributes to the mass of substance j as α_{kj}. As before, the stoichiometric coefficient of process i with respect to substance j is denoted by ν_{ij}. As the process table introduced in section 4.1 (Table 4.1) already contains one column per substance, it can easily be extended by additional rows to contain the substance composition. This is illustrated in Table 4.3. As the stoichiometric coefficients ν_{ij} can

process	substances and/or organisms					rate
elem. const.	s_1	s_2	s_3	$\cdots$	s_{n_s}	
p_1	ν_{11}	ν_{12}	ν_{13}	$\cdots$	ν_{1n_s}	ρ_1
p_2	ν_{21}	ν_{22}	ν_{23}	$\cdots$	ν_{2n_s}	ρ_2
$\vdots$	$\vdots$	$\vdots$	$\vdots$	$\ddots$	$\vdots$	$\vdots$
p_{n_p}	ν_{n_p1}	ν_{n_p2}	ν_{n_p3}	$\cdots$	$\nu_{n_pn_s}$	ρ_{n_p}
e_1	α_{11}	α_{12}	α_{13}	$\cdots$	α_{1n_s}	
e_2	α_{21}	α_{22}	α_{23}	$\cdots$	α_{2n_s}	
$\vdots$	$\vdots$	$\vdots$	$\vdots$	$\ddots$	$\vdots$	
e_{n_e}	α_{n_p1}	α_{n_p2}	α_{n_p3}	$\cdots$	$\alpha_{n_en_s}$	

Table 4.3: The extended process table summarizes process stoichiometry, rates, and the composition of all substances and/or organisms. Here p_i is the name of process i, s_j is the name of the substance/organism j, e_k is the name of the elementary constituent k, $\nu_{i,j}$ is the stoichiometric coefficient of process i with respect to substance j, ρ_i is the transformation rate of process i, and $\alpha_{k,j}$ is the "content" of elementary constituent k in substance j.

be interpreted as the relative transformation rate of substance j in process i, the product $\nu_{ij}\alpha_{kj}$ is the relative transformation rate of the elementary constituent k contained in substance j. No net production or consumption of element k implies that the sum of all of these relative transformation rates of element k of a given process must be zero. If a process description includes all involved substances that contain the element k, mass conservation of element k in process i can therefore be formulated by the following equation

$$\boxed{\sum_j \nu_{ij}\alpha_{kj} = 0} \tag{4.43}$$

For given elemental composition of substances, the set of these equations corresponding to all considered elements constrains the stoichiometric coefficients of process i that are compatible with elemental mass conservation.

In this section, we will learn how to apply equation (4.43) together with stoichiometric parameters to determine process stoichiometry. We will do this by discussing two examples of increasing complexity. We will start with a simple process model for growth and respiration of algae that considers mass conservation of nitrogen and phosphorus in section 4.3.2.1. We will then extend this model to the consideration of the five most important elements C, H, O, N and P in section 4.3.2.2. This will lead to a model that is similar to the model described in the previous section, but with parameterized composition and different composition of different organisms and organic substances.

4.3.2.1 Growth and Respiration of Algae: Nutrient Balance

As a first example, we start with a model for growth and respiration of algae with consumption and release of ammonium and phosphate. We would like to calculate the stoichiometric coefficients of these processes based on nitrogen and phosphorus conservation according to equation (4.43). We introduce the mass fractions $\alpha_{\mathrm{N,ALG}}$ (gALG-N/gALG-DM) and $\alpha_{\mathrm{P,ALG}}$ (gALG-P/gALG-DM) of nitrogen and phosphorus in dry mass of algae as model parameters. Furthermore, we measure ammonium in nitrogen mass units ($\mathrm{gNH_4^+}$-N) and phosphate in phosphorus mass units ($\mathrm{gHPO_4^{2-}}$-P). This implies that their mass fractions of nitrogen and phosphorus are equal to unity: $\alpha_{\mathrm{N,NH_4^+}} = 1$, $\alpha_{\mathrm{P,HPO_4^{2-}}} = 1$. Obviously, $\alpha_{\mathrm{P,NH_4^+}} = \alpha_{\mathrm{N,HPO_4^{2-}}} = 0$. For the growth process of algae, we set the stoichiometric coefficient of algae to unity: $\nu_{\mathrm{gro,ALG,NH_4^+\ ALG}} = 1$. Applying the mass conservation equation (4.43) to nitrogen then leads to

$$\underbrace{\nu_{\mathrm{gro,ALG,NH_4^+\ NH_4^+}} \cdot 1}_{\mathrm{NH_4^+}} + \underbrace{\nu_{\mathrm{gro,ALG,NH_4^+\ HPO_4^{2-}}} \cdot 0}_{\mathrm{HPO_4^{2-}}} + \underbrace{1 \cdot \alpha_{\mathrm{N,ALG}}}_{\mathrm{ALG}} = 0 \quad .$$

From this equation we see that $\nu_{\mathrm{gro,ALG,NH_4^+\ NH_4^+}}$ must be equal to -$\alpha_{\mathrm{N,ALG}}$ and that we cannot learn anything about the stoichiometric coefficient of phosphate, $\nu_{\mathrm{gro,ALG,NH_4^+\ HPO_4^{2-}}}$. Similarly, from phosphorus conservation, we get the equation

$$\underbrace{\nu_{\mathrm{gro,ALG,NH_4^+\ NH_4^+}} \cdot 0}_{\mathrm{NH_4^+}} + \underbrace{\nu_{\mathrm{gro,ALG,NH_4^+\ HPO_4^{2-}}} \cdot 1}_{\mathrm{HPO_4^{2-}}} + \underbrace{1 \cdot \alpha_{\mathrm{P,ALG}}}_{\mathrm{ALG}} = 0 \quad .$$

From this equation we see that $\nu_{\mathrm{gro,ALG,NH_4^+\ HPO_4^{2-}}}$ must be equal to -$\alpha_{\mathrm{P,ALG}}$ and that we cannot learn anything about the stoichiometric coefficient of ammonium, $\nu_{\mathrm{gro,ALG,NH_4^+\ NH_4^+}}$. This results in the following stoichiometric coefficients for growth of algae

$$\begin{aligned} \nu_{\mathrm{gro,ALG,NH_4^+\ ALG}} &= 1 \\ \nu_{\mathrm{gro,ALG,NH_4^+\ NH_4^+}} &= -\alpha_{\mathrm{N,ALG}} \\ \nu_{\mathrm{gro,ALG,NH_4^+\ HPO_4^{2-}}} &= -\alpha_{\mathrm{P,ALG}} \end{aligned} \tag{4.44a}$$

when expressed as gALG-DM/gALG-DM, $\mathrm{gNH_4^+}$-N/gALG-DM, and $\mathrm{gHPO_4^{2-}}$-P/gALG-DM. This equation states that production of one gALG-DM (dry mass of algae) consumes

$\alpha_{\mathrm{N,ALG}}$ g$\mathrm{NH_4^+}$-N and $\alpha_{\mathrm{P,ALG}}$ g$\mathrm{HPO_4^{2-}}$-P. As this corresponds to the nitrogen and phosphorus content of dry mass of algae, this stoichiometry is obviously in agreement with the conservation of nitrogen and phosphorus. When expressing the stoichiometric coefficients in units of gALG-DM/gALG-DM, mol$\mathrm{NH_4^+}$/gALG-DM, and mol$\mathrm{HPO_4^{2-}}$/gALG-DM we get the following stoichiometric coefficients

$$\begin{aligned}
\nu_{\mathrm{gro,ALG,NH_4^+\ ALG}} &= 1 \\
\nu_{\mathrm{gro,ALG,NH_4^+\ NH_4^+}} &= -\frac{\alpha_{\mathrm{N,ALG}}}{14\mathrm{gN/mol}} \\
\nu_{\mathrm{gro,ALG,NH_4^+\ HPO_4^{2-}}} &= -\frac{\alpha_{\mathrm{P,ALG}}}{31\mathrm{gP/mol}} \quad .
\end{aligned} \tag{4.44b}$$

Respiration is the reverse process. These two processes are summarized in Table 4.4 for mass units of nitrogen and phosphorus and in Table 4.5 for molar units.

Process		Substances / Organisms		
		$\mathrm{NH_4^+}$	$\mathrm{HPO_4^{2-}}$	ALG
Element		gN	gP	gDM
Growth of ALG,$\mathrm{NH_4^+}$		$-\alpha_{\mathrm{N,ALG}}$	$-\alpha_{\mathrm{P,ALG}}$	1
Respiration of ALG		$\alpha_{\mathrm{N,ALG}}$	$\alpha_{\mathrm{P,ALG}}$	-1
N	gN	1		$\alpha_{\mathrm{N,ALG}}$
P	gP		1	$\alpha_{\mathrm{P,ALG}}$

Table 4.4: Stoichiometry and composition tables of the simple growth and respiration model of algae based on nitrogen and phosphorus conservation. This table uses nitrogen and phosphorus mass units for nutrients; see Table 4.5 for molar units.

Process		Substances / Organisms		
		$\mathrm{NH_4^+}$	$\mathrm{HPO_4^{2-}}$	ALG
Element		mol	mol	gDM
Growth of ALG,$\mathrm{NH_4^+}$		$-\frac{\alpha_{\mathrm{N,ALG}}}{14\mathrm{gN/mol}}$	$-\frac{\alpha_{\mathrm{P,ALG}}}{31\mathrm{gP/mol}}$	1
Respiration of ALG		$\frac{\alpha_{\mathrm{N,ALG}}}{14\mathrm{gN/mol}}$	$\frac{\alpha_{\mathrm{P,ALG}}}{31\mathrm{gP/mol}}$	-1
N	gN	14gN/mol		$\alpha_{\mathrm{N,ALG}}$
P	gP		31gP/mol	$\alpha_{\mathrm{P,ALG}}$

Table 4.5: Stoichiometry and composition table of the simple growth and respiration model of algae based on nitrogen and phosphorus conservation. This table uses molar units for nutrients; see Table 4.4 for nitrogen and phosphorus mass units.

4.3.2.2 Growth, Respiration and Death of Algae and Zooplankton: Consideration of the Elements C, H, O, N and P

In this example, we extend the elemental mass fraction approach to the inclusion of all five elements C, H, O, N and P (Reichert et al., 2001) to generalize the model shown in Table 4.2 to the use of parameterized mass fractions of elements in organic material. For each organic compound, j, we introduce the five mass fractions $\alpha_{C,j}$, $\alpha_{H,j}$, $\alpha_{O,j}$, $\alpha_{N,j}$, and $\alpha_{P,j}$ and assume that they sum to unity:

$$\boxed{\alpha_{C,j} + \alpha_{H,j} + \alpha_{O,j} + \alpha_{N,j} + \alpha_{P,j} = 1} \tag{4.45}$$

This is equivalent to a chemical formula of organic matter of type j of

$$\boxed{C_{\alpha_{C,j}/12} H_{\alpha_{H,j}} O_{\alpha_{O,j}/16} N_{\alpha_{N,j}/14} P_{\alpha_{P,j}/31}} \tag{4.46}$$

which generalizes the Redfield composition given by equation (4.33). Equation (4.46) describes one g of dry organic matter. Conversely, the Redfield composition given by equation (4.33) can be expressed by mass fractions as follows

$$\begin{aligned}
\alpha_{C,ALG}^{Redfield} &= \frac{106 \cdot 12}{3550} \frac{gC}{gDM} &&\approx 0.36 \frac{gC}{gDM} \\
\alpha_{H,ALG}^{Redfield} &= \frac{263}{3550} \frac{gH}{gDM} &&\approx 0.07 \frac{gH}{gDM} \\
\alpha_{O,ALG}^{Redfield} &= \frac{110 \cdot 16}{3550} \frac{gO}{gDM} &&\approx 0.50 \frac{gO}{gDM} \\
\alpha_{N,ALG}^{Redfield} &= \frac{16 \cdot 14}{3550} \frac{gN}{gDM} &&\approx 0.06 \frac{gN}{gDM} \\
\alpha_{P,ALG}^{Redfield} &= \frac{1 \cdot 31}{3550} \frac{gP}{gDM} &&\approx 0.01 \frac{gP}{gDM} \quad .
\end{aligned} \tag{4.47}$$

Note that these mass fractions are realistic for marine plankton. In freshwater, this is often a reasonable approximation to the composition of algae and zooplankton as long as primary production is not severely limited by phosphate. If primary production is severely limited by phosphate, the phosphate mass fraction of algal biomass can be considerably smaller (Hupfer et al., 1995).

Derivation of the stoichiometric coefficients can be done by accounting for the mass fractions with the aid of equation (4.43) as it was done in section 4.3.2.1 for the elements N and P. Equivalently, we can count atoms as described in section 4.3.1 with the difference that the given numbers 106, 263, 110, 16 and 1 in $C_{106}H_{263}O_{110}N_{16}P$ are replaced by the parameterized numbers $\alpha_{C,j}/12$, $\alpha_{H,j}$, $\alpha_{O,j}/16$, $\alpha_{N,j}/14$, and $\alpha_{P,j}/31$ (which are not integers).

We will again demonstrate the derivation for the process of growth of algae with nitrate as the nitrogen source. The derivation follows the same steps as the derivation of equation (4.35) on page 48. We start by writing this process in chemical notation with unknown stoichiometric coefficients a, b, c, d, e, and f as follows:

$$\begin{aligned}
a\,HCO_3^- + b\,NO_3^- + c\,HPO_4^{2-} + d\,H^+ + e\,H_2O \\
\rightarrow C_{\alpha_{C,ALG}/12} H_{\alpha_{H,ALG}} O_{\alpha_{O,ALG}/16} N_{\alpha_{N,ALG}/14} P_{\alpha_{P,ALG}/31} + f\,O_2 \quad .
\end{aligned}$$

The six constraints for the conservation of C, O, H, N, P and charge lead to six constraining equations to determine these six parameters uniquely. First, conservation of C leads to

$$a = \frac{\alpha_{\mathrm{C,ALG}}}{12} \quad ,$$

conservation of N to

$$b = \frac{\alpha_{\mathrm{N,ALG}}}{14} \quad ,$$

and conservation of P to

$$c = \frac{\alpha_{\mathrm{P,ALG}}}{31} \quad .$$

Using these solutions, conservation of H, O and charge lead to

$$\begin{aligned}
&\frac{\alpha_{\mathrm{C,ALG}}}{12} \cdot 1 + \frac{\alpha_{\mathrm{P,ALG}}}{31} \cdot 1 + d \cdot 1 + e \cdot 2 = 1 \cdot \alpha_{\mathrm{H,ALG}} \\
&\frac{\alpha_{\mathrm{C,ALG}}}{12} \cdot 3 + \frac{\alpha_{\mathrm{N,ALG}}}{14} \cdot 3 + \frac{\alpha_{\mathrm{P,ALG}}}{31} \cdot 4 + e \cdot 1 = 1 \cdot \frac{\alpha_{\mathrm{O,ALG}}}{16} + f \cdot 2 \\
&\frac{\alpha_{\mathrm{C,ALG}}}{12} \cdot (-1) + \frac{\alpha_{\mathrm{N,ALG}}}{14} \cdot (-1) + \frac{\alpha_{\mathrm{P,ALG}}}{31} \cdot (-2) + d \cdot (+1) = 0 \quad .
\end{aligned}$$

The last equation then leads to

$$d = \frac{\alpha_{\mathrm{C,ALG}}}{12} + \frac{\alpha_{\mathrm{N,ALG}}}{14} + \frac{2\,\alpha_{\mathrm{P,ALG}}}{31} \quad ,$$

the first then to

$$e = \frac{\alpha_{\mathrm{H,ALG}}}{2} - \frac{\alpha_{\mathrm{C,ALG}}}{12} - \frac{\alpha_{\mathrm{N,ALG}}}{28} - \frac{3\,\alpha_{\mathrm{P,ALG}}}{62} \quad ,$$

and finally the second

$$f = \frac{\alpha_{\mathrm{C,ALG}}}{12} + \frac{\alpha_{\mathrm{H,ALG}}}{4} - \frac{\alpha_{\mathrm{O,ALG}}}{32} + \frac{5\,\alpha_{\mathrm{N,ALG}}}{56} + \frac{5\,\alpha_{\mathrm{P,ALG}}}{124} \quad .$$

This then results in

$$\begin{aligned}
&\frac{\alpha_{\mathrm{C,ALG}}}{12}\,\mathrm{HCO_3^-} + \frac{\alpha_{\mathrm{N,ALG}}}{14}\,\mathrm{NO_3^-} + \frac{\alpha_{\mathrm{P,ALG}}}{31}\,\mathrm{HPO_4^{2-}} \\
&\qquad + \left(\frac{\alpha_{\mathrm{C,ALG}}}{12} + \frac{\alpha_{\mathrm{N,ALG}}}{14} + \frac{2\,\alpha_{\mathrm{P,ALG}}}{31}\right)\mathrm{H^+} \\
&\qquad + \left(\frac{\alpha_{\mathrm{H,ALG}}}{2} - \frac{\alpha_{\mathrm{C,ALG}}}{12} - \frac{\alpha_{\mathrm{N,ALG}}}{28} - \frac{3\,\alpha_{\mathrm{P,ALG}}}{62}\right)\mathrm{H_2O} \\
&\rightarrow \mathrm{C}_{\alpha_{\mathrm{C,ALG}}/12}\mathrm{H}_{\alpha_{\mathrm{H,ALG}}}\mathrm{O}_{\alpha_{\mathrm{O,ALG}}/16}\mathrm{N}_{\alpha_{\mathrm{N,ALG}}/14}\mathrm{P}_{\alpha_{\mathrm{P,ALG}}/31} \\
&\qquad + \left(\frac{\alpha_{\mathrm{C,ALG}}}{12} + \frac{\alpha_{\mathrm{H,ALG}}}{4} - \frac{\alpha_{\mathrm{O,ALG}}}{32} + \frac{5\,\alpha_{\mathrm{N,ALG}}}{56} + \frac{5\,\alpha_{\mathrm{P,ALG}}}{124}\right)\mathrm{O_2}
\end{aligned} \tag{4.48}$$

This implies the following stoichiometric coefficients for algal growth with nitrate:

$$\begin{aligned}
\nu_{\mathrm{gro,ALG,NO_3^-\,HCO_3^-}} &= -\frac{\alpha_{\mathrm{C,ALG}}}{12\mathrm{gC/mol}} \\
\nu_{\mathrm{gro,ALG,NO_3^-\,NO_3^-}} &= -\frac{\alpha_{\mathrm{N,ALG}}}{14\mathrm{gN/mol}} \\
\nu_{\mathrm{gro,ALG,NO_3^-\,HPO_4^{2-}}} &= -\frac{\alpha_{\mathrm{P,ALG}}}{31\mathrm{gP/mol}} \\
\nu_{\mathrm{gro,ALG,NO_3^-\,H^+}} &= -\frac{\alpha_{\mathrm{C,ALG}}}{12\mathrm{gC/mol}} - \frac{\alpha_{\mathrm{N,ALG}}}{14\mathrm{gN/mol}} - \frac{2\,\alpha_{\mathrm{P,ALG}}}{31\mathrm{gP/mol}} \\
\nu_{\mathrm{gro,ALG,NO_3^-\,H_2O}} &= -\frac{\alpha_{\mathrm{H,ALG}}}{2\mathrm{gH/mol}} + \frac{\alpha_{\mathrm{C,ALG}}}{12\mathrm{gC/mol}} + \frac{\alpha_{\mathrm{N,ALG}}}{28\mathrm{gN/mol}} + \frac{3\,\alpha_{\mathrm{P,ALG}i}}{62\mathrm{gP/mol}} \\
\nu_{\mathrm{gro,ALG,NO_3^-\,ALG}} &= 1 \\
\nu_{\mathrm{gro,ALG,NO_3^-\,O_2}} &= \frac{\alpha_{\mathrm{C,ALG}}}{12\mathrm{gC/mol}} + \frac{\alpha_{\mathrm{H,ALG}}}{4\mathrm{gH/mol}} - \frac{\alpha_{\mathrm{O,ALG}}}{32\mathrm{gO/mol}} + \frac{5\,\alpha_{\mathrm{N,ALG}}}{56\mathrm{gN/mol}} + \frac{5\,\alpha_{\mathrm{P,ALG}}}{124\mathrm{gP/mol}}
\end{aligned} \tag{4.49}$$

Similarly we get

$$\begin{aligned}
&\frac{\alpha_{\mathrm{C,ALG}}}{12}\,\mathrm{HCO_3^-} + \frac{\alpha_{\mathrm{N,ALG}}}{14}\,\mathrm{NH_4^+} + \frac{\alpha_{\mathrm{P,ALG}}}{31}\,\mathrm{HPO_4^{2-}} \\
&\qquad + \left(\frac{\alpha_{\mathrm{C,ALG}}}{12} - \frac{\alpha_{\mathrm{N,ALG}}}{14} + \frac{2\,\alpha_{\mathrm{P,ALG}}}{31}\right)\mathrm{H^+} \\
&\qquad + \left(\frac{\alpha_{\mathrm{H,ALG}}}{2} - \frac{\alpha_{\mathrm{C,ALG}}}{12} - \frac{3\,\alpha_{\mathrm{N,ALG}}}{28} - \frac{3\,\alpha_{\mathrm{P,ALG}}}{62}\right)\mathrm{H_2O} \\
&\rightarrow \mathrm{C}_{\alpha_{\mathrm{C,ALG}}/12}\mathrm{H}_{\alpha_{\mathrm{H,ALG}}}\mathrm{O}_{\alpha_{\mathrm{O,ALG}}/16}\mathrm{N}_{\alpha_{\mathrm{N,ALG}}/14}\mathrm{P}_{\alpha_{\mathrm{P,ALG}}/31} \\
&\qquad + \left(\frac{\alpha_{\mathrm{C,ALG}}}{12} + \frac{\alpha_{\mathrm{H,ALG}}}{4} - \frac{\alpha_{\mathrm{O,ALG}}}{32} - \frac{3\,\alpha_{\mathrm{N,ALG}}}{56} + \frac{5\,\alpha_{\mathrm{P,ALG}}}{124}\right)\mathrm{O_2}
\end{aligned} \tag{4.50}$$

for algal growth with ammonium as the nitrogen source. This implies the following stoichiometric coefficients for algal growth with ammonium:

$$\begin{aligned}
\nu_{\mathrm{gro,ALG,NH_4^+\,HCO_3^-}} &= -\frac{\alpha_{\mathrm{C,ALG}}}{12\mathrm{gC/mol}} \\
\nu_{\mathrm{gro,ALG,NH_4^+\,NH_4^+}} &= -\frac{\alpha_{\mathrm{N,ALG}}}{14\mathrm{gN/mol}} \\
\nu_{\mathrm{gro,ALG,NH_4^+\,HPO_4^{2-}}} &= -\frac{\alpha_{\mathrm{P,ALG}}}{31\mathrm{gP/mol}} \\
\nu_{\mathrm{gro,ALG,NH_4^+\,H^+}} &= -\frac{\alpha_{\mathrm{C,ALG}i}}{12\mathrm{gC/mol}} + \frac{\alpha_{\mathrm{N,ALG}}}{14\mathrm{gN/mol}} - \frac{2\,\alpha_{\mathrm{P,ALG}}}{31\mathrm{gP/mol}} \\
\nu_{\mathrm{gro,ALG,NH_4^+\,H_2O}} &= -\frac{\alpha_{\mathrm{H,ALG}}}{2\mathrm{gH/mol}} + \frac{\alpha_{\mathrm{C,ALG}}}{12\mathrm{gC/mol}} + \frac{3\,\alpha_{\mathrm{N,ALG}}}{28\mathrm{gN/mol}} + \frac{3\,\alpha_{\mathrm{P,ALG}}}{62\mathrm{gP/mol}} \\
\nu_{\mathrm{gro,ALG,NH_4^+\,ALG}} &= 1\,\frac{\mathrm{g\ DM}}{\mathrm{g\ DM}} \\
\nu_{\mathrm{gro,ALG,NH_4^+\,O_2}} &= \frac{\alpha_{\mathrm{C,ALG}}}{12\mathrm{gC/mol}} + \frac{\alpha_{\mathrm{H,ALG}}}{4\mathrm{gH/mol}} - \frac{\alpha_{\mathrm{O,ALG}}}{32\mathrm{gO/mol}} - \frac{3\,\alpha_{\mathrm{N,ALG}}}{56\mathrm{gN/mol}} + \frac{5\,\alpha_{\mathrm{P,ALG}}}{124\mathrm{gP/mol}}
\end{aligned}$$

(4.51)

These process stoichiometries are summarized in the first two rows of the Tables 4.6 and 4.7. These Tables generalize Table 4.2 to parameterized elemental mass fractions that may be different from one organism or organic substance to the other.

Respiration is the reverse process to primary production with ammonium as the nitrogen source. The stoichiometries of the respiration processes of algae and zooplankton are given in the rows 3 and 6 of the Tables 4.6 and 4.7.

The death process as formulated by equation (4.40) was very simple as we assumed the composition of all organisms and organic particles to be the same. In this section, we allow the composition of different organism and organic particles to be different. If the composition of organisms is different, we could divide organic particles into classes of particles of different composition. The death process could then still be kept simple as a transfer of a living organism to a dead particle of the same composition. As it is often inconvenient to have many classes of particles of different composition, we may choose to assign an average composition to a single class of organic particles. Unfortunately, this makes it impossible to keep all elemental mass balances correct if we transfer a living organism to a dead particle without uptake or release of elements or compounds. Because organic particles will finally be mineralized, it seems meaningful to introduce a "yield", Y_{death}, for the death process that determines the fraction of the organism that becomes a dead particle (of different composition) and to assume that the remaining part of the organism will be mineralized. This "yield" should be chosen as large as possible without leading to the need for uptake of nutrients or oxygen (otherwise organisms could only die in the presence of nutrients or oxygen). This leads to stoichiometric coefficients of -1 for the organism and Y_{death} for dead particles. The six stoichiometric coefficients for the remaining compounds involved in the mineralization process (NH_4^+, HPO_4^{2-}, O_2, HCO_3^-, H^+, H_2O) can then be derived from the conservation laws of C, H, O, N, P and charge as this was demonstrated extensively for the algal growth processes on the preceding pages. The stoichiometries of the death processes of algae and zooplankton are summarized in the rows 4 and 7 of the Tables 4.6 and 4.7.

Finally, the growth process of zooplankton is a straightforward generalization of the process given in Tables 4.4 and 4.5. The stoichiometry of this process is given in row 5 of the Tables 4.6 and 4.7.

This explains the full stoichiomtric matrix shown in Tables 4.6 and 4.7. Note that we omit the more complicated expressions for some of the stoichiometric coefficients.

Process		Substances / Organisms			
		NH_4^+	NO_3^-	HPO_4^{2-}	O_2
Element		mol	mol	mol	mol
Growth of ALG,NH_4^+		$-\frac{\alpha_{N,ALG}}{14gN/mol}$		$-\frac{\alpha_{P,ALG}}{31gP/mol}$	$\frac{\alpha_{C,ALG}}{12gC/mol}+\frac{\alpha_{H,ALG}}{4gH/mol}-\frac{\alpha_{O,ALG}}{32gO/mol}-\frac{3\,\alpha_{N,ALG}}{56gN/mol}+\frac{5\,\alpha_{P,ALG}}{124gP/mol}$
Growth of ALG,NO_3^-			$-\frac{\alpha_{N,ALG}}{14gN/mol}$	$-\frac{\alpha_{P,ALG}}{31gP/mol}$	$\frac{\alpha_{C,ALG}}{12gC/mol}+\frac{\alpha_{H,ALG}}{4gH/mol}-\frac{\alpha_{O,ALG}}{32gO/mol}+\frac{5\,\alpha_{N,ALG}}{56gN/mol}+\frac{5\,\alpha_{P,ALG}}{124gP/mol}$
Respiration of ALG		$\frac{\alpha_{N,ALG}}{14gN/mol}$		$\frac{\alpha_{P,ALG}}{31gP/mol}$	$-\frac{\alpha_{C,ALG}}{12gC/mol}-\frac{\alpha_{H,ALG}}{4gH/mol}+\frac{\alpha_{O,ALG}}{32gO/mol}+\frac{3\,\alpha_{N,ALG}}{56gN/mol}-\frac{5\,\alpha_{P,ALG}}{124gP/mol}$
Death of ALG		$\frac{\alpha_{N,ALG}-Y_{ALG,death}\alpha_{N,POM}}{14gN/mol}$		$\frac{\alpha_{P,ALG}-Y_{ALG,death}\alpha_{P,POM}}{31gP/mol}$	νdeath, ALG O2
Growth of ZOO		$\frac{\frac{\alpha_{N,ALG}}{Y_{ZOO}}-\frac{f_e\alpha_{N,POM}}{Y_{ZOO}}-\alpha_{N,ZOO}}{14gN/mol}$		$\frac{\frac{\alpha_{P,ALG}}{Y_{ZOO}}-\frac{f_e\alpha_{P,POM}}{Y_{ZOO}}-\alpha_{P,ZOO}}{31gP/mol}$	νgro, ZOO O2
Respiration of ZOO		$\frac{\alpha_{N,ZOO}}{14gN/mol}$		$\frac{\alpha_{P,ZOO}}{31gP/mol}$	$-\frac{\alpha_{C,ZOO}}{12gC/mol}-\frac{\alpha_{H,ZOO}}{4gH/mol}+\frac{\alpha_{O,ZOO}}{32gO/mol}+\frac{3\,\alpha_{N,ZOO}}{56gN/mol}-\frac{5\,\alpha_{P,ZOO}}{124gP/mol}$
Death of ZOO		$\frac{\alpha_{N,ZOO}-Y_{ZOO,death}\alpha_{N,POM}}{14gN/mol}$		$\frac{\alpha_{P,ZOO}-Y_{ZOO,death}\alpha_{P,POM}}{31gP/mol}$	νdeath, ZOO O2
C	gC				
H	gH	4gH/mol		1gH/mol	
O	gO		48gO/mol	64gO/mol	32gO/mol
N	gN	14gN/mol	14gN/mol		
P	gP			31gP/mol	
charge	chu	1chu/mol	-1chu/mol	-2chu/mol	

Table 4.6: Process stoichiometry of the extended model with parameterized nitrogen and phosphorus mass fractions of organisms and organic particles (to be continued in Table 4.7). This table is expressed in molar units for inorganic compounds.

Process		Substances / Organisms					
		HCO_3^-	H^+	H_2O	ALG	ZOO	POM
Element		mol	mol	mol	gDM	gDM	gDM
Growth of ALG,NH_4^+		$-\frac{\alpha_{C,ALG}}{12gC/mol}$	$\frac{\alpha_{C,ALG}}{12gC/mol} - \frac{\alpha_{N,ALG}}{14gN/mol} + \frac{2\,\alpha_P}{31gP/mol}$	$\frac{\alpha_{H,ALG}}{2gH/mol} - \frac{\alpha_{C,ALG}}{12gC/mol} - \frac{3\,\alpha_{N,ALG}}{28gN/mol} - \frac{3\,\alpha_{P,ALG}}{62gP/mol}$	1		
Growth of ALG,NO_3^-		$-\frac{\alpha_{C,ALG}}{12gC/mol}$	$\frac{\alpha_{C,ALG}}{12gC/mol} + \frac{\alpha_{N,ALG}}{14gN/mol} + \frac{2\,\alpha_{P,ALG}}{31gP/mol}$	$\frac{\alpha_{H,ALG}}{2gH/mol} - \frac{\alpha_{C,ALG}}{12gC/mol} - \frac{\alpha_{N,ALG}}{28gN/mol} - \frac{3\,\alpha_{P,ALG}}{62gP/mol}$	1		
Respiration of ALG		$\frac{\alpha_{C,ALG}}{12gC/mol}$	$-\frac{\alpha_{C,ALG}}{12gC/mol} + \frac{\alpha_{N,ALG}}{14gN/mol} - \frac{2\,\alpha_{P,ALG}}{31gP/mol}$	$-\frac{\alpha_{H,ALG}}{2gH/mol} + \frac{\alpha_{C,ALG}}{12gC/mol} + \frac{3\,\alpha_{N,ALG}}{28gN/mol} + \frac{3\,\alpha_{P,ALG}}{62gP/mol}$	-1		
Death of ALG		$\frac{\alpha_{C,ALG} - Y_{ALG,death}\alpha_{C,POM}}{12gC/mol}$	νdeath, ALG H	νdeath, ALG H2O	-1		$Y_{ALG,death}$
Growth of ZOO		$\frac{\frac{\alpha_{C,ALG}}{Y_{ZOO}} - \frac{f_e\alpha_{C,POM}}{Y_{ZOO}} - \alpha_{C,ZOO}}{12gC/mol}$	νgro, ZOO H	νgro, ZOO H2O	$-\frac{1}{Y_{ZOO}}$	1	$\frac{f_e}{Y_{ZOO}}$
Respiration of ZOO		$\frac{\alpha_{C,ZOO}}{12gC/mol}$	$-\frac{\alpha_{C,ZOO}}{12gC/mol} + \frac{\alpha_{N,ZOO}}{14gN/mol} - \frac{2\,\alpha_{P,ZOO}}{31gP/mol}$	$-\frac{\alpha_{H,ZOO}}{2gH/mol} + \frac{\alpha_{C,ZOO}}{12gC/mol} + \frac{3\,\alpha_{N,ZOO}}{28gN/mol} + \frac{3\,\alpha_{P,ZOO}}{62gP/mol}$		-1	
Death of ZOO		$\frac{\alpha_{C,ZOO} - Y_{ZOO,death}\alpha_{C,POM}}{12gC/mol}$	νdeath, ZOO H	νdeath, ZOO H2O		-1	$Y_{ZOO,death}$
C	gC	12gC/mol			$\alpha_{C,ALG}$	$\alpha_{C,ZOO}$	$\alpha_{C,POM}$
H	gH	1gH/mol	1gH/mol	2gH/mol	$\alpha_{H,ALG}$	$\alpha_{H,ZOO}$	$\alpha_{H,POM}$
O	gO	48gO/mol		16gO/mol	$\alpha_{O,ALG}$	$\alpha_{O,ZOO}$	$\alpha_{O,POM}$
N	gN				$\alpha_{N,ALG}$	$\alpha_{N,ZOO}$	$\alpha_{N,POM}$
P	gP				$\alpha_{P,ALG}$	$\alpha_{P,ZOO}$	$\alpha_{P,POM}$
charge	chu	-1chu/mol	1chu/mol				

Table 4.7: Process stoichiometry of the extended model with parameterized nitrogen and phosphorus mass fractions of organisms and organic particles (continuation from Table 4.6). This table is expressed in molar units for inorganic compounds.

4.3.3 General Analysis and Solution of Stoichiometric Equations

The approach outlined in the previous section offers promising opportunities for a flexible description of process stoichiometry based on elemental composition of involved substances. This is particularly true, if the investigated processes and the considered substances in a model are not subject to modification. In a research context, when model modifications may be important, this approach is troublesome to apply, as the stoichiometric equations must be solved again after each modification of considered substances or elements and for new processes incorporated into the model. For this reason, it is interesting to do one further step of abstraction and provide a theoretical framework for generally solving stoichiometric equations. This framework allows the calculation of the number of additional stoichiometric constraints necessary to make a process unique and to calculate the stoichiometric coefficients for a process characterized by the set of involved substances, their composition and the required additional stoichiometric constraints (Reichert and Schuwirth, 2010).

In section 4.3.3.1 we will outline a six step procedure for the general derivation of process stoichiometries. In section 4.3.3.2 we will analyse and mathematically formulate the constraints on stoichiometric coefficients, before we provide the mathematical framework for their analysis in section 4.3.3.3. In section 4.3.3.4 we demonstrate the mathematics with the simple example discussed in section 4.3.2.1 that allows us to solve the equations analytically. Finally, in section 4.3.3.5 we will illustrate the six step procedure outlined in section 4.3.3.1 by numerically solving the governing equations of a more complex example. Chapter 15 in the appendix describes the R functions used to solve this example. These functions can be used to perform all calculations discussed in this section numerically for a transformation process system of any size.

4.3.3.1 Overview of General Procedure

To calculate the stoichiometric coefficients for a given system consisting of different substances and/or organism groups (state variables) affected by a set of processes, we propose the following procedure. First all substances/organisms which are required in addition to the modelled substances/organisms to close the mass balances have to be identified and added to the substances/organisms list. This step is often necessary as substances that are not of primary interest are not included in the model as state variables. They still do not have to be included as state variables, but they must be considered for applying conservation laws to derive stoichiometric coefficients. Examples for such substances are water and potentially H^+ ions that do not need to be included as state variables in aquatic systems (H^+ ions need to be included if pH is to be modelled (Reichert, 2001)) but are important for hydrogen and oxygen mass balances, or N_2 that is produced during denitrification and is often not included as a model state variable as it escapes the system without further interaction. Then the "elementary constituents" (e.g. chemical elements and charge) for which conservation laws are to be be applied must be identified and the composition of all involved substances/organisms with respect to these "elementary constituents" has to be defined. To calculate the stoichiometric coefficients for each individual process we then propose the following 6 step procedure (Reichert and Schuwirth, 2010):

Step 1: Select the substances/organisms involved in the process.
Not all substances/organisms are involved in all processes. Identifying those involved in the particular process is important to more strongly constrain the stoichiometric coefficients.

The signs of the corresponding stoichiometric coefficients should also be determined here based on the expected consumption/production pattern of the process (see also step 6). The selection of the involved substances/organisms and their signs must be based on chemical and/or biological knowledge about the process.

Step 2: Determine the number of additional constraints that are required to calculate the stoichiometric coefficients.
It is now a mathematical problem to determine how many constraints are required in addition to these imposed by conservation laws for "elementary constituents" to make the stoichiometry of the process unique. Those techniques will be described in sections 4.3.3.2 and 4.3.3.3, their implementation in the appendix (chapter 15) and examples will illustrate the application of these techniques in section 4.3.3.5. An example of such an additional constraint is a yield coefficient that determines the fraction of organic matter increase of a predator per unit of consumed prey.

Step 3: Define additional stoichiometric constraints if step 2 reveals that they are needed.
Specific process knowledge is required to define such additional stoichiometric constraints. In the example mentioned in step 2, the yield coefficient cannot be derived from conservation laws and must be specified based on empirical evidence or detailed process knowledge.

Step 4: Choose one coefficient and set it to a specific value.
As mentioned in section 4.1, the process stoichiometry is only defined up to an arbitrary factor. The choice is thus arbitrary, but it must be considered when specifying the process rate. Usually, one of the stoichiometric coefficients is set to plus or minus unity; the process rate is then plus or minus the transformation rate of the corresponding substance or organism by the process under consideration.

Step 5: Calculate the stoichiometric coefficients of the process.
Calculation of stoichiometric coefficients becomes now a purely mathematical problem described conceptually in sections 4.3.3.2 and 4.3.3.3, its implementation in the appendix (chapter 15) and its application to two examples in section 4.3.3.5.

Step 6: Check signs of the calculated stoichiometric coefficients.
The procedure outlined above guarantees exact fulfilment of all considered conservation laws by the process under consideration. Nevertheless, the specification of the compositions of the involved substances and of the additional stoichiometric constraints may lead to a process stoichiometry in which consumption and production patterns of substances do not correspond to the real process to be described by the model (see step 1). For this reason, this check is important. If it fails, composition parameters and/or additional stoichiometric constraints may have to be adapted (see also discussion in section 4.3.3.5).

Mathematical formulation and solution of the two steps 2 and 5 will be discussed in the following two sections.

4.3.3.2 Constraints on Stoichiometric Conditions

General Conservation Constraints

An important way of getting information about stoichiometric coefficients is to make assumptions about the composition of transformed substances and to apply conservation laws of "elementary constituents" to constrain or even derive the stoichiometric coefficients. This can only be done if all substances affected by the process are considered (all

substances have to be considered for deriving consistent stoichiometric coefficients; some of these substances may still be omitted for simulation). When dealing with substance composition, it is easiest to think of composing "elements" and their conserved "masses", although the formalism applies to any property for which a rigorous conservation law can be formulated (such as chemical elements, electrical charge, or chemical oxygen demand). This is the reason why "elementary constituents" is written in quotation marks.

For each substance, its composition can be characterized by a set of "masses" of all "elementary constituents" contributing to a unit mass of the substance. To guarantee consistency of the description, an "elementary constituent" must be quantified by the same unit across different substances. However, the units for the different "elementary constituents" can be different. Also the units of the different substances can be different. The compositions of all substances can be summarized in the composition matrix

$$\boldsymbol{\alpha} = \overbrace{\begin{pmatrix} \alpha_{11} & \alpha_{12} & \alpha_{13} & \cdots & \alpha_{1n_\mathrm{s}} \\ \alpha_{21} & \alpha_{22} & \alpha_{23} & \cdots & \alpha_{2n_\mathrm{s}} \\ \vdots & \vdots & \vdots & \ddots & \vdots \\ \alpha_{n_\mathrm{e}1} & \alpha_{n_\mathrm{e}2} & \alpha_{n_\mathrm{e}3} & \cdots & \alpha_{n_\mathrm{e}n_\mathrm{s}} \end{pmatrix}}^{\text{substances } \mathrm{s}_1, ..., \mathrm{s}_{n_\mathrm{s}}} \left.\begin{matrix} \\ \\ \\ \\ \end{matrix}\right\} \begin{matrix} \text{"elementary} \\ \text{constituents"} \\ \mathrm{e}_1, ..., \mathrm{e}_{n_\mathrm{e}} \end{matrix} \tag{4.52}$$

Here, α_{kj} denotes the "mass" of the "elementary constituent" k contributing to a unit mass of the substance j.

For a given process i, the stoichiometric coefficients, ν_{ij}, for different substances j, can be interpreted as relative conversion rates of different substances j by the process. Therefore, the products $\nu_{ij}\,\alpha_{kj}$ are the corresponding relative transformation rates of the "elementary constituent" k contained in the substances j. As it is assumed that the "mass" of the "elementary constituent" k is conserved and we assume that all substances affected by the process are included in the list of considered substances, we get the following constraints imposed by the conservation laws (4.43)

$$\sum_{j=1}^{n_\mathrm{s}} \nu_{ij}\,\alpha_{kj} = 0 \qquad \text{for all } i \text{ (processes) and } k \text{ ("elementary constituents")} \tag{4.53}$$

(Gujer and Larsen, 1995; Gujer et al., 1995; Henze et al., 1995; Gujer et al., 1999; Henze et al., 2000).

If the stoichiometric coefficients are also aggregated in a matrix (4.3)

$$\boldsymbol{\nu} = \overbrace{\begin{pmatrix} \nu_{11} & \nu_{12} & \nu_{13} & \cdots & \nu_{1n_\mathrm{s}} \\ \nu_{21} & \nu_{22} & \nu_{23} & \cdots & \nu_{2n_\mathrm{s}} \\ \vdots & \vdots & \vdots & \ddots & \vdots \\ \nu_{n_\mathrm{p}1} & \nu_{n_\mathrm{p}2} & \nu_{n_\mathrm{p}3} & \cdots & \nu_{n_\mathrm{p}n_\mathrm{s}} \end{pmatrix}}^{\text{substances } \mathrm{s}_1, ..., \mathrm{s}_{n_\mathrm{s}}} \left.\begin{matrix} \\ \\ \\ \\ \end{matrix}\right\} \begin{matrix} \text{processes} \\ \mathrm{p}_1, ..., \mathrm{p}_{n_\mathrm{p}} \end{matrix} \tag{4.54}$$

the $n_\mathrm{e} \cdot n_\mathrm{p}$ conservation constraints (4.53) can be written as

$$\boxed{\boldsymbol{\nu} \cdot \boldsymbol{\alpha}^\mathrm{T} = \mathbf{0}} \tag{4.55}$$

Equation (4.55) limits the degree of freedom for the choice of stoichiometric coefficients. On the other hand, each row vector of stoichiometric coefficients that results in zero if it is multiplied from the left to $\boldsymbol{\alpha}^{\mathrm{T}}$ is a possible process stoichiometry that does not violate conservation laws of "elementary constituents". As each linear combination of such row vectors again fulfils this property, the consistent process stoichiometries form a vector space. This vector space is called the left nullspace of the matrix $\boldsymbol{\alpha}^{\mathrm{T}}$. The dimension of this vector space determines the number of independent processes that are compatible with conservation laws. If we have a basis of this space, each consistent process stoichiometry can be written as a linear combination of the basis vectors, or each process as a composite process of the corresponding basic processes.

Process-Specific Conservation Constraints

When deriving stoichiometric coefficients for a particular process, we are interested in constraints for the stoichiometric coefficients of this process. As the specific process typically does not affect all substances considered for all processes, less degrees of freedom remain for the stoichiometric coefficients. To set up the constraining equations for a particular process i, we have to eliminate the columns of the composition matrix, $\boldsymbol{\alpha}$, that refer to substances that are not affected by the process i. This results in a reduced composition matrix, $\boldsymbol{\alpha}_{(i)}$, relevant for process i. In analogy to equation (4.55), the constraints applicable to stoichiometric coefficients for process i are then given by

$$\boxed{\boldsymbol{\nu}_i \cdot \left(\boldsymbol{\alpha}_{(i)}\right)^{\mathrm{T}} = \mathbf{0}} \tag{4.56}$$

Here, $\boldsymbol{\nu}_i$ is a row vector or a matrix of stoichiometries for process i that are consistent with respect to conservation laws for "elementary constituents". Similarly to $\boldsymbol{\alpha}_{(i)}$, this row vector or matrix only contains columns referring to substances affected by the process and have to be extended by elements with a value of zero for the other substances when combined with the other process stoichiometries to the complete stoichiometric matrix of all processes (4.3). If the dimension of the left nullspace of the matrix $\left(\boldsymbol{\alpha}_{(i)}\right)^{\mathrm{T}}$ is unity, the conservation constraints define the process stoichiometry uniquely (up to an arbitrary factor that can be determined by setting one of the stoichiometric coefficients equal to plus or minus unity). If this dimension is larger, additional stoichiometric constraints are required to make the process stoichiometry unique. Each additional constraint that is independent of the other constraints reduces the dimension of the space of stoichiometries that are compatible with conservation laws and additional constraints by one. Therefore, the number of required additional stoichiometric constraints for process i is equal to the dimension of the left nullspace of $\left(\boldsymbol{\alpha}_{(i)}\right)^{\mathrm{T}}$ minus one.

Additional Stoichiometric Constraints

Usually, for a given process i, additional stoichiometric constraints are linear equations in the stoichiometric coefficients of this process and can therefore be written in the form

$$\sum_{j=1}^{n_\mathrm{s}} \nu_{ij}\, \gamma_{(i),kj} = 0 \tag{4.57}$$

with coefficients $\gamma_{(i),kj}$ for constraint k of the process i. The sum extends over all considered substances j. If we combine all additional stoichiometric constraints for a given process i

in a matrix of constraints

$$\boldsymbol{\gamma}_{(i)} = \overbrace{\begin{pmatrix} \gamma_{(i),11} & \gamma_{(i),12} & \gamma_{(i),13} & \cdots & \gamma_{(i),1n_\mathrm{s}} \\ \gamma_{(i),21} & \gamma_{(i),22} & \gamma_{(i),23} & \cdots & \gamma_{(i),2n_\mathrm{s}} \\ \vdots & \vdots & \vdots & \ddots & \vdots \\ \gamma_{(i),n_\mathrm{c}1} & \gamma_{(i),n_\mathrm{c}2} & \gamma_{(i),n_\mathrm{c}3} & \cdots & \gamma_{(i),n_\mathrm{c}n_\mathrm{s}} \end{pmatrix}}^{\text{substances } 1,...,n_\mathrm{s}} \left.\begin{matrix} \\ \\ \\ \\ \end{matrix}\right\} \begin{matrix} \text{constraints} \\ \mathrm{c}^i_1,...,\mathrm{c}^i_{n^i_\mathrm{c}} \\ \text{for process } i \end{matrix} \tag{4.58}$$

we can write the corresponding constraining equations (4.57) in matrix form

$$\boxed{\boldsymbol{\nu}_i \cdot \left(\boldsymbol{\gamma}_{(i)}\right)^\mathrm{T} = \mathbf{0}} \tag{4.59}$$

Combining Conservation and Additional Stoichiometric Constraints

Due to the mathematical similarities of the constraining equations (4.56) and (4.59), these two equations can be combined to the equation constraining the stoichiometry of process i by conservation laws and additional stoichiometric constraints:

$$\boxed{\boldsymbol{\nu}_i \cdot \begin{pmatrix} \boldsymbol{\alpha}_{(i)} \\ \boldsymbol{\gamma}_{(i)} \end{pmatrix}^\mathrm{T} = \mathbf{0}} \tag{4.60}$$

The matrix that is transposed in this equation appends the rows of $\boldsymbol{\gamma}_{(i)}$ to the rows of $\boldsymbol{\alpha}_{(i)}$. If the number of additional stoichiometric constraints is equal to the dimension of the nullspace of the matrix $\left(\boldsymbol{\alpha}_{(i)}\right)^\mathrm{T}$ minus 1, and if all constraints are independent, there is a unique solution to this equation that describes the stoichiometric coefficients up to an arbitrary factor. This factor is usually chosen by setting one of the stoichiometric coefficients to plus or minus unity.

4.3.3.3 Analysing and Calculating Process Stoichiometry

In this section mathematical techniques for the following tasks of stoichiometric calculation will be formulated:

1. For a given process characterized by the set of affected substances of given composition, calculate the number of additional stoichiometric constraints required to make the process stoichiometry unique.

2. For a given process characterized by the set of affected substances of given composition and the constraints required to make the stoichiometry unique, calculate the stoichiometric coefficients.

As the analyses of the previous section showed, all equations (4.56), (4.59) and (4.60) to be solved for dealing with the tasks described above require the construction of the left nullspace of a matrix. We will first show how this can be done by using an algorithm that constructs the singular value decomposition of the matrix. In the following subsections, we will then develop the solutions to the individual tasks by applying this procedure to different matrices.

The singular value decomposition theorem of linear algebra (Golub and Loan, 1996) states that each $n \times m$ matrix $\mathbf{A}$ with $n \geq m$ can be decomposed into a product of three matrices $\mathbf{U}$, $\mathbf{D}$ and $\mathbf{V}^{\mathrm{T}}$

$$\mathbf{A} = \mathbf{U} \cdot \mathbf{D} \cdot \mathbf{V}^{\mathrm{T}} \tag{4.61}$$

where the three matrices $\mathbf{U}$, $\mathbf{D}$ and $\mathbf{V}$ have the following properties:

- $\mathbf{U}$ is an $n \times m$ matrix with orthonormal columns: $\mathbf{U}^{\mathrm{T}} \cdot \mathbf{U} = \mathbf{I}$.
- $\mathbf{D}$ is an $m \times m$ diagonal matrix with non-negative elements in its diagonal. These values in the diagonal of $\mathbf{D}$ are called singular values of the matrix $\mathbf{A}$.
- $\mathbf{V}$ is an $m \times m$ matrix with orthonormal columns: $\mathbf{V}^{\mathrm{T}} \cdot \mathbf{V} = \mathbf{I}$.

Figure 4.7 illustrates this decomposition graphically for a a two-dimensional case. The

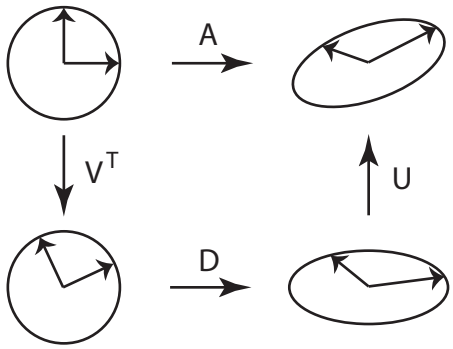

Figure 4.7: Decomposition of a linear function characterized by the matrix $\mathbf{A}$ into a rotation characterized by $\mathbf{V}^{\mathrm{T}}$, a dilatation and/or contraction along the main coordinate axes characterized by $\mathbf{D}$, and another rotation characterized by $\mathbf{U}$.

linear function represented by the matrix $\mathbf{A}$ can be decomposed into a rotation characterized by $\mathbf{V}^{\mathrm{T}}$, a dilatation and/or contraction along the main coordinate axes characterized by $\mathbf{D}$, and another rotation characterized by $\mathbf{U}$.

The matrices used in this theorem can be constructed as follows. The singular values are equal to the square roots of the eigenvalues of $\mathbf{A}^{\mathrm{T}}\mathbf{A}$ or $\mathbf{A}\mathbf{A}^{\mathrm{T}}$. The eigenvectors of $\mathbf{A}^{\mathrm{T}}\mathbf{A}$ build the columns of $\mathbf{V}$, those of $\mathbf{A}\mathbf{A}^{\mathrm{T}}$ build the columns of $\mathbf{U}$. A constructive implementation of this theorem can be used to get the left nullspace of the matrix $\mathbf{A}$. First, to get a complete basis of the left nullspace, we extend the $n \times m$ matrix $\mathbf{A}$ to the $n \times n$ matrix $\tilde{\mathbf{A}}$ by columns that contain only zero elements. All matrices are then $n \times n$. By applying the singular value decomposition theorem (4.61) to the matrix $\tilde{\mathbf{A}}$ and multiplying the decomposition equation from the left with $\tilde{\mathbf{U}}^{\mathrm{T}}$ we get

$$\tilde{\mathbf{U}}^{\mathrm{T}} \cdot \tilde{\mathbf{A}} = \tilde{\mathbf{D}} \cdot \tilde{\mathbf{V}}^{\mathrm{T}} = \tilde{\mathbf{R}} \qquad . \tag{4.62}$$

All singular values in $\tilde{\mathbf{D}}$ that are zero lead now obviously to corresponding rows in $\tilde{\mathbf{R}}$ that are zero (note that $\tilde{\mathbf{D}}$ is diagonal). The equality signs in (4.62) then imply that the corresponding rows of $\tilde{\mathbf{U}}^{\mathrm{T}}$ are elements of the nullspace of $\tilde{\mathbf{A}}$ and therefore of $\mathbf{A}$. The rows of $\tilde{\mathbf{U}}^{\mathrm{T}}$ that correspond to singular values that are not zero do not belong to the left nullspace of $\tilde{\mathbf{A}}$ and $\mathbf{A}$. As all rows of $\tilde{\mathbf{U}}^{\mathrm{T}}$ together span the n-dimensional space, the

rows corresponding to singular values that are zero form an orthonormal basis of the left nullspace of $\mathbf{A}$.

In order to apply this theorem to solve the tasks described above, we need a constructive implementation to get the rows of the matrix $\tilde{\mathbf{U}}^{\mathrm{T}}$ that correspond to singular values that are zero. Algorithms to construct the matrices the existence of which is guaranteed by the singular value decomposition theorem are described in the literature (Golub and Loan, 1996). Implementations of such algorithms are available in general packages for statistics, graphics, and computing, such as R (`http://www.r-project.org`) or Matlab (`http://www.mathworks.com`), in libraries for computational linear algebra, such as the Fortran 77 library LAPACK (`http://www.netlib.org/lapack`) or its ANSI C translation CLAPACK (`http://www.netlib.org/clapack`), and implementations are also described in the literature (Press et al., 1992b; Press et al., 1992a; Press et al., 2002). In the following subsections, we will apply such a constructive implementation of the singular value decomposition theorem to solve the mathematical problems of the two tasks described above by applying it to the matrix relevant for each task.

Calculating the Number of Required Additional Constraints

We apply the singular value decomposition theorem (4.61) in the form of equation (4.62) to the matrices

$$\mathbf{A}_2^{(i)} = \left(\boldsymbol{\alpha}_{(i)}\right)^{\mathrm{T}} \tag{4.63}$$

(see equation 4.56). The dimension of the left nullspace of this matrix is given as the number of zero diagonal elements of the matrix $\tilde{\mathbf{D}}$ gained from the singular value decomposition in the form of equation (4.62). The number of required constraints is then equal to this dimension minus 1.

Calculating Stoichiometric Coefficients

We combine the constraints induced by the substance composition matrix (4.52) with the additional constraints matrix (4.59) and delete the columns referring to substances not affected by the process. This leads to the following matrix of constraints

$$\mathbf{A}_3^{(i)} = \begin{pmatrix} \boldsymbol{\alpha}_{(i)} \\ \boldsymbol{\gamma}_{(i)} \end{pmatrix}^{\mathrm{T}} \tag{4.64}$$

(see equation 4.60) to which the singular value decomposition theorem is applied. If the input was consistent (correct number of constraints) we get a unique row vector from $\tilde{\mathbf{U}}^{\mathrm{T}}$ corresponding to a singular value that is zero. This row vector defines the stoichiometry of the process up to an arbitrary multiplicative factor.

4.3.3.4 Analytical Example: Growth of Algae on Nutrients

The simple example described in section 4.3.2.1 led to the stoichiometry given in Table 4.8 together with the mass composition of all involved substances. To simplify the expressions, throughout this section, we use α_{N} and α_{P} to characterize the nitrogen and phosphorus content of algae instead of $\alpha_{\mathrm{N,ALG}}$ and $\alpha_{\mathrm{P,ALG}}$. This model is simple enough to make an analytical construction of the matrices in the singular value decomposition theorem

Process		Substances / Organisms		
		NH_4^+	HPO_4^{2-}	ALG
Element		gN	gP	gDM
Growth of ALG,NH_4^+		$-\alpha_N$	$-\alpha_P$	1
Respiration of ALG		α_N	α_P	-1
N	gN	1	0	α_N
P	gP	0	1	α_P

Table 4.8: Stoichiometry and composition table of the simple growth and respiration model of algae based on nitrogen and phosphorus conservation.

possible. This is demonstrated in this section to clarify the approach. We first show that the solution provided earlier is consistent with the formulation of the constraints in matrix notation. Then we demonstrate that we obtain the same solution by using the singular value decomposition theorem.

The composition matrix of ammonium, phosphate and algal biomass with respect to nitrogen and phosphorus is given by

$$\boldsymbol{\alpha} = \overbrace{\begin{pmatrix} 1 & 0 & \alpha_N \\ 0 & 1 & \alpha_P \end{pmatrix}}^{NH_4^+ \; HPO_4^{2-} \; ALG} \left.\begin{matrix} \\ \end{matrix}\right\} \begin{matrix} N \\ P \end{matrix} \tag{4.65}$$

According to the solution provided in Table 4.8 the processes of growth and respiration of algae are characterized by the following stoichiometric matrix

$$\boldsymbol{\nu} = \overbrace{\begin{pmatrix} -\alpha_N & -\alpha_P & 1 \\ \alpha_N & \alpha_P & -1 \end{pmatrix}}^{NH_4^+ \quad HPO_4^{2-} \quad ALG} \left.\begin{matrix} \\ \end{matrix}\right\} \begin{matrix} \text{Growth of ALG,} NH_4^+ \\ \text{Respiration of ALG} \end{matrix} \tag{4.66}$$

It can easily be verified that these matrices fulfil the mass conservation constraints (4.55)

$$\boldsymbol{\nu} \cdot \boldsymbol{\alpha}^T = \begin{pmatrix} -\alpha_N & -\alpha_P & 1 \\ \alpha_N & \alpha_P & -1 \end{pmatrix} \cdot \begin{pmatrix} 1 & 0 \\ 0 & 1 \\ \alpha_N & \alpha_P \end{pmatrix} = \mathbf{0} \quad . \tag{4.67}$$

To get the complete nullspace of $\boldsymbol{\alpha}^T$ we extend $\boldsymbol{\alpha}$ by a row of zeros and transpose the

resulting matrix. This leads to

$$\tilde{\mathbf{A}} = \begin{pmatrix} 1 & 0 & 0 \\ 0 & 1 & 0 \\ \alpha_{\mathrm{N}} & \alpha_{\mathrm{P}} & 0 \end{pmatrix} \quad . \tag{4.68}$$

For the construction of the matrices of the singular value decomposition theorem we must calculate the eigenvalues and eigenvectors of the two matrices

$$\tilde{\mathbf{A}}^{\mathrm{T}}\tilde{\mathbf{A}} = \begin{pmatrix} 1+\alpha_{\mathrm{N}}^2 & \alpha_{\mathrm{N}}\alpha_{\mathrm{P}} & 0 \\ \alpha_{\mathrm{N}}\alpha_{\mathrm{P}} & 1+\alpha_{\mathrm{P}}^2 & 0 \\ 0 & 0 & 0 \end{pmatrix} \quad , \quad \tilde{\mathbf{A}}\tilde{\mathbf{A}}^{\mathrm{T}} = \begin{pmatrix} 1 & 0 & \alpha_{\mathrm{N}} \\ 0 & 1 & \alpha_{\mathrm{P}} \\ \alpha_{\mathrm{N}} & \alpha_{\mathrm{P}} & \alpha_{\mathrm{N}}^2+\alpha_{\mathrm{P}}^2 \end{pmatrix} \quad . \tag{4.69}$$

The eigenvalues are given by

$$\lambda_1 = 1+\alpha_{\mathrm{N}}^2+\alpha_{\mathrm{P}}^2 \quad , \quad \lambda_2 = 1 \quad , \quad \lambda_3 = 0 \tag{4.70}$$

The eigenvectors of $\tilde{\mathbf{A}}^{\mathrm{T}}\tilde{\mathbf{A}}$ are then given by

$$v_1 = \begin{pmatrix} \dfrac{\alpha_{\mathrm{N}}}{\sqrt{\alpha_{\mathrm{N}}^2+\alpha_{\mathrm{P}}^2}} \\ \dfrac{\alpha_{\mathrm{P}}}{\sqrt{\alpha_{\mathrm{N}}^2+\alpha_{\mathrm{P}}^2}} \\ 0 \end{pmatrix} \quad , \quad v_2 = \begin{pmatrix} \dfrac{\alpha_{\mathrm{P}}}{\sqrt{\alpha_{\mathrm{N}}^2+\alpha_{\mathrm{P}}^2}} \\ \dfrac{-\alpha_{\mathrm{N}}}{\sqrt{\alpha_{\mathrm{N}}^2+\alpha_{\mathrm{P}}^2}} \\ 0 \end{pmatrix} \quad , \quad v_3 = \begin{pmatrix} 0 \\ 0 \\ 1 \end{pmatrix} \quad . \tag{4.71}$$

those of $\tilde{\mathbf{A}}\tilde{\mathbf{A}}^{\mathrm{T}}$ by

$$v_1 = \begin{pmatrix} \dfrac{\alpha_{\mathrm{N}}}{\sqrt{\alpha_{\mathrm{N}}^2+\alpha_{\mathrm{P}}^2}\cdot\sqrt{1+\alpha_{\mathrm{N}}^2+\alpha_{\mathrm{P}}^2}} \\ \dfrac{\alpha_{\mathrm{P}}}{\sqrt{\alpha_{\mathrm{N}}^2+\alpha_{\mathrm{P}}^2}\cdot\sqrt{1+\alpha_{\mathrm{N}}^2+\alpha_{\mathrm{P}}^2}} \\ \dfrac{\sqrt{\alpha_{\mathrm{N}}^2+\alpha_{\mathrm{P}}^2}}{\sqrt{1+\alpha_{\mathrm{N}}^2+\alpha_{\mathrm{P}}^2}} \end{pmatrix}, \; v_2 = \begin{pmatrix} \dfrac{\alpha_{\mathrm{P}}}{\sqrt{\alpha_{\mathrm{N}}^2+\alpha_{\mathrm{P}}^2}} \\ \dfrac{-\alpha_{\mathrm{N}}}{\sqrt{\alpha_{\mathrm{N}}^2+\alpha_{\mathrm{P}}^2}} \\ 0 \end{pmatrix}, \; v_3 = \begin{pmatrix} \dfrac{-\alpha_{\mathrm{N}}}{\sqrt{1+\alpha_{\mathrm{N}}^2+\alpha_{\mathrm{P}}^2}} \\ \dfrac{-\alpha_{\mathrm{P}}}{\sqrt{1+\alpha_{\mathrm{N}}^2+\alpha_{\mathrm{P}}^2}} \\ \dfrac{1}{\sqrt{1+\alpha_{\mathrm{N}}^2+\alpha_{\mathrm{P}}^2}} \end{pmatrix} \tag{4.72}$$

Using the square root of the eigenvalues as singular values, the eigenvectors of $\tilde{\mathbf{A}}^{\mathrm{T}}\tilde{\mathbf{A}}$ as columns of $\tilde{\mathbf{V}}$, and those of $\tilde{\mathbf{A}}\tilde{\mathbf{A}}^{\mathrm{T}}$ as columns of $\tilde{\mathbf{U}}$ leads to the construction of the solution

of the singular value theorem

$$\overbrace{\begin{pmatrix} 1 & 0 & 0 \\ 0 & 1 & 0 \\ \alpha_\mathrm{N} & \alpha_\mathrm{P} & 0 \end{pmatrix}}^{\tilde{\mathbf{A}}} = \overbrace{\begin{pmatrix} \frac{\alpha_\mathrm{N}}{\sqrt{\alpha_\mathrm{N}^2+\alpha_\mathrm{P}^2}\cdot\sqrt{1+\alpha_\mathrm{N}^2+\alpha_\mathrm{P}^2}} & \frac{\alpha_\mathrm{P}}{\sqrt{\alpha_\mathrm{N}^2+\alpha_\mathrm{P}^2}} & \frac{-\alpha_\mathrm{N}}{\sqrt{1+\alpha_\mathrm{N}^2+\alpha_\mathrm{P}^2}} \\ \frac{\alpha_\mathrm{P}}{\sqrt{\alpha_\mathrm{N}^2+\alpha_\mathrm{P}^2}\cdot\sqrt{1+\alpha_\mathrm{N}^2+\alpha_\mathrm{P}^2}} & \frac{-\alpha_\mathrm{N}}{\sqrt{\alpha_\mathrm{N}^2+\alpha_\mathrm{P}^2}} & \frac{-\alpha_\mathrm{P}}{\sqrt{1+\alpha_\mathrm{N}^2+\alpha_\mathrm{P}^2}} \\ \frac{\sqrt{\alpha_\mathrm{N}^2+\alpha_\mathrm{P}^2}}{\sqrt{1+\alpha_\mathrm{N}^2+\alpha_\mathrm{P}^2}} & 0 & \frac{1}{\sqrt{1+\alpha_\mathrm{N}^2+\alpha_\mathrm{P}^2}} \end{pmatrix}}^{\tilde{\mathbf{U}}}$$

$$\cdot \underbrace{\begin{pmatrix} \sqrt{1+\alpha_\mathrm{N}^2+\alpha_\mathrm{P}^2} & & \\ & 1 & \\ & & 0 \end{pmatrix}}_{\tilde{\mathbf{D}}} \cdot \underbrace{\begin{pmatrix} \frac{\alpha_\mathrm{N}}{\sqrt{\alpha_\mathrm{N}^2+\alpha_\mathrm{P}^2}} & \frac{\alpha_\mathrm{P}}{\sqrt{\alpha_\mathrm{N}^2+\alpha_\mathrm{P}^2}} & 0 \\ \frac{\alpha_\mathrm{P}}{\sqrt{\alpha_\mathrm{N}^2+\alpha_\mathrm{P}^2}} & \frac{-\alpha_\mathrm{N}}{\sqrt{\alpha_\mathrm{N}^2+\alpha_\mathrm{P}^2}} & 0 \\ 0 & 0 & 1 \end{pmatrix}}_{\tilde{\mathbf{V}}^\mathrm{T}} \tag{4.73}$$

The last column of $\tilde{\mathbf{U}}$ now demonstrates, that the only possible stoichiometry of processes is proportional to $(-\alpha_\mathrm{N}, -\alpha_\mathrm{P}, 1)$. This corresponds to the solution given in Table 4.8.

The procedure outlined in this section seems to be a very complicated way to find this out. However, it should be noted, that the main advantage of this procedure is to provide general solutions for bigger process systems, where analytical solution is no longer so straightforward.

4.3.3.5 Numerical Example: Growth of Algae and Zooplankton

This section demonstrates how to apply the 6 step procedure to derive process stoichiometries outlined in section 4.3.3.1 (Reichert and Schuwirth, 2010). We assume that we want to build-up a lake model with the state variables ammonium (NH_4^+), nitrate (NO_3^-), phosphate (HPO_4^{2-}), dissolved oxygen (O_2), phytoplankton (ALG), zooplankton (ZOO), dead particulate organic matter (POM), and dissolved organic matter (DOM). We consider the elements nitrogen (N), phosphorus (P), carbon (C), hydrogen (H), and oxygen(O), and electric charge as elementary constituents and make appropriate assumptions of the composition of the organic components. To be able to close mass balances, for the calculation of process stoichiometries, we add the compounds bicarbonate (HCO_3^-), hydrogen ions (H^+), and water (H_2O) (see section 4.3.3 for a general explanation of this step). Note that we assume the P content of phytoplankton to be smaller than that of zooplankton due to P limitation of phytoplankton growth and the P and N content of dead organic matter to be smaller than that of zooplankton due to the higher content of carbon in the slowly degradable part of organic matter. We then proceed with the derivation of the process stoichiometries of phytoplankton growth on nitrate as the nitrogen source (primary production) and of zooplankton growth on phytoplankton (consumption) according to the 6 step procedure outlined in section 4.3.3.5.

Step 1: Select the substances/organisms involved in the process.
Phytoplankton growth on nitrate as the nitrogen source should lead to the production of phytoplankton and dissolved oxygen under consumption of nitrate, phosphate and bicarbonate. The signs of the stoichiometric coefficients of hydrogen ions and water are not a priori clear. Zooplankton growth should produce zooplankton under consumption of phytoplankton. Due to partial mineralisation of the organic material, excretion and sloppy feeding, we expect release of ammonium, phosphate, bicarbonate and particulate and dissolved organic matter and consumption of dissolved oxygen. Again, the signs of the stoichiometric coefficients of hydrogen ions and water are not a priori clear. Table 4.9 shows our current knowledge of the two processes and the composition matrix in the form of the extended process table.

process		substances and organisms											rate
elements		NH_4^+ gN	NO_3^- gN	HPO_4^{2-} gP	HCO_3^- gC	O_2 gO	H^+ mol	H_2O mol	ALG gDM	ZOO gDM	POM gDM	DOM g	
growth ALG			−	−	−	+	?	?	+				$\rho_{gro,ALG}$
growth ZOO		+		+	+	−	?	?	−	+	+	+	$\rho_{gro,ZOO}$
N	gN	1	1	0	0	0	0	0	0.06	0.06	0.04	0.04	
P	gP	0	0	1	0	0	0	0	0.005	0.01	0.007	0.007	
C	gC	0	0	0	1	0	0	0	0.365	0.360	0.483	0.483	
H	gH	0.286	0	0.032	0.083	0	1	2	0.07	0.07	0.07	0.07	
O	gO	0	3.429	2.065	4	1	0	12	0.5	0.5	0.4	0.4	
charge	ch.units	0.071	0.071	-0.065	-0.083	0	1	0	0	0	0	0	

Table 4.9: Extended process table of prior knowledge for growth of phytoplankton and zooplankton.

Step 2: Determine the number of additional constraints which are required to calculate the stoichiometric coefficients.
Application of the function `calc.stoich.basis` of our R package `stoichcalc` (see chapter 15) to the composition matrix and the list of non-zero stoichiometric coefficients but without additional constraints leads to the result that there is exactly one possible stoichiometry for phytoplankton growth but that four independent stoichiometries are still possible for zooplankton growth. This means that no additional stoichiometric constraint is needed for phytoplankton growth, but that three additional constraints are needed for zooplankton growth.

Step 3: Define additional stoichiometric constraints if step 2 reveals that they are needed.
It is clear that the yield of zooplankton growth (zooplankton biomass production per unit of phytoplankton consumed) and the release of particulate and dissolved organic matter due to excretion and sloppy feeding cannot be derived from mass conservation principles. Introducing the parameters yield, Y_{ZOO}, fraction of organic particles released per unit of phytoplankton consumed, f_{POM}, and fraction of dissolved organic matter released per unit of phytoplankton consumed, f_{DOM}, we thus obtain the following three linear constraints to the stoichiometric coefficients of zooplankton growth:

$$\nu_{\mathrm{gro,ZOO;ZOO}} = -Y_{\mathrm{ZOO}}\nu_{\mathrm{gro,ZOO;ALG}} \tag{4.74a}$$

$$\nu_{\mathrm{gro,ZOO;POM}} = -f_{\mathrm{POM}}\nu_{\mathrm{gro,ZOO;ALG}} \tag{4.74b}$$

$$\nu_{\mathrm{gro,ZOO;DOM}} = -f_{\mathrm{DOM}}\nu_{\mathrm{gro,ZOO;ALG}} \tag{4.74c}$$

Specific process knowledge is required to determine the values of these parameters. For the numerical example, we will use $Y_{\mathrm{ZOO}} = 0.2$, $f_{\mathrm{POM}} = 0.2$ and $f_{\mathrm{DOM}} = 0.1$.

Step 4: Choose one coefficient and set it to a specific value.
As we are denoting the processes "growth" (of phytoplankton and zooplankton, respectively), it is convenient to formulate the process rate as the growth rate of the corresponding organism. This requires setting the stoichiometric coefficient of the growing organism to unity. Transformation rates of other substances can then be calculated by multiplying the process rate with the stoichiometric coefficient of the substance.

Step 5: Calculate the stoichiometric coefficients of the process.
Application of the function `calc.stoich.coef` of our R package `stoichcalc` (see chapter 15) leads to the process stoichiometry shown in Table 4.10.

process elements	substances and organisms											rate
	NH_4^+ gN	NO_3^- gN	HPO_4^{2-} gP	HCO_3^- gC	O_2 gO	H^+ mol	H_2O mol	ALG gDM	ZOO gDM	POM gDM	DOM g	
growth ALG	0	−0.06	−0.0050	−0.36	1.25	−0.026	−0.0065	1	0	0	0	$\rho_{\mathrm{gro,ALG}}$
growth ZOO	0.18	0	0.0045	0.74	−1.65	0.049	0.0063	−5	1	1	0.5	$\rho_{\mathrm{gro,ZOO}}$

Table 4.10: Final process table for growth of algae and zooplankton.

Step 6: Check signs of the calculated stoichiometric coefficients.
A comparison of the signs of the stoichiometric coefficients in Tables 4.9 and 4.10 demonstrates the correct representation of the production and consumption pattern. However, due to the different contents of nutrients of the organic components, this step could lead to the identification of a problem. If we e.g. would lower the phosphorus content of phytoplankton from 0.005 to 0.004 gP/gDM, we would see that phosphate would be consumed instead of released during the growth of zooplankton. This could be corrected by lowering the yield of zooplankton growth on phytoplankton. This example demonstrates the influence of food quality on the yield (DeMott et al., 1998; Omlin et al., 2001; Hessen et al., 2002; Anderson et al., 2005).

Chapter 5

Behaviour of Solutions of Differential Equation Models

The goal of this chapter is to provide some understanding of the behaviour of solutions of initial-value problems of explicit, first-order systems of ordinary differential equations, as they often occur in the context of modelling dynamical systems (not only in ecology). For more extensive introductions, we refer to the literature (Imboden and Koch, 2003, is an example of an accessible introduction). "First-order" means that we deal with equations that involve a function and its first derivative, excluding higher-order derivatives. This is not a severe restriction as higher-order systems can be mapped to first-order systems of higher dimension by introducing new functions for the higher derivatives. "Explicit" means that we can resolve the equations for the derivatives. And finally, "ordinary differential equations" means that we are only dealing with equations that involve derivatives with respect to one variable, which, for dynamical systems, will be time, t. We omit in this chapter systems of partial differential equations that could also involve spatial derivatives or derivatives with respect to other continuous properties, such as age or size (see section 12.3.1 for examples of such models). This leads us to the following mathematical from of models to investigate the behaviour of the solutions:

$$\boxed{\frac{\mathrm{d}\mathbf{y}}{\mathrm{d}t} = \mathbf{g}(\mathbf{y}, t)} \tag{5.1}$$

The final restriction is on initial-value problems. We are interested in the time evolution of a solution of equation (5.1) from a given inital state $\mathbf{y}_0 = \mathbf{y}(t_0)$ (in contrast to boundary-value problems in which we may want to specify given values for different components of $\mathbf{y}$ at different points in time).

The first important result to mention is that under relatively weak regularity conditions (Lipschitz continuity of $\mathbf{g}$ in $\mathbf{y}$ uniformly with respect to t; we will usually have differentiable functions $\mathbf{g}$ that are even more regular than required), there exists a unique solution to this initial-value problem for some interval in time (Teschl, 2012, is an example of a book with a proof of this statement). As a solution can diverge within a finite time, the solution cannot be guaranteed for an arbitrary large time interval.

In the remaining sections of this chapter we will briefly deal with the graphical interpretation of differential equations of the form (5.1) (section 5.1), with the special case of linear systems (section 5.2) before moving to the general case of nonlinear systems (section

5.3). The chapter ends with a short outlook into elementary numerical solution techniques (section 5.4).

5.1 Graphical Interpretation

Equation (5.1) defines the derivative of $\mathbf{y}$ with respect to time as a function of the current state, $\mathbf{y}$, and time, t. For each point in time, we can plot the vector field, $\mathbf{g}$, as a function of the states, $\mathbf{y}$. This is illustrated in Figure 5.1 for a model that does not explicitly depend on time. This means that this vector field, which shows direction and speed of motion at each point in state-space, remains constant in time. Solutions can thus be drawn by following the directions of the arrows. Two such solutions are illustrated by red and green lines in Figure 5.1. This figure illlustrates a model with a so-called limit cycle, a periodic solution that is asymptotically reached from starting points within a large area of attraction.

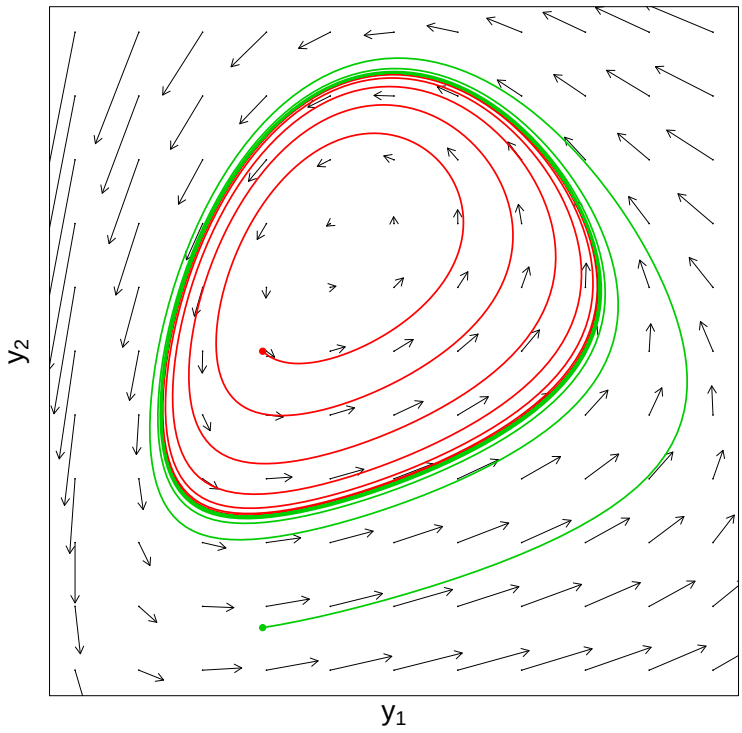

Figure 5.1: Examples of a vector field, $\mathbf{g}$, and two solutions of a two-dimensional system of ordinary differential equations of the form (5.1) without explicit time dependence (autonomous model).

5.2 Systems of Linear Ordinary Differential Equations

Although nonlinear phenomena are very important, it is worth to start the analysis of the behaviour of solutions of differential equations models with the linear case as they determine the local behaviour around steady-state solutions of nonlinear models. A linear,

first-order differential equations system can be written in the form

$$\frac{\mathrm{d}\mathbf{y}}{\mathrm{d}t} = \mathbf{A}(t)\mathbf{y} + \mathbf{b}(t) \tag{5.2}$$

where the matrix $\mathbf{A}$ defines the so-called homogeneous part and $\mathbf{b}$ is the inhomogeneity. Equation (5.2) can be solved formally, which leads to the general solution

$$\mathbf{y}(t) = \mathbf{M}(t)\mathbf{M}(t_0)^{-1}\mathbf{y}(t_0) + \mathbf{M}(t)\int_{t_0}^{t}\mathbf{M}(s)^{-1}\mathbf{b}(s)\mathrm{d}s \quad , \tag{5.3}$$

where $\mathbf{M}$ is a fundamental matrix that is invertible and solves the homogeneous system of linear ordinary differential equations

$$\frac{\mathrm{d}\mathbf{M}}{\mathrm{d}t} = \mathbf{A}(t)\mathbf{M} \quad . \tag{5.4}$$

The columns of the fundamental matrix $\mathbf{M}$ are linearly independent solutions of the homogeneous system

$$\frac{\mathrm{d}\mathbf{y}}{\mathrm{d}t} = \mathbf{A}(t)\mathbf{y} \tag{5.5}$$

so that any solution of equation (5.5) can be written in the form $\mathbf{y}(t) = \mathbf{M}(t)\mathbf{c}$ with a constant vector $\mathbf{c}$ or as $\mathbf{y}(t) = \mathbf{M}(t)\mathbf{M}(t_0)^{-1}\mathbf{y}(t_0)$ (choosing $\mathbf{c} = \mathbf{M}(t_0)^{-1}\mathbf{y}(t_0)$).

In the following paragraphs, we give an overview over the main steps for deriving the solutions of homogeneous ordinary differential equations with a constant matrix $\mathbf{A}$. The aim is to provide insight into the key ideas and concepts. For further details or proofs, we refer to the literature (Teschl, 2012). If $\mathbf{A}$ is constant, $\mathbf{M}$ is given by

$$\mathbf{M}(t) = \exp(\mathbf{A}t) \tag{5.6}$$

where the matrix exponential is defined by

$$\exp(\mathbf{A}) = \sum_{j=0}^{\infty}\frac{1}{j!}\mathbf{A}^j \quad . \tag{5.7}$$

To analyze the behaviour of the solutions of the homogeneous equation (5.5) with constant matrix $\mathbf{A}$ we can profit from the transformation of $\mathbf{A}$ to the Jordan form. According to a standard theorem of linear algebra, for any square matrix $\mathbf{A}$ there exists a unitary transformation matrix $\mathbf{U}$ so that transforms $\mathbf{A}$ to the following standard "Jordan" form:

$$\mathbf{U}\mathbf{A}\mathbf{U}^{-1} = \mathbf{J} = \begin{pmatrix} \mathbf{J}_1 & & \\ & \ddots & \\ & & \mathbf{J}_m \end{pmatrix} \quad , \quad \mathbf{J}_i = \begin{pmatrix} \lambda_i & 1 & & & \\ & \lambda_i & 1 & & \\ & & \ddots & \ddots & \\ & & & \lambda_i & 1 \\ & & & & \lambda_i \end{pmatrix} \tag{5.8}$$

Here, λ_i are the eigenvalues of the matrix $\mathbf{A}$. In many cases, in particular if all eigenvalues have multiplicity 1, the "Jordan blocks", $\mathbf{J}_i$, degenerate to the 1 x 1 matrices λ_i and $\mathbf{J}$

becomes diagonal. Nevertheless, the general form (5.8) is very important if this is not the case. Applying the unitary transformation to the homogeneous system (5.5) with constant matrix $\mathbf{A}$ leads to

$$\frac{\mathrm{d}(\mathbf{U}\mathbf{y})}{\mathrm{d}t} = \mathbf{U}\mathbf{A}\mathbf{U}^{-1}\mathbf{U}\mathbf{y} \qquad \text{or} \qquad \frac{\mathrm{d}\tilde{\mathbf{y}}}{\mathrm{d}t} = \mathbf{J}\tilde{\mathbf{y}} \quad \text{with} \quad \tilde{\mathbf{y}} = \mathbf{U}\mathbf{y} \quad . \tag{5.9}$$

This leads thus to a homogeneous system with a Jordan form matrix (for linear combinations of the original components of $\mathbf{y}$). The advantage of this form of the differential equations is that it is easier to calculate the matrix exponential (5.7). First, for block matrices, we have

$$\exp(\mathbf{J}) = \begin{pmatrix} \exp(\mathbf{J}_1) & & \\ & \ddots & \\ & & \exp(\mathbf{J}_m) \end{pmatrix} \quad , \tag{5.10}$$

so that we can focus on an individual Jordan block. Here we have

$$\exp(\mathbf{J}_i) = \exp(\lambda_i) \begin{pmatrix} 1 & 1 & \frac{1}{2!} & \cdots & \frac{1}{(k_i-1)!} \\ & 1 & 1 & \cdots & \frac{1}{(k_i-2)!} \\ & & \ddots & \ddots & \vdots \\ & & & 1 & 1 \\ & & & & 1 \end{pmatrix} \quad , \tag{5.11}$$

and for the product with time, t:

$$\exp(\mathbf{J}_i t) = \exp(\lambda_i t) \begin{pmatrix} 1 & t & \frac{t^2}{2!} & \cdots & \frac{t^{k_i-1}}{(k_i-1)!} \\ & 1 & t & \cdots & \frac{t^{k_i-2}}{(k_i-2)!} \\ & & \ddots & \ddots & \vdots \\ & & & 1 & t \\ & & & & 1 \end{pmatrix} \quad . \tag{5.12}$$

Considering the fact that for real matrices $\mathbf{A}$ complex eigenvalues occur in conjugate pairs and the structure of the (transformed) solution given by equation (5.12), we conclude that the solutions of the homogeneous equation (5.5) are of the form of the following linear combinations:

$$\boxed{\mathbf{y}(t) = \sum_{i=1}^{m} \sum_{j=0}^{k_i-1} a_{ij}\, t^j \, \exp\big(\mathrm{Re}(\lambda_i)t\big) \, \cos\big(\mathrm{Im}(\lambda_i)t + \phi_{ij}\big)} \tag{5.13}$$

where λ_i are the eigenvalues of $\mathbf{A}$, m is the number of Jordan blocks of the Jordan transformation of $\mathbf{A}$, k_i is the dimension of the i^{th} Jordan block, ϕ_{ij} are phase shifts in the oscillation term (resulting from combining the solutions of the two complex conjugate eigenvalues), and Re and Im are extracting the real and imaginary parts of the eigenvalues.

Note that the general solution (5.13) is very easy to interpret: A single, linear, homogeneous differential equation $\mathrm{d}y/\mathrm{d}t = \lambda y$ has the solution $y(t) = a\exp(\lambda t)$. For real

eigenvalues, this is still the core part of the solution given by equation (5.13). For the general solution (5.13), we need three extensions: First, we have to consider multiple eigenvalues, which leads to multiple terms of the form $\exp(\lambda_i t)$. Second, we have to consier that $\mathbf{A}$ may not be diagonizable which, as a consequence of the Jordan form, results in additional factors of the form t^j. And third, eigenvalues may be complex (in conjugate pairs). Real and imaginary parts of the complex solutions are then real solutions. Because of the identity $\exp(a + ib) = \exp(a)(\cos(b) + i\sin(b))$ this leads to the final cosine term in equation (5.13) (in addition to the exponential term that is also present for real eigenvalues).

Figure 5.2 demonstrates the most important solution behaviours resulting from equation (5.13).Note that the solution converges to zero if the real parts of all eigenvalues λ_i are negative; if there are complex eigenvalues, the solutions with components corresponding to these eigenvalues are oscillating with decreasing amplitude. If any of the real parts of the eigenvalues are positive, most solutions (those with non-zero contributions with these terms) diverge, again with oscillations with increasing amplitude in case of the involvement of complex eigenvalues. The factors t^j in equation (5.13) do not qualitatively alter this behaviour that results from the exponential term as divergence or convergence to zero of the exponential factor is stronger than the powers of t.

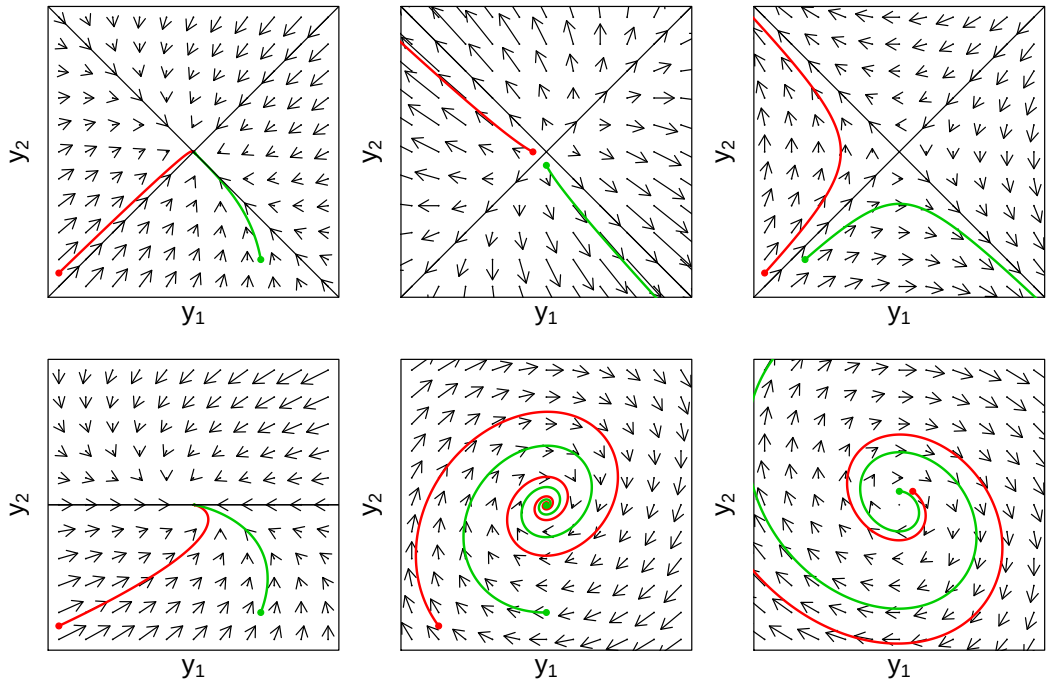

Figure 5.2: Examples of vector fields and two solutions each for the cases with two negative eigenvalues (top, left), two positive eigenvalues (top, middle), one negative, and one positive eigenvalue (top, right), one double negative eigenvalue with only one eigenvector (bottom, left), a pair of complex eigenvalues with negative real part (bottom, middle), and a pair of complex eigenvalues with positive real part (bottom, right).

5.3 Systems of Nonlinear Ordinary Differential Equations

The geometric interpretation discussed in section 5.1 limits the options for structurally different solutions of autonomous models (without explicit time dependence) in low dimensions. As the vector field defined by the right-hand side of equation (5.1) and shown in Figure 5.1 defines a unique direction (and speed) of development at each point in the system's state space, crossing of solution trajectories is not possible. This limits the possible behaviour of solutions in one dimension to fixed points (steady-state solutions) and transients towards or away from fixed points and divergent solutions. In two dimensions, periodic solutions, in particular limit cycles, as shown in Figure 5.1 are additional possible elements. In three dimensions, much more complicated solutions are possible as will be discussed in section 5.3.3. The analysis of nonlinear differential equations systems starts naturally with fixed points or steady-state solutions as discussed in the next section.

5.3.1 Fixed Points and their Stability

The behaviour of the solutions of ordinary differential equations systems is very difficult to analyze, in particular in dimensions larger than two (see discussion above). It is, however, straightforward to start with an analysis of fixed points or steady-state solutions. For autonomous models (no explicit time-dependence)

$$\frac{\mathrm{d}\mathbf{y}}{\mathrm{d}t} = \mathbf{g}(\mathbf{y}) \quad , \tag{5.14}$$

these are given as the solutions of the implicit equation

$$\mathbf{g}(\mathbf{y}_{\mathrm{fix}}) = 0 \quad . \tag{5.15}$$

At these points, according to equation (5.14), $\mathrm{d}\mathbf{y}/\mathrm{d}t = 0$ and thus the solution stays in this state.

Once the fixed points are determined, we are interested in their stability. A fixed point is called **stable**, if there exists a local neighbourhood of the fixed point for which all solutions starting from initial values within the neighbourhood converge to the fixed point. If we use the approximation

$$\mathbf{g}(\mathbf{y}) \approx \mathbf{g}(\mathbf{y}_{\mathrm{fix}}) + (\mathbf{y} - \mathbf{y}_{\mathrm{fix}}) \left.\frac{\partial \mathbf{g}}{\partial \mathbf{y}^{\mathrm{T}}}\right|_{\mathbf{y}=\mathbf{y}_{\mathrm{fix}}} \tag{5.16}$$

we see that small deviations from the fixed point, $\boldsymbol{\delta} = \mathbf{y} - \mathbf{y}_{\mathrm{fix}}$, approximately fulfill a linear, homogeneous differential equation (5.5) replacing $\mathbf{A}$ by the **Jacobian matrix** $\mathrm{Jac}(\mathbf{g}) = \partial\mathbf{g}/\partial\mathbf{y}^{\mathrm{T}}$ of the function $\mathbf{g}$ at the fixed point:

$$\mathbf{A} = \mathrm{Jac}(\mathbf{g}) = \left.\frac{\partial \mathbf{g}}{\partial \mathbf{y}^{\mathrm{T}}}\right|_{\mathbf{y}=\mathbf{y}_{\mathrm{fix}}} \quad . \tag{5.17}$$

If we use the notation

$$\mathbf{g}(\mathbf{y}_{\mathrm{fix}}) = 0 \quad \text{and} \quad \{\lambda_i\}_{i=1}^{m} = \text{eigenvalues of } \left.\frac{\partial \mathbf{g}}{\partial \mathbf{y}^{\mathrm{T}}}\right|_{\mathbf{y}=\mathbf{y}_{\mathrm{fix}}} \tag{5.18}$$

and consider the discussion at the end of section 5.2, we find the following stability criteria:

$$\boxed{\text{if } \mathrm{Re}(\lambda_i) < 0 \; \forall \; \lambda_i \;\Rightarrow\; \mathbf{y}_{\text{fix}} \text{ is a stable fixed point}} \tag{5.19}$$

and

$$\boxed{\text{if } \exists i : \; \mathrm{Re}(\lambda_i) > 0 \;\Rightarrow\; \mathbf{y}_{\text{fix}} \text{ is an unstable fixed point}} \tag{5.20}$$

Note that if no $\lambda_i > 0$ but there exist $\lambda_i = 0$, we need higher order analysis to determine the stability of the fixed point.

Note that the linear stability analysis only applies locally and cannot be used to analyse the **domain of attraction** of a stable fixed point. The domain of attraction consists of all points from which, when chosen as initial values, the fixed point is asymptotically reached.

5.3.2 Limit Cycles

The next essential element after fixed points and transient solutions already possible in two dimensions are limit cycles, as shown in Figure 5.1. Limit cycles are periodic solutions that are asymptotically reached from initial values within a **domain of attraction** of the structure.

Dividing the state space of a model into domains of attraction of different structures and domains from which solutions diverge is a very important means for qualitative understanding of the behaviour of a model. **Bifurcation theory** deals with understanding qualitative changes in these pattern as a function of model parameters or external driving forces. As an example, a stable fixed point can become unstable as a function of a change in model parameters while developing a stable limit cycle of increasing amplitude around it (this is the so-called Hopf-bifurcation).

5.3.3 Chaos

The paper by Lorenz in 1963 about "deterministic nonperiodic flow" led to a break-through in the insight of complex behaviour already of very simple nonlinear systems of ordinary differential equations (Lorenz, 1963). More specifically, Lorenz studied the behaviour of solutions of a three-dimensional model of the form (5.14) with the following function

$$\mathbf{g}(\mathbf{y}) = \begin{pmatrix} a(y_2 - y_1) \\ by_1 - y_2 - y_1 y_3 \\ y_1 y_2 - cy_3 \end{pmatrix} \quad . \tag{5.21}$$

Figure 5.3 shows the behaviour of a solution of this model.

The insight into the possible complexity of the solutions of such models and into the sensitivity to initial conditions (solutions with very close initial conditions separate very quickly) founded the so-called "deterministic chaos theory" which builds the bases of the understanding for poor predictability of the behaviour even of deterministic systems. As the initial condition can only be observed or reproduced with a limited accuracy, a deterministic system that is sensitive to initial conditions, looses predictability very quickly with an increasing forecast time horizon. This is the reason for the limited forecast horizon of weather forecasts that extends only very slowly with increasing resolution of the observation network.

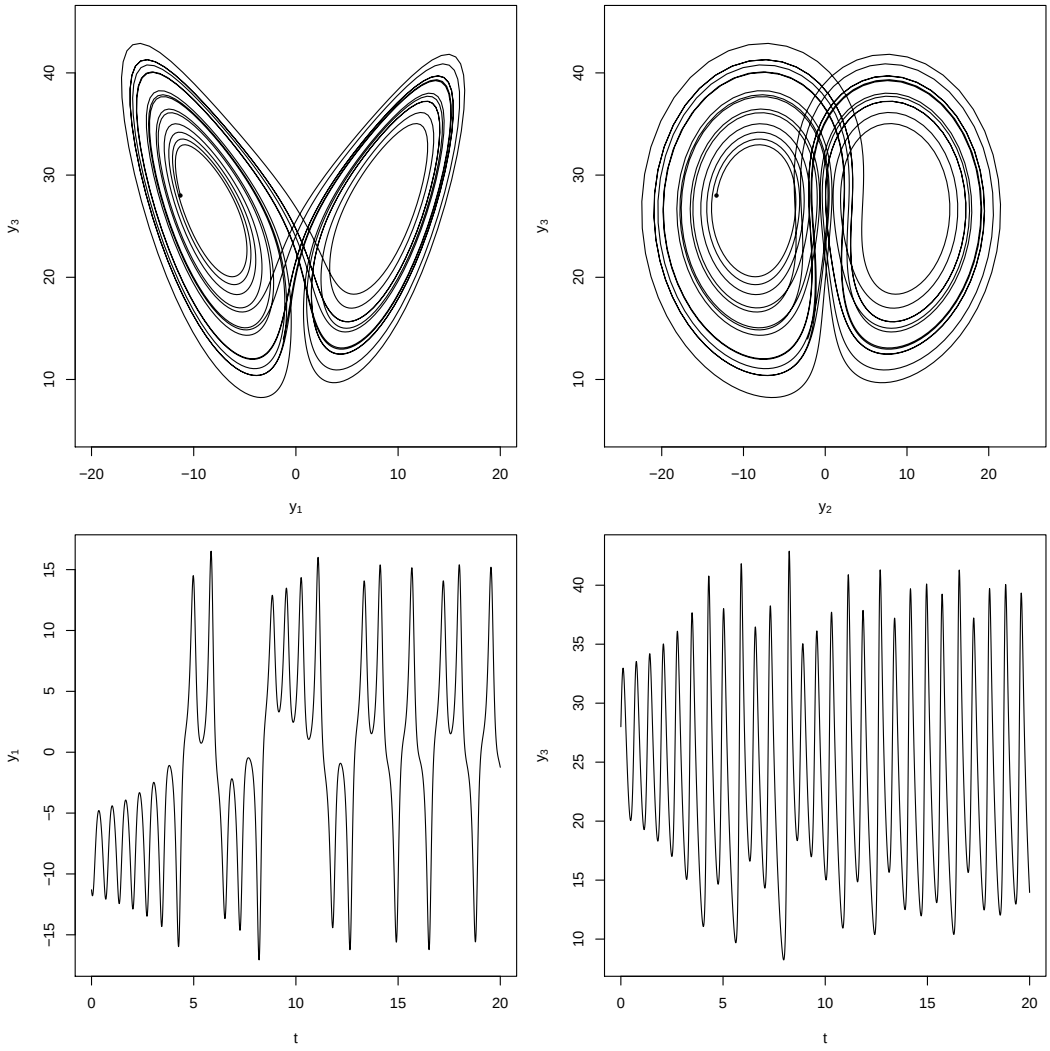

Figure 5.3: Two projections of a trajectory of the Lorenz system (5.21) in state space (top row) and the time series of two of the components (bottom row) demonstrate the potential complexity of solutions already possible with a simple three-dimensional model (parameter values $a = 10$, $b = 28$, $c = 8/3$; initial value $\mathbf{y} =$ (-11.3,-13.3,28)).

5.4 Numerical Solution of Ordinary Differential Equations

In this section we give a short description of the most elementary techniques for the solution of systems of ordinary differential equations. This description should help to identify numerical problems and to give support for their solution. For more efficient and more precise techniques than those described in this chapter we refer to the literature (Shampine, 1994; Soetaert et al., 2012).

The simplest technique for the discretization of a system of ordinary differential equations

$$\boxed{\frac{\mathrm{d}\mathbf{y}}{\mathrm{d}t} = \mathbf{g}(\mathbf{y}, t)} \tag{5.22}$$

is the explicit Euler technique. In its simplest form, this technique discretizes the time axis into equidistant points

$$t_j = t_0 + j \cdot \Delta t \tag{5.23}$$

If we abbreviate the solutions at each points in time by

$$\mathbf{y}_j = \mathbf{y}(t_j) \tag{5.24}$$

we can substitute the following approximations into the differential equations given above:

$$\boxed{\begin{array}{lcl} \mathbf{y} & \rightarrow & \mathbf{y}_j \\ \dfrac{\mathrm{d}\mathbf{y}}{\mathrm{d}t} & \rightarrow & \dfrac{\mathbf{y}_{j+1} - \mathbf{y}_j}{\Delta t} \end{array}} \tag{5.25}$$

This transforms the system of differential equations into a system of difference equations:

$$\boxed{\mathbf{y}_{j+1} = \mathbf{y}_j + \Delta t\, \mathbf{g}(\mathbf{y}_j, t_j)} \tag{5.26}$$

As these equations can be solved explicitly for the solution at the next time point, $\mathbf{y}_{j+1}$, this discretization scheme is is called **explicit Euler scheme**.

If we replace the substitution scheme (5.25) by

$$\boxed{\begin{array}{lcl} \mathbf{y} & \rightarrow & \mathbf{y}_j \\ \dfrac{\mathrm{d}\mathbf{y}}{\mathrm{d}t} & \rightarrow & \dfrac{\mathbf{y}_j - \mathbf{y}_{j-1}}{\Delta t} \end{array}} \tag{5.27}$$

and shift the index by one unit, we get the alternative discretization scheme

$$\boxed{\mathbf{y}_{j+1} = \mathbf{y}_j + \Delta t\, \mathbf{g}(\mathbf{y}_{j+1}, t_{j+1})} \tag{5.28}$$

In this scheme, the solution at the next time point, $\mathbf{y}_{j+1}$, is present at both sides of the equation and even as an argument of the generally nonlinear function $\mathbf{g}$. For this reason, this discretization scheme is called **implicit Euler scheme**. This equation must be solved

iteratively at each time step. This makes each single integration step numerically much more expensive compared to the explicit Euler scheme.

The advantage of the implicit technique compared to the explicit technique is that it makes it possible to perform the integration with significantly bigger times steps if the system of differential equations is stiff. A system of differential equations is called "stiff", if neighbouring solutions of the solution to be found converge much quicker to this solution than the time scale of changes of this solution. Figure 5.4 illustrates the behaviour of solutions of a stiff system of differential equations together with numerical approximations by the explicit and the implicit Euler schemes. Because of the stiffness of

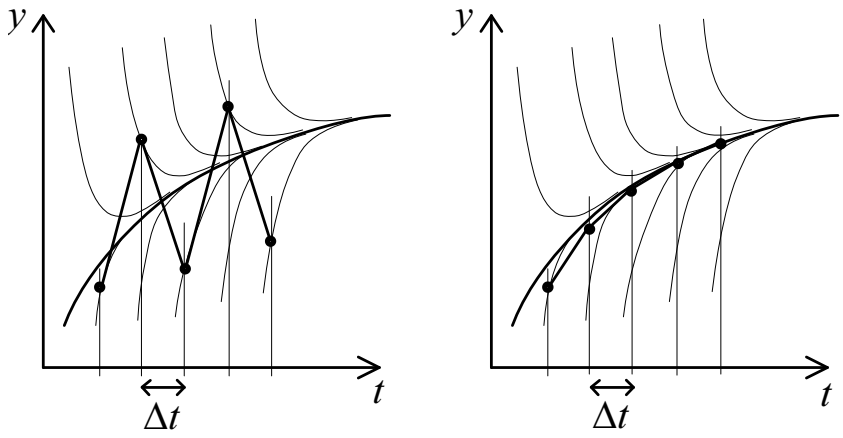

Figure 5.4: Numerical solutions of a stiff system of differential equations using an explicit (left panel) and an implicit (right panel) Euler scheme with the same time step.

the system of differential equations the slopes of the solutions (thin lines) in the vicinity of the solution to be found (thick line) are significantly larger than the slope of the solution to be found. Extrapolation of this slope by the explicit Euler scheme leads to oscillations of the numerical solution at the time step used for drawing the figure. These oscillations could only be eliminated with this scheme by reducing the time step drastically to the time scale of the fast, neighbouring solutions. In contrast to this numerical solution based on the explicit Euler scheme, the solution based on the implicit scheme behaves much less problematic. The reason is that this technique tries to find a numerical solution that has the correct slope at the end of the time step. Due to this better behaviour, this scheme allows much larger time steps for stiff systems of differential equations. If the stiffness problem is severe enough, the higher expense at each time step is then overcompensated by the smaller number of steps that have to be carried out to integrate over a given time domain. For this reason, for stiff systems of differential equations, implicit schemes should be used. To get a higher integration accuracy, not the simple implicit Euler scheme is used, but this scheme is replaced by an implicit technique of higher order. These techniques replace the approximations of the derivatives in equation (5.27) by approximations that consider higher order terms in the Taylor series of the solutions at time t_j. In addition, the order of the scheme and the time step are adapted dynamically in order to optimally follow

the true solution. As the true solution is unknown, this is usually achieved by comparing different solutions with different time step or different approximation order (Gear, 1971b; Gear, 1971a; Gear, 1971c; Hindmarsh, 1983; Petzold, 1983; Brenan et al., 1989; Shampine, 1994; Soetaert et al., 2012).

Part II

Formulation of Ecosystem Processes

Chapter 6

Physical Processes

In this chapter, we introduce the mathematical formulation of the physical processes transport and mixing (section 6.1), sedimentation (section 6.2), gas exchange (section 6.3), and detachment or resuspension (section 6.4).

6.1 Transport and Mixing

This section provides a brief overview of transport and mixing in surface waters and on how they can be considered in aquatic ecosystem models. For a more detailed exposition, we refer to the literature (Fischer et al., 1979, and many more).

6.1.1 Transport and Mixing in Lakes and Reservoirs

In this section, we give an overview of substance transport and mixing processes in lakes and reservoirs. The section is structured into four subsections: In section 6.1.1.1 we discuss density stratification in lakes and reservoirs. Then, in section 6.1.1.2 we discuss plunging inflows as a consequence of the density difference between the inflow and upper lake layers. Finally, in the sections 6.1.1.3 and 6.1.1.4 we discuss the underlying physics and the mathematical description of horizontal and vertical spreading of substances in lakes and reservoirs.

6.1.1.1 Density Stratification of Lakes and Reservoirs

Due to the dependence of the density of water on temperature and dissolved substances, undisturbed water bodies tend to be stratified, particularly when heated from the top. Denser (usually colder) water layers are below layers of less dense (usually warmer) water (density stratification).

Temperature dependence of the density of water is in many cases the most important cause of density stratification. In temperature ranges that are typical for natural water bodies, the density of pure water can be approximated by the following function (Bührer and Ambühl, 1975):

$$\rho_{\mathrm{w}}(T) \approx 999.84298\ \mathrm{kg/m^3} + 10^{-3}\ \mathrm{kg/m^3}\Big(0.059385\ {}^{o}\mathrm{C}^{-3}\ \cdot\ T^3 - 8.56272\ {}^{o}\mathrm{C}^{-2}\ \cdot\ T^2 + 65.4891\ {}^{o}\mathrm{C}^{-1}\ \cdot\ T\Big) \quad (6.1)$$

Between 0 and 24 ^{o}C, this equation approximates the density of water with a relative error of less than 10^{-5}. Figure 6.1 shows the dependence of the density of water on temperature according to equation (6.1).

Due to incoming solar radiation and heat exchange with the atmosphere the surface layer of the water column is heated in spring and summer. In our climate, this typically leads to a division of the water body into three zones. Due to daily variation in temperature and wind-induced turbulence, a surface layer of 1 to 5 m thickness, the epilimnion, remains quite well mixed. Below the epilimnion, in a depth of about 5 - 20 m, there is a strong temperature gradient. This zone is called the metalimnion. The zone below the metalimnion, the hypolimnion, is significantly less affected by yearly changes in temperature. The strong stratification in the metalimnion leads to a strong reduction in turbulent exchange of dissolved substances between hypolimnion and epilimnion (see section 6.1.1.4). Figure 6.2 shows, with an example from Lake Hallwil, a typical density stratification as it occurs in spring (Scheidegger, 1992). In the late autumn and winter, cooling of the lake at its surface supported by wind-induced mixing often destroys the density stratification of the lake. Besides temperature, dissolved and particulate substances can also have an effect on density of water that is relevant for stratification.

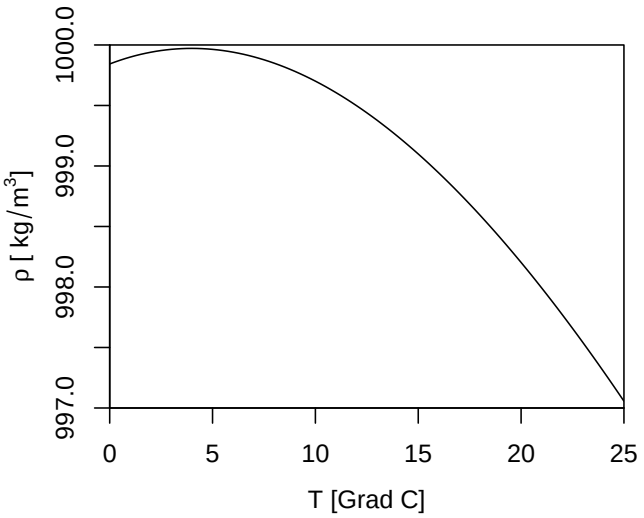

Figure 6.1: Density of pure water as a function of temperature.

6.1.1.2 Plunging of Inflows

Inflows into a stratified water body that have a higher density than the surface layers plunge below the surface layers. This process is illustrated in Figure 6.3. After the discharge into the surface layer entrainment of surrounding water into the plume leads to a decrease in flow velocity. After sufficient deceleration, the plume starts to plunge into deeper layers. Further entrainment of surrounding water and sedimentation of particles further reduces the density of the plume. Finally the plume reaches a depth in which the density of the surrounding water is the same as that of the plume. In this depth, the plume spreads horizontally across the water body. Vertical spreading can be strongly suppressed if the water body has a large density gradient.

Figure 6.4 shows that the difference in electrical conductivity between the River Muota and Lake Lucerne can be used to trace the plume of the Muota close to the river mouth.

The conductivity signal clearly shows that the river plunges into a depth between 10 and 14 m. The electrical conductivity of Lake Lucerne is much smaller than that of the River Muota because of the large fraction of its catchment dominated by cristalline rocks. In contrast, the catchment of the river Muota is dominated by sedimentary rocks. The situation shown in Figure 6.4 is typical for summer and autumn. During this time there is a very strong density gradient in the metalimnion that offers all densities that occur in the inflow. For this reason, the inflow always plunges into the metalimnion. During the winter, the lake is well mixed with only small density differences beween top and bottom. During this time, very cold inflows or inflows with a high sediment load can plunge down to the lake bottom.

6.1.1.3 Horizontal Spreading of Dissolved Substances

Horizontal transport and spreading in lakes and reservoirs is caused by directed, advective flow and turbulent diffusion. Because of the existence of much larger eddies in horizontal than in vertical direction, the distinction between advective flow and diffusive eddies depends on the spatial scale and extension of the spreading substance patch. For a small

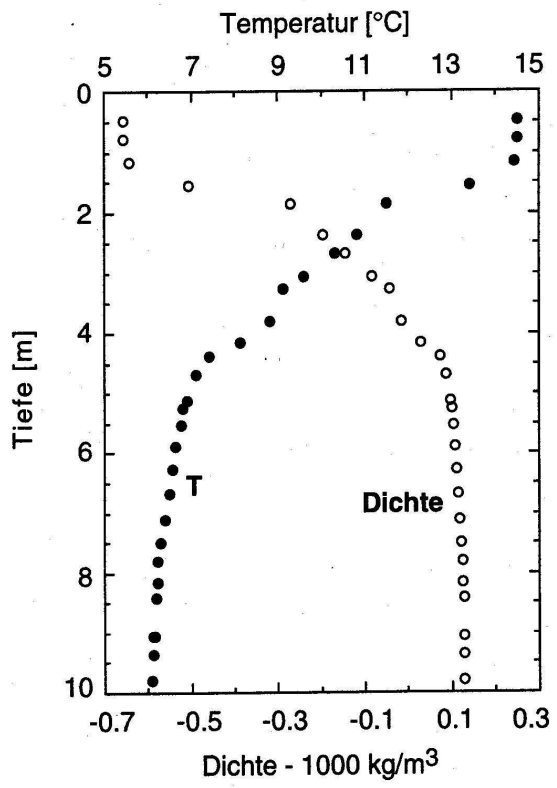

Figure 6.2: Temperature and density in the surface layers of Lake Hallwil in spring 1992 (Scheidegger, 1992).

substance patch, a large eddy leads to advection, whereas for a large patch, the same eddy leads to spreading. For this reason, the strength of turbulent diffusivity increases with the size of the substance patch which spreads across the lake.

Spreading by turbulent diffusion can be described by the following diffusion equation:

$$\frac{\partial C}{\partial t} = K_{xy}\left(\frac{\partial^2 C}{\partial x^2} + \frac{\partial^2 C}{\partial y^2}\right) \tag{6.2}$$

Here, K_{xy} is the coefficient of horizontal turbulent diffusion. The simplest solution of this equation for a substance pulse of mass m, which is distributed over the depth h, is given by

$$C(x,y,t) = \frac{m}{h}\frac{1}{2\pi}\frac{1}{\sigma_{xy}(t)^2}\exp\left(-\frac{(x-x_0)^2+(y-y_0)^2}{2\sigma_{xy}(t)^2}\right) \tag{6.3}$$

with

$$\sigma_{xy}(t) = \sqrt{2K_{xy}t} \tag{6.4}$$

The width of the substance distribution can be estimated by four standard deviations of this distribution, the maximum concentration by a rectangular distribution with half of

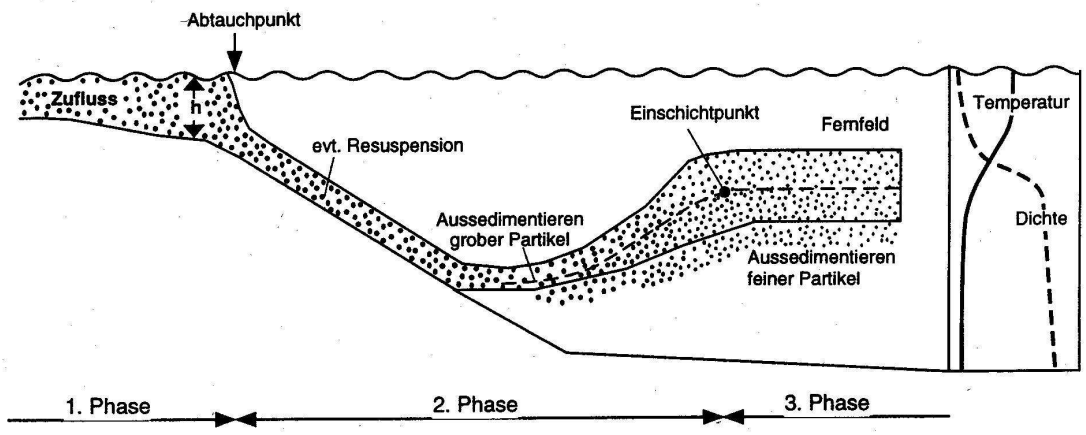

Figure 6.3: Illustration of the plunging process of an inflow into a stratified water body (Johny Wüest, Eawag).

this width:

$$\boxed{\begin{aligned} L_{xy}(t) &\approx 4\sigma_{xy}(t) = 4\sqrt{2K_{xy}t} \\ C_{\max} &\approx \frac{m}{h}\frac{1}{4\sigma_{xy}(t)^2} = \frac{m}{h}\frac{1}{8K_{xy}t} \end{aligned}} \tag{6.5}$$

The coefficient of horizontal turbulent diffusion, K_{xy}, is within a range

$$\boxed{K_{xy} \approx 10^4 - 10^6 \text{ m}^2/\text{d}} \tag{6.6}$$

where small values apply to smaller patches and large values to large patches. When applying this estimate, care has to be taken to advective flows due to wind, tributaries and the lake outlet that shift the center of mass in addition to the spreading process.

Example 6.1: The following figure shows an example of horizontal tracer spreading in 18 m depth in Lake Lucerne (Peeters et al., 1996).

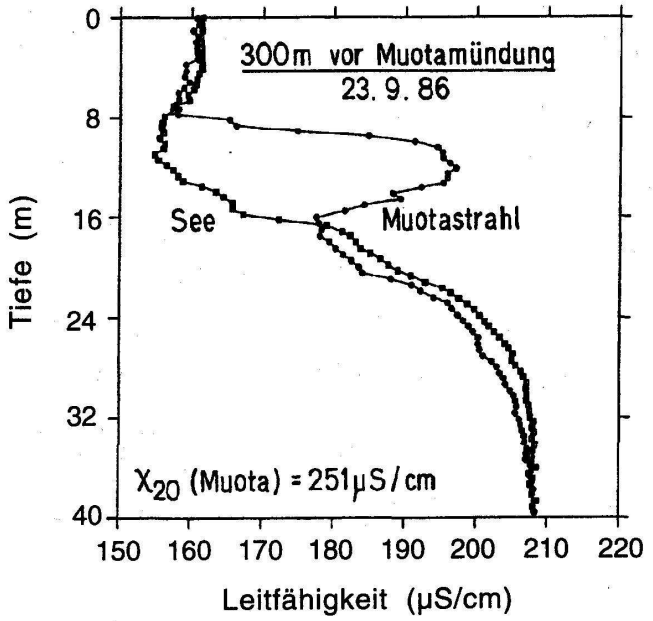

Figure 6.4: Conductivity signal of the River Muota in Lake Lucerne close to the river mouth (Wüest et al., 1988).

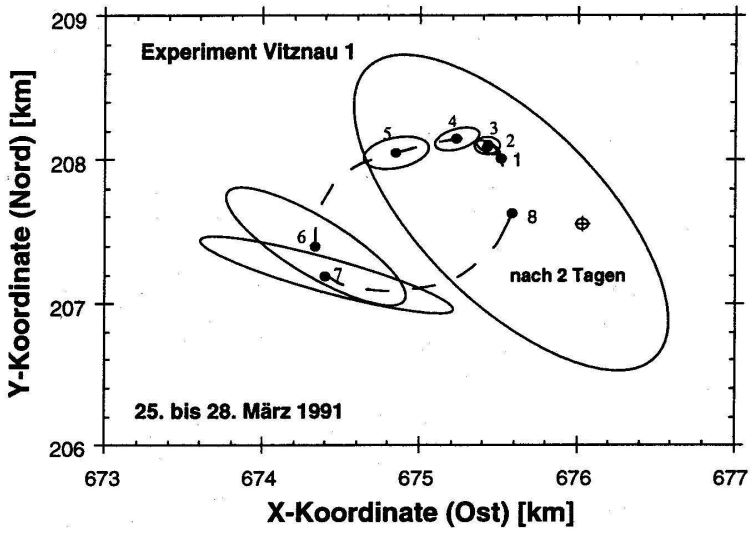

It is obvious that initially, when the tracer cloud is small, large eddies shift the tracer cloud and only small eddies contribute to its enlargement. When the cloud grows, an eddy of the same size as the one that originally shifted the whole cloud, now contributes to mixing. An estimate of the coefficient of horizontal turbulent diffusion for the first two days according to equation (6.5) leads to a value of about 10^5 m^2/d. This is within the range of values given by equation (6.6).

6.1.1.4 Vertical Spreading of Dissolved Substances

The differential equation for vertical mixing of a horizontally distributed substance in a lake is given by

$$\frac{\partial C}{\partial t} = K_z \frac{\partial^2 C}{\partial z^2} \tag{6.7}$$

Here, C is the horizontally averaged substance concentration, z the vertical distance from the lake surface, t time and K_z the coefficient of vertical turbulent diffusion. The simplest solution of this equation for a pulse of mass m of a substance is given by

$$C(z,t) = \frac{m}{A} \frac{1}{\sqrt{2\pi}} \frac{1}{\sigma_z(t)} \exp\left(-\frac{(z-z_0)^2}{2\sigma_z(t)^2}\right) \tag{6.8}$$

with

$$\sigma_z(t) = \sqrt{2K_z t} \tag{6.9}$$

Here, A is the horizontal cross-sectional area of the lake at the depth of the tracer cloud, z_0, and t time since tracer input. We can estimate the width of the tracer pulse by four standard deviations, $\sigma_z(t)$, of this distribution and the maximum concentration as the concentration of a rectangular distribution with half of this width:

$$\boxed{\begin{aligned} L_z(t) &\approx 4\sigma_z(t) = 4\sqrt{2K_z t} \\ C_{\max} &\approx \frac{m}{A}\frac{1}{2\sigma_z(t)} = \frac{m}{A}\frac{1}{2\sqrt{2K_z t}} \end{aligned}} \tag{6.10}$$

Typical values of coefficients of turbulent diffusion in epilimnion, metalimnion and hypolimnion are in the ranges given by

$$\boxed{\begin{aligned} K_{z,\text{epi}} &\approx 100 \text{ m}^2/\text{d} \\ K_{z,\text{meta}} &\approx 0.01 - 0.1 \text{ m}^2/\text{d} \\ K_{z,\text{hypo}} &\approx 0.1 - 10 \text{ m}^2/\text{d} \end{aligned}} \tag{6.11}$$

The large value in the epilimnion serves to approximate complete mixing. This value can be used for the whole lake during winter, if the water column in the deep hypolimnion is not stabilized chemically.

Example 6.2: The following figure shows profiles of temperature, of the coefficient of vertical turbulent diffusion and of the concentration of an artificial tracer in Lake Cadagno at different points in time after tracer input.

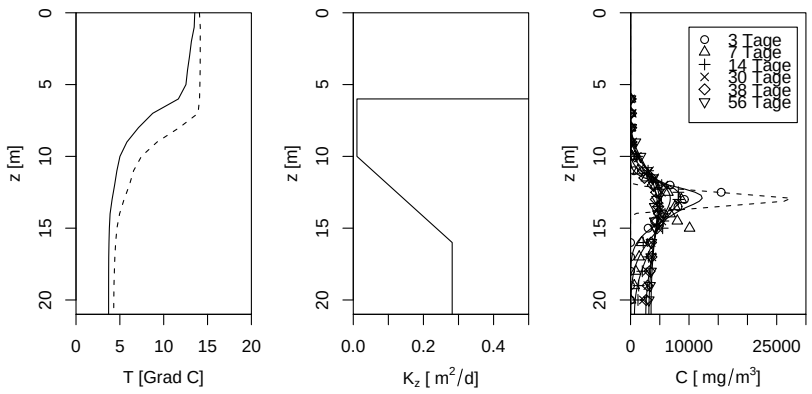

The figure shows temperature profiles (left) at the beginning (solid line), and at the end (dashed) of the measurement series, the coefficient of vertical turbulent diffusion (middle), and measured (markers) and calculated (lines) tracer profiles after 3, 7, 14, 30, 38 and 56 days after tracer input (right). It is obvious that the strong stratification keeps the tracer away from the epilimnion, whereas it diffuses much quicker down to the hypolimnion. The values of the coefficient of turbulent vertical diffusion are within the range given by the equation (6.11).

If a lake is approximated by a system of mixed reactors, equation (6.7) is replaced by the system of ordinary differential equations of the form (3.12). The two most frequently used options are a two-box model for epilimnion and hypolimnion and a multi-box model for water layers in the lake. For the two-box model, the metalimnion could be described by a link with fluxes of

$$\mathbf{J}_{\text{diff}}^{\text{epi hypo}} = A_{\text{meta}}\, K_{\text{z,meta}}\, \frac{\mathbf{C}^{\text{epi}} - \mathbf{C}^{\text{hypo}}}{h_{\text{meta}}} \tag{6.12}$$

where A_{meta} is the cross-sectional area of the lake in the depth of the metalimnion, $K_{\text{z,meta}}$ is the turbulent diffusivity in the metalimnion, and h_{meta} is the thickness of the metalimnion. This corresponds to a diffusive flux according to equation (3.17) with an exchange coefficient of

$$q_{\text{diff}}^{\text{epi hypo}} = A_{\text{meta}}\, \frac{K_{\text{z,meta}}}{h_{\text{meta}}} \tag{6.13}$$

For a multi-box model, the fluxes between box k and box $k+1$ are given by

$$\mathbf{J}_{\text{diff}}^{k\,k+1} = A_{k,k+1}\, K_{\text{z},k,k+1}\, \frac{\mathbf{C}^{k} - \mathbf{C}^{k+1}}{h_{\text{box}}} \tag{6.14}$$

where $A_{k,k+1}$ is the cross-sectional area of the lake between the boxes k and $k+1$, $K_{\text{z},k,k+1}$ is the coefficient of turbulent diffusion between the boxes k and $k+1$, and h_{box} is the height of the boxes. This corresponds to a diffusive exchange coefficient of

$$q_{\text{diff}}^{k\,k+1} = A_{k,k+1}\, \frac{K_{\text{z},k,k+1}}{h_{\text{box}}} \tag{6.15}$$

In addition to these diffusive fluxes, we will need a sedimentation flux of settling particles as described in section 6.2.

6.1.2 Transport and Mixing in Rivers

In this section, we give an overview of substance transport and mixing processes in rivers. The section is structured into four subsections: In section 6.1.2.1 we discuss the estimation of average flow velocity and water depth under steady-state hydraulic conditions. This is the condition under which we discuss substance transport and mixing in the following sections. In section 6.1.2.2 we discuss vertical mixing, in section 6.1.2.3 lateral mixing, and in section 6.1.2.4 longitudinal transport and dispersion in rivers. We only give a crude overview as a basis for formulating simple ecological models. For more details we refer to the literature (Fischer et al., 1979; Rutherford, 1994, and many more).

6.1.2.1 Steady-State River Hydraulics

The crucial function characterizing cross-sectionally averaged steady-state hydraulics in rivers is the dependence of the mean velocity, v, on discharge, Q, and the geometry of the river bed.

Flow in a river is caused by the gravitational force. Along a river reach that is not influenced by backwater effects of hydraulic constructions or changes in river bed geometry, the accelerating component (parallel to the river bed) of the gravitational force divided by its component normal to the river bed is given by the slope of the river bed:

$$S_0 = -\frac{\mathrm{d}z_\mathrm{b}}{\mathrm{d}x} \tag{6.16}$$

Here, z_b is the vertical coordinate of the sole of the river (if necessary smoothed to eliminate variation at spatial scales that are not relevant at the spatial scale of modelling) and x is the distance along the river. For uniform flow the accelerating component of the gravitational force is compensated by the decelerating frictional force. Friction is caused by surface roughness and irregularities of the river bed, by irregularities in channel geometry, obstructions, vegetation and curves. All these causes affect river flow and generate turbulence and, finally, energy dissipation. This is a very complicated process that cannot be accounted for mechanistically in a simple, one-dimensional model. For this reason, the friction force is parameterized as a function of cross-sectionally averaged flow quantitites, the geometry of the river bed, and surface roughness. Usually, the friction force is made non-dimensional by division through the gravitational force of the fluid. The two most frequently used formulations of this non-dimensional friction force, the so-callled friction-slope, S_f, are

$$S_\mathrm{f} = \frac{f}{8g}\frac{1}{R}\frac{Q^2}{A^2} \tag{6.17}$$

(Darcy-Weisbach) and

$$S_\mathrm{f} = \frac{1}{K_\mathrm{st}^2}\frac{1}{R^{4/3}}\frac{Q^2}{A^2} = n^2\frac{1}{R^{4/3}}\frac{Q^2}{A^2} \qquad , \qquad n = \frac{1}{K_\mathrm{st}} \tag{6.18}$$

(Manning-Strickler). In these equations f is the non-dimensional friction factor (the factor 8 was introduced for compatibility with pipe flow), g is the gravitational acceleration, Q is the river discharge, A is the wetted cross-sectional area, K_st is the friction coefficient according to Strickler, n is the friction coefficient according to Manning,

$$R = \frac{A}{P} \tag{6.19}$$

is the hydraulic radius, and P is the perimeter of the wetted cross-section of the river bed.

In the first approach (6.17) it is assumed that the friction force, F_f, for a water body of length L along the channel is proportional to the water density, ρ, to the contact area between the water body and the river bed, PL, and to the average flow velocity squared, v^2:

$$F_\mathrm{f} \propto \rho \cdot PL \cdot v^2 \tag{6.20}$$

Dividing this expression by the gravitational force

$$F_\mathrm{g} = \rho \cdot g \cdot AL \tag{6.21}$$

and using the expression

$$v = \frac{Q}{A} \tag{6.22}$$

for the average flow velocity at a given discharge, Q, we get

$$S_\mathrm{f} \propto \frac{\rho \cdot PL \cdot v^2}{\rho \cdot g \cdot AL} = \frac{1}{g}\frac{P}{A}\frac{Q^2}{A^2} = \frac{1}{g}\frac{1}{R}\frac{Q^2}{A^2} \tag{6.23}$$

This corresponds to equation (6.17) with a non-dimensional constant of proportionality of $f/8$. The approach (6.18) corrects this formulation sightly according to empirical evidence.

The water body is accelerated by the component of the gravitational force along the river and decelerated by the friction force that increases with flow velocity. Along a sufficiently long prismatic river reach (no change in the cross-sectional shape of the river bed) with constant friction coefficient, this leads to an equilibrium between gravitational and friction forces. Using the non-dimensional forces introduced above, this equilibrium can be formulated as

$$S_\mathrm{f} = S_0 \tag{6.24}$$

(see Figure 6.5). This equation allows us to estimate the mean flow velocity in a prismatic channel of known geometry and friction as a function of discharge. To get a typical functional relationship without having to bother with complicated geometric expression, in the following, we assume the river bed to be prismatic with a rectangular cross-section characterized by its width, w, and to have a constant slope, S_0. We further assume the river to be much wider than the water depth, h. This leads to the following geometric expressions:

$$A = wh \quad , \quad P = w + 2h \approx w \quad , \quad R = A/P \approx A/w \approx h \tag{6.25}$$

Substituting the friction equations (6.17) or (6.18), into equation (6.24), using $R \approx A/w$ from equation (6.25), and $A = Q/v$ from equation (6.22), we get the following dependences of the flow velocity, v, on discharge, Q, river bed width, w, and river bed slope, S_0:

$$v = \left(\frac{8g}{f} S_0 \frac{Q}{w}\right)^{\frac{1}{3}} \tag{6.26}$$

(based on the friction approach 6.17) or

$$\boxed{v = \left(K_\mathbf{st}\sqrt{S_0}\right)^{\frac{3}{5}} \left(\frac{Q}{w}\right)^{\frac{2}{5}} = \left(\frac{\sqrt{S_0}}{n}\right)^{\frac{3}{5}} \left(\frac{Q}{w}\right)^{\frac{2}{5}}} \tag{6.27}$$

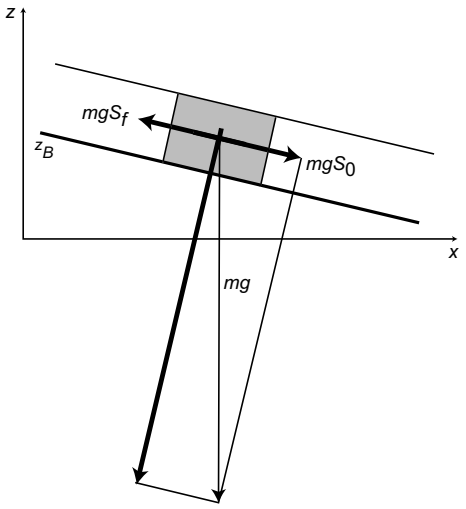

Figure 6.5: Equilibrium of gravitational and friction forces for steady-state hydraulics in a prismatic channel without changes in friction and slope, away from backwater influences, and with the approximation of a small angle of the slope, α: $\sin(\alpha) \approx \tan(\alpha) = S_0$.

(based on the friction approach 6.18). To use these equations, we need an estimate of the friction factor f, the friction coefficient, K_{st}, according to Strickler, or the friction coefficient, $n = 1/K_{\mathrm{st}}$ according to Manning.

There are many approaches for estimating friction coefficients based on properties of the river bed. One such approach for estimating the Manning coefficient, n, is shown in Table 6.1. This approach distinguishes the following contributions to the production of friction:

1. surface roughness of the river bed;
2. irregularities in the surface of the river bed;
3. irregularities in the river cross-section;
4. obstructions in the river bed;
5. vegetation;
6. effect of curves.

The total friction coefficient, n is then the sum of six terms according to

$$n = \sum_{i=1}^{6} n_i \tag{6.28}$$

Typical contributions, n_i, in this sum can be estimated according to the guidelines outlined in Table 6.1 (Cowan, 1956; French, 1985). Due to its seasonal dynamics, vegetation is a particularly difficult contribution to estimate.

Within reaches influenced by backwater effects, e.g. due to weirs, equation (6.27) is not valid. Here, the average velocity in the reservoir can be estimated from its volume,

Category	Property	Contribution to friction		
Surface material	earth	$n_1 =$	0.020	$\mathrm{s/m^{1/3}}$
of the river bed	fine gravel		0.024	$\mathrm{s/m^{1/3}}$
	coarse gravel		0.028	$\mathrm{s/m^{1/3}}$
Irregularities	smooth	$n_2 =$	0.000	$\mathrm{s/m^{1/3}}$
of the river bed	minor		0.005	$\mathrm{s/m^{1/3}}$
	moderate		0.010	$\mathrm{s/m^{1/3}}$
	severe		0.020	$\mathrm{s/m^{1/3}}$
Variation of shape	gradual	$n_3 =$	0.000	$\mathrm{s/m^{1/3}}$
of the cross-section	occasional		0.005	$\mathrm{s/m^{1/3}}$
	frequent		0.010 - 0.015	$\mathrm{s/m^{1/3}}$
Obstructions in	negligible	$n_4 =$	0.000	$\mathrm{s/m^{1/3}}$
the river bed	minor		0.010 - 0.015	$\mathrm{s/m^{1/3}}$
	appreciable		0.020 - 0.030	$\mathrm{s/m^{1/3}}$
	severe		0.040 - 0.060	$\mathrm{s/m^{1/3}}$
Vegetation	none	$n_5 =$	0.000	$\mathrm{s/m^{1/3}}$
	low		0.005 - 0.010	$\mathrm{s/m^{1/3}}$
	medium		0.010 - 0.025	$\mathrm{s/m^{1/3}}$
	high		0.025 - 0.050	$\mathrm{s/m^{1/3}}$
	very high		0.050 - 0.100	$\mathrm{s/m^{1/3}}$
Effect of curves	minor	$n_6 =$	0.000	$\mathrm{s/m^{1/3}}$
	appreciable		$0.15 \sum_{i=1}^{5} n_i$	
	severe		$0.30 \sum_{i=1}^{5} n_i$	

Table 6.1: Contributions of different causes of turbulence production in rivers to the total friction coefficient according to (Cowan, 1956). See the original reference for a more precise definition of the terms.

V, and length, L:

$$\boxed{v = \frac{QL}{V} = \frac{Q}{\bar{A}}} \tag{6.29}$$

Here, $\bar{A} = V/L$ is the average cross-sectional area of the reservoir.

From the mean flow velocity and the width of the river, the mean depth can be estimated as

$$\boxed{h = \frac{Q}{wv}} \tag{6.30}$$

Example 6.3: Glatt River downstream of Bülach: the Glatt River is strongly influenced by vegetation. This has a significant effect on its friction coefficient:

winter				summer			
n_1	=	0.028	s/m$^{1/3}$	n_1	=	0.028	s/m$^{1/3}$
n_2	=	0.005	s/m$^{1/3}$	n_2	=	0.005	s/m$^{1/3}$
n_3	=	0.000	s/m$^{1/3}$	n_3	=	0.000	s/m$^{1/3}$
n_4	=	0.000	s/m$^{1/3}$	n_4	=	0.000	s/m$^{1/3}$
n_5	=	0.010	s/m$^{1/3}$	n_5	=	0.050	s/m$^{1/3}$
n_6	=	0.000	s/m$^{1/3}$	n_6	=	0.000	s/m$^{1/3}$
n	=	0.043	s/m$^{1/3}$	n	=	0.083	s/m$^{1/3}$
K_{st}	=	23	m$^{1/3}$/s	K_{st}	=	12	m$^{1/3}$/s

With a mean width of about 16 m, a slope of 0.34 % and a discharge of 4 m^3/s we get the following values for mean flow velocity and mean depth:

winter				summer			
v	=	0.68	m/s	v	=	0.46	m/s
h	=	0.36	m	h	=	0.54	m

This demonstrates that vegetation can have a significant effect on flow velocity and water depth.

6.1.2.2 Vertical Mixing

To get a simple estimate of dispersal of a substance transported in a river using analytical solutions of the transport equation, we have to make simplifying assumptions regarding water flow. We assume the flow to have a constant velocity, v, in time and across the river cross-section and assume a constant vertical turbulent diffusion coefficient, K_z, and a constant lateral diffusion and dispersion coefficient, e_y. The combined diffusion and dispersion coefficient in lateral direction, e_y, considers the effect of secondary currents in addition to turbulence on lateral mixing. We have then the following transport equation:

$$\frac{\partial C}{\partial t} = -v\frac{\partial C}{\partial x} + e_y\frac{\partial^2 C}{\partial y^2} + K_z\frac{\partial^2 C}{\partial z^2} \tag{6.31}$$

Here, C is the concentration of the substance dissolved or suspended in the water column, t is time, x is distance along the river, y is distance across the river, z is vertical elevation, v is flow velocity (in x-direction), K_z is the coefficient of vertical turbulent diffusion, and e_y is the coefficient of lateral turbulent diffusion and dispersion.

If we limit our analysis of vertical mixing to a situation in which the substance enters the river homogeneously spread over the river width, we can omit the lateral dimension and get the following simplified steady-state equation:

$$v\frac{\partial C}{\partial x} = K_z\frac{\partial^2 C}{\partial z^2} \tag{6.32}$$

If the substance enters the river at the water surface (elevation z_0), we get the following analytical solution to this equation, which is valid as long as no considerable concentration reaches the river bed:

$$C(x,y,z) = \frac{J}{w}\frac{1}{v}\frac{2}{\sqrt{2\pi}}\frac{1}{\sigma_z(x)}\exp\left(-\frac{(z-z_0)^2}{2\sigma_z(x)^2}\right) \tag{6.33}$$

with

$$\sigma_z(x) = \sqrt{2K_z \frac{x}{v}} \tag{6.34}$$

Here, J is the mass flux of the substance entering the river at its surface, w is the river width, and z_0 is the z-coordinate of the river surface. For longer distances along the river, this solution must be extended to

$$C(x,y,z) = \frac{J}{w}\frac{1}{v}\frac{2}{\sqrt{2\pi}}\frac{1}{\sigma_z(x)}\sum_{n=-\infty}^{\infty}\exp\left(-\frac{(z-z_0-2nh)^2}{2\sigma_z(x)^2}\right) \tag{6.35}$$

This form considers the increase in concentration due to the no-flux boundary condition at the river bed. Because of the quick decrease of the exponential function, in most situations only a small number of terms must be considered in this sum.

Vertical mixing is a continuous process that approaches a uniform distribution asymptotically. Under such conditions there is no unique definition of a mixing distance. We define the mixing distance as the distance, after which the standard deviation, $\sigma_z(x)$, of the vertical substance distribution according to equation (6.34), is equal to the depth of the river. We then get the following expressions for the vertical mixing distance (horizontal distance, after which the substance is nearly homogeneously mixed over the depth of the river):

$$\boxed{s_{\mathrm{mix},z} \approx \frac{h^2}{2K_z}v} \tag{6.36}$$

Because of its quadratic dependence on the water depth, the mixing distance is reduced by a factor of four if the substance enters the river at half of the depth. Figure 6.6 shows the standard deviation of the substance distribution and corresponding substance distributions at flow distances of 1%, 10%, 25%, 50% and 100% of $s_{\mathrm{mix},z}$ according to equation (6.35). Equation (6.35) can be used to calculate the concentration difference between top and bottom of the river after the mixing distance according to equation (6.36). This relative difference is smaller than 3%.

To apply the equations (6.33), (6.34), (6.35) and (6.36) we need estimates of the mean flow velocity, v, of the mean water depth, h, and of the coefficient of vertical turbulent diffusion, K_z. For a wide rectangular channel (6.25) and in the absence of backwater effects, the mean velocity and the depth can be estimated with the aid of the equations (6.27) and (6.30). To get an estimate of the coefficient of vertical turbulent diffusion, we need an estimate of the bottom shear stress that produces turbulence. In the absence of backwater effects, when the equilibrium (6.24) applies, we get

$$\tau_0 \approx \rho g h S_0 \tag{6.37}$$

Here, τ_0 is the bottom shear stress, ρ is the density of the flowing medium, and g is the gravitational acceleration. In hydraulics, shear stresses are often expressed after division by the density and taking the square root. This leads to the shear velocity

$$u^* = \sqrt{\frac{\tau_0}{\rho}} \tag{6.38}$$

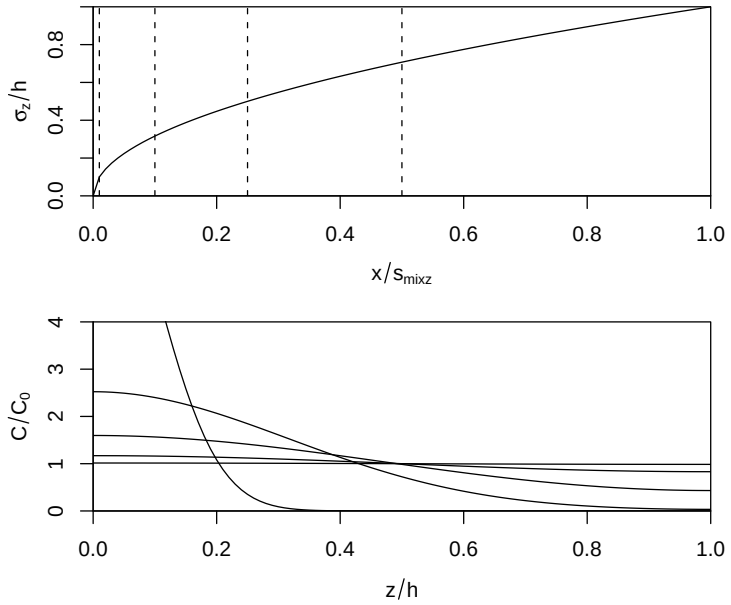

Figure 6.6: Behaviour of the standard deviation, σ_z, of the substance distribution as a function of distance, x, along the river (top) and substance distribution across the depth of the river after 1%, 10%, 25%, 50% and 100% of $s_{\mathrm{mix},z}$ (these positions are marked with dashed lines in the top figure). $C_0 = J/Q = J/(Av) \approx J((hwv)$ is the concentration after complete mixing across the river cross-section.

In the absence of backwater effects, we then get:

$$\boxed{u^* \approx \sqrt{ghS_0}} \tag{6.39}$$

The vertical profile of the flow velocity follows approximatively the logarithmic law of turbulent boundary layers:

$$v(z) = v + \frac{u^*}{\kappa}\left(1 + \log\left(\frac{z - z_{\mathrm{B}}}{h}\right)\right) \tag{6.40}$$

where $\kappa \approx 0.4$ is the Karman constant and v without argument is the depth-averaged flow velocity. We can now express the shear stress based on two different reasonings. Due to the linear decrease of shear-producing overlaying mass with increasing distance from the river bed, the shear stress decreases linearly with the distance from the river bed:

$$\tau(z) = \tau_0 \frac{z_{\mathrm{B}} + h - z}{h} = \rho u^{*2} \frac{z_{\mathrm{B}} + h - z}{h} \tag{6.41}$$

On the other hand, we can express the shear stress by the turbulent viscosity, ν_{t}, the density of water, ρ, and the velocity gradient:

$$\tau(z) = \nu_{\mathrm{t}} \rho \frac{\mathrm{d}v(z)}{\mathrm{d}z} \tag{6.42}$$

Taking the derivative of equation (6.40) and substituting it into this equation leads to

$$\tau(z) = \nu_{\mathrm{t}} \rho \frac{u^*}{\kappa} \frac{1}{z - z_{\mathrm{B}}} \tag{6.43}$$

This equation can be solved for the turbulent viscosity to yield

$$\nu_t = \frac{\tau(z)}{\rho \frac{u^*}{\kappa} \frac{1}{z - z_B}} = \kappa u^* \frac{1}{h}(z - z_B)(z_B + h - z) \tag{6.44}$$

where the linear shear stress profile (6.41) has been substituted into the first equation. We finally get the turbulent mixing coefficient, K_z, by averaging the turbulent viscosity over the depth:

$$K_z = \bar{\nu_t} = \kappa u^* \frac{1}{h^2} \int_{z_B}^{z_B+h} (z - z_B)(z_B + h - z) \mathrm{d}z = \kappa u^* h \int_0^1 \eta(1 - \eta) \mathrm{d}\eta \tag{6.45}$$

This leads to the following final expression for the coefficient of vertical turbulent diffusion:

$$\boxed{K_z \approx \frac{1}{6} \kappa u^* h \approx 0.07 u^* h} \tag{6.46}$$

Together with the equations (6.27), (6.30) and (6.39) we can get estimates of all variables of the equations (6.33), (6.35) and (6.36).

Example 6.4: Glatt River downstream of Bülach: With the data from example 6.3 (page 101) we get:

winter				summer			
K_z	=	0.0028	m^2/s	K_z	=	0.0051	m^2/s
$s_{mix,z}$	=	17	m	$s_{mix,z}$	=	14	m

The vertical mixing distances do not differ significantly for the summer and winter situation because the difference in the mixing coefficient is partially compensated by the difference in water depth (equal to the distance across which mixing must take place): The larger depth in summer leads to a larger shear force and therefore to stronger turbulence. This is partially compensated by the larger distance across which mixing must take place.

6.1.2.3 Lateral Mixing

To get a simple estimate of dispersal of a substance transported in a river using analytical solutions of the transport equation, we have to make simplifying assumptions regarding water flow. We assume the flow to have a constant velocity, v, in time and across the river cross-section and assume a constant vertical turbulent diffusion coefficient, K_z, and a constant lateral diffusion and dispersion coefficient, e_y. The combined diffusion and dispersion coefficient in lateral direction, e_y, considers the effect on secondary currents in addition to turbulence on lateral mixing. We have then the following transport equation (as in the preceding section):

$$\frac{\partial C}{\partial t} = -v \frac{\partial C}{\partial x} + e_y \frac{\partial^2 C}{\partial y^2} + K_z \frac{\partial^2 C}{\partial z^2} \tag{6.47}$$

If we limit our analysis to steady-state mixing of a substance across the river that enters the river well mixed over the river depth, we can ignore the vertical dimension and time dependence and get the following simplified equation:

$$v \frac{\partial C}{\partial x} = e_y \frac{\partial^2 C}{\partial y^2} \tag{6.48}$$

For a substance entering the river at its bank, we get the following solution, that is valid as long as the substance does not reach the other bank at considerable concentration

$$C(x,y,z) = \frac{J}{h}\frac{1}{v}\frac{2}{\sqrt{2\pi}}\frac{1}{\sigma_y(x)}\exp\left(-\frac{(y-y_0)^2}{2\sigma_y(x)^2}\right) \tag{6.49}$$

with

$$\sigma_y(x) = \sqrt{2e_y\frac{x}{v}} \tag{6.50}$$

Here, J is the mass flux of the substance entering the river at its bank, and y_0 the y-coordinate of this bank. For larger flow distances, the no-flux boundary condition at the other bank must be taken into account which leads to the following extension of the solution given above:

$$C(x,y,z) = \frac{J}{h}\frac{1}{v}\frac{2}{\sqrt{2\pi}}\frac{1}{\sigma_y(x)}\sum_{n=-\infty}^{\infty}\exp\left(-\frac{(y-y_0-2nw)^2}{2\sigma_y(x)^2}\right) \tag{6.51}$$

Due to the fast decrease of the exponential function, in most cases only a small number of terms must be considered in this sum. Close to the point of entrance into the river, the lateral extension of the substance distribution can be estimated by twice the standard deviation of the normal distribution, the maximum concentration with a rectangular distribution with half of this width. Far from the input site, the maximum concentration is equal to the concentration after complete mixing across the cross-sectional area. This leads to the following estimates of the width and the maximum concentration of the substance distribution:

$$\boxed{\begin{aligned} L_y &\approx 2\sigma_y(x) = 2\sqrt{2e_y\frac{x}{v}} \\ C_{\max} &\approx \frac{J}{hv}\frac{1}{\min(\sigma_y(x),w)} = \frac{J}{hv}\frac{1}{\min\left(\sqrt{2e_y\frac{x}{v}},w\right)} \end{aligned}} \tag{6.52}$$

Similarly to the vertical case, we define the lateral mixing distance (i.e. the distance along the river after which the substance is approximately evenly distributed in lateral direction) by the criterion that the standard deviation, $\sigma_y(x)$, of the substance distribution is equal to the river width. This leads to the following estimate for the lateral mixing distance:

$$\boxed{s_{\mathrm{mix},y} \approx \frac{w^2}{2e_y}v} \tag{6.53}$$

Because of the quadratic dependence of the mixing distance on river width, the mixing distance is reduced to one fourth if the substance enters the river in its centre instead of the bank. Figure 6.7 shows the dependence of the width $\sigma_y(x)$ of the substance distribution along the river according to eqation (6.50) and typical distributions of concentration across the river width according to equation (6.51). The relative difference in substance concentration between the river banks is smaller than 3% after a transport distance of $s_{\mathrm{mix},y}$ according to equation (6.53).

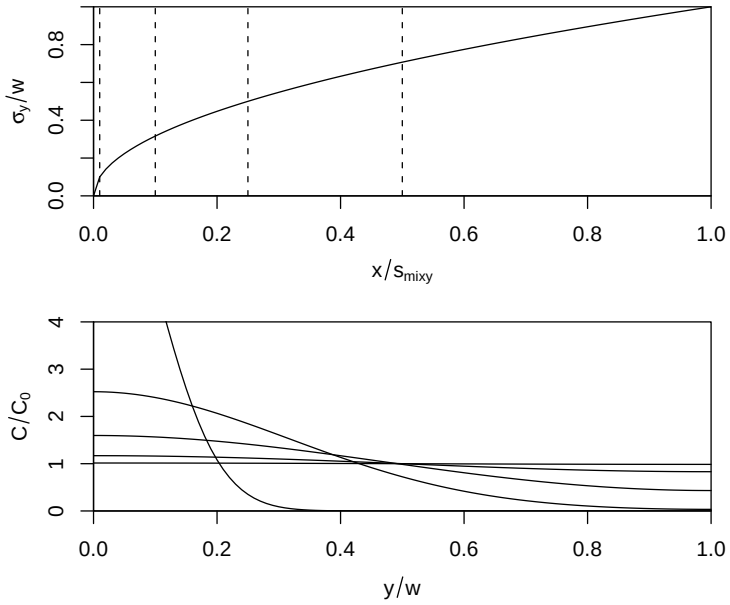

Figure 6.7: Dependence of the width of the substance distribution along the river (top) and typical shapes of the substance distribution across the river after 1%, 10%, 25%, 50% and 100% of $s_{\mathrm{mix},y}$ (these positions are marked with dashed lines in the top figure). $C_0 = J/Q = J/(Av) \approx J((hwv)$ is the concentration after complete mixing across the river cross-section.

To apply the equations (6.49), (6.50), (6.51), (6.52) and (6.53) we need estimates of the mean flow velocity, v, of the mean water depth, h and of the coefficient of lateral turbulent diffusion plus dispersion, e_y. As rivers are usually not thermally stratified, the coefficient of lateral turbulent diffusion is of a similar size as that of vertical turbulent diffusion (see section 6.1.2.2). However, due to the larger width compared to the depth, we can have larger turbulent eddies which increase the coefficient of turbulent diffusion. Analogously to the coefficient of vertical turbulent diffusion (6.46) we then get

$$K_x \approx K_y \approx \theta_K u^* h \tag{6.54}$$

with a somewhat larger proportionality factor

$$\theta_K \approx 0.15 \quad . \tag{6.55}$$

The coefficient of lateral diffusion plus dispersion includes additionally to turbulence the effect of secondary currents on lateral mixing (such currents are often induced by curves). With the same approach as above, we then get

$$\boxed{e_y \approx \theta_e u^* h} \tag{6.56}$$

with a larger proportionality factor

$$\boxed{\theta_e \approx 0.6} \tag{6.57}$$

For very strongly meandering rivers, this factor can even be much larger up to values in the order of 2.5 (Fischer et al., 1979).

Example 6.5: Glatt River downstream of Bülach: Using the data of example 6.3 (page 101; see also example 6.4 on page 104) we get:

winter				summer			
e_y	=	0.024	m^2/s	e_y	=	0.043	m^2/s
$s_{mix,y}$	=	3600	m	$s_{mix,y}$	=	1400	m

Please note that mixing distances in a river with a width of 16 m can already be of considerable length. This must be considered when taking water samples downstream of tributaries or pollutant discharge sites.

6.1.2.4 Transport and Longitudinal Dispersion

As it is clearly visible in Figure 6.8, the lateral velocity profile has a strong influence on longitudinal dispersion. Dissolved or suspended substances are transported much slower close to the river banks than in the centre of the river. Lateral mixing moves substance

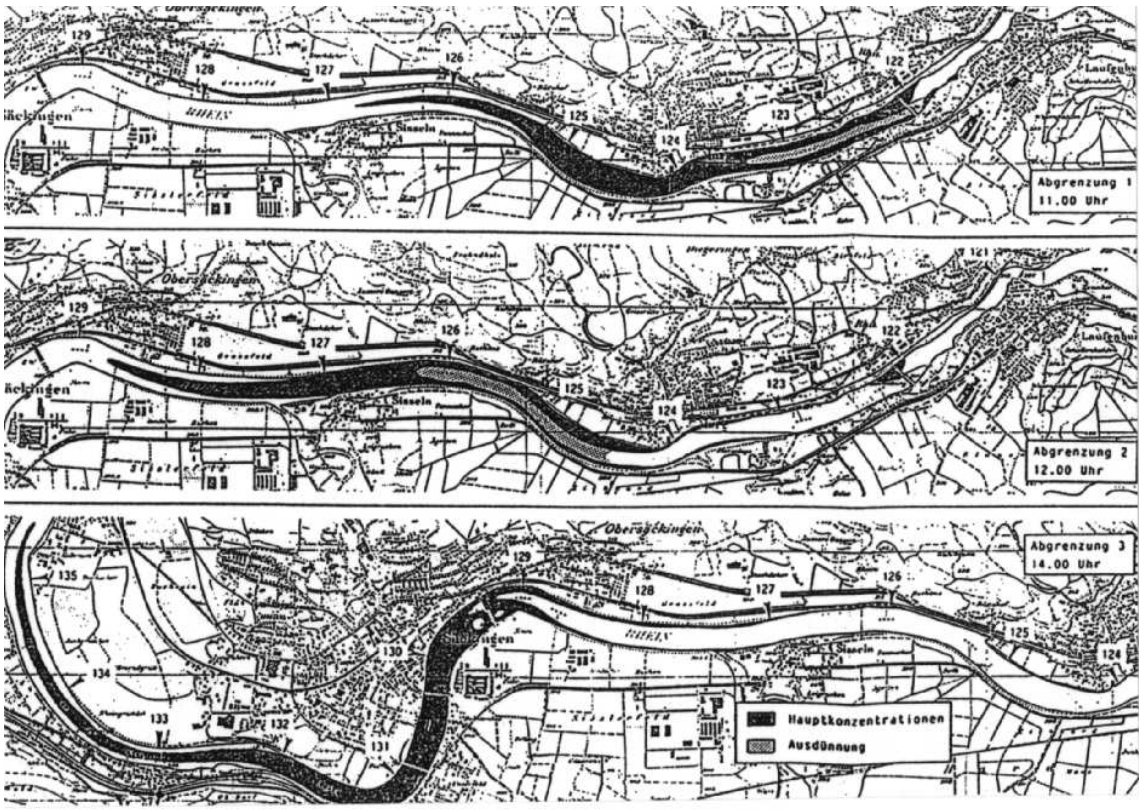

Figure 6.8: Transport and spreading of a fluorescence dye pulse in the Rhine River at three different points in time (Leibundgut et al., 1988).

particles or molecules between the zones of different longitudinal transport velocity. The differences in longitudinal transport velocities are the main cause for longitudinal spreading of a substance pulse in the river. This effect is much larger than the effect of longitudinal turbulent diffusion. As high turbulent diffusion leads to a fast exchange between the zones of different advective velocities, longitudinal dispersion decreases with increasing lateral turbulence.

To get simple estimates of longitudinal dispersion based on analytical solutions of the transport equation for distances large compared to the lateral mixing distance, we describe longitudinal transport by a one-dimensional advection-diffusion (or -dispersion) equation:

$$\frac{\partial C}{\partial t} = -v\frac{\partial C}{\partial x} + E_x\frac{\partial^2 C}{\partial x^2} \tag{6.58}$$

In this equation, E_x is the coefficient of longitudinal dispersion. The solution to this equation for a pulse input of mass m is given by

$$C(x,t) = \frac{m}{hw}\frac{1}{\sqrt{2\pi}}\frac{1}{\sigma_x(t)}\exp\left(-\frac{(x-vt)^2}{2\sigma_x(t)^2}\right) \tag{6.59}$$

with

$$\sigma_x(t) = \sqrt{2E_x t} \tag{6.60}$$

This solution describes advective transport of the pulse with mean velocity v and spreading of the pulse due to longitudinal dispersion quantified by the dispersion coefficient E_x.

To use the equation given above, in addition to the mean flow velocity, v, we need an estimate of the longitudinal dispersion coefficient, E_x. Such an estimate is given by (Fischer, 1967; Fischer et al., 1979):

$$\boxed{E_x \approx c_f\frac{w^2v^2}{u^*h}} \tag{6.61}$$

where the non-dimensional proportionality factor can be estimated by

$$\boxed{c_f \approx 0.011} \tag{6.62}$$

Equation (6.61) shows the effect of different mechanisms that contribute to longitudinal dispersion:

- Dispersion increases with increasing velocity differences across the river. As velocity is (close to) zero at the river bank and the shape of the velocity profile does not change too strongly from one river to the other, the velocity differences can be parameterized with the mean velocity (the effect of the velocity profile influences the value of the coefficient c_f). The increasing effect of increasing velocity differences on dispersion is expressed by the proportionality to v^2.

- Dispersion increases with increasing width of the river, because increasing width significantly decreases lateral mixing. This leads to the proportionality with w^2.

- Dispersion decreases with increasing lateral turbulent diffusivity, as this increases mixing across the river. This leads to the proportionality with $1/(u^*h)$ (see equation 6.56).

The position of the pulse can be estimated with the aid of the mean flow velocity, the length with four times the standard deviation of the substance distribution, and the

maximum concentration with a rectangular pulse with half of this length. This leads to the following estimates:

$$\boxed{\begin{aligned} s_x &\approx vt \\ L_x &\approx 4\sigma_x(t) = 4\sqrt{2E_x t} \\ C_{\max} &\approx \frac{m}{hw}\frac{1}{2\sigma_x(t)} = \frac{m}{hw}\frac{1}{2\sqrt{2E_x t}} \end{aligned}} \tag{6.63}$$

The second of these equations is derived from the property of the normal distribution (6.59) that 95% of the substance mass is within a length of four times the standard deviation. This can also be used as a rough estimate of the length of a concentration pulse that is not normally distributed.

Example 6.6: Glatt River downstream of Bülach: With the data from example 6.3 (page 101; see also examples 6.4 and 6.5 on pages 104 and 107) we get:

winter				summer			
E_x	=	33	m^2/s	E_x	=	8	m^2/s

The significantly stronger mixing across the width of the river (see example 6.5 on page 107) reduces longitudinal dispersion considerably in summer compared to the winter situation. Note that the length of the pulse (6.63) depends only on the square root of E_x.

Many simple models of rivers approximate the river by a sequence of mixed reactors. The distance along the river is divided into sections of length Δx. For a river with mean width, w, mean depth, h, and discharge, Q, the description uses mixed reactors of volume

$$\boxed{V = wh\Delta x} \tag{6.64}$$

Mixing within these boxes results in longitudinal dispersion with an equivalent dispersion coefficient given by

$$\boxed{E_x = \frac{v\Delta x}{2} = \frac{Q\Delta x}{2wh}} \tag{6.65}$$

This effect is called “numerical diffusion”.

6.2 Sedimentation

Sedimentation is an important process as it transports organic and inorganic particles to the sediment where heterotrophic bacteria degrade organic matter. As the bacterial density is usually much higher in the sediment than in the water column, the degradation rate is much higher in the sediment. In lakes, slowly degradable organic particles accumulate together with inorganic particles in the sediment. In rivers, periodic resuspension events during floods may remobilize the sediment and transport it further downstream. However, also in rivers, there may be zones of sediment accumulation, particularly upstream of dams or in zones that are only slightly coupled to the main channel.

According to Stokes' Law, the sedimentation velocity of small particles in laminar conditions is given by

$$v_{\text{sed}} = f_{\text{st}} \, \frac{g}{18} \, \frac{\rho_{\text{p}} - \rho_{\text{w}}}{\mu} \, d_{\text{p}}^2 \tag{6.66}$$

The symbols in this equation have the following meaning:

- g: gravitational acceleration (LT^{-2}).
- ρ_{p}: density of the particle (ML^{-3}).
- ρ_{w}: density of water (ML^{-3}).
- μ: dynamic viscosity of water ($\text{ML}^{-1}\text{T}^{-1}$).
- d_{p}: particle diameter (L).
- f_{st}: shape factor (1.0 for spheres).

Settling velocities depend strongly on particle size and are in the following ranges

$$\boxed{\begin{array}{lcl} v_{\text{sed,ALG}} & \approx & 0.0 - 0.3 \text{ m/d} \\ v_{\text{sed,POM}} & \approx & 0.2 - 2.5 \text{ m/d} \\ v_{\text{sed,clay}} & \approx & 0.3 - 1.0 \text{ m/d} \\ v_{\text{sed,silt}} & \approx & 3.0 - 30 \text{ m/d} \end{array}} \tag{6.67}$$

where ALG refers to algae, POM to dead organic particles, and clay ($< 4\mu$m) and silt (4-63μm) are size fractions of inorganic suspended particles. There is experimental (Ruiz et al., 2005) and theoretical (Bosse and Kleiser, 2005) evidence, that settling velocities tend to increase under turbulent conditions.

Sedimentation is represented by a downward flux

$$\boxed{J_{\text{sed,POM}} = A_{\text{sed}} \, v_{\text{sed,POM}} \, C_{\text{POM}}} \tag{6.68}$$

where A_{sed} is the cross-sectional area of the water column and sediment and C_{POM} is the concentration of particulate organic particles in the water column. The formulation of the sediment flux for the other compounds is analogous. This flux can be used as an interface flux between mixed boxes or in a model with continuous vertical space resolution (see sections 3.3 and 3.4 for more details).

6.3 Gas Exchange

Mineralization, primarily in the sediment, can lead to very strong oxygen depletion in the water column. This is particularly the case in the deep hypolimnion of a lake or during night in a river, when the loss is not compensated by oxygen produced by primary production. For this reason, oxygen exchange across the water surface is extremely important to compensate for this oxygen loss. On the other hand, oxygen transfer across the water surface helps limiting supersaturation during strong primary production periods. Besides dissolved oxygen, carbon dioxide is another important gas exchanged across the water surface. Due to carbon dioxide uptake during periods of strong primary production, inorganic carbon (usually dominated by bicarbonate) concentrations can be reduced significantly. If this is not balanced by carbon dioxide uptake from the atmosphere, this can lead to very strong pH changes, or in extreme cases, even to a carbon limitation of growth.

In equilibrium, the concentration in the water phase would be equal to the equilibrium concentration, which, according to Henry's law, is given by

$$C_{\mathrm{w,eq}}(C_{\mathrm{a}}) = \frac{C_{\mathrm{a}}}{H} \tag{6.69}$$

where C_{w} is the concentration in the water phase, C_{a} is the concentration in the air phase, and H is the non-dimensional Henry's law coefficient. If there is consumption or production of the gas in one of the phases, the concentrations will no longer be in equilibrium and a gas exchange flux will be established that tends to reestablish the equilibrium. The simplest model of such a gas exchange process assumes two molecular boundary layers at the water and air sides of the interface which limit the gas exchange (Whitman, 1923). Figure 6.9 illustrates this concept. At the interface, there is an equilibrium between the

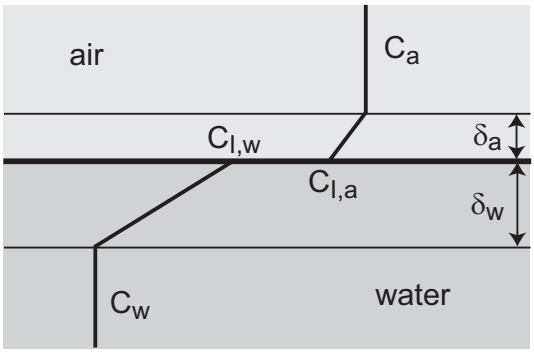

Figure 6.9: Illustration of two-film gas exchange model (see text for more explanations).

concentrations in the gas-phase and in the water-phase:

$$C_{\mathrm{I,w}} = \frac{C_{\mathrm{I,a}}}{H} \tag{6.70}$$

where $C_{\mathrm{I,w}}$ is the concentration in the water at the interface to the air, $C_{\mathrm{I,a}}$ is the concentration in the air at the interface to the water. As there is no accumulation of the gas at the interface, the fluxes across the two boundary layers must both be equal to the flux across the interface:

$$J_{\mathrm{gasex}} = AD_{\mathrm{w}}\frac{C_{\mathrm{I,w}} - C_{\mathrm{w}}}{\delta_{\mathrm{w}}} = AD_{\mathrm{a}}\frac{C_{\mathrm{a}} - C_{\mathrm{I,a}}}{\delta_{\mathrm{a}}} \tag{6.71}$$

where D_w is the coefficient of molecular diffusion of the substance in the water phase, D_a is the coefficient of molecular diffusion of the substance in the air phase, δ_w is the thickness of the molecular boundary layer in the water phase, δ_a is the thickness of the molecular boundary layer in the air phase, and A is the interface area. When substituting the equilibrium equation (6.70) into this equation, we can solve the equality of the fluxes through the two layers for the interface concentration in the air phase

$$C_\mathrm{I,a} = \frac{\delta_\mathrm{w} D_\mathrm{a} C_\mathrm{a} + \delta_\mathrm{a} D_\mathrm{w} C_\mathrm{w}}{\frac{\delta_\mathrm{a} D_\mathrm{w}}{H} + \delta_\mathrm{w} D_\mathrm{a}} \tag{6.72}$$

Substituting this expression back into the flux in the air boundary layer yields

$$\boxed{J_\mathrm{gasex} = A\, v_\mathrm{ex} \left(C_\mathrm{w,eq}(C_\mathrm{a}) - C_\mathrm{w} \right)} \tag{6.73}$$

with the gas exchange velocity

$$v_\mathrm{ex} = \frac{D_\mathrm{a} D_\mathrm{w}}{\frac{\delta_\mathrm{a} D_\mathrm{w}}{H} + \delta_\mathrm{w} D_\mathrm{a}} \tag{6.74}$$

Note that equation (6.73) expresses the gas flux across the interface as a function of the concentration in the water phase and the equilibrium concentration corresponding to the concentration in the air phase. The concentrations at the interface are eliminated from this final equation to estimate the flux. We can write the gas exchange velocity as

$$\boxed{v_\mathrm{ex} = \frac{1}{\frac{1}{v_\mathrm{ex,a}} + \frac{1}{v_\mathrm{ex,w}}} \quad \text{with} \quad v_\mathrm{ex,a} = H \frac{D_\mathrm{a}}{\delta_\mathrm{a}} \quad \text{and} \quad v_\mathrm{ex,w} = \frac{D_\mathrm{w}}{\delta_\mathrm{w}}} \tag{6.75}$$

This equation demonstrates that the gas exchange resistance $1/v_\mathrm{ex}$ is the sum of the resistance in the air boundary layer $1/v_\mathrm{ex,a}$ and the resistance in the water boundary layer $1/v_\mathrm{ex,w}$.

We will use the gas exchange formulation given by equation (6.73) with using an empirical estimate for the gas exchange velocity, v_ex. In many practical cases, the resistance of one boundary layer dominates over the other in equation (6.75). In this case the gas exchange velocity is proportional to the molecular diffusion coefficient in the phase that dominates the gas exchange resistance. This means that gas exchange velocities of different substances, the exchange of which is limited by the boundary layer in the same phase, are related to each other by the ratio of the molecular diffusion coefficients in that phase. Note that other models (Higbie, 1935; Danckwerts, 1951) lead to a multiplication with the square root of the ratio of the diffusion coefficients instead of the ratio itself.

The equilibrium concentration of dissolved oxygen in water that is in contact with the atmosphere (with its given oxygen concentration) is of particular importance. It can be estimated by (Mortimer, 1981):

$$C_{\mathrm{w,eq,O_2}}(T,p) = \exp\bigl(7.7117 - 1.31403 \log(T/1^\circ\mathrm{C} + 45.93)\bigr) \cdot 1\mathrm{gO/m^3} \cdot \frac{p}{1013.25\,\mathrm{hPa}} \,. \tag{6.76}$$

In this equation, T is temperature in °C and p is air pressure in hPa.

6.4 Detachment and Resuspension

Besides respiration and death with subsequent mineralization, detachment or resuspension are important mechanisms to diminish periphyton and sediment deposits in rivers.

We can formulate the detachment or resuspension flux of particles from the sediment as a maximum flux that depends on the bottom shear stress and the dissipation power of the river and a limitation term with respect to the surface density of particles. For organic particles, POM, this leads to the following detachment flux:

$$\boxed{J_{\text{det,POM}} = J_{\text{det,POM,max}} \frac{D_{\text{SPOM}}}{K_{\text{SPOM,det}} + D_{\text{SPOM}}}} \tag{6.77}$$

We assume the maximum flux to be zero unless a certain threshold of the bottom shear stress is exceeded. This threshold depends on the particle density and size. Under uniform flow conditions, the bottom shear stress is given by

$$\tau_0 = \rho_{\text{w}} g h S_0 \tag{6.78}$$

where ρ_{w} is the density of water, g the gravitational acceleration, h the water depth, and S_0 the slope of the river bed. This shear stress leads to the following force when integrated over the surface of the particle (for simplicity assumed of quadratic shape)

$$F_{\text{s}} = \rho_{\text{w}} g h S_0 \cdot d_{\text{p}}^2 \tag{6.79}$$

where d_{p} is the particle diameter. This force has to be compared with the gravitational force acting against lift forces on the particle (again for simplicity, we assume a cubic form of the particle)

$$F_{\text{p}} = (\rho_{\text{p}} - \rho_{\text{w}})\ g\ d_{\text{p}}^3 \tag{6.80}$$

where ρ_{p} is the density of the particle. The ratio of these two forces is the non-dimensional shear force

$$\boxed{\theta = \frac{F_{\text{s}}}{F_{\text{p}}} = \frac{h\ S_0}{\frac{\rho_{\text{p}} - \rho_{\text{w}}}{\rho_{\text{w}}}\ d_{\text{p}}}} \tag{6.81}$$

This non-dimensional shear stress allows us to formulate a universal critical shear stress, θ_{cr}, below which there is no detachment or resuspension. This critical non-dimensional shear stress is in the order of

$$\theta_{\text{cr}} \approx 0.047 \tag{6.82}$$

This threshold is of particular importance when applied to the gravel particles of the river bed. Above the threshold we can assume bed movement of gravel. This leads to catastrophic elimination of sessile algae that are attached to the gravel surfaces.

For lighter or smaller particles that can be suspended in the water column, we assume that a constant fraction, f_{entr}, of the dissipation power of the river is used for particle entrainment when the bottom shear stress is above the critical threshold. The dissipation

power of a river with uniform flow per surface area is given by (weight per surface area times vertical velocity):

$$p_{\text{river}} = \rho_{\text{w}} g h \cdot v S_0 \tag{6.83}$$

The power per surface area required to lift sediment particles by $h/2$ is given by (specific weight times volume flux times elevation difference):

$$p_{\text{entr}} = (\rho_{\text{p}} - \rho_{\text{w}}) g \cdot \frac{J_{\text{det,POM,max}}}{\rho_{\text{p}}} \cdot \frac{h}{2} \tag{6.84}$$

Assuming a fixed fraction, f_{entr}, of the dissipation power to be used to resuspend sediment particles if the non-dimensional shear stress exceeds a critical value leads to the following expression for the maximum resuspension flux:

$$\boxed{J_{\text{det,POM,max}} = \begin{cases} 2\ f_{\text{entr}}\ v\ S_0\ \dfrac{\rho_{\text{p}} \rho_{\text{w}}}{\rho_{\text{p}} - \rho_{\text{w}}} & \text{for } \theta > \theta_{\text{cr}} \\ 0 & \text{for } \theta \leq \theta_{\text{cr}} \end{cases}} \tag{6.85}$$

Chapter 7

Chemical Processes

The most important chemical processes for biogeochemical-ecological lake models are chemical equilibria and sorption processes.

The consideration of chemical equilibria in the process formulation of models as used in this manuscript is discussed in section 7.1 with the examples of the equilibria of self-ionization of water, speciation of inorganic carbon, nitrogen and phosphorus compounds, and calcite precipitation and dissolution.

Sorption of chemical substances to particles in the water column can play an important role in aquatic systems. In particular, sorption of dissolved substances to sedimenting particles can increase the elimination rate of substances from the water column considerably. However, one should be aware that resuspension or mineralization of such particles can be accompanied by desorption and release of the adsorbed substances. Sorption is of particular interest for organic pollutants, heavy metals, and phosphate. The formulation of adsorption and desorption processes or of adsorption/desorption equilibria are discussed in section 7.2.

7.1 Chemical Equilibria

Table 7.1 summarizes the most important chemical equilibria for modelling speciation of inorganic carbon, nitrogen, and phosphorus compounds, precipitation and dissolution of calcite, and pH in ecological-biogeochemical models. Under typical pH conditions of natural waters between 7 and 9 the number of equilibria can even be reduced by neglecting the compounds H_2CO_3, H_3PO_4, and PO_4^{3-}. We discuss here how these speciation processes can be included in ecological-biogeochemical models. For a more extensive discussion of chemical equilibria in water we refer to the literature (Stumm and Morgan, 1981; Appelo and Postma, 2005).

Another important process for the calculation of carbonate equilibria is the dissolution of atmospheric carbon dioxide in the water since the equilibrium concentration of dissolved carbon species depends on the partial pressure of carbon dioxide in the atmosphere. Rapid consumption of inorganic carbon compounds by primary production can exceed transfer across the air-water interface. This can lead to significant deviations of dissolved carbon dioxide concentrations from equilibrium and thus requires a dynamic calculation of the gas-transfer process. This process is described in chapter 6.3.

From a chemical point of view, the most straightforward way of modelling the equilibria listed in Table 7.1 would be to formulate forward and backward reactions as shown in Table 7.2 with the last two rates given by

$$\rho_{\mathrm{CaCO_3,prec}} = \begin{cases} k_{\mathrm{CaCO_3,prec}}(\Omega_{\mathrm{CaCO_3}} - 1) & \text{if } \Omega_{\mathrm{CaCO_3}} > 1 \\ 0 & \text{if } \Omega_{\mathrm{CaCO_3}} \leq 1 \end{cases} \tag{7.1}$$

$$\rho_{\mathrm{CaCO_3,diss}} = \begin{cases} 0 & \text{if } \Omega_{\mathrm{CaCO_3}} \geq 1 \\ k_{\mathrm{CaCO_3,diss}}(1 - \Omega_{\mathrm{CaCO_3}}) \dfrac{D_{\mathrm{CaCO_3}}}{K_{\mathrm{CaCO_3}} + D_{\mathrm{CaCO_3}}} & \text{if } \Omega_{\mathrm{CaCO_3}} < 1 \end{cases} \tag{7.2}$$

with

$$\Omega_{\mathrm{CaCO_3}} = \frac{C_{\mathrm{Ca^{2+}}} C_{\mathrm{CO_3^{2-}}}}{K_{\mathrm{CaCO_3}}} \tag{7.3}$$

Ω is a measure for the saturation state of the solution with respect to a certain mineral and is calculated as the ratio between the ion activity product (IAP) and the solubility constant (K). If Ω is > 1, the solution is oversaturated and if Ω is < 1, the solution is undersaturated with respect to the considered mineral.

For each equilibrium, this process formulation leads to two processes with one kinetic parameter for each process. As the equilibrium is characterized by the same forward and backward transformation rates of all species and we used the same stoichiometric coefficients with reversed sign, the equilibrium is characterized by the condition that the process rates of forward and backward reaction are the same (principle of detailed balancing). This leads to the following relations between kinetic parameters (lower case "k", see Table 7.2) and equilibrium parameters (upper case "K", see Table 7.1):

$$K_{\mathrm{w}} = \frac{k_{\mathrm{w,fw}}}{k_{\mathrm{w,bw}}} \tag{7.4}$$

Process	Chemical equation	Equilibrium condition
Self-ionization of water	$H_2O \leftrightarrow H^+ + OH^-$	$C_{OH^-} \cdot C_{H^+} = K_w$
Carbonate equilibria	$CO_2(aq) + H_2O \leftrightarrow H_2CO_3$	$\frac{C_{CO_2}}{C_{H_2CO_3}} = K_{CO_2,H_2CO_3}$
	$H_2CO_3 \leftrightarrow H^+ + HCO_3^-$	$\frac{C_{H^+} \cdot C_{HCO_3^-}}{C_{H_2CO_3}} = K_{HCO_3^-,H_2CO_3}$
	$HCO_3^- \leftrightarrow H^+ + CO_3^{2-}$	$\frac{C_{H^+} \cdot C_{CO_3^{2-}}}{C_{HCO_3^-}} = K_{CO_3^{2-},HCO_3^-}$
Composite carbonate equilibrium $C_{H_2CO_3^*} = C_{H_2CO_3} + C_{CO_2}$	$H_2CO_3^* \leftrightarrow H^+ + HCO_3^-$	$\frac{C_{H^+} \cdot C_{HCO_3^-}}{C_{H_2CO_3} + C_{CO_2}} = \frac{C_{H^+} \cdot C_{HCO_3^-}}{C_{H_2CO_3^*}} = \frac{K_{HCO_3^-,H_2CO_3}}{1 + K_{CO_2,H_2CO_3}} = K_{HCO_3^-,H_2CO_3^*}$
Phosphate equilibria	$H_3PO_4 \leftrightarrow H^+ + H_2PO_4^-$	$\frac{C_{H^+} \cdot C_{H_2PO_4^-}}{C_{H_3PO_4}} = K_{H_2PO_4^-,H_3PO_4}$
	$H_2PO_4^- \leftrightarrow H^+ + HPO_4^{2-}$	$\frac{C_{H^+} \cdot C_{HPO_4^{2-}}}{C_{H_2PO_4^-}} = K_{HPO_4^{2-},H_2PO_4^-}$
	$HPO_4^{2-} \leftrightarrow H^+ + PO_4^{3-}$	$\frac{C_{H^+} \cdot C_{PO_4^{3-}}}{C_{HPO_4^{2-}}} = K_{PO_4^{3-},HPO_4^{2-}}$
Ammonium equilibrium	$NH_4^+ \leftrightarrow H^+ + NH_3$	$\frac{C_{H^+} \cdot C_{NH_3}}{C_{NH_4^+}} = K_{NH_3,NH_4^+}$
Calcite equilibrium	$Ca^{2+} + CO_3^{2-} \leftrightarrow CaCO_3$	$C_{Ca^{2+}} \cdot C_{CO_3^{2-}} = K_{CaCO_3}$

Table 7.1: Most important chemical equilibria in aquatic systems. Note that the composite carbonate equilibrium can be used instead of the first two carbonate equilibria listed above (it is not an additional equilibrium). This is often introduced because of the analytical difficulty of distinguishing H_2CO_3 from CO_2.

Process	H_2O mol	H^+ mol	OH^- mol	CO_2 gC	H_2CO_3 gC	HCO_3^- gC	CO_3^{2-} gC	H_3PO_4 gP	$H_2PO_4^-$ gP	HPO_4^{2-} gP	PO_4^{3-} gP	NH_4^+ gN	NH_3 gN	Ca^{2+} mol	$CaCO_3$ mol	Rate
$H_2O \rightarrow H^+ + OH^-$	−1	1	1													$k_{w,fw}$
$H_2O \leftarrow H^+ + OH^-$	1	−1	−1													$k_{w,bw} C_{H^+} C_{OH^-}$
$CO_2 + H_2O \rightarrow H_2CO_3$	−1/12			−1	1											$k_{CO_2,H_2CO_3} C_{CO_2}$
$CO_2 + H_2O \leftarrow H_2CO_3$	1/12			1	−1											$k_{H_2CO_3,CO_2} C_{H_2CO_3}$
$H_2CO_3 \rightarrow H^+ + HCO_3^-$		1/12			−1	1										$k_{H_2CO_3,HCO_3^-} C_{H_2CO_3}$
$H_2CO_3 \leftarrow H^+ + HCO_3^-$		−1/12			1	−1										$k_{HCO_3^-,H_2CO_3} C_{H^+} C_{HCO_3^-}$
$HCO_3^- \rightarrow H^+ + CO_3^{2-}$		1/12				−1	1									$k_{HCO_3^-,CO_3^{2-}} C_{HCO_3^-}$
$HCO_3^- \leftarrow H^+ + CO_3^{2-}$		−1/12				1	−1									$k_{CO_3^{2-},HCO_3^-} C_{H^+} C_{CO_3^{2-}}$
$H_3PO_4 \rightarrow H^+ + H_2PO_4^-$		1/31						−1	1							$k_{H_3PO_4,H_2PO_4^-} C_{H_3PO_4}$
$H_3PO_4 \leftarrow H^+ + H_2PO_4^-$		−1/31						1	−1							$k_{H_2PO_4^-,H_3PO_4} C_{H^+} C_{H_2PO_4^-}$
$H_2PO_4^- \rightarrow H^+ + HPO_4^{2-}$		1/31							−1	1						$k_{H_2PO_4^-,HPO_4^{2-}} C_{H_2PO_4^-}$
$H_2PO_4^- \leftarrow H^+ + HPO_4^{2-}$		−1/31							1	−1						$k_{HPO_4^{2-},H_2PO_4^-} C_{H^+} C_{HPO_4^{2-}}$
$HPO_4^{2-} \rightarrow H^+ + PO_4^{3-}$		1/31								−1	1					$k_{HPO_4^{2-},PO_4^{3-}} C_{HPO_4^{2-}}$
$HPO_4^{2-} \leftarrow H^+ + PO_4^{3-}$		−1/31								1	−1					$k_{PO_4^{3-},HPO_4^{2-}} C_{H^+} C_{PO_4^{3-}}$
$NH_4^+ \rightarrow H^+ + NH_3$		1/14										−1	1			$k_{NH_4^+,NH_3} C_{NH_4^+}$
$NH_4^+ \leftarrow H^+ + NH_3$		−1/14										1	−1			$k_{NH_3,NH_4^+} C_{H^+} C_{NH_3}$
$Ca^{2+} + CO_3^{2-} \rightarrow CaCO_3$							−12							−1	1	$\rho_{CaCO_3,prec}$
$Ca^{2+} + CO_3^{2-} \leftarrow CaCO_3$							12							1	−1	$\rho_{CaCO_3,diss}$

Table 7.2: Process table of forward and backward reactions of the equilibria listed in Table 7.1.

$$K_{CO_2,H_2CO_3} = \frac{k_{H_2CO_3,CO_2}}{k_{CO_2,H_2CO_3}} \tag{7.5a}$$

$$K_{HCO_3^-,H_2CO_3} = \frac{k_{H_2CO_3,HCO_3^-}}{k_{HCO_3^-,H_2CO_3}} \tag{7.5b}$$

$$K_{CO_3^{2-},HCO_3^-} = \frac{k_{HCO_3^-,CO_3^{2-}}}{k_{CO_3^{2-},HCO_3^-}} \tag{7.5c}$$

$$K_{H_2PO_4^-,H_3PO_4} = \frac{k_{H_3PO_4,H_2PO_4^-}}{k_{H_2PO_4^-,H_3PO_4}} \tag{7.6a}$$

$$K_{HPO_4^{2-},H_2PO_4^-} = \frac{k_{H_2PO_4^-,HPO_4^{2-}}}{k_{HPO_4^{2-},H_2PO_4^-}} \tag{7.6b}$$

$$K_{PO_4^{3-},HPO_4^{2-}} = \frac{k_{HPO_4^{2-},PO_4^{3-}}}{k_{PO_4^{3-},HPO_4^{2-}}} \tag{7.6c}$$

$$K_{NH_3,NH_4^+} = \frac{k_{NH_4^+,NH_3}}{k_{NH_3,NH_4^+}} \tag{7.7}$$

An alternative formulation of the equilibria would be to use only one process for the approach to equilibrium (Reichert et al., 2001).

When considering the constraints (7.4) to (7.7), the process formulation used in Table 7.2 for the equilibria between dissolved compounds requires the specification of the equilibrium parameter, K, and one of the kinetic parameters, k. As the kinetics of these processes are very fast, inclusion of these processes leads to stiffness problems of the differential equations to be solved for calculating the dynamic solution (see chapter 5.4). To decrease the severity of these numerical problems, kinetics of chemical equilibria are usually not described by realistic kinetics in ecological-biogeochemical models. Instead, kinetic parameters are chosen to be sufficiently large that the involved compounds will be very close to equilibrium for the given time scale of external influence factors and biological and physical processes, but as small as possible to not increase the numerical burden unnecessarily.

7.2 Sorption

In this section implementation of the processes of adsorption of chemical substances to and desorption of substances from particles in the water column or the sediment are introduced.

Analogously to the chemical equilibria described in section 7.1, reversible sorption processes can be formulated as a forward (adsorption) and a backward (desorption) reaction. The stoichiometries of the adsorption and desorption processes are simple, as the processes consist of attachment of the compound to a solid surface or detachment of the compound from the surface without transformation of the compound. Table 7.3 shows a process table of the adsorption and desorption processes of a substance j to a solid surface.

Process	Substances		Rate
	dissolved subst. j	adsorbed subst. j	
	g	g	
Adsorption of substance j	-1	1	$\rho_{\mathrm{ads},j}$
Desorption of substance j	1	-1	$\rho_{\mathrm{des},j}$

Table 7.3: Process table of adsorption and desorption of a substance to a particle or solid surface.

To formulate the rate expressions, $\rho_{\mathrm{ads},j}$ and $\rho_{\mathrm{des},j}$, respectively, we need to quantify the amount of dissolved and adsorbed substances. The dissolved substance is characterized by its concentration in the water phase, i.e. the dissolved substance mass per unit volume of water, C_j. The adsorbed substance is usually characterized by the adsorbed substance mass per unit mass of the sorbent (the solids with the surface to which the substance adsorbs), S_j. When describing sorption to particles that are present in small concentration in the water (particles do not significantly contribute to the volume of the suspension), the total concentration of dissolved and particulate substances is given by

$$C_j^{\mathrm{tot}} = C_j + C_{\mathrm{s}} S_j \tag{7.8a}$$

where C_{s} is the concentration of the particles. If the particles contribute significantly to the volume, e.g. in the sediment of an aquatic system, the total concentration (total mass per total volume) is given as

$$C_j^{\mathrm{tot}} = \theta C_j + (1-\theta)\rho_{\mathrm{s}} S_j \tag{7.8b}$$

where θ is the porosity (fraction of the volume filled by water), and ρ_{s} is the density of the solid material (filling the remaining fraction of $1-\theta$ of the volume). Please note that the conversion factors

$$f_{S\to C}^{C_{\mathrm{s}}} = C_{\mathrm{s}} \quad , \quad f_{S\to C}^{\theta,\rho_{\mathrm{s}}} = \frac{1-\theta}{\theta}\,\rho_{\mathrm{s}} \tag{7.9}$$

must be considered in addition to the stoichiometry given in Table 7.3, when calculating mass balances of the adsorption and desorption processes using the units of S_j and C_j.

The simplest formulation of kinetics of adsorption and desorption are linear rates given by the following expressions:

$$\rho_{\mathrm{ads},j} = k_{\mathrm{ads},j} \cdot C_j \tag{7.10}$$

$$\rho_{\mathrm{des},j} = k_{\mathrm{des},j} \cdot S_j \tag{7.11}$$

Sorption equilibrium is achieved when the process rates of adsorption and desorption are the same ($\rho_{\mathrm{ads},j} = \rho_{\mathrm{des},j}$). This leads to the following relation between the kinetic parameters k and the equilibrium constant K_{D}:

$$S_{\mathrm{eq},j}(C_j) = \frac{k_{\mathrm{ads},j}}{k_{\mathrm{des},j}} \cdot C_j = K_{\mathrm{D},j} \cdot C_j \tag{7.12}$$

If the sorption sites become limiting, equation (7.10) is no longer realistic as it does not take into account that less free sorption sites will be available when more sites are already filled. The simplest assumption is then to formulate the adsorption rate as being proportional to the free sorption sites given by the total available sites ($S_{\max}$) minus the filled sites (S_j). In this case the process rate can be formulated proportional to the saturation level:

$$\rho_{\mathrm{ads},j} = k_{\mathrm{ads},j} \cdot C_j \cdot (S_{\max} - S_j) \tag{7.13}$$

In equilibrium, where $\rho_{\mathrm{ads},j}$ equals $\rho_{\mathrm{des},j}$, we get the so-called Langmuir Isotherm (Appelo and Postma, 2005):

$$S_{\mathrm{eq},j}(C_j) = \frac{S_{\max} \cdot C_j}{K_{\mathrm{L}} + C_j} \tag{7.14}$$

(as they are usually measured at constant temperature, the relationships between dissolved and sorbed concentrations in equilibrium, such as those given by equations 7.12 and 7.14, are called isotherms). The Langmuir isotherm shows that the sorbed concentration of the substance j in equilibrium ($S_{\mathrm{eq},j}$) increases linearly with the dissolved concentration (C_j) if $C_j \ll K_{\mathrm{L}}$. If the dissolved concentration is high ($C_j \gg K_{\mathrm{L}}$), the surface becomes saturated, and $S_j \approx S_{\max}$.

The rate of fast reversible sorption processes can alternatively be described by the following equation:

$$\rho_{\mathrm{sorb}} = k_j \cdot (S_{\mathrm{eq},j}(C_j) - S_j) \tag{7.15}$$

It describes relaxation of the actually sorbed concentration to the equilibrium concentration with a rate constant k_j. If k_j is set to a sufficiently large value, this model is a good approximation to equilibrium sorption. The stoichiometry of this process is the same as that for the desorption process shown in Table 7.3. Any other sorption isotherm can be implemented in a similar way.

Chapter 8

Biological Processes

In this chapter, we introduce the mathematical formulation of important biological transformation processes. We discuss process formulations for primary production (section 8.1), respiration (section 8.2), death (section 8.3), consumption (section 8.4), mineralization (section 8.5), nitrification (section 8.6), and bacterial growth (section 8.8).

All process stoichiometries formulated in this chapter approximate the composition of organic matter as consisting of the five elements C, H, O, N and P. This is inspired by the "Redfield-composition" introduced in section 4.3.1 and given by equation (4.33)

$$(CH_2O)_{106}(NH_3)_{16}(H_3PO_4)_1 = C_{106}H_{263}O_{110}N_{16}P \tag{8.1}$$

but we formulate all processes for an arbitrary composition of organic material consisting of these five elements.

8.1 Primary Production

Primary production is the production of organic material from inorganic nutrients through photosynthesis. This process provides the food for the higher trophic levels of the ecosystem foodweb (growth of nitrifiers is another autotrophic process that is important for nitrification but not relevant for food production; see section 8.8.2). The energy source for primary production is the photosynthetically active radiation (PAR) which consists of radiation between wavelengths of 400 and 700 nm and corresponds to about 50% of the global radiation (GLR) of sunlight. Photosynthesis can be parameterized either using PAR or GLR. In deep aquatic systems, algae and some bacteria contribute to primary production, in shallow systems plants may contribute also. Note that there is some overlap of this section with chapter 4 as primary production by algae was used as an example to introduce our process notation.

We formulate the stoichiometry of primary production considering the elements C, H, O, N and P as constituents of organic material. We distinguish two processes based on ammonium (NH_4^+) or nitrate (NO_3^-) as the nitrogen source. Phosphate (HPO_4^{2-}) is the source of phosphorus. Most algae grow with carbon dioxide (CO_2) as the carbon source. However, at normal pH values, most of the carbon in water is in the form of bicarbonate (HCO_3^-). For this reason, considerable uptake of carbon dioxide (CO_2) is only possible because, due to the fast chemical equilibrium, carbon dioxide taken by algae is quickly replaced by the reaction $HCO_3^- + H^+ \rightarrow H_2O + CO_2$ (see section 7.1 for more details). For this reason, we get a better overview of induced pH changes, when formulating primary production as uptake of bicarbonate (HCO_3^-). As organic matter contains less oxygen than these constituents, primary production is associated with release of dissolved oxygen. This leads to the qualitative stoichiometry of primary production shown in Table 8.1. In this

Process	Substances / Organisms								Rate
	NH_4^+	NO_3^-	HPO_4^{2-}	HCO_3^-	O_2	H^+	H_2O	ALG	
	gN	gN	gP	gC	gO	mol	mol	gDM	
Pri. prod. NH_4^+	−		−	−	+	?	?	1	$\rho_{\text{gro,ALG,NH}_4^+}$
Pri. prod. NO_3^-		−	−	−	+	?	?	1	$\rho_{\text{gro,ALG,NO}_3^-}$

Table 8.1: Process table of primary production with ammonium (NH_4^+) or nitrate (NO_3^-) as the nitrogen source.

table, "−" indicates a negative stoichiometric coefficient, "+" a positive stoichiometric coefficient, and "?" a stoichiometric coefficient the sign of which may depend on the composition of organic material. The six missing stoichiometric coefficients in each row are uniquely determined by the six conservation laws for C, H, O, N, P and charge. They can be calculated as described in section 4.3. The R package `stoichcalc` described in section 15 can be used for this purpose.

Typically, the process rate of primary production by algae is formulated as a linear function in algae concentration considering temperature, light and nutrient dependence of the specific growth rate of algae. If these dependences are formulated using a multiplicative approach as described in section 4.2 and using a preference factor $p_{\text{NH}_4^+,\text{ALG}}$ for uptake of ammonium relative to unity for nitrate, we end with the following process rates for

primary production with ammonium and nitrate as the nitrogen source:

$$\rho_{\mathrm{gro,ALG,NH_4^+}} = k_{\mathrm{gro,ALG},T_0} \cdot \exp\Big(\beta_{\mathrm{ALG}}(T-T_0)\Big) \cdot \frac{I}{K_I+I} \cdot \min\left(\frac{C_{\mathrm{HPO_4^{2-}}}}{K_{\mathrm{HPO_4^{2-},ALG}}+C_{\mathrm{HPO_4^{2-}}}}, \frac{C_{\mathrm{NH_4^+}}+C_{\mathrm{NO_3^-}}}{K_{\mathrm{N,ALG}}+C_{\mathrm{NH_4^+}}+C_{\mathrm{NO_3^-}}}\right) \cdot \frac{p_{\mathrm{NH_4^+,ALG}} C_{\mathrm{NH_4^+}}}{p_{\mathrm{NH_4^+,ALG}} C_{\mathrm{NH_4^+}} + C_{\mathrm{NO_3^-}}} \cdot C_{\mathrm{ALG}} \quad (8.2)$$

$$\rho_{\mathrm{gro,ALG,NO_3^-}} = k_{\mathrm{gro,ALG},T_0} \cdot \exp\Big(\beta_{\mathrm{ALG}}(T-T_0)\Big) \cdot \frac{I}{K_I+I} \cdot \min\left(\frac{C_{\mathrm{HPO_4^{2-}}}}{K_{\mathrm{HPO_4^{2-},ALG}}+C_{\mathrm{HPO_4^{2-}}}}, \frac{C_{\mathrm{NH_4^+}}+C_{\mathrm{NO_3^-}}}{K_{\mathrm{N,ALG}}+C_{\mathrm{NH_4^+}}+C_{\mathrm{NO_3^-}}}\right) \cdot \frac{C_{\mathrm{NO_3^-}}}{p_{\mathrm{NH_4^+,ALG}} C_{\mathrm{NH_4^+}} + C_{\mathrm{NO_3^-}}} \cdot C_{\mathrm{ALG}} \quad (8.3)$$

Note that we could use alternative formulations for temperature, nutrient and light dependence as described in section 4.2. As outlined in section 4.2.4, when approximating a lake layer by a well mixed box of height h and we assume constant light extinction coefficient λ, we have to apply the following depth-averaged rates

$$\rho_{\mathrm{gro,ALG,NH_4^+}} = k_{\mathrm{gro,ALG},T_0} \cdot \exp\Big(\beta_{\mathrm{ALG}}(T-T_0)\Big) \cdot \frac{1}{\lambda h} \log\left(\frac{K_I+I_0}{K_I+I_0\exp(-\lambda h)}\right) \cdot \min\left(\frac{C_{\mathrm{HPO_4^{2-}}}}{K_{\mathrm{HPO_4^{2-},ALG}}+C_{\mathrm{HPO_4^{2-}}}}, \frac{C_{\mathrm{NH_4^+}}+C_{\mathrm{NO_3^-}}}{K_{\mathrm{N,ALG}}+C_{\mathrm{NH_4^+}}+C_{\mathrm{NO_3^-}}}\right) \cdot \frac{p_{\mathrm{NH_4^+,ALG}} C_{\mathrm{NH_4^+}}}{p_{\mathrm{NH_4^+,ALG}} C_{\mathrm{NH_4^+}} + C_{\mathrm{NO_3^-}}} \cdot C_{\mathrm{ALG}} \quad (8.4)$$

$$\rho_{\mathrm{gro,ALG,NO_3^-}} = k_{\mathrm{gro,ALG},T_0} \cdot \exp\Big(\beta_{\mathrm{ALG}}(T-T_0)\Big) \cdot \frac{1}{\lambda h} \log\left(\frac{K_I+I_0}{K_I+I_0\exp(-\lambda h)}\right) \cdot \min\left(\frac{C_{\mathrm{HPO_4^{2-}}}}{K_{\mathrm{HPO_4^{2-},ALG}}+C_{\mathrm{HPO_4^{2-}}}}, \frac{C_{\mathrm{NH_4^+}}+C_{\mathrm{NO_3^-}}}{K_{\mathrm{N}}+C_{\mathrm{NH_4^+}}+C_{\mathrm{NO_3^-}}}\right) \cdot \frac{C_{\mathrm{NO_3^-}}}{p_{\mathrm{NH_4^+,ALG}} C_{\mathrm{NH_4^+}} + C_{\mathrm{NO_3^-}}} \cdot C_{\mathrm{ALG}} \quad (8.5)$$

These rates depend on the light intensity I_0 at the water surface instead of the in-situ light intensity $I = I_0 \exp(-\lambda z)$. This is the form that must be applied in box models.

8.2 Respiration

Respiration is the inverse process of photosynthesis (see primary production in section 8.1). It is a metabolic process by which organic substances are broken down to simpler products with the release of energy (Lucas, 1996). It is an important process for the survival of organisms as it frees energy for life maintenance processes (including locomotion activity and reproduction) (Clarke, 1987). As a first approximation, the process of respiration can be simplified to the transformation of organism biomass to nutrients, being aware of the fact that this is a combination of different steps of reactions including the mineralization of dissolved organic material to nutrients. We concentrate on oxic respiration.

Table 8.2 shows the stoichiometry of respiration. The stoichiometric coefficients of this

Process	Substances / Organisms							Rate
	NH_4^+	HPO_4^{2-}	HCO_3^-	O_2	H^+	H_2O	ALG	
	gN	gP	gC	gO	mol	mol	gDM	
Respiration	+	+	+	−	?	?	−1	$\rho_{\text{resp,ALG}}$

Table 8.2: Process table of respiration of algae. Respiration of other organisms is formulated analogously.

process are the same as those for primary production with ammonium as the nitrogen source but with reversed signs (see Table 8.1 in section 8.1).

As (oxic) respiration requires dissolved oxygen, we need a limitation term with respect to dissolved oxygen. Furthermore it seems natural to use a temperature dependence to account for different activity levels at different temperatures. This leads to the following process rate for respiration:

$$\rho_{\text{resp,ALG}} = k_{\text{resp,ALG},T_0} \cdot \exp\Big(\beta_{\text{ALG}}(T - T_0)\Big) \cdot \frac{C_{\text{O}_2}}{K_{\text{O}_2,\text{ALG}} + C_{\text{O}_2}} \cdot C_{\text{ALG}} \tag{8.6}$$

8.3 Death

Death transfers living organisms into dead organic particles. The accumulation of dead particles due to death, sloppy feeding and excretion (see section 8.4) leads, due to oxygen consumption of mineralization processes, to anoxic and anaerobic environments. Natural organic particles have a wide spectrum of biodegradability. In models of ecological systems, this is often represented by a (quickly) degradable and an inert fraction of organic matter. In this context "inert" means that there is no significant degradation within the time frame of investigation; it is not "truly" inert.

If the composition of dead particles is the same as that of the living organisms, death has a simple stoichiometry with a single stoichiometric parameter, f_I, specifying which fraction of dying organisms ends in inert organic particles ($1 - f_\mathrm{I}$ will be converted into degradable organic particles). As different organisms often have different composition (e.g. algae and bacteria) this would require to introduce state variables for dead organisms of any type. This could lead to a large number of state variables. For this reason, we are looking for a description of the death process that can transfer organisms into dead particles of different composition without violating elemental mass conservation. A possible solution to this problem is to assume some mineralization during the death process. This may not be very realistic, but it is in accordance with biogeochemical cycles, as the dominant fraction of organic particles will be mineralized also. For this reason, we introduce a "yield" coefficient for death, $Y_{\mathrm{ALG,death}}$ (here formulated for death of algae), that specifies the fraction of dying organisms that end in dead organic particles whereas the rest of the organic material will be respired. This leads to the process table shown in Table 8.3 (POMD represents degradable particulate organic matter, POMI inert particulate organic matter). In this table, stoichiometric coefficients indicated by "0/+" should not

Process	Substances / Organisms									Rate
	NH_4^+	HPO_4^{2-}	HCO_3^-	O_2	H^+	H_2O	ALG	POMD	POMI	
	gN	gP	gC	gO	mol	mol	gDM	gDM	gDM	
Death	0/+	0/+	0/+	0/+	?	?	−1	$(1-f_\mathrm{I})$ $\cdot Y_{\mathrm{ALG,death}}$	f_I $\cdot Y_{\mathrm{ALG,death}}$	$\rho_{\mathrm{death,ALG}}$

Table 8.3: Process table of death of algae. Death of other organisms is formulated analogously.

be negative, because otherwise the death process would require ammonium, phosphate, bicarbonate or dissolved oxygen. This process contains 9 stoichiometric coefficients. One is given by normalization. We are then left with 8 unknowns which are uniquely determined by six conservation laws for the elements C, H, O, N, P and charge and the two constraints parameterized by the "yield" coefficient and by the fraction of inert particles produced by the process. These two constraints can be formulated as

$$\nu_{\mathrm{death,ALG\ ALG}} \cdot Y_{\mathrm{ALG,death}} + \nu_{\mathrm{death,ALG\ POMD}} + \nu_{\mathrm{death,ALG\ POMI}} = 0 \tag{8.7}$$

and

$$f_\mathrm{I}\ (\nu_{\mathrm{death,ALG\ POMD}} + \nu_{\mathrm{death,ALG\ POMI}}) = \nu_{\mathrm{death,ALG\ POMI}} \tag{8.8}$$

or

$$f_\mathrm{I}\ \nu_{\mathrm{death,ALG\ POMD}} - (1 - f_\mathrm{I})\nu_{\mathrm{death,ALG\ POMI}} = 0 \tag{8.9}$$

The constraints (8.7) and (8.9) are of the required form (4.57) or (4.59) and can easily be integrated in software using the R package `stoichcalc` described in section 15. These equations have a meaningful solution as long as the composition differences are not too large and dead organic particles have a lower oxygen content than the organisms (this increases the fraction of organic matter that can be respired to get rid of excess nutrients without leading to the consumption of dissolved oxygen). For very large composition differences between different organisms it may be better to introduce more fractions of organic particles with different composition.

Usually, a very simple process rate

$$\rho_{\text{death,ALG}} = k_{\text{death,ALG}} \cdot C_{\text{ALG}} \tag{8.10}$$

is used for death. The specific death rate, $k_{\text{death,ALG}}$, will in many cases depend on external influence factors, such as zooplankton for algae or fish for zooplankton if these other organisms are not internalized to the model.

8.4 Consumption

Consumption of one type of organisms by another is a very important ecological process that is the basis of all food webs extending primary production. We discuss the formulation of predation processes with the example of zooplankton feeding on algae.

The yield, Y_{ZOO}, which determines the produced zooplankton biomass per unit of consumed algal biomass is an obvious stoichiometric parameter associated with any predation process. Predation is accompanied by the production of dead organic particles due to sloppy feeding and excretion. We introduce the fraction of consumed algal biomass that becomes dead organic particles due to sloppy feeding and excretion, f_{e}, as a stoichiometric parameter. As for the death process (see section 8.3) we distinguish the production of degradable (POMD) and inert (POMI) dead organic particles. Also similarly to the death process, we introduce the parameter f_{I} as describing the fraction of the produced particles that is inert. These three constraints can be formulated as

$$\nu_{\mathrm{gro,ZOO\ ZOO}} + \nu_{\mathrm{gro,ZOO\ ALG}} Y_{\mathrm{ZOO}} = 0 \tag{8.11}$$

$$\nu_{\mathrm{gro,ZOO\ POMD}} + \nu_{\mathrm{gro,ZOO\ POMI}} + \nu_{\mathrm{gro,ZOO\ ALG}} f_{\mathrm{e}} = 0 \tag{8.12}$$

$$\nu_{\mathrm{gro,ZOO\ POMD}} f_{\mathrm{I}} - \nu_{\mathrm{gro,ZOO\ POMI}} (1 - f_{\mathrm{I}}) = 0 \tag{8.13}$$

This leads to the process stoichiometry shown in Table 8.4 The unknown stoichiometric

Process	Substances / Organisms										Rate
	NH_4^+ gN	HPO_4^{2-} gP	HCO_3^- gC	O_2 gO	H^+ mol	H_2O mol	ALG gDM	ZOO gDM	POMD gDM	POMI gDM	
Growth ZOO	+	+	+	−	?	?	$\frac{-1}{Y_{\mathrm{ZOO}}}$	1	$\frac{(1-f_{\mathrm{I}})f_{\mathrm{e}}}{Y_{\mathrm{ZOO}}}$	$\frac{f_{\mathrm{I}} f_{\mathrm{e}}}{Y_{\mathrm{ZOO}}}$	$\rho_{\mathrm{gro,ZOO}}$

Table 8.4: Process table of a consumption process for the example of predation of zooplankton on algae.

coefficients can easily be calculated using the constraints given above and the conservation laws for C, H, O, N, P and charge as outlined in section 4.3.

It is natural to assume the rate to be proportional to the concentration of predators. The process rate obviously needs a limitation with respect to decreasing oxygen levels and a dependence on food availability. This is fulfilled by the following process rate:

$$\rho_{\mathrm{gro,ZOO}} = k_{\mathrm{gro,ZOO},T_0} \cdot \exp\Big(\beta_{\mathrm{ZOO}}(T - T_0)\Big) \cdot \frac{C_{\mathrm{O_2}}}{K_{\mathrm{O_2,ZOO}} + C_{\mathrm{O_2}}} \cdot \frac{C_{\mathrm{ALG}}}{K_{\mathrm{ALG,ZOO}} + C_{\mathrm{ALG}}} \cdot C_{\mathrm{ZOO}} \tag{8.14}$$

In many applications, we will remain in the linear branch of the limitation term with respect to algae. In this case, the parameterization

$$\rho_{\mathrm{gro,ZOO}} = k'_{\mathrm{gro,ZOO},T_0} \cdot \exp\Big(\beta_{\mathrm{ZOO}}(T - T_0)\Big) \cdot \frac{C_{\mathrm{O_2}}}{K_{\mathrm{O_2,ZOO}} + C_{\mathrm{O_2}}} \cdot C_{\mathrm{ALG}} \cdot C_{\mathrm{ZOO}} \tag{8.15}$$

without explicit consideration of saturation with respect to algae is more convenient. However, the rate constant $k'_{\mathrm{gro,ZOO},T_0}$ has then more complicated units.

Process rates for growth of omnivorous or carnivorous zooplankton and of predators can be formulated analogously. However, if multiple food sources are available, additional preference factors as described in section 4.2.5 will be required.

8.5 Mineralization

Oxic mineralization transforms organic matter to dissolved nutrients and carbon dioxide under consumption of oxygen. In the absence of dissolved oxygen (primarily in the sediment), mineralization can use nitrate, manganese oxide, iron hydroxide or sulphate for oxidizing organic matter. Finally, methanogenesis can convert organic matter to nutrients, carbon dioxide and methane. In this section, we describe the stoichiometry and possible process kinetics of mineralization as it can be used in aquatic ecosystem models. The bacterially mediated mechanisms of mineralization are only taken into account in this section by an appropriate choice of the mineralization rate coefficient. See section 8.8.1 for a description of growth of heterotrophic bacteria on organic substrate under oxic or anoxic conditions to get a more detailed description of mineralization mechanisms. As mineralization is caused by bacteria and bacterial concentrations vary considerably from one (part of the) system to another, mineralization rate coefficients vary over many orders of magnitude from one system to another.

8.5.1 Oxic Mineralization

Table 8.5 shows the process table for oxic mineralization when considering the elements C, H, O, N and P as constituents of organic matter. Unknown stoichiometric coefficients

Process	Substances / Organisms							Rate
	NH_4^+	HPO_4^{2-}	HCO_3^-	O_2	H^+	H_2O	POM	
	gN	gP	gC	gO	mol	mol	gDM	
Oxic mineralization	+	+	+	−	?	?	−1	$\rho_{\text{miner,ox,POM}}$

Table 8.5: Process table of oxic mineralization.

for which it is evident that they are positive are indicated by "+", negative ones by "−", and coefficients the sign of which is not clear or depends on the composition of organic material are indicated by "?". As we have 6 unknown stoichiometric coefficients and 6 conservation laws (C, H, O, N, P and charge) there is no need for additional stoichiometric parameters and the unknown coefficients can easily be calculated as described in section 4.3. The R package `stoichcalc` described in section 15 can be used for this purpose.

The stoichiometric coefficient of oxic mineralization with respect to dissolved oxygen determines the "chemical oxygen demand" (COD) of an organic compound. If the definition of "chemical oxygen demand" is extended to inorganic compounds, generalized oxygen budgets can be formulated. This built the basis of process formulations in activated sludge models (Henze et al., 1986; Gujer and Henze, 1991; Henze et al., 1995; Gujer et al., 1995; Gujer and Larsen, 1995; Henze et al., 1999; Gujer et al., 1999; Henze et al., 2000). When using COD, one has to be aware, that the definition of COD is based on oxidation of organic material with release of ammonium and not nitrate. Nitrification of ammonium to nitrate will require additional oxygen (see section 8.6). For this reason, COD is sometimes called "carbonaceous" oxygen demand, to which the "nitrogenous" oxygen demand required for nitrification must be added to get the total oxygen demand.

As oxic mineralization consumes dissolved oxygen, we need a rate limitation by dissolved oxygen. Considering in addition a temperature dependence of the transformation

rate and assuming simple, first order kinetics with respect to organic material, we get the following mineralization rate

$$\rho_{\text{miner,ox,POM}} = k_{\text{miner,ox,POM},T_0} \cdot \exp\Big(\beta_{\text{BAC}}(T - T_0)\Big) \cdot \frac{C_{\text{O}_2}}{K_{\text{O}_2,\text{miner}} + C_{\text{O}_2}} \cdot C_{\text{POM}} \quad (8.16)$$

8.5.2 Anoxic Mineralization

Table 8.6 shows the process table for anoxic mineralization when considering the elements C, H, O, N and P as constituents of organic matter. In contrast to oxic mineralization as shown in Table 8.5, the required oxygen for mineralization is gained by reduction of nitrate to molecular nitrogen instead of using dissolved oxygen. We have now 7 unknown

Process	Substances / Organisms								Rate
	NH_4^+	NO_3^-	N_2	HPO_4^{2-}	HCO_3^-	H^+	H_2O	POM	
	gN	gN	gN	gP	gC	mol	mol	gDM	
Anoxic miner.	+	−	+	+	+	?	?	−1	$\rho_{\text{miner,anox,POM}}$

Table 8.6: Process table of anoxic mineralization.

stoichiometric coefficients and 6 conservation laws (C, H, O, N, P and charge). This means that we need one additional constraint. This constraint is given by the assumption that nitrate is reduced to molecular nitrogen and none of it to ammonium. This is expressed by the constraint

$$\nu_{\text{miner,anox NO3}} + \nu_{\text{miner,anox N2}} = 0 \quad (8.17)$$

With this additional constraint the unknown coefficients can easily be calculated as described in section 4.3. The R package `stoichcalc` described in section 15 can be used for this purpose.

As anoxic mineralization requires nitrate, we need a limitation of this process rate by nitrate. Because oxic mineralization requires less energy, it is preferred to anoxic mineralization if dissolved oxygen is available. This can be considered by using an oxygen inhibition term

$$\left(1 - \frac{C_{\text{O}_2}}{K_{\text{O}_2,\text{miner}} + C_{\text{O}_2}}\right) = \frac{K_{\text{O}_2,\text{miner}}}{K_{\text{O}_2,\text{miner}} + C_{\text{O}_2}} \quad (8.18)$$

This factor switches off anoxic mineralization if dissolved oxygen is available. Note that parallel to this, oxic mineralization is switched on by the rate expression (8.16). Again considering temperature dependence and assuming a first-order process with respect to organic matter, we get the following rate

$$\rho_{\text{miner,anox,POM}} = k_{\text{miner,anox,POM,T0}} \cdot \exp\Big(\beta_{\text{BAC}}(T - T_0)\Big) \cdot \frac{K_{\text{O}_2,\text{miner}}}{K_{\text{O}_2,\text{miner}} + C_{\text{O}_2}} \cdot \frac{C_{\text{NO}_3^-}}{K_{\text{NO}_3^-,\text{miner}} + C_{\text{NO}_3^-}} \cdot C_{\text{POM}} \quad (8.19)$$

8.5.3 Anaerobic Mineralization

Table 8.7 shows the process table for oxic, anoxic and anaerobic mineralization when considering the elements C, H, O, N and P as constituents of organic matter. In addition to (1) oxic (in the presence of dissolved oxygen) and (2) anoxic mineralization (in the absence of dissolved oxygen but presence of nitrate), we introduce (3) mineralization by manganese oxide reduction (under release of Mn^{2+}), (4) mineralization by iron hydroxide reduction (under release of Fe^{2+}), (5) mineralization by sulphate reduction (under release of HS^-), and (6) methanogenesis (with production of CH_4). The anaerobic mineralization processes are of particular importance in the sediment where the diffusion limitation of transport of dissolved oxygen and nitrate leads to anaerobic conditions. The reduced substances Mn^{2+}, Fe^{2+} and HS^- are diffusing to higher sediment layers and into the water column where they consume dissolved oxygen when being oxidized. As already discussed in sections 8.5.1 and 8.5.2, there are 6 unknown stoichiometric coefficients for the first mineralization process and 6 conservation laws (C, H, O, N, P and charge). Therefore, there is no need for additional stoichiometric parameters. The anoxic mineralization process needs an additional constraint that is given by assuming all nitrate being converted to molecular nitrogen. The anaerobic mineralization processes (3), (4) and (5) have 7 unknown stoichiometric coefficients. However, in addition to the conservation laws mentioned above for these processes there is one additional conservation law for manganese, iron, or sulphur, respectively. The sixth mineralization process has again 6 unknown coefficients for the same 6 conservation laws as used for the first process. For this reason, there is no need for additional stoichiometric constraints in any of the anaerobic mineralization processes.

Similar kinetic expressions can be given for anaerobic mineralization as those for oxic (8.16) and anoxic mineralization (8.19). This requires the introduction of additional limitation and inhibition factors.

Process	Substances / Organisms														Rate
	NH_4^+ gN	NO_3^- gN	N_2 gN	HPO_4^{2-} gP	HCO_3^- gC	CH_4 gC	O_2 gO	SO_4^{2-} mol	HS^- mol	Mn^{2+} mol	Fe^{2+} mol	H^+ mol	H_2O mol	MnO_2 mol	FeOOH mol	POM gDM	
Oxic mineral.	+			+	+		−					?	?			−1	$\rho_{\text{miner,ox,POM}}$
Anoxic mineral.	+	−	+	+	+							?	?			−1	$\rho_{\text{miner,anox,POM}}$
Mn oxide red.	+		+	+	+					+		?	?	−		−1	$\rho_{\text{miner,MnO2,POM}}$
Fe hydrox. red.	+		+	+	+						+	?	?		−	−1	$\rho_{\text{miner,FeOOH,POM}}$
Sulphate red.	+		+	+	+			−	+			?	?			−1	$\rho_{\text{miner,SO4,POM}}$
Methanogenesis	+			+	+	+						?	?			−1	$\rho_{\text{miner,CH4,POM}}$

Table 8.7: Process table of mineralization processes.

8.6 Nitrification

Nitrification is the biologically mediated oxidation of ammonium over nitrite to nitrate. Under aerobic conditions ammonium has potential energy relative to the more oxidized forms nitrite and nitrate. Some chemoautotrophic bacteria are able to use this stored potential energy to allow for carbon fixation by the process of nitrification (Dodds, 2002). It can either be modelled as a one step process combining the two sub-steps or the model can represent these two oxidation steps separately. Both formulations are discussed in the following two subsections. See section 8.8.2 for a more detailed description of the growth of autotrophic nitrifying bacteria due to this process.

8.6.1 Nitrification as a One Step Process

Table 8.8 shows the stoichiometry of the one-step nitrification process.

Process	Substances / Organisms					Rate
	NH_4^+	NO_3^-	O_2	H^+	H_2O	
	gN	gN	gO	mol	mol	
Nitrification	-1	$+$	$-$	?	?	ρ_{nitri}

Table 8.8: Process table of nitrification modelled as a one step oxidation process from ammonium to nitrate.

This stoichiometry has the obvious unique solution

$$NH_4^+ + 2\,O_2 \rightarrow NO_3^- + 2\,H^+ + H_2O \tag{8.20}$$

The process rate needs a limitation by dissolved oxygen and ammonium concentrations and a temperature dependence:

$$\rho_{\text{nitri}} = k_{\text{nitri},T_0} \cdot \exp\Big(\beta_{\text{BAC}}(T - T_0)\Big) \cdot \min\left(\frac{C_{NH_4^+}}{K_{NH_4^+,\text{nitri}} + C_{NH_4^+}}, \frac{C_{O_2}}{K_{O_2,\text{nitri}} + C_{O_2}}\right) \tag{8.21}$$

8.6.2 Nitrification as a Two Step Process

Table 8.9 shows the stoichiometries of the two steps of the two-step nitrification process. These stoichiometries have the obvious unique solution

Process	Substances / Organisms						Rate
	NH_4^+	NO_2^-	NO_3^-	O_2	H^+	H_2O	
	gN	gN	gN	gO	mol	mol	
Ammonium oxidation	-1	$+$		$-$	?	?	ρ_{nitri1}
Nitrite oxidation		-1	$+$	$-$	?	?	ρ_{nitri2}

Table 8.9: Process table of nitrification modelled as a two step process from ammonium to nitrite and from nitrite to nitrate.

$$NH_4^+ + \frac{3}{2}\,O_2 \rightarrow NO_2^- + 2\,H^+ + H_2O \tag{8.22}$$

$$\mathrm{NO_2^-} + \frac{1}{2}\,\mathrm{O_2} \rightarrow \mathrm{NO_3^-} \tag{8.23}$$

The process rates need a limitation by dissolved oxygen and ammonium concentrations and by dissolved oxygen and nitrite concentrations, respectively. Adding an exponential temperature dependence leads to

$$\rho_{\mathrm{nitri1}} = k_{\mathrm{nitri1},T_0} \cdot \exp\Big(\beta_{\mathrm{N1}}(T - T_0)\Big) \cdot \min\left(\frac{C_{\mathrm{NH_4^+}}}{K_{\mathrm{NH_4^+,nitri}} + C_{\mathrm{NH_4^+}}}, \frac{C_{\mathrm{O_2}}}{K_{\mathrm{O_2,nitri}} + C_{\mathrm{O_2}}}\right) \tag{8.24}$$

$$\rho_{\mathrm{nitri2}} = k_{\mathrm{nitri2},T_0} \cdot \exp\Big(\beta_{\mathrm{N2}}(T - T_0)\Big) \cdot \min\left(\frac{C_{\mathrm{NO_2^-}}}{K_{\mathrm{NO_2^-,nitri}} + C_{\mathrm{NO_2^-}}}, \frac{C_{\mathrm{O_2}}}{K_{\mathrm{O_2,nitri}} + C_{\mathrm{O_2}}}\right) \tag{8.25}$$

8.7 Hydrolysis

Particulate organic substances cannot directly be consumed or degraded by microorganisms. Heterotrophic microorganisms, mainly bacteria, need dissolved organic substrate for their growth. In section 8.5, the mineralization process is described as degradation of organic particles. This is a simplified, aggregated description of a more complicated sequence of steps involving transformation of particulate organic matter to the dissolved phase, uptake of dissolved organic substrate by heterotrophic microorganisms, growth of these microorganisms with partial mineralization of organic material, and subsequent respiration and death. The dead microorganisms lead to a partial feedback to this sequence of processes of "mineralization" of particulate organic material.

A reaction in which a water molecule (or hydroxide ion) substitutes for another atom or group of atoms in an organic molecule is called a hydrolysis reaction (Schwarzenbach et al., 2003). Through this hydrolysis reaction, large organic molecules are broken down into smaller molecules that are often easier to degrade biologically. In simple ecosystem and sewage treatment process models, the transformation of hardly degradable organic particles into quickly degradable dissolved organic matter is called "hydrolysis" although there is not a unique relationship between the properties of organic material of being particulate or dissolved and being hardly or quickly degradable. Despite the imprecise use of the term, we will use the term "hydrolysis" here also as denoting the transformation process from the model components of degradable particulate organic material to dissolved organic material that can serve as a substrate for heterotrophic microorganisms. Table 8.10 shows the stoichiometry of this process. Similarly to the death process described in section 8.3, we introduce a "yield" that makes it possible to account for differences in composition of particulate and dissolved organic material by mineralizing a part of the organic material. This makes it possible to limit the number of modelled compounds. Again, the symbol

Process	Substances / Organisms								Rate
	NH_4^+	HPO_4^{2-}	HCO_3^-	O_2	H^+	H_2O	POM	DOM	
	gN	gP	gC	gO	mol	mol	gDM	g	
Hydrolysis	0/+	0/+	0/+	0/+	?	?	-1	Y_{hyd}	$\rho_{\text{hyd,POM}}$

Table 8.10: Process table of hydrolysis.

"0/+" in Table 8.10 indicates a stoichiometric coefficient that should not be negative. If it is not possible to find a reasonable composition and reasonable stoichiometric parameters to achieve fulfilment of these non-negativity conditions, different fractions of dissolved organic material must be introduced, as it may also be necessary for particulate organic material (see section 8.3 for a similar discussion). The six conservation equations for the elements C, H, O, N and P and for charge together with the constraint for the "yield"

$$\nu_{\text{hyd DOM}} + \nu_{\text{hyd POM}} Y_{\text{hyd}} = 0 \tag{8.26}$$

lead to the seven constraining equations that are required to calculate the seven unknown stoichiometric coefficients in Table 8.10 according to the techniques described in section 4.3. The R package `stoichcalc` described in section 15 can be used for this purpose.

As our "hydrolysis" process is an aggregate process of much more complicated processes in reality, it is difficult to parameterize. We use a simple first order rate expression

$$\rho_{\mathrm{hyd,POM}} = k_{\mathrm{hyd,POM},T_0} \cdot \exp\Big(\beta_{\mathrm{hyd}}(T - T_0)\Big) \cdot C_{\mathrm{POM}} \tag{8.27}$$

and shift the difficulty to the reasonable choice of the coefficient $k_{\mathrm{hyd,POM},T_0}$.

8.8 Bacterial Growth

Many biogeochemical processes in ecosystems, such as mineralization (see section 8.5) and nitrification (see section 8.6), are performed by bacteria or other microorganisms. This implies that their rates depend not only on the concentrations of substances transformed by the processes and external influence factors, but also on the density of bacteria present at a given location in the ecosystem. This leads to a large range of rates that can be observed in ecosystems and, consequently, to a lack of universality of model parameters.

If there is a significant temporal change of the bacterial community in the investigated system or if the model should be made more universal by using specific growth and death rates of bacteria instead of overall rate coefficients, the bacterial community or their dominant functional group(s) must be explicitly considered in the model. We can learn how to do this from models for activated sludge sewage treatment plants (Henze et al., 1986; Gujer and Henze, 1991; Henze et al., 1995; Gujer et al., 1995; Henze et al., 1999; Gujer et al., 1999; Henze et al., 2000).

Bacteria (and other organisms) can be classified according to the energy source and the metabolism of their growth process. The reductive process of biomass formation requires a substance that is oxidised, the electron donor. Table 8.11 shows the classification of growth processes according to the energy source, electron donor, and carbon source (Lampert and Sommer, 1997). This classification determines which substances have to be included when

energy source		electron donor		carbon source	
light:	**photo-**	organic comp.:	**organo-**	organic comp.:	**hetero-**
redox process:	**chemo-**	inorganic comp.:	**litho-**	inorganic comp.:	**auto-**

Table 8.11: Classification of growth processes according to the energy source, electron donor, and carbon source. The type consists of one or several of the keywords listed above (at most one per column) extended by the word **-trophic**.

deriving the stoichiometry of the growth process. Note that algae and macrophytes (see section 8.1) are of the photolithoautotrophic type, heterotrophic bacteria as described in section 8.8.1 would more precisely be called chemoorganoheterotrophic organisms, and nitrifiers (see section 8.8.2) are of the chemolithoautotrophic type.

8.8.1 Growth of Heterotrophic Bacteria

Heterotrophic organisms, such as bacteria and fungi are responsible for the decomposition of organic material. This process can be modelled as "hydrolysis" of particulate organic material to the dissolved form as described in section 8.7 and subsequent growth of heterotrophic microorganisms on dissolved substrate. Table 8.12 shows the stoichiometry of this process. We distinguish oxic growth of heterotrophic microorganisms using ammonium or nitrate as the nitrogen source (if the food does not contain enough nitrogen) and anoxic growth of heterotrophic microorganisms. For all of these processes the yield leads to the constraining equations

$$\nu_{\mathrm{gro,HET,ox,NH_4^+\ HET}} + \nu_{\mathrm{gro,HET,ox,NH_4^+\ DOM}} Y_{\mathrm{HET}} = 0 \tag{8.28}$$

Process	Substances / Organisms										Rate
	NH_4^+ gN	NO_3^- gN	N_2 gN	HPO_4^{2-} gP	HCO_3^- gC	O_2 gO	H^+ mol	H_2O mol	DOM g	HET gDM	
Oxic gro. HET NH_4^+	?			?	+	−	?	?	$-\frac{1}{Y_{\text{HET}}}$	1	$\rho_{\text{gro,HET,ox,NH}_4^+}$
Oxic gro. HET NO_3^-		?		?	+	−	?	?	$-\frac{1}{Y_{\text{HET}}}$	1	$\rho_{\text{gro,HET,ox,NO}_3^-}$
Anox. gro. HET		−	+	?	+		?	?	$-\frac{1}{Y_{\text{HET}}}$	1	$\rho_{\text{gro,HET,anox}}$

Table 8.12: Process oxic and anoxic growth of heterotrophic microorganisms.

$$\nu_{\text{gro,HET,ox,NO}_3^-\ \text{HET}} + \nu_{\text{gro,HET,ox,NO}_3^-\ \text{DOM}} Y_{\text{HET}} = 0 \tag{8.29}$$

$$\nu_{\text{gro,HET,anox,NH}_4^+\ \text{HET}} + \nu_{\text{gro,HET,anox,NH}_4^+\ \text{DOM}} Y_{\text{HET}} = 0 \tag{8.30}$$

Note that for a steady-state bacterial population, the corresponding mineralization processes described in the sections 8.5.1 and 8.5.2 consist of these growth processes together with respiration of these microorganisms, death and succeeding mineralization of the dead organisms (which again consists of hydrolysis, heterotrophic growth, respiration, and death).

Process rates for growth of heterotrophic microorganisms must take into account limitations by organic substrate and dissolved oxygen (oxic growth) or nitrate (anoxic growth). Depending on the signs of the stoichiometric coefficients, additional limitations with respect to nitrogen and phosphorus may be required.

$$\begin{aligned}\rho_{\text{gro,HET,ox,NH}_4^+} = k_{\text{gro,HET,ox},T_0} \cdot \exp\Big(\beta_{\text{BAC}}(T - T_0)\Big) \left[\cdot \frac{p_{\text{NH}_4^+,\text{HET}} C_{\text{NH}_4^+}}{p_{\text{NH}_4^+,\text{HET}} C_{\text{NH}_4^+} + C_{\text{NO}_3^-}}\right] \\ \cdot \min\left(\frac{C_{\text{DOM}}}{K_{\text{DOM,HET}} + C_{\text{DOM}}}, \frac{C_{\text{O}_2}}{K_{\text{O}_2,\text{HET}} + C_{\text{O}_2}}, \right. \\ \left. \left[\frac{C_{\text{HPO}_4^{2-}}}{K_{\text{HPO}_4^{2-},\text{HET}} + C_{\text{HPO}_4^{2-}}}\right], \left[\frac{C_{\text{NH}_4^+} + C_{\text{NO}_3^-}}{K_{\text{N,HET}} + C_{\text{NH}_4^+} + C_{\text{NO}_3^-}}\right]\right) \cdot C_{\text{HET}}\end{aligned} \tag{8.31}$$

$$\begin{aligned}\rho_{\text{gro,HET,ox,NO}_3^-} = k_{\text{gro,HET,ox},T_0} \cdot \exp\Big(\beta_{\text{BAC}}(T - T_0)\Big) \left[\cdot \frac{C_{\text{NO}_3^-}}{p_{\text{NH}_4^+,\text{HET}} C_{\text{NH}_4^+} + C_{\text{NO}_3^-}}\right] \\ \cdot \min\left(\frac{C_{\text{DOM}}}{K_{\text{DOM,HET}} + C_{\text{DOM}}}, \frac{C_{\text{O}_2}}{K_{\text{O}_2,\text{HET}} + C_{\text{O}_2}}, \right. \\ \left. \left[\frac{C_{\text{HPO}_4^{2-}}}{K_{\text{HPO}_4^{2-},\text{HET}} + C_{\text{HPO}_4^{2-}}}\right], \left[\frac{C_{\text{NH}_4^+} + C_{\text{NO}_3^-}}{K_{\text{N,HET}} + C_{\text{NH}_4^+} + C_{\text{NO}_3^-}}\right]\right) \cdot C_{\text{HET}}\end{aligned} \tag{8.32}$$

$$\rho_{\text{gro,HET,anox}} = k_{\text{gro,HET,anox},T_0} \cdot \exp\Big(\beta_{\text{BAC}}(T - T_0)\Big) \cdot \frac{K_{\text{O}_2,\text{HET}}}{K_{\text{O}_2,\text{HET}} + C_{\text{O}_2}}$$
$$\cdot \min\left(\frac{C_{\text{DOM}}}{K_{\text{DOM,HET}} + C_{\text{DOM}}}, \frac{C_{\text{NO}_3^-}}{K_{\text{NO}_3^-,\text{HET}} + C_{\text{NO}_3^-}}, \left[\frac{C_{\text{HPO}_4^{2-}}}{K_{\text{HPO}_4^{2-},\text{HET}} + C_{\text{HPO}_4^{2-}}}\right]\right) \cdot C_{\text{HET}} \tag{8.33}$$

In these equations, the terms in square brackets only apply, if the corresponding stoichiometric coefficients are negative.

8.8.2 Growth of Nitrifiers

To model nitrification activities, populations of nitrifying bacteria must be modelled. There are different organisms responsible for the first step of nitrification from ammonium to nitrite (e.g. *Nitrosomonas*) (see section 8.6) than for the second step from nitrite to nitrate (e.g. *Nitrobacter*) (see section 8.6) (Dodds, 2002). We denote these two classes of nitrifying bacteria by "N1" (for the fist step) and "N2" (for the second step). Table 8.13 shows the stoichiometry of these two nitrification processes. Note that nitrifiers are

Process	Substances / Organisms										Rate
	NH_4^+ gN	NO_2^- gN	NO_3^- gN	HPO_4^{2-} gP	HCO_3^- gC	O_2 gO	H^+ mol	H_2O mol	N1 gDM	N2 gDM	
Growth of N1	$-\frac{1}{Y_{\text{N1}}}$	+		−	−	−	?	?	1		$\rho_{\text{gro,N1}}$
Growth of N2		$-\frac{1}{Y_{\text{N2}}}$	+	−	−	−	?	?		1	$\rho_{\text{gro,N2}}$

Table 8.13: Growth of first and second stage nitrifiers.

autotrophic bacteria that use the energy obtained through oxidation of ammonium or nitrite, or nitrite to nitrate for the synthesis of organic material. There is one stoichiometric constraint for each of the two processes: The "yields" Y_{N1} and Y_{N2} specify, how many g NH_4^+-N and how many g NO_2^--N are consumed per unit of produced dry biomass unit of nitrifiers. Note that this is considerably more than the nitrogen fraction of the biomass, as the oxidation of the inorganic nitrogen compounds is the energy source for growth.

The process rates must account for the limitations by ammonium or nitrite and dissolved oxygen:

$$\rho_{\text{gro,N1}} = k_{\text{gro,N1},T_0} \cdot \exp\Big(\beta_{\text{N1}}(T - T_0)\Big)$$
$$\cdot \min\left(\frac{C_{\text{NH}_4^+}}{K_{\text{NH}_4^+,\text{nitri}} + C_{\text{NH}_4^+}}, \frac{C_{\text{O}_2}}{K_{\text{O}_2,\text{nitri}} + C_{\text{O}_2}}, \frac{C_{\text{HPO}_4^{2-}}}{K_{\text{HPO}_4^{2-},\text{nitri}} + C_{\text{HPO}_4^{2-}}}\right) \cdot C_{\text{N1}} \tag{8.34}$$

$$\rho_{\text{gro,N2}} = k_{\text{gro,N2},T_0} \cdot \exp\Big(\beta_{\text{N2}}(T - T_0)\Big)$$
$$\cdot \min\left(\frac{C_{\text{NO}_2^-}}{K_{\text{NO}_2^-,\text{nitri}} + C_{\text{NO}_2^-}}, \frac{C_{\text{O}_2}}{K_{\text{O}_2,\text{nitri}} + C_{\text{O}_2}}, \frac{C_{\text{HPO}_4^{2-}}}{K_{\text{HPO}_4^{2-},\text{nitri}} + C_{\text{HPO}_4^{2-}}}\right) \cdot C_{\text{N2}} \tag{8.35}$$

8.9 Colonization

Colonization can be an important process to accelerate the increase of biological populations after a catastrophic event. In addition, colonization protects the solution of the model from reaching extremely low concentrations from which it would take a very long time to recover by a process the rate of which is linear in the organism concentration.

Colonization is a transfer process of organisms from either one compartment of the system to the other or from the part of the world outside of the system boundaries into the system. Consequently, it is described by flux

$$J_{\mathrm{col},i} \tag{8.36}$$

across the system boundaries. This flux can often be assumed to be constant, but it can also have a seasonal dependence, or, if between compartments described by the model, the net colonization rate could be made dependent on the difference of the concentrations of the organism in both compartments. Usually, the colonization flux would be selected to be so small that it does not lead directly to a significant change of biomass. Its main effect is to stimulate the growth process which then takes place within the system boundaries and relies on internal resources of the system. A small colonization rate is sufficient to protect the solution from reaching extremely small concentrations and thus significantly increases growth in the initial phase after a near extinction.

Part III

Stochasticity, Uncertainty and Parameter Estimation

Chapter 9

Consideration of Stochasticity and Uncertainty

9.1 Causes of Stochasticity and Uncertainty

9.1.1 Stochasticity of Dynamics

So far, we described the dynamics of densities of functional groups of organisms by deterministic differential equations. This means that no randomness is involved in the dynamics so that the same initial conditions and driving forces always lead to the same results. There are three main reasons, why this is only an approximate description of reality even if the structure and function of the ecosystem would be perfectly known.

First, **genetic stochasticity** leads to non-deterministic changes in the genetic composition of a population and in related properties of the individuals even in the absence of selective forces. As a consequence, this leads to non-deterministic population or community dynamics. Together with selection processes, such genetic changes leads to evolutionary processes.

Second, populations and communities consist of individual organisms, the fate of which can only be described by probabilistic processes. This is in particular true for birth and death processes (we can formulate a survival probability, but will never know, when exactly an individual organism will die), but applies also to food uptake followed by respiration and growth. These stochastic processes at the individual level introduce random elements into population or community dynamics, so-called **demographic stochasticity**. This is particularly important to consider for populations or communities that consist of a small number of organisms, in particular when calculating probabilities of extinction. On the other hand, the relative variability of population and community dynamics due to demographic stochasticity becomes smaller with an increasing number of organisms in the population. For this reason, the equations as discussed in the previous chapters can be interpreted as descriptions for the limiting case of very large populations where demographic stochasticity can be neglected.

A third reason for non-deterministic dynamics is that environmental conditions were described very simplistically in our models so far (e.g. seasonal and smooth variation of light and temperature in a homogeneous environment). Short-term variability and heterogeneity of inputs that are not resolved by the available data, effects of influence

factors that are not considered by the model, etc. lead to regular and irregular deviations from the behaviour of the deterministic models described so far. The irregular component of these deviations is called **environmental stochasticity** and is also relevant for large populations and communities.

All three elements of stochasticity in ecosystem dynamics discussed above lead to uncertainty about the behaviour of the system even if structure and function of the ecosystem would be perfectly known. For this reason, when considering any of these sources of stochasticity, model predictions for given initial conditions and parameters will no longer be certain outcomes and their uncertainty may have to be considered.

9.1.2 Uncertainty of Model Structure, Input and Parameters

Due to our incomplete knowledge of driving forces and ecosystem structure and function, model predictions would be uncertain even in cases in which stochasticity of ecosystem dynamics could be neglected (see previous sections for sources of stochasticity). Input uncertainty can usually be estimated based on the uncertainty of sampling procedures and measurement devices. However, despite choosing a spatial domain to be modelled with well-defined boundaries, fluxes across these boundaries are often difficult to quantify due to their spatial dimension and the heterogeneity of the fluxes. Model parameters that have a direct mechanistic meaning can sometimes be estimated from experiments in the laboratory (e.g. from observed growth rates of species as a function of driving conditions) or from data that are independent of the biological processes in the model (e.g. temperature profiles provide information on the intensity of mixing processes in a lake which also affect plankton dynamics). However, even parameters that have a conceptual meaning can often not be estimated independently of the model due to the aggregated description by the model (e.g. growth rate parameters of a community of many different species, hydrological parameters that represent processes averaged over a heterogeneous landscape). Uncertainty of model structure is even more difficult to consider than input and parameter uncertainty. Ideally, several conceptually different models should be used for calibration and prediction to make it possible to at least roughly estimate the effect of structural uncertainty. However, due to limited resources, this is often not possible in practice.

9.2 Probabilistic Framework

We use random variables to describe stochasticity in the dynamics of ecological systems as well as uncertainty due to incomplete knowledge about the structure and function of these systems. Random variables describe random events or uncertain knowledge and are characterized by their probability distributions. In the following three subsections, we briefly describe some basic terms of probability theory that we will apply to the description of ecological systems in the next section.

9.2.1 Univariate Random Variables and Distributions

A scalar random variable can be characterized by its probability distribution. Figure 9.1 illustrates discrete and continuous probability distributions for a one-dimensional random variable Z. For continuous random variables, probabilities of the outcome being in an interval can be calculated as the integral of the density, f, over this interval (as an example,

the grey area in the right panel of Fig. 9.1 represents the probability that the outcome is in the interval $[z_1, z_2]$). Figure 9.2 shows the cumulative probabilities of the outcome being smaller than or equal to the value at the x-axis for the two cases shown in Fig. 9.1.

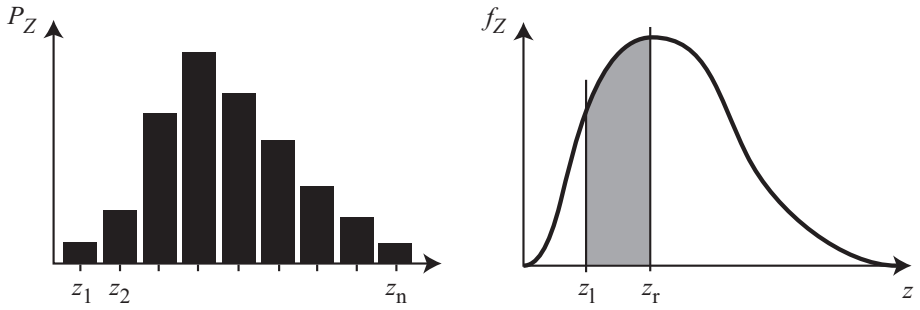

Figure 9.1: Examples of discrete probabilities of a probability distribution of a discrete random variable (left) and a probability density of a continuous random variable (right).

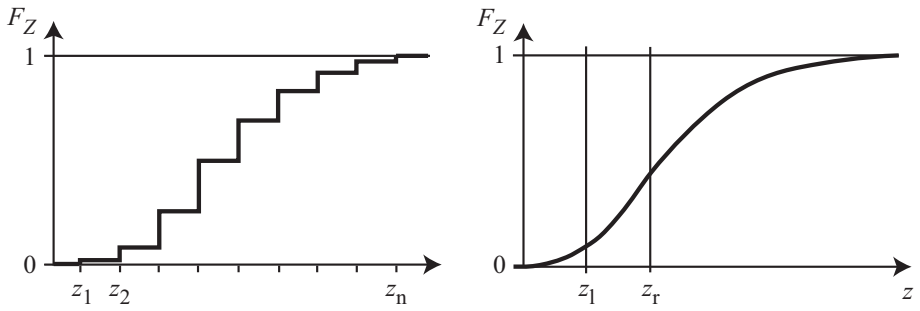

Figure 9.2: Examples of distribution functions of a discrete (left) and a continuous random variable (right).

9.2.2 Multivariate Random Variables and Distributions

Multivariate distributions are characterized by their joint probability distribution. For continuous multivariate random variables, the joint propability density, f, describes the probability of an outcome per unit of all of its components. Consequently, analogously to the univariate case, the probability of an outcome in any part of the outcome space, A, is equal to the integral of the joint density over this space (in this section, we illustrate all equations and figures for the two-dimensional case):

$$P(A) = \int_A f(x, y)\, \mathrm{d}x\, \mathrm{d}y \quad . \tag{9.1}$$

When we are interested in the associated probability distribution of some of the components of a multivariate random variable, it is important to distinguish the marginal and the conditional distributions. The marginal distribution of x is the distribution of x

when no knowledge about y (besides that induced by the joint distribution) is available. Consequently, we have to integrate the joint distribution over y:

$$f(x) = \int f(x, y)\, \mathrm{d}y \quad . \tag{9.2}$$

In contrast, the conditional distribution represents the knowledge about x when we know that y has a given value of y_0. Thus, we have to keep y fixed at y_0 and renormalize the resulting distribution:

$$f(x \mid y_0) = \frac{f(x, y_0)}{f(y_0)} = \frac{f(x, y_0)}{\int f(x', y_0)\, \mathrm{d}x'} \quad . \tag{9.3}$$

Figure 9.3 illustrates the concepts of joint, marginal and conditional distributions with a two-dimensional example. We will come back to these important concepts when dealing with Bayesian inference in section 10.3.

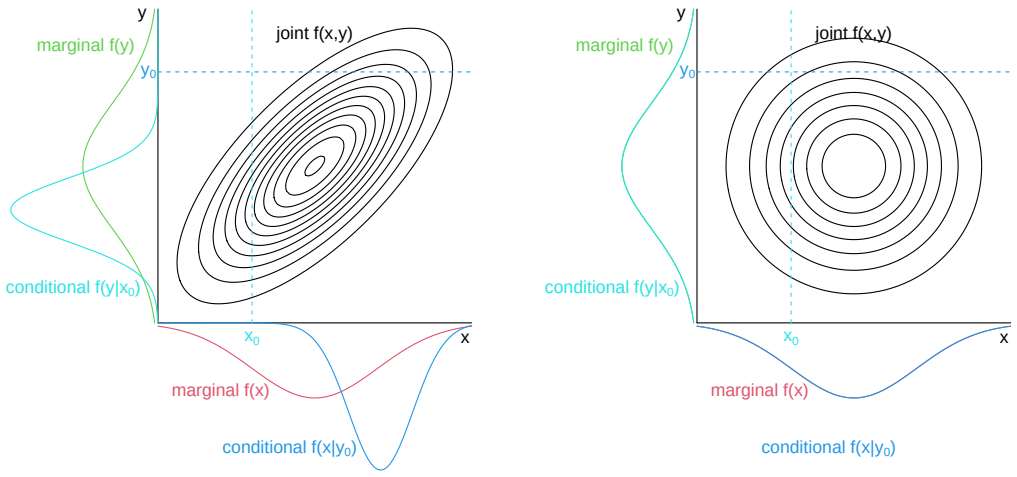

Figure 9.3: Examples of bivariate random variables with (left) and without dependence (right) between the two components. The figures show the bivariate probability density by isolines as well as marginal and conditional density functions of the two components. Note that for a joint distribution of independent random variables ($f(x, y) = f(x)f(y)$), the conditional and marginal distributions are the same.

9.2.3 Stochastic Processes

A stochastic process in time is a set of random variables, one for each point in time. When using a stochastic process to describe a parameter that is influenced by stochastic external driving forces, it is often convenient to define this stochastic process as a solution of a stochastic differential equation. The simplest stochastic differential equation that does not lead to an ever increasing variance is the equation for the mean-reverting Ornstein–Uhlenbeck process given by

$$\mathrm{d}\Theta_t = \frac{1}{\tau}(\mu - \Theta_t)\, \mathrm{d}t + \sqrt{\frac{2}{\tau}}\sigma\, \mathrm{d}W_t \quad . \tag{9.4}$$

Here, Θ_t, is the time-dependent variable (as a random process, i.e. a set of random variables for all points of time, t), μ is its mean, σ its asymptotic standard deviation, τ the correlation time of the mean-reverting process, and W_t is a continuous-time random walk process (also called Brownian motion or Wiener process). The first term (so-called drift term) on the right hand side of this stochastic differential equation describes a relaxation of the parameter Θ_t back to its mean, μ, with a correlation time τ, the second term (so-called diffusion term) describes the effect of noise. The long-term behaviour of this process leads to continuous random walks around the mean, μ, with a standard deviation σ. Figure 9.4 shows some examples of realizations of Ornstein-Uhlenbeck processes.

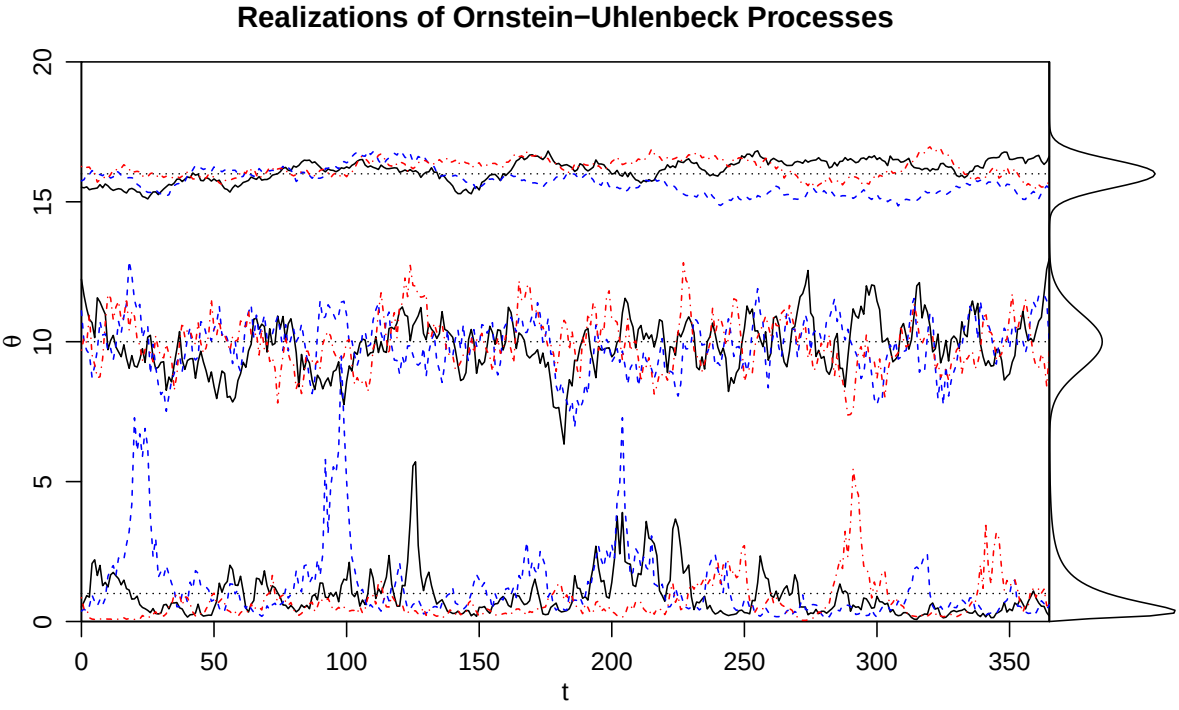

Figure 9.4: Examples of realizations of Ornstein-Uhlenbeck processes. Top: $\mu = 16$, $\sigma = 0.5$, $\tau = 50$. Middle: $\mu = 10$, $\sigma = 1$, $\tau = 5$. Bottom: exp of realizations of an Ornstein-Uhlenbeck process with $\tau = 10$; mean, m, and standard deviation, s, of the underlying Ornstein-Uhlenbeck process (log of the plotted time series) are chosen such that that $\mu = 1$ and $\sigma = 1$ on the plotted scale (see section 14.3, equations 14.27 to 14.30 for the required transformations between (μ, σ) and (m, s)). The asymptotic densities (for $t \gg \tau$) of the processes are shown in the right margin of the plot.

The stochastic differential equation (9.4) can be solved analytically and leads to a Normal distribution at any value of the time, t, with the expected value, variance and covariance given by

$$\mathrm{E}[\Theta_t \mid \Theta_{t_0} = \theta_0] = \mu + (\theta_0 - \mu) \exp\left(-\frac{t - t_0}{\tau}\right) \quad , \tag{9.5}$$

$$\mathrm{Var}[\Theta_t \mid \Theta_{t_0} = \theta_0] = \sigma^2 \left[1 - \exp\left(-2\frac{t - t_0}{\tau}\right)\right] \quad , \tag{9.6}$$

$$\mathrm{Cov}[\Theta_t, \Theta_s \mid \Theta_{t_0} = \theta_0] = \sigma^2 \left[\exp\left(-\frac{\mid t - s \mid}{\tau} \right) - \exp\left(-\frac{t + s - 2t_0}{\tau} \right) \right] \quad . \tag{9.7}$$

This analytical solution demonstrates that when the time $t - t_0$ is large compared to τ, the process will vary around its mean with an approximate standard deviation of σ. The closer to the time t_0, the smaller the variance and the closer the mean to the value at t_0. It is easy to draw discretized realizations of the process given by the equations (9.5) and (9.6).

9.3 Stochasticity and Uncertainty in Ecological Models

If we summarize all model output variables at time points and locations of interest in a model output vector, $\mathbf{y}_{\mathrm{out}}$, the deterministic models used in the previous chapters can be represented by the (vector-valued) function

$$\mathbf{y}_{\mathrm{out}}(\mathbf{x}, \boldsymbol{\theta}) \quad , \tag{9.8}$$

where $\mathbf{x}$ are the inputs and $\boldsymbol{\theta}$ the model parameters.

9.3.1 Genetic or Demographic Stochasticity

Considering genetic or demographic stochasticity leads to a probabilistic rather than a deterministic description of population or community dynamics. This leads to probability distributions of outcomes instead of precise results even for given inputs and model parameters. Formally, considering this kind of stochasticity, requires the replacement of the deterministic model function (9.8) by a vector of random variables

$$\mathbf{Y}_{\mathrm{out}}(\mathbf{x}, \boldsymbol{\theta}) \quad . \tag{9.9}$$

In this case, the vector of random variables, $\mathbf{Y}_{\mathrm{out}}$, is characterized by a joint probability distribution

$$p_{\mathrm{out}}(\mathbf{y}_{\mathrm{out}} \mid \mathbf{x}, \boldsymbol{\theta}) \tag{9.10}$$

for the variables $\mathbf{y}_{\mathrm{out}}$ conditional on inputs, $\mathbf{x}$, and model parameters, $\boldsymbol{\theta}$. For continuous random variables, p describes a joint probability density and is usually denoted, f; for discrete random variables, it describes a joint discrete probability distribution and is typically denoted P.

Demographic stochasticity can be described by discrete indviduals or individual-based models. The dynamics of a discrete individuals population of community model can be described by a so-called master equation, a differential equation describing how the probability of the system being in a given state changes over time (Black and McKane, 2012). In the simplest case, the state of a population or community is described by the number of organisms of a specific species or the numbers of different species in the community. The master equation is then the differential equation that describes the dynamics of the probability distribution of the number of species or of a vector of the numbers of different species of organisms (see section 12.3.2 for an example of how such a differential equation can be constructed). More complex individual-based models even model each organism separately, differentiating properties of different organisms of the same species (see section 12.3.3).

9.3.2 Environmental Stochasticity

Through the dependence of inputs, mass fluxes and process rates on environmental conditions, environmental stochasticity leads to associated fluctuations in mass fluxes and process rates. The most straightforward way of considering the effet of these fluctuations on the behaviour of the ecosystem is to make inputs or model parameters stochastic processes in time. This results in replacing the given inputs, $\mathbf{x}$, and/or the given model parameters, $\boldsymbol{\theta}$, by stochastic processes, $\mathbf{X}$, and/or $\boldsymbol{\Theta}$ as shown in Figure 9.4. Dependent on whether there is no additional intrinsic stochasticity or there is additional intrinsic stochasticity, we then get the model description

$$\mathbf{y}_{\text{out}}(\mathbf{X}, \boldsymbol{\Theta}) \tag{9.11}$$

or

$$\mathbf{Y}_{\text{out}}(\mathbf{X}, \boldsymbol{\Theta}) \quad . \tag{9.12}$$

9.3.3 Uncertainty due to Incomplete Knowledge

In addition to uncertainty induced in the predictions due to genetic, demographic, and environmental stochasticity, we have uncertainty due to incomplete knowledge about input, mechanisms, parameterizations and parameter values. In contrast to uncertainty due to stochasticity, for the description of which probability calculus provides the obvious mathematical framework, it is less clear, which is the best mathematical framework to describe incomplete knowledge. There are the following reasons, why probabilities are also a good framework to describe uncertainty due to incomplete knowledge (Howson and Urbach, 1989; Gillies, 1991; Reichert et al., 2015):

First, to describe incomplete knowledge, probabilities are interpreted as degrees of belief of an individual or a group (so-called subjective or intersubjective probabilities), rather than as limits of observed frequencies for a large number of observations as they are interpreted for the description of stochasticity. It can be shown, that if such degrees of belief are operationalized by indifference statements between lotteries and if the person stating his or her beliefs wants to avoid the possibility of sure loss when someone chooses between the lotteries he or she is indifferent, these degrees of belief must follow the laws of probability (Ramsey - De Finetty theorem) (Howson and Urbach, 1989).

Another argument in favour of using probabilities is the need to be able to consistently express conditional beliefs (how would the system develop under certain management measures or environmental conditions). This is also best possible when using probabilities (Cox, 1946).

Finally, there is another very important argument for using probabilities to describe scientific knowledge that is rarely discussed in the literature (Reichert et al., 2015). Uncertainty of the outcome of a perfectly known system that is affected by randomness can be characterized by objective probabilities. Once the random event has been realized, but the outcome has not yet been observed, uncertainty becomes uncertainty due to lack of knowledge. Here, the underlying objective probability serves as the natural, characterization of the uncertainty of the outcome due to incomplete knowledge. Such a transfer of objective probabilities to intersubjective degrees of belief is only consistently possible in a framework that also uses probabilities to describe these beliefs.

When using probabilities to describe and quantify scientific knowledge, it is important to acquire the information in an intersubjective way. Subjective probabilities are useful to characterize individual beliefs and are required to understand individual behaviour. However, the "current state of scientific knowledge" can only be described by "defendable" probability distributions constructed from empirical evidence extracted from the literature or by intersubjective probabilities aggregated from individual scientists or elicited from groups of scientists. Note that this procedure is in accordance with the scientific standard of quality control by peer review.

In conclusion, we will formulate the uncertainty of input, model parameterization or model parameters in the form of a joint probability distribution of inputs and model parameters. The model is then again described by the equations (9.11) or (9.12) but the bold symbols mean here vectors of random variables rather than random processes. If there is environmental stochasticity, the uncertaint random variables become the parameters of the stochastic processes that describe the fluctuating inputs or parameters.

In many practical cases the joint distribution of inputs and parameters will be the product of independent marginals. Three particularly important univariate probability distributions used for such marginals are the Uniform, the Normal and the Lognormal distributions. These distributions are described in Appendix 14.

9.4 Numerical Approximation by Monte Carlo Simulation

The model functions (9.10), (9.11) and (9.12) require the calculation of probability distributions of model output resulting from intrinsic stochasticity (equation 9.10), from the propagation of random variables or random processes through a deterministic model (equation 9.11), or the evaluation of a stochastic model for random model parameters (equation 9.12). With the exception of a very small category of (mostly linear) models, this cannot be done analytically.

The most universal numerical technique to propagate uncertainties while accounting for model nonlinearities is Monte Carlo simulation. To do so, a random sample is drawn from the parameter, input or intrinsic variable distribution, the model results are calculated for all of these parameter sets and the empirical frequency distribution of these model results is then used as an approximation to the probability density of the results. Figure 9.5 illustrates this procedure for a deterministic model $y(\theta)$.

If the model is stochastic, this Monte Carlo approach is extended by also drawing a realization from the probability distribution of model results for each realization of the model parameters. If model stochasticity is formulated by the use of stochastic, time-dependent parameters as described in section 9.3, this consists of drawing a realization of the Ornstein-Uhlenbeck processes for each time-dependent parameter as shown in Fig. 9.4 and then evaluating the model (e.g. by numerically integrating the differential equations). This will be illustrated in section 11.7.

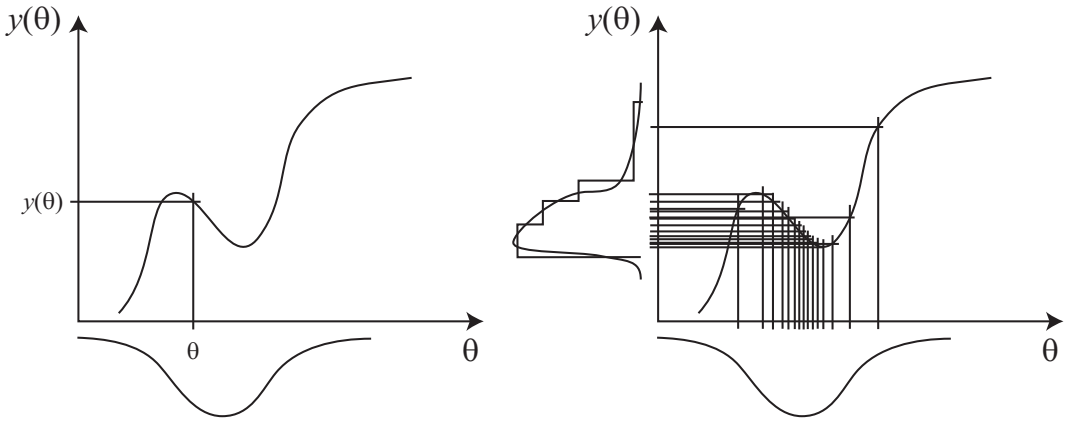

Figure 9.5: Illustration of the idea underlying the propagation of a probability distribution of parameters to model results by Monte Carlo simulation.

Chapter 10

Parameter Estimation

Chapter 9 was devoted to the consideration of stochasticity and uncertainty in model input, structure and parameters for calculating probabilistic model predictions. In this chapter, we are interested in the reverse problem, to learn from observational data about model parameters. As parameter estimation or 'statistical inference' is based on observations, in section 10.1 the model representations introduced in chapter 9 are extended to consider observation error. In the two subsequent sections 10.2 and 10.3 the concepts underlying the two most important general inference techniques, maximum likelihood parameter estimation and Bayesian inference, respectively, are briefly introduced.

10.1 Observation Error and Likelihood Function

In chapter 9 we were interested in describing our knowledge about the 'true' system state by model output. To learn from observations, we first need an extension of these models to describe observation error. The simplest way to do that, is to formulate an additive observation error term, $\mathbf{E}_{\text{obs}}$, to either the deterministic, $\mathbf{y}_{\text{out}}$, or the stochastic, $\mathbf{Y}_{\text{out}}$, model output:

$$\mathbf{Y}_{\text{obs}}(\mathbf{x}, \boldsymbol{\theta}) = \mathbf{y}_{\text{out}}(\mathbf{x}, \boldsymbol{\theta}) + \mathbf{E}_{\text{obs}}(\mathbf{x}, \boldsymbol{\theta}) \tag{10.1}$$

or

$$\mathbf{Y}_{\text{obs}}(\mathbf{x}, \boldsymbol{\theta}) = \mathbf{Y}_{\text{out}}(\mathbf{x}, \boldsymbol{\theta}) + \mathbf{E}_{\text{obs}}(\mathbf{x}, \boldsymbol{\theta}) \quad . \tag{10.2}$$

Note that, due to the observation error, $\mathbf{Y}_{\text{obs}}$ is always a vector of random variables, even in case of a deterministic model and is defined by the joint probability distribution of all observations $\mathbf{y}_{\text{obs}}$ given inputs $\boldsymbol{x}$ and parameters $\boldsymbol{\theta}$:

$$p_{\text{obs}}(\mathbf{y}_{\text{obs}} \mid \mathbf{x}, \boldsymbol{\theta}) \quad . \tag{10.3}$$

When substituting the actual observations for $\mathbf{y}_{\text{obs}}$ and the actual inputs into equation (10.3), the resulting function of the model parameters, $\boldsymbol{\theta}$, is called the **likelihood function** of the model (given the data). The term 'likelihood' was chosen as this function is not a probability distribution of $\boldsymbol{\theta}$ (it is derived as a probability distribution of $\mathbf{y}_{\text{obs}}$), but it seems reasonable to assume that parameters with a large value of p_{obs} are more 'likely' than parameters with smaller values of p_{obs} (for given input and observations) because these parameter values make the observations probable. This is the basis of the simplest universal parameter estimation technique as outlined in the next subsection.

10.2 Maximum Likelihood Parameter Estimation

In frequentist statistics, statistical inference is about finding good approximations to the unique, true parameter values. In this interpretation of statistics, only quantities that can repeatedly be observed, are random variables characterized by probability distributions. Unless model parameters can directly be measured with a random observation error, this is not true for model parameters. In contrast to that interpretation, in section 9.3.3 we adopted a Bayesian approach in which we describe our knowledge about parameter values by probabilitiy distributions. Still, in the absence of prior knowledge, we can get a point estimate of parameter values, $\hat{\boldsymbol{\theta}}$, by maximizing the likelihood function introduced in section 10.1:

$$\hat{\boldsymbol{\theta}}_{\mathrm{ML}} = \mathrm{argmax}_{\boldsymbol{\theta}} \left[p_{\mathrm{obs}}(\mathbf{y}_{\mathrm{obs}} \mid \mathbf{x}, \boldsymbol{\theta}) \right] \quad . \tag{10.4}$$

Unless we calculate frequentist confidence regions, this just provides us with a point estimate but can still be useful for an initial analysis without prior knowledge. The more typical approach of doing Bayesian inference is described in the next subsection.

10.3 Bayesian Inference

The strength of Bayesian inference is to combine prior knowledge about parameter values with information from data using a model. In the environmental sciences this is extremely useful as there is often a lot of defendable, prior information about model parameters available from investigations of similar systems and there may not be sufficient data available from the modeled system to infer all parameters without relying partly on prior knowledge. Under some circumstances, the strength may be a weakness, as it introduces a "bias" from prior knowledge into the analysis. In such cases, frequentist statistics may be the better choice.

To introduce Bayesian inference, we need two important equations from probability theory. Note that we again use the letter P for probabilities of discrete random variables and f for probability densities of continuous random variables. First, marginal probabilities can be gained from joint probabilities by summing or integrating over the variables we are not interested in:

$$P(a) = \sum_b P(a, b) \quad , \quad f(a) = \int f(a, b) \, \mathrm{d}b \qquad . \tag{10.5}$$

Second, conditional probabilities are defined as the quotient of the joint probability and the marginal on which to condition:

$$P(a \mid b) = \frac{P(a, b)}{P(b)} \quad , \quad f(a \mid b) = \frac{f(a, b)}{f(b)} \qquad . \tag{10.6}$$

In these equations, $P(a, b)$ and $f(a, b)$ are joint, discrete probabilities and probability densities, respectively. Combining the two equations, we get

$$P(a \mid b) = \frac{P(a, b)}{P(b)} = \frac{P(b \mid a) \, P(a)}{\sum_{a'} P(b \mid a') \, P(a')} \quad , \quad f(a \mid b) = \frac{f(a, b)}{f(b)} = \frac{f(b \mid a) \, f(a)}{\int_{a'} f(b \mid a') \, f(a') \, \mathrm{d}a'} \tag{10.7}$$

These equations are the basis of Bayesian inference.

When replacing a by the model parameters, $\boldsymbol{\theta}$, and b by the observations, $\mathbf{y}_{\text{obs}}$, in equation (10.7), adding conditioning on the inputs, $\mathbf{x}$, and adding labels to the probability densities, we get the following equation for updating prior to posterior information about the model parameters:

$$f_{\text{post}}(\boldsymbol{\theta} \mid \mathbf{x}, \mathbf{y}_{\text{obs}}) = \frac{f_{\text{pri}}(\boldsymbol{\theta})\ f_{\text{obs}}(\mathbf{y}_{\text{obs}} \mid \mathbf{x}, \boldsymbol{\theta})}{\int f_{\text{pri}}(\boldsymbol{\theta}')\ f_{\text{obs}}(\mathbf{y}_{\text{obs}} \mid \mathbf{x}, \boldsymbol{\theta}')\ \mathrm{d}\boldsymbol{\theta}'} \propto f_{\text{pri}}(\boldsymbol{\theta})\ f_{\text{obs}}(\mathbf{y}_{\text{obs}} \mid \mathbf{x}, \boldsymbol{\theta}) \quad . \tag{10.8}$$

In this equation, f_{post} is the probability density characterizing the posterior knowledge on model parameters combining prior knowledge with information from data using the model, f_{pri} describes the prior knowledge on model parameters, and $f_{\text{obs}}(\mathbf{y}_{\text{obs}} \mid \mathbf{x}, \boldsymbol{\theta}')$ is the likelihood function of the model (the probability density of modelled observations given parameters and input as introduced by the equations 10.1 and 10.3 with actual observations and input substituted for $\mathbf{y}_{\text{obs}}$ and $\mathbf{x}$.

Unless there is conflicting information between prior knowledge and data, equation (10.8) typically leads to narrowing prior information about model parameters to posterior information. The more data is available and the smaller the observation uncertainty, the more information from data influences the posterior. In contrast, few and inaccurate data lead only to minor changes in prior information. Similarly to the maximum likelihood estimate (10.4), the maximum posterior provides a point estimate

$$\hat{\boldsymbol{\theta}}_{\text{MP}} = \text{argmax}_{\boldsymbol{\theta}} \left[p_{\text{pri}}(\boldsymbol{\theta}) p_{\text{obs}}(\mathbf{y}_{\text{obs}} \mid \mathbf{x}, \boldsymbol{\theta}) \right] \tag{10.9}$$

of the model parameters that may be useful for initial analyses or for initiating numerical algorithms for sampling from the posterior as explained in the next subsection.

Figure 10.1 shows a very simple example of sequential Bayesian inference for a parameter that is directly observable.

Updating prior information with data to posterior knowledge by Bayesian inference is illustrated in the first row of plots. The second row shows how the posterior from the first step can be used as a prior for new data that was collected independently of the first data set. The posterior that combines this new prior with the new data is exactly the same as if the original prior would have been updated with all data in one step. This property makes Bayesian inference a consistent learning algorithm.

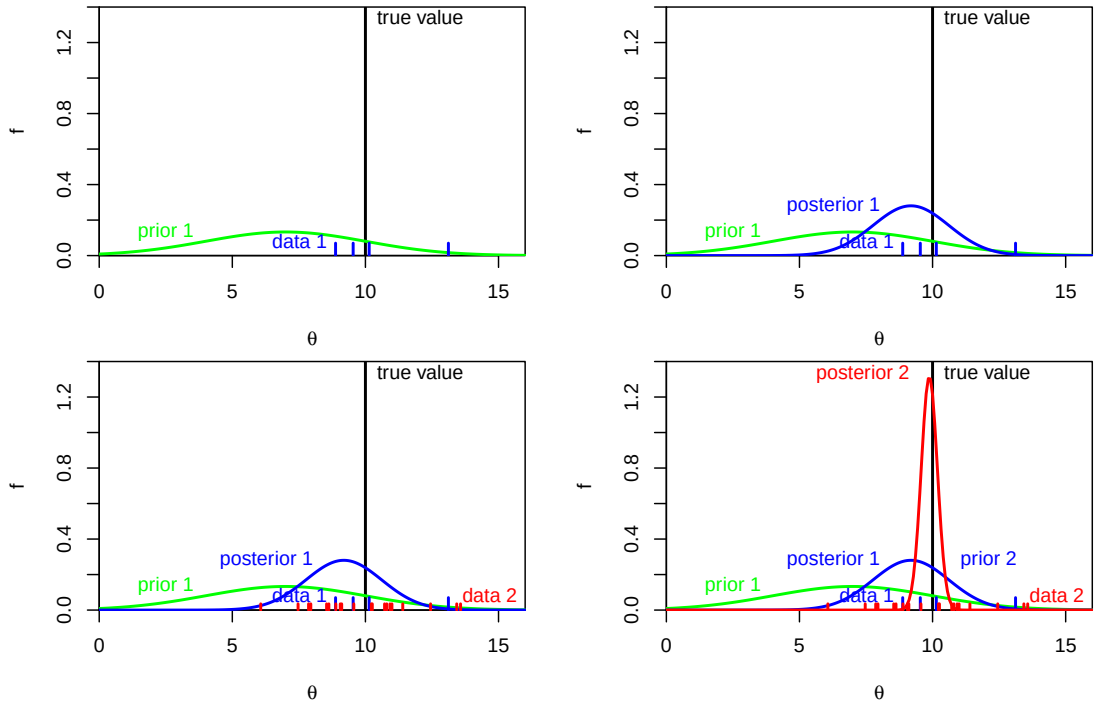

Figure 10.1: Illustration of Bayesian inference. Top left panel: prior, data and true value (which will not be known in a real application). Top right panel: the posterior is a compromise between prior information and information from the data. Bottom left panel: additional data becomes available (data 2). Bottom right panel: the posterior becomes now the prior for the new data and leads to a new posterior that is closer to the data.

10.4 Markov Chain Monte Carlo for Posterior Sampling

There are only very few probability distributions and models for which Bayesian inference can be done analytically. For this reason, numerical techniques for Bayesian inference are very important. Most of these are based on Monte Carlo simulation. However, there is an additional difficulty to forward Monte Carlo simulation as discussed in section 9.4. Equation (10.8) only specifies the posterior probability distribution up to a proportionality constant. This makes it difficult to sample from the posterior and specific techniques have been developed to resolve this issue. The most important of these is Markov chain Monte Carlo sampling. In the following, we deal with continuous parameters and thus replace the symbol for a general probability distributions, p, by the symbol for probability densities, f.

A Markov Chain is a special type of a random process. It consists of a sequence of random variables with the property that the probability density of each random variable in the chain conditional on the immediate predecessor is independent of any other random variable of the chain. We are thus able to characterize a Markov chain by its "transition probability density", $f_{\text{trans}}(\boldsymbol{\theta}^{\text{new}} \mid \boldsymbol{\theta}^{\text{old}})$, which is the conditional probability density for reaching a new state, $\boldsymbol{\theta}^{\text{new}}$, given the previous one, $\boldsymbol{\theta}^{\text{old}}$. We will assume our Markov chains to be homogeneous in time. This means that the transition probability density is the same for the whole chain.

Homogeneous Markov chains may have a **stationary distribution**, f_{stat}, that is invariant under executing a step:

$$\int f_{\text{stat}}(\boldsymbol{\theta}')\, f_{\text{trans}}(\boldsymbol{\theta} \mid \boldsymbol{\theta}')\, \mathrm{d}\boldsymbol{\theta}' = f_{\text{stat}}(\boldsymbol{\theta}) \qquad \forall\, \boldsymbol{\theta} \qquad . \tag{10.10}$$

The stationary distribution may also be referred to as **invariant distribution** or **equilibrium distribution**.

A sufficient, although not necessary, condition that a Markov chain has a stationary distribution is the condition of detailed balance:

$$f_{\text{stat}}(\boldsymbol{\theta})\, f_{\text{trans}}(\boldsymbol{\theta}' \mid \boldsymbol{\theta}) = f_{\text{stat}}(\boldsymbol{\theta}')\, f_{\text{trans}}(\boldsymbol{\theta} \mid \boldsymbol{\theta}') \quad \forall \boldsymbol{\theta}, \boldsymbol{\theta}' \quad . \tag{10.11}$$

This condition represents reversibility in the sense that for every pair of parameter states, $\boldsymbol{\theta}, \boldsymbol{\theta}'$, the probabilities of being in one state and transitioning to the other are equal.

If a Markov chain has a stationary distribution and it is aperiodic and recurrent (i.e. ergodic), then the Markov chain will converge to its (in this case unique) stationary distribution. It has been shown that most of the chains used in Markov Chain Monte Carlo simulation fulfill this property (Tierney, 1994; Gamerman, 1997) and can thus be used as samples from the stationary distribution.

The idea underlying Markov Chain Monte Carlo simulation for Bayesian inference is to design a Markov chain that has the posterior as its stationary distribution. We can then calculate a sample of this Markov Chain and use it to calculate approximate characteristics of the posterior (Tierney, 1994; Gelman et al., 1995; Gamerman, 1997).

Some Markov Chain Monte Carlo procedures decompose the transition density, $f_{\text{trans}}(\boldsymbol{\theta}' \mid \boldsymbol{\theta})$, into a proposal density, $f_{\text{prop}}(\boldsymbol{\theta}' \mid \boldsymbol{\theta})$, and an acceptance probability, $P_{\text{accept}}(\boldsymbol{\theta}' \mid \boldsymbol{\theta})$.

Denoting the probability of staying at the same point by

$$P_{\text{stay}}(\boldsymbol{\theta}) = 1 - \int f_{\text{prop}}(\boldsymbol{\theta}' \mid \boldsymbol{\theta})\, P_{\text{accept}}(\boldsymbol{\theta}' \mid \boldsymbol{\theta})\, \mathrm{d}\boldsymbol{\theta}' \quad , \tag{10.12}$$

the transition density is then formulated as

$$f_{\text{trans}}(\boldsymbol{\theta}' \mid \boldsymbol{\theta}) = f_{\text{prop}}(\boldsymbol{\theta}' \mid \boldsymbol{\theta})\, P_{\text{accept}}(\boldsymbol{\theta}' \mid \boldsymbol{\theta}) + P_{\text{stay}}(\boldsymbol{\theta})\, \delta(\boldsymbol{\theta} - \boldsymbol{\theta}') \quad . \tag{10.13}$$

Given a proposal density, the condition of detailed balance (10.11) leads to a condition that has to be fulfilled by the acceptance probability:

$$P_{\text{accept}}(\boldsymbol{\theta}' \mid \boldsymbol{\theta}) = \frac{f_{\text{stat}}(\boldsymbol{\theta}')}{f_{\text{stat}}(\boldsymbol{\theta})}\, \frac{f_{\text{prop}}(\boldsymbol{\theta} \mid \boldsymbol{\theta}')}{f_{\text{prop}}(\boldsymbol{\theta}' \mid \boldsymbol{\theta})}\, P_{\text{accept}}(\boldsymbol{\theta} \mid \boldsymbol{\theta}') \quad \text{for } \boldsymbol{\theta} \neq \boldsymbol{\theta}' \quad . \tag{10.14}$$

It can easily be verified that the transition density (10.13) leads to the fulfillment of the stationarity condition (10.10) if the acceptance probability fulfills the condition (10.14):

$$\begin{aligned} \int f_{\text{stat}}(\boldsymbol{\theta}')\, f_{\text{trans}}(\boldsymbol{\theta} \mid \boldsymbol{\theta}')\, \mathrm{d}\boldsymbol{\theta}' &= \int f_{\text{stat}}(\boldsymbol{\theta}')\, f_{\text{prop}}(\boldsymbol{\theta} \mid \boldsymbol{\theta}')\, P_{\text{accept}}(\boldsymbol{\theta} \mid \boldsymbol{\theta}')\, \mathrm{d}\boldsymbol{\theta}' + f_{\text{stat}}(\boldsymbol{\theta})\, P_{\text{stay}}(\boldsymbol{\theta}) \\ &= f_{\text{stat}}(\boldsymbol{\theta}) \left(\int f_{\text{prop}}(\boldsymbol{\theta}' \mid \boldsymbol{\theta})\, P_{\text{accept}}(\boldsymbol{\theta}' \mid \boldsymbol{\theta})\, \mathrm{d}\boldsymbol{\theta}' + P_{\text{stay}}(\boldsymbol{\theta}) \right) = f_{\text{stat}}(\boldsymbol{\theta}) \quad . \end{aligned} \tag{10.15}$$

Here, for the first equal sign we used (10.13), for the second (10.14), and for the third (10.12). Thus, any proposal distribution that leads to a recurrent transition distribution and which is associated with an acceptance probability that fulfills the condition (10.14) leads to a Markov chain that can be used to sample from the given stationary distribution. As we only need the ratio of the stationary density at different points in equation (10.14), we can develop such a numerical scheme for a given distribution even if we know its density only up to an unknown normalization factor. This is a crucial property for Bayesian inference, as we usually do not know the normalization factor of the posterior. The procedures discussed in the next two subsections are two slightly different implementations of this more general procedure.

The simplest sampling scheme based on the equations (10.12) to (10.14) assumes a symmetric proposal density ($f_{\text{prop}}(\boldsymbol{\theta}' \mid \boldsymbol{\theta}) = f_{\text{prop}}(\boldsymbol{\theta} \mid \boldsymbol{\theta}')\ \forall\ \boldsymbol{\theta}, \boldsymbol{\theta}'$). As the factor $f_{\text{prop}}(\boldsymbol{\theta} \mid \boldsymbol{\theta}')/f_{\text{prop}}(\boldsymbol{\theta}' \mid \boldsymbol{\theta})$ then cancels from the condition for the acceptance probability (10.14), the acceptance probability

$$P_{\text{accept}}(\boldsymbol{\theta}' \mid \boldsymbol{\theta}) = \min\left(\frac{f_{\text{stat}}(\boldsymbol{\theta}')}{f_{\text{stat}}(\boldsymbol{\theta})}, 1 \right) \tag{10.16}$$

fulfills equation (10.14).

This leads to the following sampling scheme (Metropolis et al., 1953; Gelman et al., 1995; Gamerman, 1997):

1. Select a starting value $\boldsymbol{\theta}^{(0)}$.

2. Based on the current point, $\boldsymbol{\theta}^{(i)}$, draw a random point, $\boldsymbol{\theta}^*$, from the proposal distribution, $f_{\text{prop}}\big(\boldsymbol{\theta}^* \mid \boldsymbol{\theta}^{(i)}\big)$.

3. Calculate the ratio

$$r = \frac{f(\boldsymbol{\theta}^*)}{f(\boldsymbol{\theta}^{(i)})} \tag{10.17}$$

of the densities at the suggested point and at the previous point of the chain.

4. Set

$$\boldsymbol{\theta}^{(i+1)} = \begin{cases} \boldsymbol{\theta}^* & \text{with probability } \min(r, 1) \\ \boldsymbol{\theta}^{(i)} & \text{with probability } 1 - \min(r, 1) \end{cases} \tag{10.18}$$

and proceed with step 2.

This can easily be applied to posterior sampling, as the unknown normalization factor of the posterior density cancels when calculating the ratio (10.17). Figure 10.2 illustrates the first steps of the procedure outlined above.

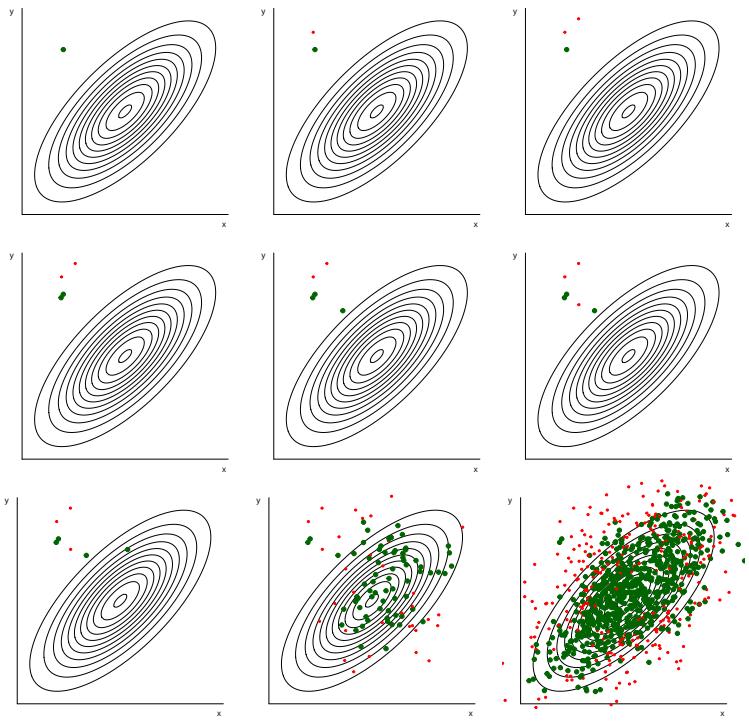

Figure 10.2: The algorithm starts with an initial point (top, left). It then proposes a new point, of which the acceptance probability can be calculated according to equation (10.17). In this case, it is rejected, indicated in red (top, center). The next proposal is again rejected (top, right). The next two proposals are accepted and indicated in green (middle, left and center). Then, again a proposal is rejected and indicated in red (middle, right). This process continues as shown in the bottom plots and at the end, the points marked in green constitute the sample from the distribution (note that, due to rejected proposals, most of the green points are multiple samples).

The general Metropolis scheme still leaves a lot of freedom in choosing the proposal distribution, $f_{\text{prop}}(\boldsymbol{\theta}' \mid \boldsymbol{\theta})$. A simple choice is the use of a Normal distribution for an

individual step of a random walk

$$f_{\text{prop}}(\boldsymbol{\theta}' \mid \boldsymbol{\theta}) \sim \text{N}(\boldsymbol{\theta}, \boldsymbol{\Sigma}) \tag{10.19}$$

where the variance-covariance matrix, $\boldsymbol{\Sigma}$, must be carefully chosen in order to achieve a good efficiency of the procedure.

The choice of the initial point and the proposal distribution affects the convergence of the Markov Chain to the posterior distribution considerably. It is recommendable to start the Markov Chain close to the maximum of the posterior calculated by a numerical optimization routine. This avoids a long "burn-in" phase of the Markov Chain. The acceptance frequency can be influenced by the shape (correlation structure) and size (standard deviations) of the proposal distribution. It should be in the range of 25 to 45 % with lower values for higher dimensions (Gelman et al., 1995). An iterative procedure of adapting the correlation structure of the proposal distribution to that of the posterior (estimated from the previous Markov Chain) and adjusting the step size to achieve a reasonable acceptance probability, is recommended for getting a good Markov Chain.

Figures 10.3 and 10.4 illustrate common convergence problems of Markov chains for the example of a Metropolis algorithm with a Normal proposal distribution.

Please note that, due to the much higher dimensionality and the absence of an analytical form of the posterior, the analyst will typically only have Figure 10.4 available for diagnostic purposes.

The six cases shown in these figures can be interpreted as follows.

The top left case shows a poor coverage of the distribution due to a too small step size of the algorithm. The analyst can identify this problems (i) by the too low rejection frequency of 0.04 and by the slow coverage of the range of parameter θ_1 by the chain in the top left panel of Figure 10.4 (the chain should oscillate much more frequently within the range of the distribution).

The top right case shows poor convergence due to a too large step size of the algorithm. This is identifiable through the too high rejection rate of 0.97 and the long constant values in the Markov chain shown in Figure 10.4. Note that the coverage of the distribution in this case is much better than in the case of the too small step size in the top left panel.

The middle left panel shows a Markov chain with a reasonable step size. This results in a rejection frequency of 0.52 and the chain oscillates much more strongly than it does in the cases shown in the top row. Still, a longer chain would be required to achieve good convergence.

The middle right panel shows the problem of a burn-in period. Due to a poor initial condition, the first 100 points of the chain are required for an approach to parameter regions with high probability density. It is very important to cut such burn-in periods before using the sample for inference, as the sample very much overestimates the probability in these regions. Burn-in problems can be avoided if empirical maximization of the posterior is used prior to starting the Markov chain algorithm and the algorithm is then started close to the maximum.

The bottom left case demonstrates that a poor correlation structure of the proposal distribution can deteriorate convergence. This phenomenon is indicated by a reasonable rejection rate, but still a poor coverage of the parameter range in the bottom left panel in Figure 10.4. An analysis of this figure would lead to the recommendation of increasing

the step size. But significant increases in step size are difficult due to the inadequate correlation structure of the proposal distribution. It is recommendable to calculate the correlation structure of the preliminary sample to achieve iteratively a better correlation structure of the proposal distribution that then finally allows to increase the step size.

The bottom right panel finally shows a Markov chain with a proposal distribution with an adequate correlation structure. This adequate correlation structure allows the analyst to increase the step size. Obviously, convergence is much faster than in the case shown in the middle left panel that has also an adequate step size, but does not account for the correlation structure of the distribution.

This discussion demonstrates the importance of analyzing the Markov chains graphically for hints of how to improve the transition probability distribution for accelerated convergence. In the simple case of a Metropolis algorithm with a Normal proposal distribution this is done by adjusting the correlation structure of the proposal distribution to the preliminary correlation structure of the posterior from the last run, and by scaling the standard deviations of the proposal distribution proportional to those of the posterior in order to achieve a reasonable rejection rate. In addition, several chains should be started with different initial values to verify (or corroborate) the convergence to the same limiting distribution. In addition to such a visual assessment, statistical techniques have been developed to support Markov Chain Monte Carlo diagnostics (Cowles and Carlin, 1996; Brooks and Roberts, 1998).

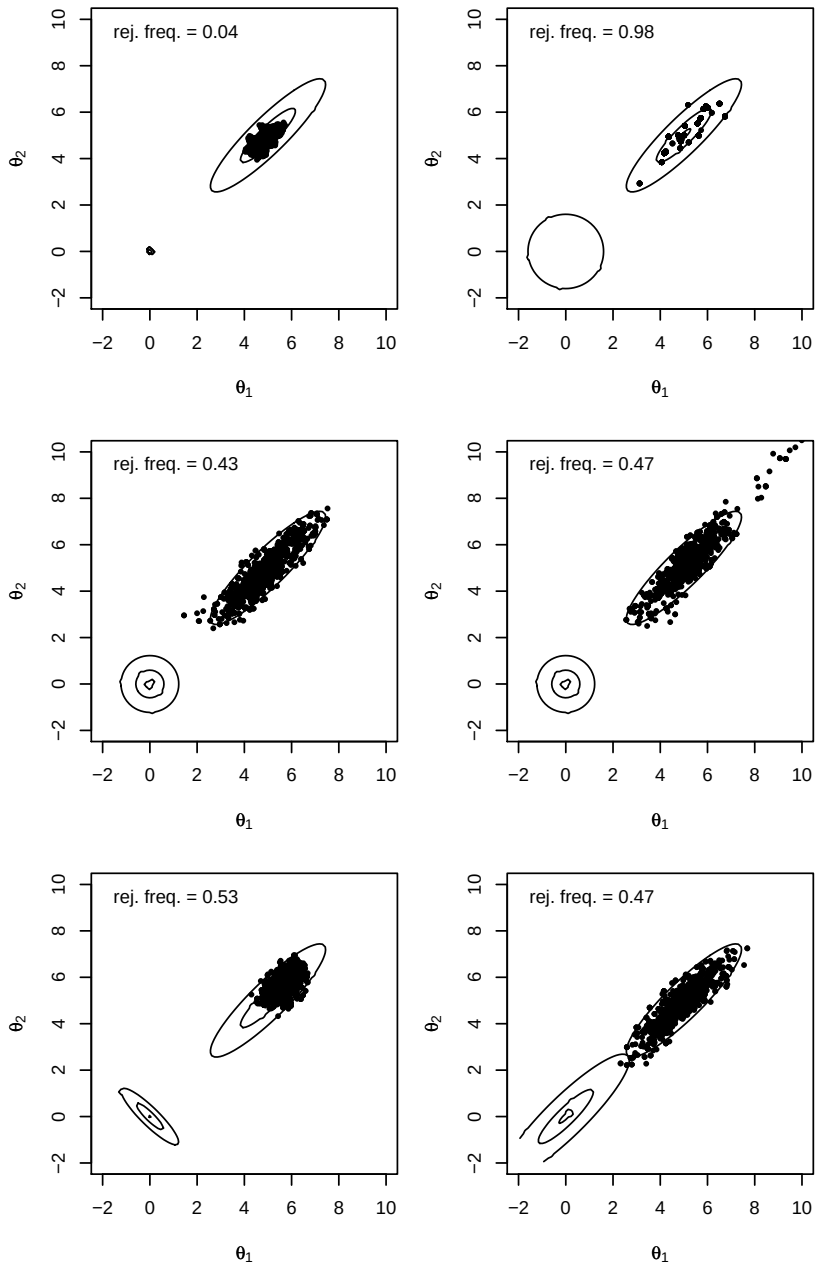

Figure 10.3: Markov chains of length 1000 for a bivariate normal distribution illustrated by its highest probability region boundaries with content of 0.05, 0.5 and 0.95 probability centered at (5,5). The distribution centered at (0,0) represents the normal proposal distribution. See Figure 10.4 for the chains for component θ_1).

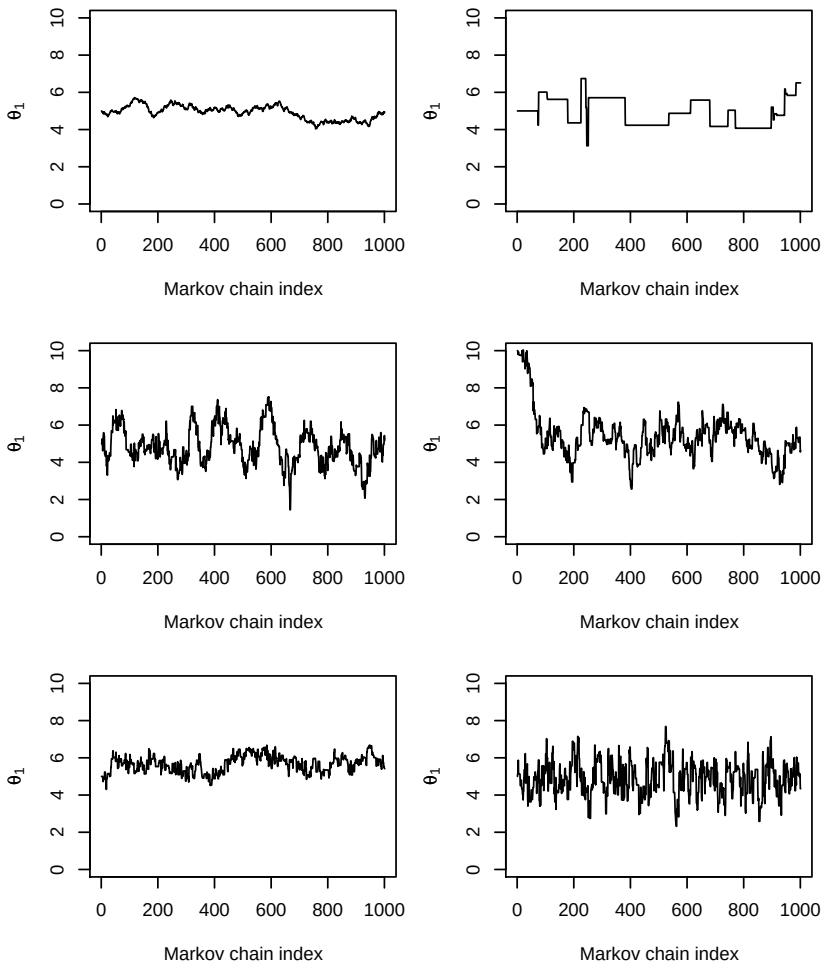

Figure 10.4: Component θ_1 of the Markov chains shown in Figure 10.3.

Part IV

Simple Models of Aquatic Ecosystems

Chapter 11

Simple Models of Aquatic Ecosystems

In this chapter we formulate a series of aquatic ecosystem models of increasing complexity and analyse their behaviour. It is recommended that readers switch to this chapter as soon as possible. The examples and applications introduced here can guide learning how aquatic ecosystem models are built and how we can learn about ecosystem function by working with models. To support this procedure, at the start of each section, we list the chapters and sections required for the understanding of the introduced didactic ecosystem model. Reading this manuscript can be guided by this chapter. Going through all the sections of this chapter and reading the required sections of the previous part before starting to read the didactic example can be an excellent strategy to learn the material of this manuscript. This would have to be complemented by reading chapter 13 that extend the basic knowledge acquired with the didactic models to an overview of models and simulation programs currently in use for research and management support. The content of this chapter can be deepened by implementing the models with the software described in chapters 15 and 16 in the appendix and practice their application and analysis.

This chapter starts with the introduction of a very simple lake phosphorus and phytoplankton model in section 11.1. In section 11.2 this lake phytoplankton model is extended by zooplankton grazing on phytoplankton. The next important extension is to distinguish the epilimnion and hypolimnion of the lake and describing mineralization of organic particles in the sediment. This is done in section 11.3. Section 11.4 provides a further extension of this model to the nitrogen cycle. Section 11.5 introduces a model for the oxygen, phosphorus and nitrogen household in a river for a given density of benthic organisms. This is followed in section 11.6 by a model for the benthic population in rivers. Finally, in section 11.7, the lake plankton model described in section 11.2 is extended to the consideration of environmental stochasticity and uncertainty as described in chapter 9.

11.1 Lake Phytoplankton Model

This model is based on the chapters and sections 1, 2, 3.1, 3.2, 4.1, 4.2, 8.1, and 8.3. It provides the opportunity to deepen the basic concepts of ecosystem model formulation with a very simple model for soluble reactive phosphorus and phytoplankton in the epilimnion of a lake. Despite its simplicity, this model is already able to demonstrate some important behavioural properties of such a system that will remain features of more complicated models. The model will be made more realistic by adding more elements in the following sections.

A very simple model of ecological processes in a lake consists of mass balances for the limiting nutrient soluble reactive phosphorus (for stoichiometric purposes assumed to be phosphate, HPO_4^{2-}) and phytoplankton, in the following referred to as algae (ALG), growing on this nutrient through the process of primary production. This model considers the two transformation processes growth (by primary production, see section 8.1) and death (see section 8.3) of algae. In this simple example, we do not consider zooplankton and dead organic particles and their mineralization. These processes will be added later (sections 11.2 and 11.3). When denoting the phosphorus content of algae by $\alpha_{\mathrm{P,ALG}}$ and formulating simple process rates according to the principles described in section 4.2, we get the process table shown as Table 11.1.

Process	Substances / Organisms		Rate
	HPO_4^{2-}	ALG	
	gP	gDM	
Growth of algae	$-\alpha_{\mathrm{P,ALG}}$	1	$\rho_{\mathrm{gro,ALG}}$
Death of algae		-1	$\rho_{\mathrm{death,ALG}}$

Table 11.1: Process table of a simple lake phytoplankton model.

In a first version of the model, we assume the dependences of process rates on current concentrations of phosphate and algae shown in Table 11.2. The process rate of algal

Rate	Rate expression
$\rho_{\mathrm{gro,ALG}}$	$k_{\mathrm{gro,ALG}} \dfrac{C_{HPO_4^{2-}}}{K_{HPO_4^{2-},\mathrm{ALG}} + C_{HPO_4^{2-}}} C_{\mathrm{ALG}}$
$\rho_{\mathrm{death,ALG}}$	$k_{\mathrm{death,ALG}}\, C_{\mathrm{ALG}}$

Table 11.2: Process rates of the first version of the simple lake phytoplankton model.

growth considers a growth limitation by phosphate that reaches saturation at high phosphate concentrations according to equation (4.11). Combining the process stoichiometry given in Table 11.1 with the transformation rates given in Table 11.2, we get the following transformation rates of $C_{HPO_4^{2-}}$ and C_{ALG}:

$$r_{HPO_4^{2-}} = -\alpha_{\mathrm{P,ALG}} \cdot k_{\mathrm{gro,ALG}} \frac{C_{HPO_4^{2-}}}{K_{HPO_4^{2-},\mathrm{ALG}} + C_{HPO_4^{2-}}} C_{\mathrm{ALG}} \quad , \tag{11.1}$$

$$r_{\mathrm{ALG}} = k_{\mathrm{gro,ALG}} \frac{C_{\mathrm{HPO_4^{2-}}}}{K_{\mathrm{HPO_4^{2-},ALG}} + C_{\mathrm{HPO_4^{2-}}}} C_{\mathrm{ALG}} - k_{\mathrm{death,ALG}}\, C_{\mathrm{ALG}} \quad . \tag{11.2}$$

In order to extend this transformation model to an ecosystem model, we need a description of the physical environment in which these transformations take place. We choose the simplest option of describing the epilimnion of a lake by a mixed reactor of constant volume. This leads to the differential equations (3.9)

$$\frac{\mathrm{d}\mathbf{C}}{\mathrm{d}t} = \frac{Q_{\mathrm{in}}}{V}\Big(\mathbf{C}_{\mathrm{in}} - \mathbf{C}\Big) + \frac{\mathbf{J}_{\mathrm{int}}}{V} + \mathbf{r} \quad . \tag{11.3}$$

for the substance vector

$$\mathbf{C} = \begin{pmatrix} C_{\mathrm{HPO_4^{2-}}} \\ C_{\mathrm{ALG}} \end{pmatrix} \tag{11.4}$$

If we assume an inflow concentration of $C_{\mathrm{in,HPO_4^{2-}}}$ for phosphate and neglect algae in the inflow we get the input concentration vector

$$\mathbf{C}_{\mathrm{in}} = \begin{pmatrix} C_{\mathrm{in,HPO_4^{2-}}} \\ 0 \end{pmatrix} \tag{11.5}$$

and we end up with the following differential equations for concentrations of phosphate, $C_{\mathrm{HPO_4^{2-}}}$, and algae, C_{ALG}:

$$\frac{\mathrm{d}C_{\mathrm{HPO_4^{2-}}}}{\mathrm{d}t} = \frac{Q_{\mathrm{in}}}{V}\Big(C_{\mathrm{in,HPO_4^{2-}}} - C_{\mathrm{HPO_4^{2-}}}\Big) + r_{\mathrm{HPO_4^{2-}}} \quad , \tag{11.6}$$

$$\frac{\mathrm{d}C_{\mathrm{ALG}}}{\mathrm{d}t} = -\frac{Q_{\mathrm{in}}}{V} C_{\mathrm{ALG}} + r_{\mathrm{ALG}} \quad . \tag{11.7}$$

Combining these equations with the rate expressions given above leads to

$$\frac{\mathrm{d}C_{\mathrm{HPO_4^{2-}}}}{\mathrm{d}t} = \frac{Q_{\mathrm{in}}}{V}\Big(C_{\mathrm{in,HPO_4^{2-}}} - C_{\mathrm{HPO_4^{2-}}}\Big) - \alpha_{\mathrm{P,ALG}} \cdot k_{\mathrm{gro,ALG}} \frac{C_{\mathrm{HPO_4^{2-}}}}{K_{\mathrm{HPO_4^{2-},ALG}} + C_{\mathrm{HPO_4^{2-}}}} C_{\mathrm{ALG}} \quad , \tag{11.8}$$

$$\frac{\mathrm{d}C_{\mathrm{ALG}}}{\mathrm{d}t} = -\frac{Q_{\mathrm{in}}}{V} C_{\mathrm{ALG}} + k_{\mathrm{gro,ALG}} \frac{C_{\mathrm{HPO_4^{2-}}}}{K_{\mathrm{HPO_4^{2-},ALG}} + C_{\mathrm{HPO_4^{2-}}}} C_{\mathrm{ALG}} - k_{\mathrm{death,ALG}}\, C_{\mathrm{ALG}} \quad . \tag{11.9}$$

Note that we wrote all these equations for this first ecosystem model to clarify our notation. For the other ecosystem models we will only show the process table (in this case Table 11.1) and the equations for the process rates (in this case Table 11.2), provide a description

of the physical environment, and define the inputs. This is sufficient to uniquely define the model.

As discussed in section 5.3 such a two-dimensional system could only develop solutions that asymptotically converge to fixed points, that converge to limit cycles, or that diverge. To explore the potential behaviour analytically, as described in section 5.3.1, we naturally start with identifying steady-state solutions (fixed points) and determine their stability. The most straigtforward fixed point solution (when setting the right-hand side of the equations 11.8 and 11.9 to zero is

$$C^{\text{fix},1}_{\text{HPO}_4^{2-}} = C_{\text{in,HPO}_4^{2-}} \quad , \tag{11.10}$$

$$C^{\text{fix},1}_{\text{ALG}} = 0 \quad . \tag{11.11}$$

as the second equation sets the right hand side of (11.9) to zero and subsequently, the first (11.8). As we did not have to make any assumptions on the model parameters, this solution exists for arbitrary values of the model parameters (only nonnegative values make sense). This obviously the solution we would get in the absence of any algae. Let us find out later, whether this solution is also relevant under other cricumstances. To find other solutions, we assume $C_{\text{ALG}} > 0$, divide the right-hand side of equation (11.9) by C_{ALG}, then set it to zero and resolve for $C_{\text{HPO}_4^{2-}}$. Then we substitute this value into equation 11.8, set the right-hand side to zero and resolve for C_{ALG}. This leads to

$$C^{\text{fix},2}_{\text{HPO}_4^{2-}} = \frac{K_{\text{HPO}_4^{2-},\text{ALG}}}{\frac{k_{\text{gro,ALG}}}{k_{\text{death,ALG}} + \frac{Q_{\text{in}}}{V}} - 1} \quad , \tag{11.12}$$

$$C^{\text{fix},2}_{\text{ALG}} = \frac{1}{\alpha_{\text{P,ALG}}} \frac{\frac{Q_{\text{in}}}{V}}{k_{\text{death,ALG}} + \frac{Q_{\text{in}}}{V}} \left(C_{\text{in,HPO}_4^{2-}} - \frac{K_{\text{HPO}_4^{2-},\text{ALG}}}{\frac{k_{\text{gro,ALG}}}{k_{\text{death,ALG}} + \frac{Q_{\text{in}}}{V}} - 1} \right) \quad . \tag{11.13}$$

As phosphate and algae concentrations need to be positive, this solution exists only if both of the two following conditions are fulfilled:

$$k_{\text{gro,ALG}} > k_{\text{death,ALG}} + \frac{Q_{\text{in}}}{V} \quad \text{and} \quad C_{\text{in,HPO}_4^{2-}} > \frac{K_{\text{HPO}_4^{2-},\text{ALG}}}{\frac{k_{\text{gro,ALG}}}{k_{\text{death,ALG}} + \frac{Q_{\text{in}}}{V}} - 1} \quad . \tag{11.14}$$

These conditions are easy to understand, at least qualitiatively. The first condition clarifies that positive algae concentrations are only possible if the maximum specific growth rate exceed death and dilution of algae in the reactor. The second condition sets a lower bound on the phosphate inflow concentration to allow net growth under the actual specific growth rate (which, in steady-state, will be equal to the death rate plus the dilution rate).

Next, we are interested in the stability of these steady-state solutions. According to section 5.3.1, we have to calculate the Jacobian matrix of our system of differential

equations (11.8) and (11.9). This is given by

$$\mathrm{Jac}(\mathbf{g}) = \begin{pmatrix} -\frac{Q_{\mathrm{in}}}{V} - \alpha_{\mathrm{P,ALG}} k_{\mathrm{gro,ALG}} C_{\mathrm{ALG}} \frac{K_{\mathrm{HPO_4^{2-},ALG}}}{\left(K_{\mathrm{HPO_4^{2-},ALG}} + C_{\mathrm{HPO_4^{2-}}}\right)^2} & -\alpha_{\mathrm{P,ALG}} k_{\mathrm{gro,ALG}} \frac{C_{\mathrm{HPO_4^{2-}}}}{K_{\mathrm{HPO_4^{2-},ALG}} + C_{\mathrm{HPO_4^{2-}}}} \\ k_{\mathrm{gro,ALG}} C_{\mathrm{ALG}} \frac{K_{\mathrm{HPO_4^{2-},ALG}}}{\left(K_{\mathrm{HPO_4^{2-},ALG}} + C_{\mathrm{HPO_4^{2-}}}\right)^2} & k_{\mathrm{gro,ALG}} \frac{C_{\mathrm{HPO_4^{2-}}}}{K_{\mathrm{HPO_4^{2-},ALG}} + C_{\mathrm{HPO_4^{2-}}}} - \frac{Q_{\mathrm{in}}}{V} - k_{\mathrm{death,ALG}} \end{pmatrix} \tag{11.15}$$

Substituting the fixed point 1 (equations 11.10 and 11.11) into the Jacobian (11.15) and solving for the eigenvalues, we get:

$$\lambda_1^{\mathrm{fix},1} = -\frac{Q_{\mathrm{in}}}{V} \quad , \quad \lambda_2^{\mathrm{fix},1} = k_{\mathrm{gro,ALG}} \frac{C_{\mathrm{in,HPO_4^{2-}}}}{K_{\mathrm{HPO_4^{2-},ALG}} + C_{\mathrm{in,HPO_4^{2-}}}} - \frac{Q_{\mathrm{in}}}{V} - k_{\mathrm{death,ALG}} \tag{11.16}$$

This means that fixed point 1 is stable if

$$k_{\mathrm{gro,ALG}} < k_{\mathrm{death,ALG}} + \frac{Q_{\mathrm{in}}}{V} \quad \text{or} \quad C_{\mathrm{in,HPO_4^{2-}}} < \frac{K_{\mathrm{HPO_4^{2-},ALG}}}{\frac{k_{\mathrm{gro,ALG}}}{k_{\mathrm{death,ALG}} + \frac{Q_{\mathrm{in}}}{V}} - 1} \tag{11.17}$$

Note that, according to equation (11.14), when both of these conditions are violated, the fixed point 2 starts to exist. The stability of the fixed point 2 can be accessed similarly, but it leads to more complicated expressions. The result is that this fixed point is stable whenever it exists and the eigenvalues can be real or complex.

From the fixed points and the stability analysis outlined above, and when choosing $C_{\mathrm{in,HPO_4^{2-}}}$ as a driving variable, we can derive the bifurcation diagrams shown if Figure 11.1.

It is interesting to realize that for the steady-state solution (11.12) and (11.13) the concentration of phosphate is determined by kinetic parameters of the model and dilution and not by the input concentration of phosphate to the lake. This is because the steady-state dynamics is flux-driven and not concentration-driven. Irrespective of the input (as long as the conditions 11.14 are fulfilled), in the steady-state all phosphate feeding the lake is consumed by phytoplankton. The phosphate concentration in the lake then just represents a dynamic equilibrium that is the lower, the lower the half-saturation concentration of the algae with respect to phosphate is. On the other hand, the input concentration of phosphate has a significant influence on the concentration of algae.

The constant driving forces considered so far may be a reasonable approximation for the description of the ecosystem over weeks or a few months. However, to describe the behaviour over significant fractions of a year or even several years, we have to consider seasonal variation in environmental conditions. A simple way of doing this is by adding temperature and light dependence factors to the growth rate of phytoplankton as it was described by the equations (4.10) and (4.29). This leads to the modified process rates shown in Table 11.3. We can then use seasonally varying functions for temperature, T, and for the light intensity at the lake surface, I_0. A linear dependence of the light extinction

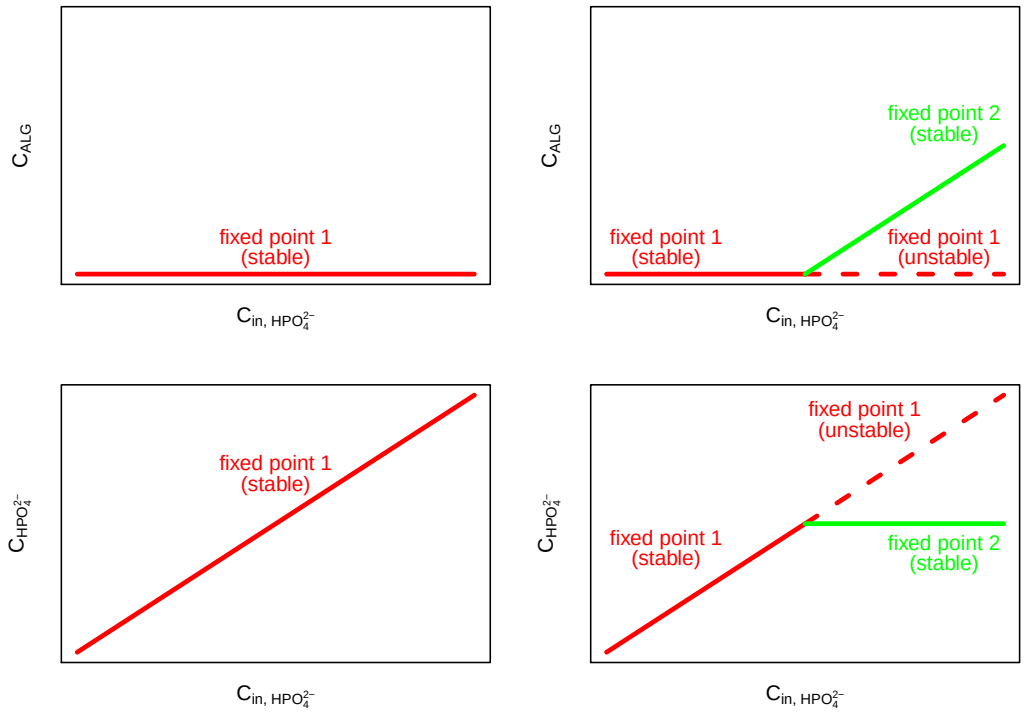

Figure 11.1: Bifurcation diagrams of the fixed points of the model defined by the equations 11.8 and 11.9 as a function of the inflow concentration of phosphate, $C_{\mathrm{in,HPO_4^{2-}}}$. Solid lines indicate stable fixed points, dashed lines unstable fixed points. The left set of plots shows the situation for $k_{\mathrm{gro,ALG}} < k_{\mathrm{death,ALG}} + \frac{Q_{\mathrm{in}}}{V}$ where only the fixed point 1 exists and stays stable. The right set of plots is for $k_{\mathrm{gro,ALG}} > k_{\mathrm{death,ALG}} + \frac{Q_{\mathrm{in}}}{V}$ where at a sufficiently high inflow concentration the fixed point 2 starts to exist and becomes stable.

coefficient on algae concentration

$$\lambda = \lambda_1 + \lambda_2 \cdot C_{\mathrm{ALG}} \tag{11.18}$$

considers basic extinction of water as well as the (self-)shading effect of algae. This leads to an interference between internally generated population dynamics with external periodicity in driving forces and can lead to complicated, irregular behaviour of the solutions (Huppert et al., 2005).

In chapter 16 we show how simple aquatic ecosystem models can be implemented in the graphics and statistics software R (`http://www.r-project.org`) with the aid of the R package `ecosim`.

Figure 11.2 shows a dynamic simulation of the model defined by the processes given in Table 11.1 with rate formulations according to Table 11.2 in a mixed reactor as defined by equation (11.3) with constant values for inflow, inflow concentration, light and temperature. The figure shows a relaxation of algae and phosphate concentrations to the steady-state solution given by the equations (11.12) and (11.13).

Figure 11.3 shows results of the extended model using the growth rates given in Table 11.3 with periodic input for temperature and light according to

Rate	Rate expression
$\rho_{\text{gro,ALG}}$	$k_{\text{gro,ALG},T_0} \cdot \exp\Big(\beta_{\text{ALG}}(T - T_0)\Big) \cdot \frac{1}{\lambda h} \log\left(\frac{K_I + I_0}{K_I + I_0 \exp(-\lambda h)}\right) \cdot \frac{C_{\text{HPO}_4^{2-}}}{K_{\text{HPO}_4^{2-},\text{ALG}} + C_{\text{HPO}_4^{2-}}} \cdot C_{\text{ALG}}$
$\rho_{\text{death,ALG}}$	$k_{\text{death,ALG}}\, C_{\text{ALG}}$

Table 11.3: Process rates of the extended version of the simple lake phytoplankton model.

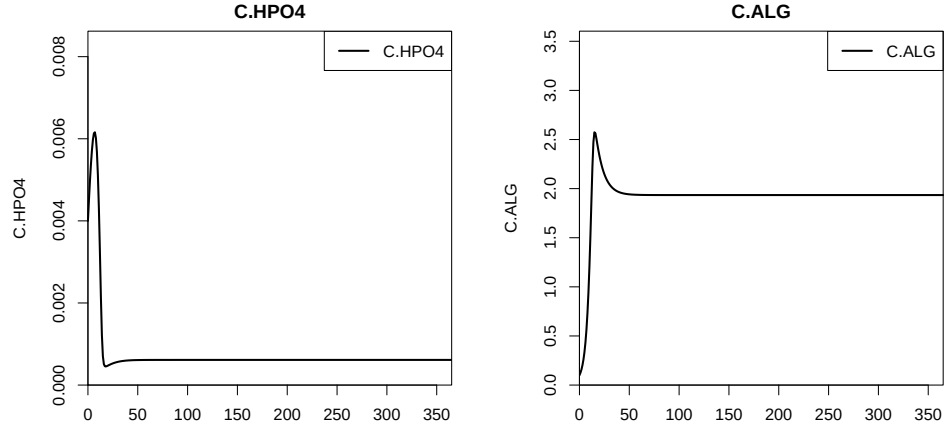

Figure 11.2: Results of a simulation of the phytoplankton model with constant driving forces and environmental conditions. Phosphate concentrations are in gP/m^3, algae concentrations in gDM/m^3, and time in days.

$$T(t) = \frac{T_{\max} + T_{\min}}{2} + \frac{T_{\max} - T_{\min}}{2} \cos\left(2\pi \frac{t - t_{\max}}{t_{\text{per}}}\right) \tag{11.19}$$

and

$$I_0(t) = \frac{I_{0,\max} + I_{0,\min}}{2} + \frac{I_{0,\max} - I_{0,\min}}{2} \cos\left(2\pi \frac{t - t_{\max}}{t_{\text{per}}}\right) \quad . \tag{11.20}$$

In these equations $T_{\max}$ and $T_{\min}$ are maximum and minimum temperature, $I_{0,\max}$ and $I_{0,\min}$ are maximum and minimum light intensity at the lake surface, $t_{\max}$ is the point in time at which temperature and light intensity are at their maxima, and t_{per} is the period, in this case one year. The results shown in Figure 11.3 demonstrate that the steady-state solution reached under constant driving forces shown in Figure 11.2 are replaced by seasonal variation in phosphate and algae. During summer, when temperature and light intensity is high, phosphate concentration is very low, as the incoming phosphate is consumed to the degree depending on the half-saturation concentration, $K_{\text{HPO}_4^{2-},\text{ALG}}$, of algae with respect to phosphate. During winter, when algae growth is reduced, phosphate concentrations increase.

As a next step towards a lake ecosystem model, we will extend this model by zooplankton. This will be done in the next section.

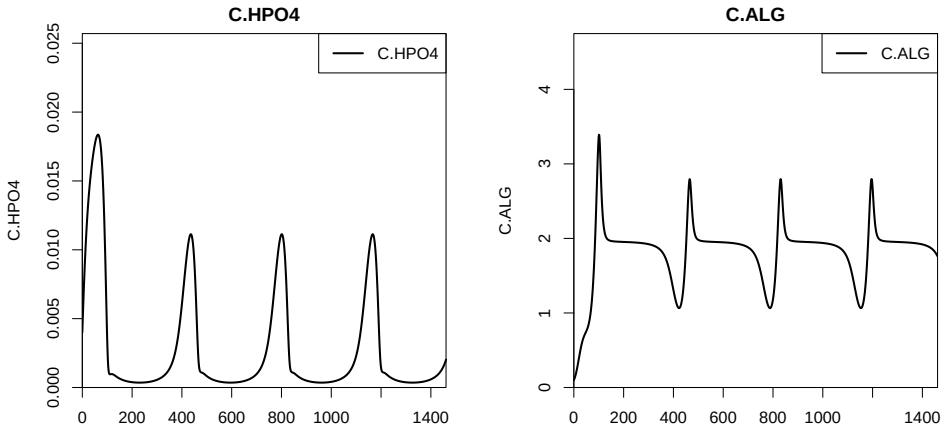

Figure 11.3: Results of a simulation of the phytoplankton model with periodic environmental conditions for temperature and light. Phosphate concentrations are in gP/m^3, algae concentrations in gDM/m^3, and time in days.

11.2 Lake Phyto- and Zooplankton Model

This model is based on the chapters and sections 1, 2, 3.1, 3.2, 4.1, 4.2, 8.1, 8.3, 8.4, and 11.1. It extends the lake phytoplankton model discussed in section 11.1 by zooplankton.

A simple ecological model for describing the most important transformation processes for phyto- and zooplankton in a lake requires the three state variables soluble reactive phosphorus (for stoichiometric purposes assumed to be phosphate, HPO_4^{2-}) as a growth-limiting nutrient, algae (ALG) as primary producers, and zooplankton (ZOO) as secondary producers. We consider growth (see sections 8.1 and 8.4) and death (see section 8.3) of both plankton groups. When denoting the phosphorus content of algae by $\alpha_{\mathrm{P,ALG}}$ and the yield of grazing by zooplankton by Y_{ZOO}, we get the process table shown as Table 11.4.

Process	Substances / Organisms			Rate
	HPO_4^{2-}	ALG	ZOO	
	gP	gDM	gDM	
Growth of algae	$-\alpha_{\mathrm{P,ALG}}$	1		$\rho_{\mathrm{gro,ALG}}$
Death of algae		-1		$\rho_{\mathrm{death,ALG}}$
Growth of zooplankton		$-\frac{1}{Y_{\mathrm{ZOO}}}$	1	$\rho_{\mathrm{gro,ZOO}}$
Death of zooplankton			-1	$\rho_{\mathrm{death,ZOO}}$

Table 11.4: Process table of a simple lake plankton model.

Similarly to the model described in section 11.1, we set up a first model version only considering nutrient limitation for the growth of algae and limitation of zooplankton growth by the available algae. This leads to the transformation rates shown in Table 11.5. The process rate of algal growth considers a growth limitation by phosphate that

Rate	Rate expression
$\rho_{\mathrm{gro,ALG}}$	$k_{\mathrm{gro,ALG}} \frac{C_{HPO_4^{2-}}}{K_{HPO_4^{2-},\mathrm{ALG}} + C_{HPO_4^{2-}}} C_{\mathrm{ALG}}$
$\rho_{\mathrm{death,ALG}}$	$k_{\mathrm{death,ALG}}\, C_{\mathrm{ALG}}$
$\rho_{\mathrm{gro,ZOO}}$	$k_{\mathrm{gro,ZOO}}\, C_{\mathrm{ALG}}\, C_{\mathrm{ZOO}}$
$\rho_{\mathrm{death,ZOO}}$	$k_{\mathrm{death,ZOO}}\, C_{\mathrm{ZOO}}$

Table 11.5: Process rates of the first version of the simple lake phyto- and zooplankton model.

reaches saturation at high phosphate concentrations according to equation (4.11). The process rate of zooplankton growth is proportional to algae as well as zooplankton concentrations. This considers the dependence of zooplankton growth on algae as their food. Note that this process model is exactly the same as the one discussed in example 4.2.

As in section 11.1, we apply this transformation process model in a completely mixed reactor describing the epilimnion of the lake. We assume the input concentration of phosphate to be given by $C_{\mathrm{in},HPO_4^{2-}}$ and no input for algae and zooplankton. Other transfer processes across interfaces are neglected.

When driving the model described above with constant inflow and inflow concentrations, there is a stronger tendency than in the model dicussed in the previous section for periodic behaviour. For the latter solutions, the cycle starts with the development of algae. The population of zooplankton increases with some delay due to increasing food resources by increasing algae concentrations. Once the zooplankton population becomes too large, the phytoplankton population breaks down. Due to starvation, the zooplankton population also breaks down and allows the algae to start their development again. There is no seasonality in this behaviour.

A simple way to introduce seasonality is to consider temperature and light dependence of the phytoplankton growth rate according to (4.10) and (4.29) (see also Table 11.3) and temperature dependence of the zooplankton growth rate. This leads to the process rates shown in Table 11.6. We can then use seasonally varying functions for temperature, T,

Rate	Rate expression
$\rho_{\text{gro,ALG}}$	$k_{\text{gro,ALG},T_0} \cdot \exp\Big(\beta_{\text{ALG}}(T - T_0)\Big) \cdot \frac{1}{\lambda h} \log\left(\frac{K_I + I_0}{K_I + I_0 \exp(-\lambda h)}\right) \cdot \frac{C_{\text{HPO}_4^{2-}}}{K_{\text{HPO}_4^{2-},\text{ALG}} + C_{\text{HPO}_4^{2-}}} \cdot C_{\text{ALG}}$
$\rho_{\text{death,ALG}}$	$k_{\text{death,ALG}}\, C_{\text{ALG}}$
$\rho_{\text{gro,ZOO}}$	$k_{\text{gro,ZOO},T_0} \cdot \exp\Big(\beta_{\text{ZOO}}(T - T_0)\Big) \cdot C_{\text{ALG}}\, C_{\text{ZOO}}$
$\rho_{\text{death,ZOO}}$	$k_{\text{death,ZOO}}\, C_{\text{ZOO}}$

Table 11.6: Process rates of the extended version of the simple lake phyto- and zooplankton model.

and for the light intensity at the lake surface, I_0. This leads to an interference between internally generated periodicity of population behaviour with external periodicity in driving forces and can lead to complicated, irregular behaviour of the solutions (Huppert et al., 2005).

Figure 11.4 shows a dynamic simulation of the model defined by the processes given in

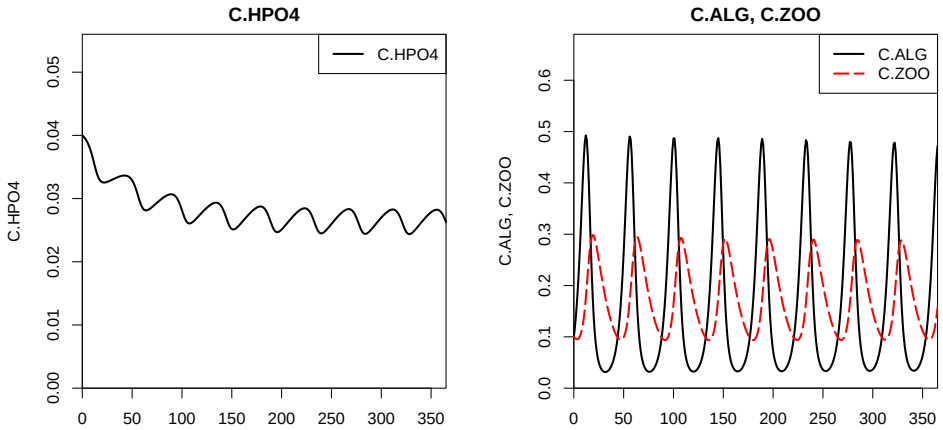

Figure 11.4: Results of a simulation of the phytoplankton-zooplankton lake model with constant driving forces and environmental conditions. Phosphate concentrations are in gP/m^3, algae and zooplankton concentrations in gDM/m^3, and time in days.

Table 11.4 with rate formulations given in Table 11.5 and in a mixed reactor as defined by equation (11.3) with constant values for inflow and inflow concentrations. These solutions were calculated using the graphics and statistics software R (`http://www.r-project.org`) with the aid of the R package `ecosim`.

Figure 11.5 shows results of the extended model with the growth rates given in Table 11.5 replaced by those given in Table 11.6 and with periodic input for temperature and light according to the equations (11.19) and (11.20). The results demonstrate that the

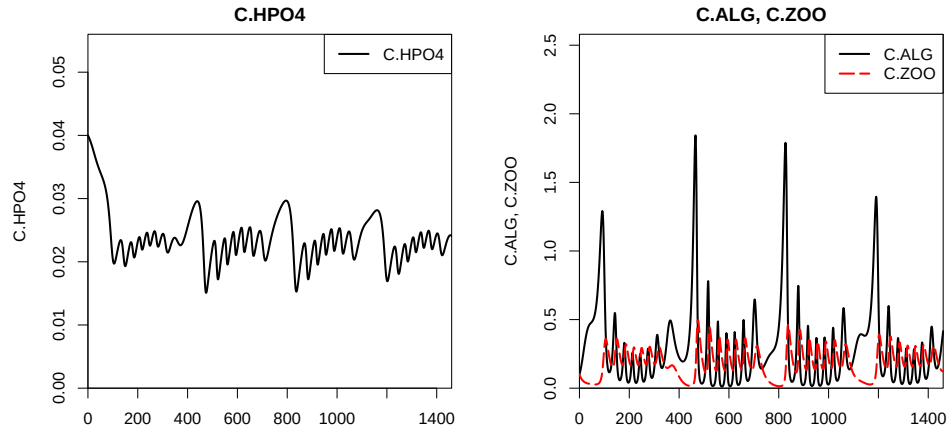

Figure 11.5: Results of a simulation of the phytoplankton-zooplankton model with periodic environmental conditions for temperature and light. Phosphate concentrations are in gP/m^3, algae and zooplankton concentrations in gDM/m^3, and time in days.

interference of the external with the internal periodicity leads to a yearly succession of several cycles of algae and zooplankton peaks. During summer when light intensity and temperature are high, growth can take place and oscillations of algae, zooplankton and phosphate occur. During winter the growth rates of algae and zooplankton are very low due to the low light intensity and temperature. During algal blooms, phosphate concentration is very low, between blooms and in winter, when algal growth is significantly reduced, phosphate concentration is high.

The model discussed in this section is nice to discuss the basic features of how to build-up an ecosystem model for an aquatic system and to start training of model implementation. However, it has severe deficits. The major deficit is the assumption of zero fluxes across the interfaces of the epilimnion. Dead plankton, fecal pellets and other organic particles are sedimenting out of the epilimnion down to the sediment of the lake. These particles are mineralized and release nutrients that diffuse back through the water column to the epilimnion. This leads to significant feedback mechanisms and retardation of the reaction of concentrations in the lake to changes in phosphate input. In addition, the mineralization processes consume dissolved oxygen or, in the absence of oxygen, nitrate. This leads to effects on the concentrations of these substances in the water column. In the next two sections, we will further extend this model to a more realistic model of a lake ecosystem that considers these processes. Even more realistic, but also more complicated lake ecosystem models will be discussed in chapter 13.

11.3 Two Box Oxygen and Phosphorus Lake Model

The lake model provided in section 11.2 demonstrated the succession of phyto- and zooplankton in the epilimnion of a lake. In this section we extend the phosphorus cycle of this model, improve the spatial resolution of the water column, and add dissolved oxygen as an additional compound considered in the model. In addition to the chapters and sections 1, 2, 3.1, 3.2, 4.1, 4.2, 8.1, 8.3, 8.4, and 11.1 required for the previous model and to the section 11.2 in which the previous model is defined, this model requires knowledge of the sections 3.3, 4.3, 6.1.1, 6.2, 6.3, 8.2, and 8.5.

To make the lake ecosystem model described in section 11.2 more realistic we make the following changes:

- We add dissolved oxygen (O_2), suspended particulate organic matter (POM), and sedimented particulate organic matter (SPOM) as additional substances to be modelled as state variables.
- We divide the water column into two mixed reactors describing epilimnion and hypolimnion and introduce gas exchange at the lake surface, turbulent diffusion through the metalimnion, and sedimentation from the epilimnion to the hypolimnion as additional transport processes.
- We add sedimented organic particles (SPOM) as an additional model component to get a very simple "flat" sediment model and add sedimentation of suspended organic particles from the hypolimnion to the sediment as an additional process.
- We add respiration of algae and zooplankton, mineralization of suspended and sedimented particulate organic compounds as additional processes.

This leads to a much more realistic description of the dissolved oxygen and phosphorus balance in the lake.

Table 11.7 shows the process table of this model. In this table, Y_{ZOO} is the yield of zooplankton growth (see section 8.4 for details), f_{e} is the fraction of particle production by grazing zooplankton due to excretion and sloppy feeding (see section 8.4 for details), $Y_{\mathrm{ALG,death}}$ and $Y_{\mathrm{ZOO,death}}$ are the yields of algae and zooplankton death (see section 8.3 for details), and the remaining stoichiometric coefficients can be calculated by applying the techniques outlined in section 4.3. Note that we need the additional substances HCO_3^-, H^+ and H_2O to derive the correct stoichiometry for dissolved oxygen although we do not include these substances in the model. Negative signs "−" in Table 11.7 indicate negative stoichiometric coefficients, positive signs "+" positive coefficients and, "0/+" indicate coefficients that should be made non-negative by an appropriate choice of compositional parameters.

The process rates in this model are given in Table 11.8. These are quite straightforward, with the exception of the last one which is a transfer and not a transformation process. Because of the simple "flat" sediment model and our concept of distinguishing dissolved and suspended substances in a mixed rector from those attached to a surface, the transfer from suspended to attached must be formulated as a transformation process. This is done by the last equation in Table (11.8) which only applies in the hypolimnion.

Process	Substances / Organisms						Rate
	HPO_4^{2-} gP	O_2 gO	ALG gDM	ZOO gDM	POM gDM	SPOM gDM	
Growth of algae	$-$	$+$	1				$\rho_{\text{gro,ALG}}$
Respiration of algae	$+$	$-$	-1				$\rho_{\text{resp,ALG}}$
Death of algae	$0/+$	$0/+$	-1		$Y_{\text{ALG,death}}$		$\rho_{\text{death,ALG}}$
Growth of zooplankton	$0/+$	$-$	$\frac{-1}{Y_{\text{ZOO}}}$	1	$\frac{f_{\text{e}}}{Y_{\text{ZOO}}}$		$\rho_{\text{gro,ZOO}}$
Respiration of zoopl.	$+$	$-$		-1			$\rho_{\text{resp,ZOO}}$
Death of zooplankton	$0/+$	$0/+$		-1	$Y_{\text{ZOO,death}}$		$\rho_{\text{death,ZOO}}$
Mineral. of org. part.	$+$	$-$			-1		$\rho_{\text{miner,POM}}$
Min. of org. part. in sed.	$+$	$-$				-1	$\rho_{\text{miner,SPOM}}$
Sed. of org. particles					-1	1	$\rho_{\text{sed,POM}}$

Table 11.7: Process table of the oxygen-phosphorus lake model.

In addition to the transformation processes we have to describe oxygen exchange with the atmosphere as an interface flux to the epilimnion

$$J^{\text{epi}}_{\text{int,O}_2} = v_{\text{ex,O}_2}\ A\ (C_{\text{O}_2,\text{sat}} - C_{\text{O}_2}) \tag{11.21}$$

where $v_{\text{ex,O}_2}$ is the gas exchange velocity of oxygen, A is the surface area of the lake, and $C_{\text{O}_2,\text{sat}}$ is the saturation concentration of dissolved oxygen in the epilimnion. See section 6.3 for more details on this process. Furthermore we need a diffusive exchange describing turbulent mixing between epilimnion and hypolimnion that applies to all substances. According to the equations (3.17) and (6.12) this exchange flux is given by

$$\mathbf{J}^{\text{epi meta}} = A_{\text{meta}}\ \frac{K_{\text{z,meta}}}{h_{\text{meta}}}\ (\mathbf{C}^{\text{epi}} - \mathbf{C}^{\text{hypo}}) \tag{11.22}$$

where A_{meta} is the cross-sectional area of the metalimnion, $K_{\text{z,meta}}$ the coefficient of turbulent diffusivity in the metalimnion, and h_{meta} is the thickness of the metalimnion. Finally, we need a sedimentation flux for suspended organic particles from the epilimnion to the metalimnion. This flux is given by

$$J^{\text{epi meta}}_{\text{POM}} = A_{\text{meta}}\ v_{\text{sed,POM}}\ C^{\text{epi}}_{\text{POM}} \tag{11.23}$$

where $v_{\text{sed,POM}}$ is the sedimentation velocity of suspended organic particles.

Figure 11.6 shows examples of results for this model for a simulation of one year. During the stratification period (about days 150 to 350) algal growth leads to a significant decrease in phosphate concentrations in the epilimnion whereas the hypolimnion concentrations increase due to mineralisation of organic material in the sediment. Dissolved oxygen shows supersaturation in the epilimnion during strong production peaks and a decrease

Rate	Rate expression
$\rho_{\text{gro,ALG}}$	$k_{\text{gro,ALG},T_0} \cdot \exp\Big(\beta_{\text{ALG}}(T-T_0)\Big) \cdot \frac{1}{\lambda h} \log\left(\frac{K_I + I_0}{K_I + I_0 \exp(-\lambda h)}\right) \cdot \frac{C_{\text{HPO}_4^{2-}}}{K_{\text{HPO}_4^{2-},\text{ALG}} + C_{\text{HPO}_4^{2-}}} \cdot C_{\text{ALG}}$
$\rho_{\text{resp,ALG}}$	$k_{\text{resp,ALG},T_0} \cdot \exp\Big(\beta_{\text{ALG}}(T-T_0)\Big) \cdot \frac{C_{\text{O}_2}}{K_{\text{O}_2,\text{ALG}} + C_{\text{O}_2}} \cdot C_{\text{ALG}}$
$\rho_{\text{death,ALG}}$	$k_{\text{death,ALG}} \cdot C_{\text{ALG}}$
$\rho_{\text{gro,ZOO}}$	$k_{\text{gro,ZOO},T_0} \cdot \exp\Big(\beta_{\text{ZOO}}(T-T_0)\Big) \cdot \frac{C_{\text{O}_2}}{K_{\text{O}_2,\text{ZOO}} + C_{\text{O}_2}} \cdot C_{\text{ALG}} \cdot C_{\text{ZOO}}$
$\rho_{\text{resp,ZOO}}$	$k_{\text{resp,ZOO},T_0} \cdot \exp\Big(\beta_{\text{ZOO}}(T-T_0)\Big) \cdot \frac{C_{\text{O}_2}}{K_{\text{O}_2,\text{ZOO}} + C_{\text{O}_2}} \cdot C_{\text{ZOO}}$
$\rho_{\text{death,ZOO}}$	$k_{\text{death,ZOO}} \cdot C_{\text{ZOO}}$
$\rho_{\text{miner,POM}}$	$k_{\text{miner,POM},T_0} \cdot \exp\Big(\beta_{\text{BAC}}(T-T_0)\Big) \cdot \frac{C_{\text{O}_2}}{K_{\text{O}_2,\text{miner}} + C_{\text{O}_2}} \cdot C_{\text{POM}}$
$\rho_{\text{miner,SPOM}}$	$k_{\text{miner,SPOM},T_0} \cdot \exp\Big(\beta_{\text{BAC}}(T-T_0)\Big) \cdot \frac{C_{\text{O}_2}}{K_{\text{O}_2,\text{miner}} + C_{\text{O}_2}} \cdot \frac{D_{\text{SPOM}}}{K_{\text{SPOM,miner,sed}} + D_{\text{SPOM}}}$
$\rho_{\text{sed,POM}}$	$\frac{v_{\text{sed,POM}}}{h_{\text{hypo}}} \cdot C_{\text{POM}}$

Table 11.8: Process rates of the oxygen-phosphorus lake model.

in the hypolimnion due to mineralisation of organic material in the sediment. Algae and zooplankton show similar oscillations as in the model shown in section 11.2 with a different period due to different parameter values. Concentrations of particulate organic matter in the epilimnion follow the pattern of algae and zooplankton due to death, sloppy feeding and excretion, the concentrations in the hypolimnion follow the same pattern due to sedimentation. Finally, the surface densities in the sediment follow the pattern with a damped amplitude due to accumulation and mineralization. During winter mixing takes place. Combined with lower light intensities and temperatures this leads to a decrease in plankton growth and concentrations.

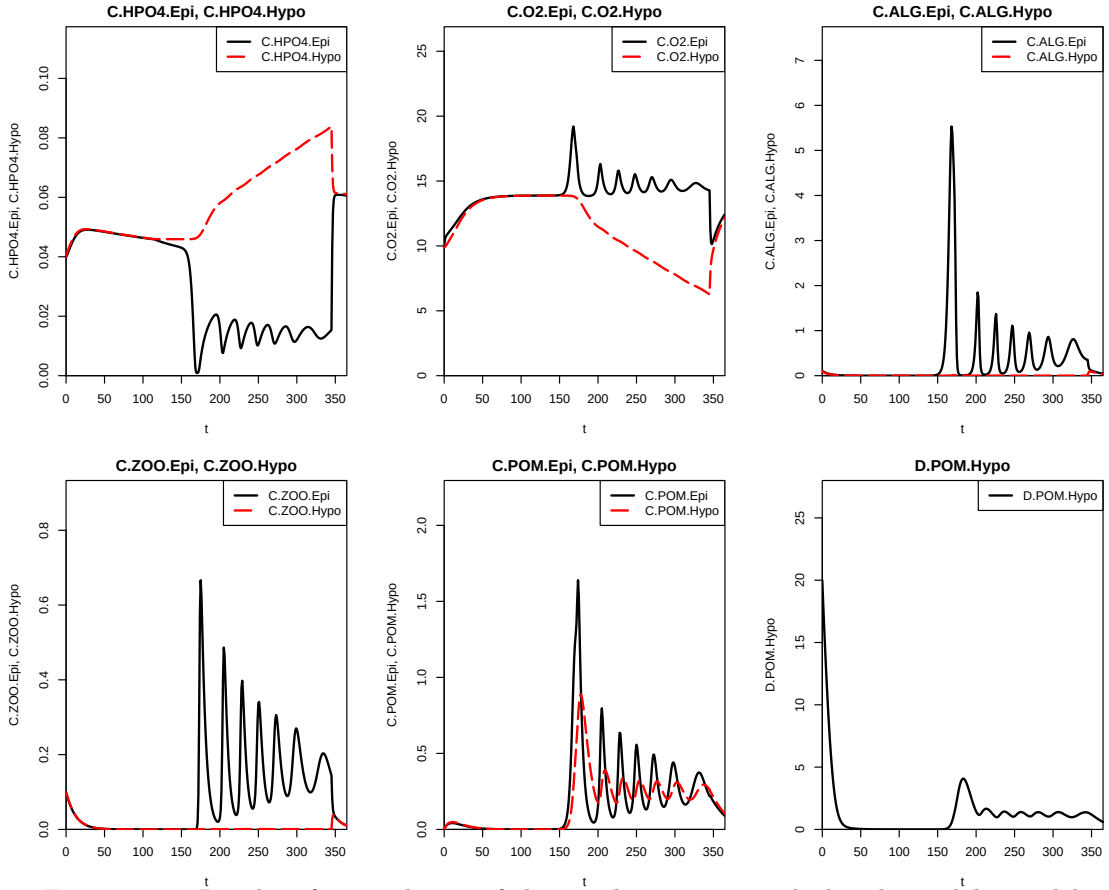

Figure 11.6: Results of a simulation of the two box oxygen and phosphorus lake model. Phosphate concentrations are in gP/m^3, oxygen concentrations in gO/m^3, algae, zooplankton and suspended particulate organic matter concentrations in gDM/m^3, sedimented particulate organic matter in gDM/m^2, and time in days.

11.4 Model of Biogeochemical Cycles in a Lake

The lake models discussed in sections 11.2 and 11.3 demonstrated succession of phyto- and zooplankton and major elements of the phosphorus and oxygen household of a lake. The model described in this section further improves the oxygen and phosphorus cycle of this model and it adds the nitrogen cycle. In addition to the chapters and sections 1, 2, 3.1, 3.2, 3.3, 4.1, 4.2, 4.3. 6.1.1, 6.2, 6.3, 8.1, 8.3, 8.4, 8.2, 8.5, and 11.1 required for the previous model and to the section 11.3 in which the previous model is defined, this model requires knowledge of the section 8.6.

To make the lake ecosystem model described in section 11.3 more complete and more realistic we make the following changes.

- We divide suspended and sedimented particulate organic matter (POM, SPOM) into degradable (POMD, SPOMD) and inert (POMI, SPOMI) fractions to account for the wide spectrum of degradability of these compounds.
- We add ammonium (NH_4^+) and nitrate (NO_3^-), distinguish primary production into a process that consumes ammonium and a process that consumes nitrate to satisfy the nitrogen need, and we consider the nitrogen content of all organic fractions.
- We add anoxic mineralization in the sediment as an additional process leading to denitrification.

Table 11.9 shows the process table of this model. The new stoichiometric parameter f_I quantifies the fraction of inert organic particles produced due to death, excretion and sloppy feeding. The stoichiometric coefficients that are not specified quantitatively in Table 11.9 can be calculated by applying the techniques outlined in section 4.3. Note that we need the additional substances N_2, HCO_3^-, H^+ and H_2O to derive the correct stoichiometric coefficients although we do not include these substances in the model. Negative signs "−" in Table 11.9 indicate negative stoichiometric coefficients, positive signs "+" positive coefficients, and "0/+" indicate coefficients that should be made non-negative by an appropriate choice of compositional parameters.

The process rates in this model are shown in Table 11.10.

Process	Substances / Organisms										Rate
	HPO_4^{2-} gP	NH_4^+ gN	NO_3^- gN	O_2 gO	ALG gDM	ZOO gDM	POMD gDM	POMI gDM	SPOMD gDM	SPOMI gDM	
Growth of algae NO_3^-	$-$		$-$	$+$	1						$\rho_{\text{gro,ALG,NO}_3^-}$
Growth of algae NH_4^+	$-$	$-$		$+$	1						$\rho_{\text{gro,ALG,NH}_4^+}$
Respiration of algae	$+$	$+$		$-$	-1						$\rho_{\text{resp,ALG}}$
Death of algae	$0/+$	$0/+$		$0/+$	-1		$(1-f_{\text{I}})Y_{\text{ALG,death}}$	$f_{\text{I}}Y_{\text{ALG,death}}$			$\rho_{\text{death,ALG}}$
Growth of zooplankton	$+$	$+$		$-$	$\frac{-1}{Y_{\text{ZOO}}}$	1	$\frac{(1-f_{\text{I}})f_{\text{e}}}{Y_{\text{ZOO}}}$	$\frac{f_{\text{I}}f_{\text{e}}}{Y_{\text{ZOO}}}$			$\rho_{\text{gro,ZOO}}$
Respiration of zoopl.	$+$	$+$		$-$		-1					$\rho_{\text{resp,ZOO}}$
Death of zooplankton	$0/+$	$0/+$		$0/+$		-1	$(1-f_{\text{I}})Y_{\text{ZOO,death}}$	$f_{\text{I}}Y_{\text{ZOO,death}}$			$\rho_{\text{death,ZOO}}$
Nitrification		-1	$+$	$-$							ρ_{nitri}
Oxic mineral. of org. part.	$+$	$+$		$-$			-1				$\rho_{\text{miner,ox,POMD}}$
Ox. min. of org. part. in sed.	$+$	$+$		$-$					-1		$\rho_{\text{miner,ox,SPOMD}}$
Anox. min. of org. part. in sed.	$+$	$+$	$-$						-1		$\rho_{\text{miner,anox,SPOMD}}$
Sed. of deg. org. part.							-1		1		$\rho_{\text{sed,POMD}}$
Sed. of inert org. part.								-1		1	$\rho_{\text{sed,POMI}}$

Table 11.9: Process table of the model for biogeochemical cycles in a lake.

Rate	Rate expression
$\rho_{\text{gro,ALG,NH}_4^+}$	$k_{\text{gro,ALG},T_0} \cdot \exp\Big(\beta_{\text{ALG}}(T-T_0)\Big) \cdot \frac{1}{\lambda h} \log\left(\frac{K_I + I_0}{K_I + I_0 \exp(-\lambda h)}\right)$ $\cdot \min\left(\frac{C_{\text{HPO}_4^{2-}}}{K_{\text{HPO}_4^{2-},\text{ALG}} + C_{\text{HPO}_4^{2-}}}, \frac{C_{\text{NH}_4^+} + C_{\text{NO}_3^-}}{K_{\text{N,ALG}} + C_{\text{NH}_4^+} + C_{\text{NO}_3^-}}\right) \cdot \frac{p_{\text{NH}_4^+} C_{\text{NH}_4^+}}{p_{\text{NH}_4^+} C_{\text{NH}_4^+} + C_{\text{NO}_3^-}} \cdot C_{\text{ALG}}$
$\rho_{\text{gro,ALG,NO}_3^-}$	$k_{\text{gro,ALG},T_0} \cdot \exp\Big(\beta_{\text{ALG}}(T-T_0)\Big) \cdot \frac{1}{\lambda h} \log\left(\frac{K_I + I_0}{K_I + I_0 \exp(-\lambda h)}\right)$ $\cdot \min\left(\frac{C_{\text{HPO}_4^{2-}}}{K_{\text{HPO}_4^{2-},\text{ALG}} + C_{\text{HPO}_4^{2-}}}, \frac{C_{\text{NH}_4^+} + C_{\text{NO}_3^-}}{K_{\text{N,ALG}} + C_{\text{NH}_4^+} + C_{\text{NO}_3^-}}\right) \cdot \frac{C_{\text{NO}_3^-}}{p_{\text{NH}_4^+} C_{\text{NH}_4^+} + C_{\text{NO}_3^-}} \cdot C_{\text{ALG}}$
$\rho_{\text{resp,ALG}}$	$k_{\text{resp,ALG},T_0} \cdot \exp\Big(\beta_{\text{ALG}}(T-T_0)\Big) \cdot \frac{C_{\text{O}_2}}{K_{\text{O}_2,\text{ALG}} + C_{\text{O}_2}} \cdot C_{\text{ALG}}$
$\rho_{\text{death,ALG}}$	$k_{\text{death,ALG}} \cdot C_{\text{ALG}}$
$\rho_{\text{gro,ZOO}}$	$k_{\text{gro,ZOO},T_0} \cdot \exp\Big(\beta_{\text{ZOO}}(T-T_0)\Big) \cdot \frac{C_{\text{O}_2}}{K_{\text{O}_2,\text{ZOO}} + C_{\text{O}_2}} \cdot C_{\text{ALG}} \cdot C_{\text{ZOO}}$
$\rho_{\text{resp,ZOO}}$	$k_{\text{resp,ZOO},T_0} \cdot \exp\Big(\beta_{\text{ZOO}}(T-T_0)\Big) \cdot \frac{C_{\text{O}_2}}{K_{\text{O}_2,\text{ZOO}} + C_{\text{O}_2}} \cdot C_{\text{ZOO}}$
$\rho_{\text{death,ZOO}}$	$k_{\text{death,ZOO}} \cdot C_{\text{ZOO}}$
ρ_{nitri}	$k_{\text{nitri},T_0} \cdot \exp\Big(\beta_{\text{BAC}}(T-T_0)\Big) \cdot \min\left(\frac{C_{\text{NH}_4^+}}{K_{\text{NH}_4^+,\text{nitri}} + C_{\text{NH}_4^+}}, \frac{C_{\text{O}_2}}{K_{\text{O}_2,\text{nitri}} + C_{\text{O}_2}}\right)$
$\rho_{\text{miner,ox,POMD}}$	$k_{\text{miner,ox,POMD},T_0} \cdot \exp\Big(\beta_{\text{BAC}}(T-T_0)\Big) \cdot \frac{C_{\text{O}_2}}{K_{\text{O}_2,\text{miner}} + C_{\text{O}_2}} \cdot C_{\text{POMD}}$
$\rho_{\text{miner,ox,SPOMD}}$	$k_{\text{miner,ox,SPOMD},T_0} \cdot \exp\Big(\beta_{\text{BAC}}(T-T_0)\Big) \cdot \frac{C_{\text{O}_2}}{K_{\text{O}_2,\text{miner}} + C_{\text{O}_2}} \cdot \frac{D_{\text{SPOMD}}}{K_{\text{SPOM,miner,sed}} + D_{\text{SPOMD}}}$
$\rho_{\text{miner,anox,SPOMD}}$	$k_{\text{miner,anox,SPOMD},T_0} \cdot \exp\Big(\beta_{\text{BAC}}(T-T_0)\Big) \cdot \frac{C_{\text{NO}_3^-}}{K_{\text{NO}_3^-,\text{miner}} + C_{\text{NO}_3^-}} \cdot \left(\frac{D_{\text{SPOMD}}}{K_{\text{SPOM,miner,sed}} + D_{\text{SPOMD}}}\right)^2$
$\rho_{\text{sed,POMD}}$	$\frac{v_{\text{sed,POM}}}{h_{\text{hypo}}} \cdot C_{\text{POMD}}$
$\rho_{\text{sed,POMI}}$	$\frac{v_{\text{sed,POM}}}{h_{\text{hypo}}} \cdot C_{\text{POMI}}$

Table 11.10: Process rates of the model for biogeochemical cycles in a lake.

The stoichiometry (Table 11.9) and rates (Table 11.10) of primary production using ammonium or nitrate are discussed in section 8.1 (Table 8.1 and equations 8.4 and 8.5). The stoichiometry (Table 11.9) and process rate (Table 11.10) of respiration of algae are discussed in section 8.2 (Table 8.2 and equation 8.6). The respiration process of zooplankton (Tables 11.9 and 11.10) is formulated analogously. The stoichiometry (Table 11.9) and process rate (Table 11.10) of death of algae are discussed in section 8.3 (Table 8.3 and equation 8.10). The death process of zooplankton (Tables 11.9 and 11.10) is formulated analogously. The stoichiometry (Table 11.9) and process rate (Table 11.10) of growth of zooplankton is discussed in a more general context of consumption in section 8.4 (Table 8.4 and equation 8.15). The stoichiometry (Table 11.9) and process rate (Table 11.10) of nitrification is discussed in section 8.6 (Table 8.8 and equation 8.21). The stoichiometry (Table 11.9) and process rate (Table 11.10) of oxic mineralization is discussed in section 8.5.1 (Table 8.5 and equation 8.16).

The stoichiometry of oxic mineralization in the sediment is the same (Table 11.9) as in the water column. However, to account for our simple "flat" sediment model which does not account for dissolved substance concentrations within the sediment, we do not use the process rate recommended in section 8.5.1. This rate was based on oxygen concentration at the place where mineralization takes place. In our simplified approach, we have to formulate oxic mineralization as a function of dissolved oxygen concentration in the water column. Oxic mineralization of sedimented organic particles will be limited by diffusion of dissolved oxygen into the sediment. In a thin sediment layer, where we have no diffusion limitation, we could use the description used in the free water column (Table 11.10). However, with increasing depth of the sediment layer proportionality with organic particles cannot longer be maintained as dissolved oxygen will only be available in the top layer. Thus, we need a process formulation which is proportional to particle density at small densities but reaches a constant saturation value when the particle density increases. This is done with a Monod-term in the surface density of sedimented degradable organic particles (Table 11.10). The half-saturation concentration in this term must correspond to a sediment density at which diffusion limitation becomes relevant.

The stoichiometry of anoxic mineralization in the sediment (Table 11.9) is discussed in section 8.5.2 (Table 8.6). The process rate would usually be formulated with an inhibition term with respect to dissolved oxygen and a limitation by nitrate as shown by equation (8.19). This formulation cannot be used in our simple sediment model that is based on concentrations of dissolved substances in the water column (rather than in-situ concentrations varying with the depth of the sediment). In a real sediment we would have a depletion of dissolved oxygen in the top layer and then depletion of nitrate in a layer below. This means that in a thin sediment layer, we would only have oxic mineralization. In a thicker sediment layer we would in addition (in deeper layers) have anoxic mineralization. With further increasing sediment thickness, both rates would become constant as additional thickness only leads to sediment layers that are depleted of dissolved oxygen and nitrate. A very simple description of this behaviour can be achieved by a quadratic Monod-term as shown in equation (Table 11.10). This term leads to the dominance of oxic mineralization at small sediment thickness followed by a slower approach to saturation of anoxic mineralization as compared to oxic mineralization.

The last two transformation rates in Table 11.10 describe sedimentation of degradable and inert organic particles as a process transforming suspended to sedimented substances

of the same condition. This process is mathematically formulated as a transformation process, because we distinguish these two types of state variables in a mixed reactor; physically, this is a transfer process. This process would also in our model become a transfer process, if we would model sediment layers by individual mixed boxes.

Similarly to the previous model described in section 11.3 we have transfer fluxes between the epilimnion and hypolimnion boxes and two compartments not described by the model. Oxygen exchange with the atmosphere is described as an interface flux to the epilimnion

$$J^{\text{epi}}_{\text{int},\text{O}_2} = v_{\text{ex},\text{O}_2}\ A\ (C_{\text{O}_2,\text{sat}} - C_{\text{O}_2}) \tag{11.24}$$

where v_{ex,O_2} is the gas exchange velocity of oxygen, A is the surface area of the lake, and $C_{\text{O}_2,\text{sat}}$ is the saturation concentration of dissolved oxygen in the epilimnion. See section 6.3 for more details on this process.

Furthermore we need a diffusive exchange describing turbulent mixing between epilimnion and hypolimnion that applies to all substances. According to the equations (3.17) and (6.12) this exchange flux is given by

$$\mathbf{J}^{\text{epi hypo}} = A_{\text{meta}}\ \frac{K_{\text{z,meta}}}{h_{\text{meta}}}\ (\mathbf{C}^{\text{epi}} - \mathbf{C}^{\text{hypo}}) \tag{11.25}$$

where A_{meta} is the cross-sectional area of the metalimnion, $K_{\text{z,meta}}$ the coefficient of turbulent diffusivity in the metalimnion, and h_{meta} is the thickness of the metalimnion. Note that the turbulent diffusivity will have a strong seasonal variation, being small during the stratification period in spring and summer and large during the overturn period in winter. Finally, we need sedimentation fluxes of suspended degradable and inert organic particles from the epilimnion to the metalimnion. These fluxes are given by

$$J^{\text{epi hypo}}_{\text{POMD}} = A_{\text{meta}}\ v_{\text{sed,POM}}\ C^{\text{epi}}_{\text{POMD}} \tag{11.26}$$

$$J^{\text{epi hypo}}_{\text{POMI}} = A_{\text{meta}}\ v_{\text{sed,POM}}\ C^{\text{epi}}_{\text{POMI}} \tag{11.27}$$

where $v_{\text{sed,POM}}$ is the (common) sedimentation velocity of suspended organic particles.

Figure 11.7 shows an example of a two year run of this model. Algae and zooplankton still qualitatively reflect the succession behaviour we have seen in the simple didactical model in section 11.2. This leads to corresponding depletion of nitrate and phosphate during the stratification and (simultaneously) production period. Note that phosphate shows a stronger relative depletion and, therefore, becomes limiting before ammonium and nitrate. Due to sedimenting dead degradable organic particles and their mineralization in the sediment, nitrate and phosphate released by mineralization accumulate in the hypolimnion during the stratified period. At the same time, also due to mineralization, dissolved oxygen is depleted. The time courses of organic particles just reflect their production as they are transported relatively quickly to the sediment. Degradable organic particles are accumulated in the sediment during production periods, but are quickly degraded when production is small, whereas inert organic particles accumulate in the sediment from year to year. Note that this distinction of organic particles into degradable

and inert is a very simple approximation of a wide spectrum of degradation rates for different organic constituents. Due to mixing and lower light intensities and temperatures in winter this oscillation is interrupted. As in the previous examples growth rates are very low during the mixing period in winter.

The time courses of concentrations of all relevant compounds in the lake shown in Figure 11.7 can be used to calculate the corresponding mass fluxes. Table 11.11 shows the average phosphorus and nitrogen mass fluxes of the simulations shown in Figure 11.7. Since we did not include molecular nitrogen as a state variable in the model, the amount of molecular nitrogen that is produced by the dentirification of nitrate appears as a gap in the mass balance. For phosphorus the mass balance is closed. There might appear just a very small gap due to the numerical inaccuracy of the numerical simulation of the model.

Flux	Substances	Phosphorus (t/a)	Nitrogen (t/a)
Input	HPO_4^{2-}, NO_3^-	**12.6**	**158**
Output	HPO_4^{2-}, NO_3^-, NH_4^+	**9.3**	**127**
	ALG, ZOO, POMD, POMI	1.2	11.5
Accumulation	HPO_4^{2-}, NO_3^-, NH_4^+	**1.2**	**-7.4**
	ALG, ZOO, POMD, POMI	0.0	0.0
	SPOMD	0.0	0.2
	SPOMI	**1.0**	**8.6**
Loss	Denitrification of NO_3^-	0.0	**17.9**

Table 11.11: Average mass fluxes, accumulation and loss rates over the simulation period shown in Figure 11.7.

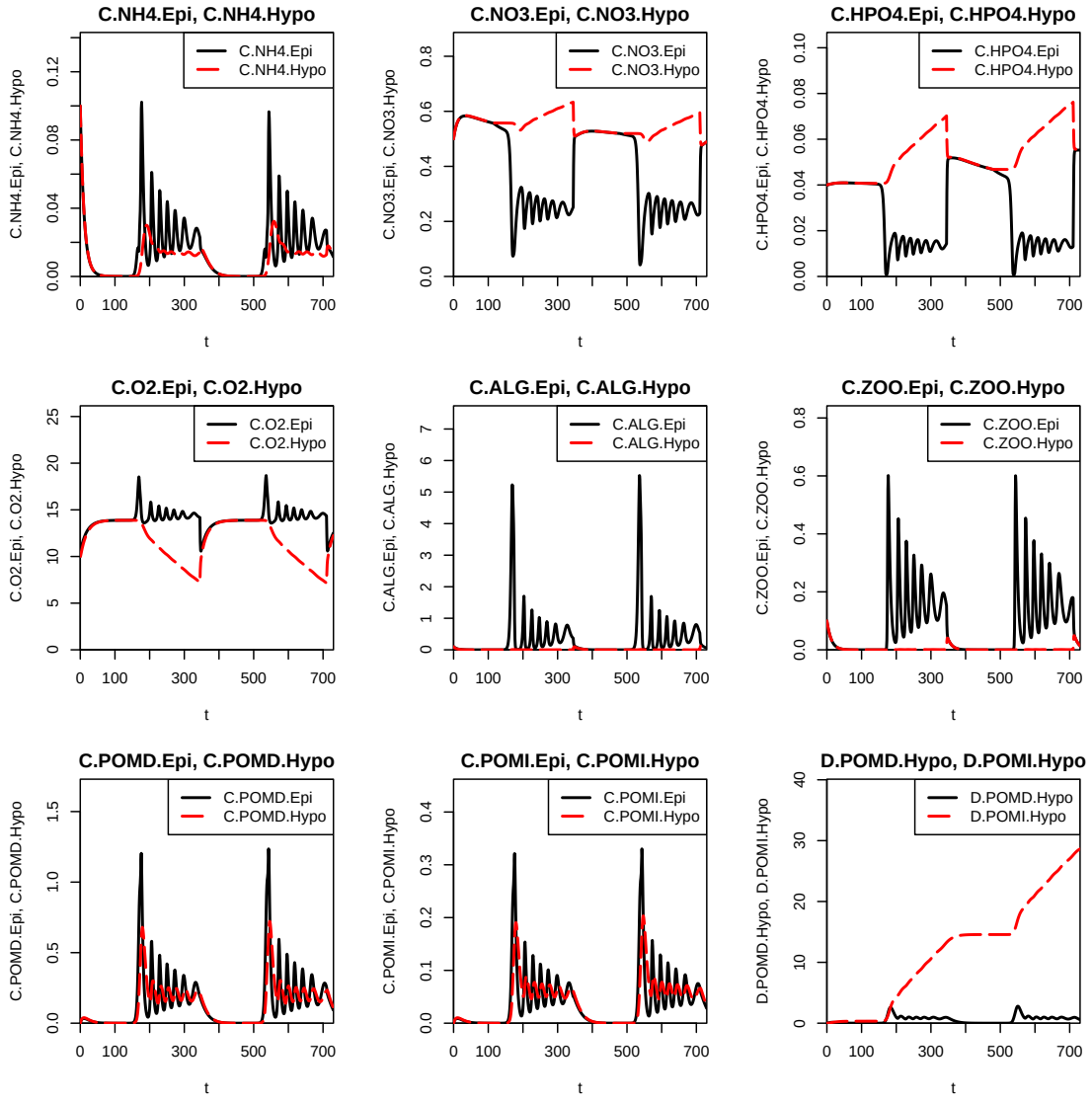

Figure 11.7: Results of a simulation of the two box model for biogeochemical cycles in a lake. Ammonium and nitrate concentrations are in gN/m^3, phosphate concentrations in gP/m^3, oxygen concentrations in gO/m^3, algae, zooplankton and suspended particulate organic matter concentrations in gDM/m^3, sedimented particulate organic matter in gDM/m^2, and time in days.

11.5 Oxygen and Nutrient Household Model of a River

In this section we construct a simple model for the oxygen and nutrient household in a river as it results from conversion processes of benthic organisms. We will extend this model to describe these benthic organisms in section 11.6.

The model discussed in this section is based on the conceptual development discussed in sections 1, 2, 3.1, 3.2, 3.3, 4.1, 4.2, and 4.3. Furthermore, we need knowledge of the processes discussed in sections 6.1.2, 6.3, 8.1, 8.2, 8.5, and 8.6.

Table 11.12 shows the process table of the model. Growth of benthic algae consumes

Process	Substances / Organisms							Rate
	HPO_4^{2-} gP	NH_4^+ gN	NO_2^- gN	NO_3^- gN	O_2 gO	SALG gDM	SPOM gDM	
Growth of algae NH_4^+	−	−			+	1		$\rho_{\text{gro,SALG,NH}_4^+}$
Growth of algae NO_3^-	−			−	+	1		$\rho_{\text{gro,SALG,NO}_3^-}$
Respiration of algae	+	+			−	−1		$\rho_{\text{resp,SALG}}$
First step of nitrification		−1	+		−			ρ_{nitri1}
Second step of nitrification			−1	+	−			ρ_{nitri2}
Mineralization	+	+			−		−1	$\rho_{\text{miner,SPOM}}$

Table 11.12: Process table of a model for oxygen and nutrient dynamics in a river.

phosphate and ammonium or nitrate from the water column and produces dissolved oxygen. Respiration of benthic algae requires consumption of dissolved oxygen from the water column and leads to release of phosphate and ammonium. Nitrification oxydizes ammonium to nitrite and nitrite to nitrate. Finally, mineralization transforms organic particles deposited in the sediment under consumption of dissolved oxygen to dissolved nutrients. By adding HCO_3^-, H^+ and H_2O to the substance list, we have 6 unknown stoichiometric coefficients to determine for each process. This can uniquely be done without additional constraints or stoichiometric parameters by applying the techniques described in section 4.3. The routines from the R package `stoichcalc` described in section 15 can be used for this purpose.

The process rates of the model are given in Table 11.13. For algae growth we use the rates given by the equations (8.2) and (8.3) given in section 8.1 with using the in-situ light intensity

$$I = I_0 \exp(-\lambda h) \tag{11.28}$$

at the river bed below a water column of height h. Note that we do not have to average the production rate over the water column as we did it for the lake models, as we model benthic algae here. However, we consider self-shading of algae in the benthic biofilm by a limitation term in the algae area density with a parameter $K_{\text{sha,SALG}}$ that represents the algae area density at which the growth rate is reduced to 50% due to self-shading. Respiration of benthic algae is formulated analogously to that of suspended algae given by

Rate	Rate expression
$\rho_{\mathrm{gro,ALG,NH_4^+}}$	$k_{\mathrm{gro,SALG},T_0} \cdot \exp\Big(\beta_{\mathrm{ALG}}(T-T_0)\Big) \cdot \dfrac{I_0 \exp(-\lambda h)}{K_I + I_0 \exp(-\lambda h)}$ $\cdot \min\left(\dfrac{C_{\mathrm{HPO_4^{2-}}}}{K_{\mathrm{HPO_4^{2-},ALG}} + C_{\mathrm{HPO_4^{2-}}}}, \dfrac{C_{\mathrm{NH_4^+}} + C_{\mathrm{NO_3^-}}}{K_{\mathrm{N,ALG}} + C_{\mathrm{NH_4^+}} + C_{\mathrm{NO_3^-}}}\right)$ $\cdot \dfrac{p_{\mathrm{NH_4^+}} C_{\mathrm{NH_4^+}}}{p_{\mathrm{NH_4^+}} C_{\mathrm{NH_4^+}} + C_{\mathrm{NO_3^-}}} \dfrac{K_{\mathrm{sha,SALG}}}{K_{\mathrm{sha,SALG}} + D_{\mathrm{SALG}}} \cdot D_{\mathrm{SALG}}$
$\rho_{\mathrm{gro,ALG,NO_3^-}}$	$k_{\mathrm{gro,SALG},T_0} \cdot \exp\Big(\beta_{\mathrm{ALG}}(T-T_0)\Big) \cdot \dfrac{I_0 \exp(-\lambda h)}{K_I + I_0 \exp(-\lambda h)}$ $\cdot \min\left(\dfrac{C_{\mathrm{HPO_4^{2-}}}}{K_{\mathrm{HPO_4^{2-},ALG}} + C_{\mathrm{HPO_4^{2-}}}}, \dfrac{C_{\mathrm{NH_4^+}} + C_{\mathrm{NO_3^-}}}{K_{\mathrm{N,ALG}} + C_{\mathrm{NH_4^+}} + C_{\mathrm{NO_3^-}}}\right)$ $\cdot \dfrac{C_{\mathrm{NO_3^-}}}{p_{\mathrm{NH_4^+}} C_{\mathrm{NH_4^+}} + C_{\mathrm{NO_3^-}}} \dfrac{K_{\mathrm{sha,SALG}}}{K_{\mathrm{sha,SALG}} + D_{\mathrm{SALG}}} \cdot D_{\mathrm{SALG}}$
$\rho_{\mathrm{resp,ALG}}$	$k_{\mathrm{resp,SALG},T_0} \cdot \exp\Big(\beta_{\mathrm{ALG}}(T-T_0)\Big) \cdot \dfrac{C_{\mathrm{O_2}}}{K_{\mathrm{O_2,ALG}} + C_{\mathrm{O_2}}} \cdot D_{\mathrm{SALG}}$
ρ_{nitri1}	$k_{\mathrm{nitri1},T_0} \cdot \exp\Big(\beta_{\mathrm{nitri1}}(T-T_0)\Big) \cdot \min\left(\dfrac{C_{\mathrm{NH_4^+}}}{K_{\mathrm{NH_4^+,nitri}} + C_{\mathrm{NH_4^+}}}, \dfrac{C_{\mathrm{O_2}}}{K_{\mathrm{O_2,nitri}} + C_{\mathrm{O_2}}}\right)$
ρ_{nitri2}	$k_{\mathrm{nitri2},T_0} \cdot \exp\Big(\beta_{\mathrm{nitri2}}(T-T_0)\Big) \cdot \min\left(\dfrac{C_{\mathrm{NO_2^-}}}{K_{\mathrm{NO_2^-,nitri}} + C_{\mathrm{NO_2^-}}}, \dfrac{C_{\mathrm{O_2}}}{K_{\mathrm{O_2,nitri}} + C_{\mathrm{O_2}}}\right)$
$\rho_{\mathrm{miner,SPOM}}$	$k_{\mathrm{miner,SPOM},T_0} \cdot \exp\Big(\beta_{\mathrm{BAC}}(T-T_0)\Big) \cdot \dfrac{C_{\mathrm{O_2}}}{K_{\mathrm{O_2,miner}} + C_{\mathrm{O_2}}} \cdot D_{\mathrm{SPOM}}$

Table 11.13: Process rates of the model for oxygen and nutrient dynamics in a river.

equation 8.6 in section 8.2. The process rates of nitrification are given by the equations (8.24) and (8.25) in section 8.6. Finally, the process rate of mineralization is given by applying equation (8.16) from section 8.5 to sedimented particulate organic material.

This model is applied to a river section modelled by three reaches, R_1-R_3, represented by mixed reactors in sequence. The volume of each of these reactors is calculated as the product of the mean river width, the mean depth and the length of the reach

$$V_{R_i} = L_{R_i} \cdot w_{R_i} \cdot h_{R_i} \tag{11.29}$$

All dissolved substances are transported with the water from one reactor to the next

$$\mathbf{J}^{R_i\, R_{i+1}} = Q\, \mathbf{C}^{R_i} \tag{11.30}$$

where Q is the river discharge. In addition, there is dissolved oxygen exchange across the water surface in each reactor as described in section 6.3

$$J^{R_i}_{\mathrm{int,O_2}} = K_2\, V_{R_i}\, (C_{\mathrm{O_2,sat}} - C^{R_i}_{\mathrm{O_2}}) \tag{11.31}$$

where K_2 is the oxygen exchange coefficient.

Figure 11.8 shows results of a simulation of the model described in this section for 3 days.

For this simulation, the model was operated with constant values of benthic biomass (SALG) and of sedimented organic particles (SPOM). The figure clearly shows that the

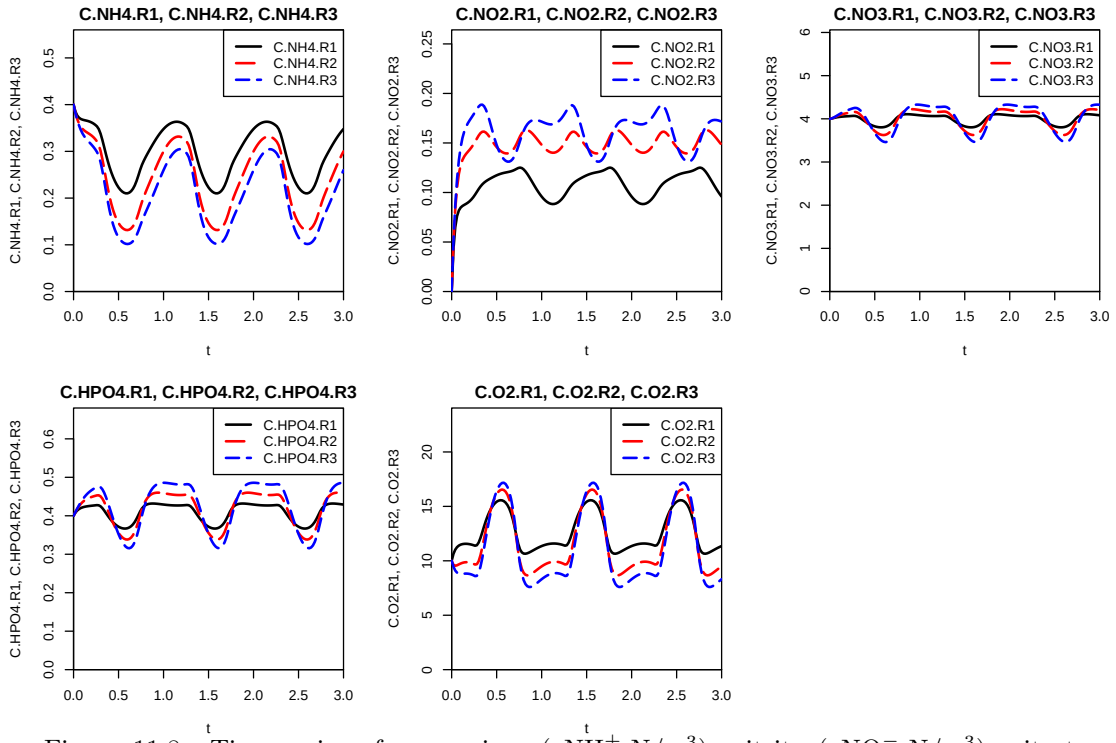

Figure 11.8: Time series of ammonium (gNH_4^+-N/m^3), nitrite (gNO_2^--N/m^3), nitrate (gNO_3^--N/m^3), phosphate ($gHPO_4^{2-}$-P/m^3), and dissolved oxygen (gO_2/m^3) in all three river reaches.

light and temperature dependent primary production leads to strong diurnal variations in ammonium, phosphate and dissolved oxygen. The temperature dependence of respiration, nitrification and mineralization leads to additional diurnal variations in the concentration of ammonium, phosphate and dissolved oxygen. As ammonium is oxidized to nitrite and nitrate, the variation in ammonium leads to similar variation in nitrite. Nitrate is much less affected as the concentration is much larger than that of ammonium or nitrite. Mineralization and respiration lead to release of ammonium and phosphate. As ammonium is nitrified and ammonium and phosphate are consumed by primary production during the day, this results only in an increase of phosphate concentrations during the night. Oxygen is consumed by the processes of respiration of algae, nitrification, and mineralization of organic particles. Oxygen concentration depends furthermore on the gas exchange with the atmosphere. For this reason, it is necessary to know the oxygen exchange coefficient to estimate parameters of primary production and mineralization with the help of oxygen concentrations in the water column. The differences in substance concentrations in the three different reaches of the river occur due to the differences in the input concentrations of each reach. In reach R1 the input concentrations are explicitly given. In reach R2 and R3 the input concentrations are calculated as the output concentrations of the previous reach R1 and R2, respectively.

11.6 Benthic Population Model of a River

In this section, the simple model for the oxygen and nutrient household in a river introduced in section 11.5 is extended to describe the benthic organisms causing the transformation processes.

The model discussed in this section is based on the model described in section 11.5. We need the conceptual development discussed in the sections 1, 2, 3.1, 3.2, 3.3, 4.1, 4.2, and 4.3. Furthermore, we need knowledge of the processes discussed in the sections 6.1.2, 6.3, 8.1, 8.2, 8.3, 8.7, and 8.8.

Table 11.14 shows the process table of the model. We distinguish four groups of organisms: Benthic algae (SALG), benthic heterotrophic bacteria (SHET), benthic bacteria that perform the first nitrification step (SN1), and benthic bacteria that perform the second nitrification step (SN2). For all four groups of organisms, we distinguish growth, death and respiration processes. Growth is described in section 8.1 for algae, in section 8.8.1 for heterotrophic bacteria, and in section 8.8.2 for nitrifiers. We complement these rate expressions with limitation terms due to self-shading of algae (see section 11.5) and another, similar limitation term to empirically describe the limitaton of bacterial growth due to diffusion limitation of nutrients and oxygen into the biofilm. Respiration is described in section 8.2 and death in section 8.3. As a last process, hydrolysis is represented as described in section 8.7. When considering the additional substances HCO_3^-, H^+, and H_2O and the conservation laws for C, H, O, N, P and charge, all stoichiometric coefficients are uniquely determined when we introduce yields for heterotrophic growth, both steps of nitrification, and death (see Table 11.14).

The process rates are given in Table 11.15.

Process	Substances / Organisms											Rate
	HPO_4^{2-} gP	NH_4^+ gN	NO_2^- gN	NO_3^- gN	O_2 gO	DOM g	SALG gDM	SHET gDM	SN1 gDM	SN2 gDM	SPOM gDM	
Growth of algae NH_4^+	−	−			+		1					$\rho_{\text{gro,SALG,NH}_4^+}$
Growth of algae NO_3^-	−			−	+		1					$\rho_{\text{gro,SALG,NO}_3^-}$
Respiration of algae	+	+			−		−1					$\rho_{\text{resp,SALG}}$
Death of algae	0/+	0/+			0/+		−1				$Y_{\text{ALG,death}}$	$\rho_{\text{death,SALG}}$
Growth of het. bact. NH_4^+	?	?			−	$\frac{-1}{Y_{\text{HET}}}$		1				$\rho_{\text{gro,SHET,NH}_4^+}$
Growth of het. bact. NO_3^-	?			?	−	$\frac{-1}{Y_{\text{HET}}}$		1				$\rho_{\text{gro,SHET,NO}_3^-}$
Respiration of het. bact.	+	+			−			−1				$\rho_{\text{resp,SHET}}$
Death of het. bact.	0/+	0/+			0/+			−1			$Y_{\text{HET,death}}$	$\rho_{\text{death,SHET}}$
Growth of N1	−	$\frac{-1}{Y_{\text{N1}}}$	+		−				1			$\rho_{\text{gro,SN1}}$
Respiration of N1	+	+			−				−1			$\rho_{\text{resp,SN1}}$
Death of N1	0/+	0/+			0/+				−1		$Y_{\text{N1,death}}$	$\rho_{\text{death,SN1}}$
Growth of N2	−		$\frac{-1}{Y_{\text{N2}}}$	+	−					1		$\rho_{\text{gro,SN2}}$
Respiration of N2	+	+			−					−1		$\rho_{\text{resp,SN2}}$
Death of N2	0/+	0/+			0/+					−1	$Y_{\text{N2,death}}$	$\rho_{\text{death,SN2}}$
Hydrolysis	0/+	0/+			0/+	Y_{hyd}					−1	ρ_{hyd}

Table 11.14: Process table of a model for the benthic population and oxygen and nutrient dynamics in a river.

Rate	Rate expression
$\rho_{\text{gro,SALG,NH}_4^+}$	$k_{\text{gro,ALG},T_0} \cdot \exp\Big(\beta_{\text{ALG}}(T-T_0)\Big) \cdot \frac{I_0 \exp(-\lambda h)}{K_I + I_0 \exp(-\lambda h)} \cdot \min\left(\frac{C_{\text{HPO}_4^{2-}}}{K_{\text{HPO}_4^{2-},\text{ALG}} + C_{\text{HPO}_4^{2-}}}, \frac{C_{\text{NH}_4^+} + C_{\text{NO}_3^-}}{K_{\text{N,ALG}} + C_{\text{NH}_4^+} + C_{\text{NO}_3^-}}\right) \cdot \frac{p_{\text{NH}_4^+,\text{ALG}} C_{\text{NH}_4^+}}{p_{\text{NH}_4^+,\text{ALG}} C_{\text{NH}_4^+} + C_{\text{NO}_3^-}} \frac{K_{\text{sha,SALG}}}{K_{\text{sha,SALG}} + D_{\text{SALG}}} \cdot D_{\text{SALG}}$
$\rho_{\text{gro,SALG,NO}_3^-}$	$k_{\text{gro,ALG},T_0} \cdot \exp\Big(\beta_{\text{ALG}}(T-T_0)\Big) \cdot \frac{I_0 \exp(-\lambda h)}{K_I + I_0 \exp(-\lambda h)} \cdot \min\left(\frac{C_{\text{HPO}_4^{2-}}}{K_{\text{HPO}_4^{2-},\text{ALG}} + C_{\text{HPO}_4^{2-}}}, \frac{C_{\text{NH}_4^+} + C_{\text{NO}_3^-}}{K_{\text{N,ALG}} + C_{\text{NH}_4^+} + C_{\text{NO}_3^-}}\right) \cdot \frac{C_{\text{NO}_3^-}}{p_{\text{NH}_4^+,\text{ALG}} C_{\text{NH}_4^+} + C_{\text{NO}_3^-}} \frac{K_{\text{sha,SALG}}}{K_{\text{sha,SALG}} + D_{\text{SALG}}} \cdot D_{\text{SALG}}$
$\rho_{\text{resp,SALG}}$	$k_{\text{resp,ALG},T_0} \cdot \exp\Big(\beta_{\text{ALG}}(T-T_0)\Big) \cdot \frac{C_{\text{O}_2}}{K_{\text{O}_2,\text{ALG}} + C_{\text{O}_2}} \cdot D_{\text{SALG}}$
$\rho_{\text{death,SALG}}$	$k_{\text{death,ALG}} \cdot D_{\text{SALG}}$
$\rho_{\text{gro,SHET,NH}_4^+}$	$k_{\text{gro,HET},T_0} \cdot \exp\Big(\beta_{\text{HET}}(T-T_0)\Big) \cdot \frac{p_{\text{NH}_4^+,\text{HET}} C_{\text{NH}_4^+}}{p_{\text{NH}_4^+,\text{HET}} C_{\text{NH}_4^+} + C_{\text{NO}_3^-}} \cdot \min\left(\frac{C_{\text{DOM}}}{K_{\text{DOM,HET}} + C_{\text{DOM}}}, \frac{C_{\text{O}_2}}{K_{\text{O}_2,\text{HET}} + C_{\text{O}_2}}, \frac{C_{\text{HPO}_4^{2-}}}{K_{\text{HPO}_4^{2-},\text{HET}} + C_{\text{HPO}_4^{2-}}}, \frac{C_{\text{NH}_4^+} + C_{\text{NO}_3^-}}{K_{\text{N,HET}} + C_{\text{NH}_4^+} + C_{\text{NO}_3^-}}\right) \frac{K_{\text{lim,SHET}}}{K_{\text{lim,SHET}} + D_{\text{SHET}}} \cdot D_{\text{SHET}}$
$\rho_{\text{gro,SHET,NO}_3^-}$	$k_{\text{gro,HET},T_0} \cdot \exp\Big(\beta_{\text{HET}}(T-T_0)\Big) \cdot \frac{C_{\text{NO}_3^-}}{p_{\text{NH}_4^+,\text{HET}} C_{\text{NH}_4^+} + C_{\text{NO}_3^-}} \cdot \min\left(\frac{C_{\text{DOM}}}{K_{\text{DOM,HET}} + C_{\text{DOM}}}, \frac{C_{\text{O}_2}}{K_{\text{O}_2,\text{HET}} + C_{\text{O}_2}}, \frac{C_{\text{HPO}_4^{2-}}}{K_{\text{HPO}_4^{2-},\text{HET}} + C_{\text{HPO}_4^{2-}}}, \frac{C_{\text{NH}_4^+} + C_{\text{NO}_3^-}}{K_{\text{N,HET}} + C_{\text{NH}_4^+} + C_{\text{NO}_3^-}}\right) \frac{K_{\text{lim,SHET}}}{K_{\text{lim,SHET}} + D_{\text{SHET}}} \cdot D_{\text{SHET}}$
$\rho_{\text{resp,SHET}}$	$k_{\text{resp,HET},T_0} \cdot \exp\Big(\beta_{\text{HET}}(T-T_0)\Big) \cdot \frac{C_{\text{O}_2}}{K_{\text{O}_2,\text{HET}} + C_{\text{O}_2}} \cdot D_{\text{SHET}}$
$\rho_{\text{death,SHET}}$	$k_{\text{death,HET}} \cdot D_{\text{SHET}}$
$\rho_{\text{gro,SN1}}$	$k_{\text{gro,N1},T_0} \cdot \exp\Big(\beta_{\text{N1}}(T-T_0)\Big) \cdot \min\left(\frac{C_{\text{NH}_4^+}}{K_{\text{NH}_4^+,\text{nitri}} + C_{\text{NH}_4^+}}, \frac{C_{\text{O}_2}}{K_{\text{O}_2,\text{nitri}} + C_{\text{O}_2}}, \frac{C_{\text{HPO}_4^{2-}}}{K_{\text{HPO}_4^{2-},\text{nitri}} + C_{\text{HPO}_4^{2-}}}\right) \frac{K_{\text{lim,SN}}}{K_{\text{lim,SN}} + D_{\text{SN1}}} \cdot D_{\text{SN1}}$
$\rho_{\text{resp,SN1}}$	$k_{\text{resp,N1},T_0} \cdot \exp\Big(\beta_{\text{N1}}(T-T_0)\Big) \cdot \frac{C_{\text{O}_2}}{K_{\text{O}_2,\text{nitri}} + C_{\text{O}_2}} \cdot D_{\text{SN1}}$
$\rho_{\text{death,SN1}}$	$k_{\text{death,N1}} \cdot D_{\text{SN1}}$
$\rho_{\text{gro,SN2}}$	$k_{\text{gro,N2},T_0} \cdot \exp\Big(\beta_{\text{N2}}(T-T_0)\Big) \cdot \min\left(\frac{C_{\text{NO}_2^-}}{K_{\text{NO}_2^-,\text{nitri}} + C_{\text{NO}_2^-}}, \frac{C_{\text{O}_2}}{K_{\text{O}_2,\text{nitri}} + C_{\text{O}_2}}, \frac{C_{\text{HPO}_4^{2-}}}{K_{\text{HPO}_4^{2-},\text{nitri}} + C_{\text{HPO}_4^{2-}}}\right) \frac{K_{\text{lim,SN}}}{K_{\text{lim,SN}} + D_{\text{SN2}}} \cdot D_{\text{SN2}}$
$\rho_{\text{resp,SN2}}$	$k_{\text{resp,N2},T_0} \cdot \exp\Big(\beta_{\text{N2}}(T-T_0)\Big) \cdot \frac{C_{\text{O}_2}}{K_{\text{O}_2,\text{nitri}} + C_{\text{O}_2}} \cdot D_{\text{SN2}}$
$\rho_{\text{death,SN2}}$	$k_{\text{death,N2}} \cdot D_{\text{SN2}}$
$\rho_{\text{hyd,SPOM}}$	$k_{\text{hyd,SPOM},T_0} \cdot \exp\Big(\beta_{\text{hyd}}(T-T_0)\Big) \cdot D_{\text{SPOM}}$

Table 11.15: Process rates of the model for benthic population and oxygen and nutrient dynamics in a river.

These formulations are according to the sections 8.1 for growth of algae, 8.8.1 for growth of heterotrophic bacteria, 8.8.2 for growth of nitrifiers, 8.2 for respiration processes, 8.3 for death processes, and 8.7 for hydrolysis with minor adaptations for the formulation for benthic instead of suspended organisms.

This model is applied to a river section modelled by three reaches, R_1-R_3, represented by mixed reactors in sequence. The volume of each of these reactors is calculated as the product of the mean river width, the mean depth and the length of the reach

$$V_{R_i} = L_{R_i} \cdot w_{R_i} \cdot h_{R_i} \tag{11.32}$$

All dissolved substances are transported with the water from one reactor to the next

$$\mathbf{J}^{R_i\, R_{i+1}} = Q\, \mathbf{C}^{R_i} \tag{11.33}$$

where Q is the river discharge. In addition, there is dissolved oxygen exchange across the water surface in each reactor as described in section 6.3

$$J^{R_i}_{\mathrm{int,O_2}} = K_2\, V_{R_i}\, (C_{\mathrm{O_2,sat}} - C^{R_i}_{\mathrm{O_2}}) \tag{11.34}$$

where K_2 is the oxygen exchange coefficient.

Figure 11.9 shows results of a simulation of the model for given, constant benthic organism densities, Figure 11.10 for allowing the organisms to grow. These figures show

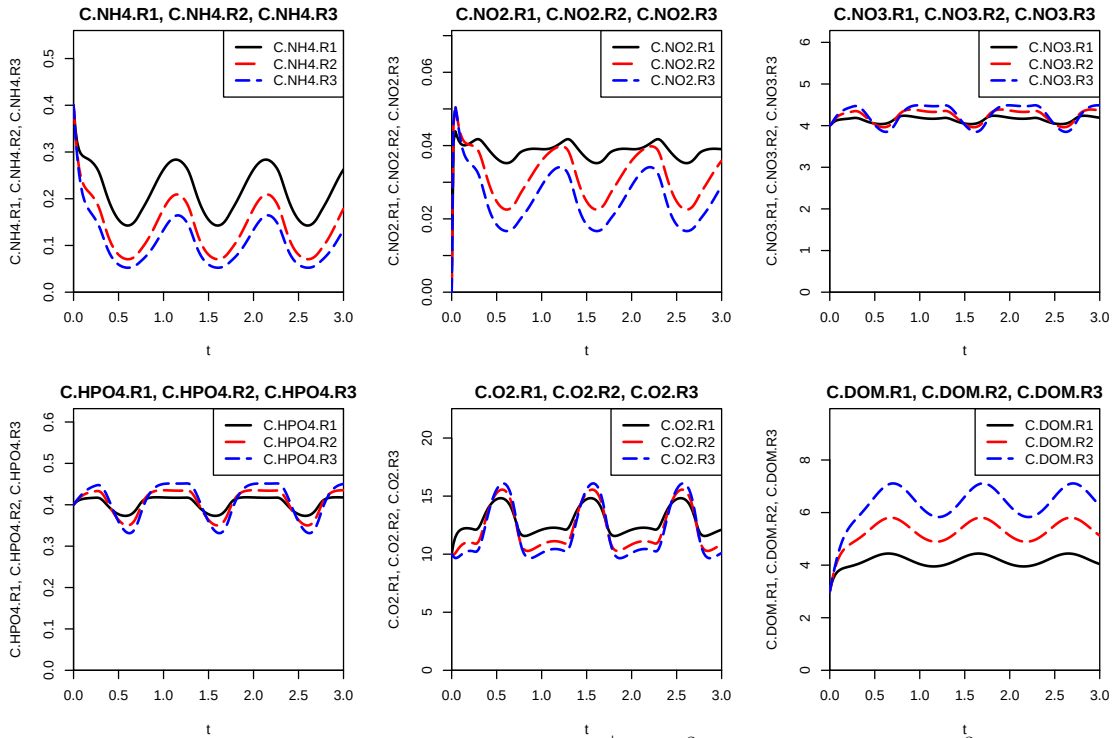

Figure 11.9: Time series of ammonium ($\mathrm{gNH_4^+}$-N/$\mathrm{m^3}$), nitrite ($\mathrm{gNO_2^-}$-N/$\mathrm{m^3}$), nitrate ($\mathrm{gNO_3^-}$-N/$\mathrm{m^3}$), phosphate ($\mathrm{gHPO_4^{2-}}$-P/$\mathrm{m^3}$), dissolved oxygen ($\mathrm{gO_2/m^3}$), and dissolved organic matter ($\mathrm{gDOM/m^3}$) in all three river reaches for a simulation with constant benthic organism densities.

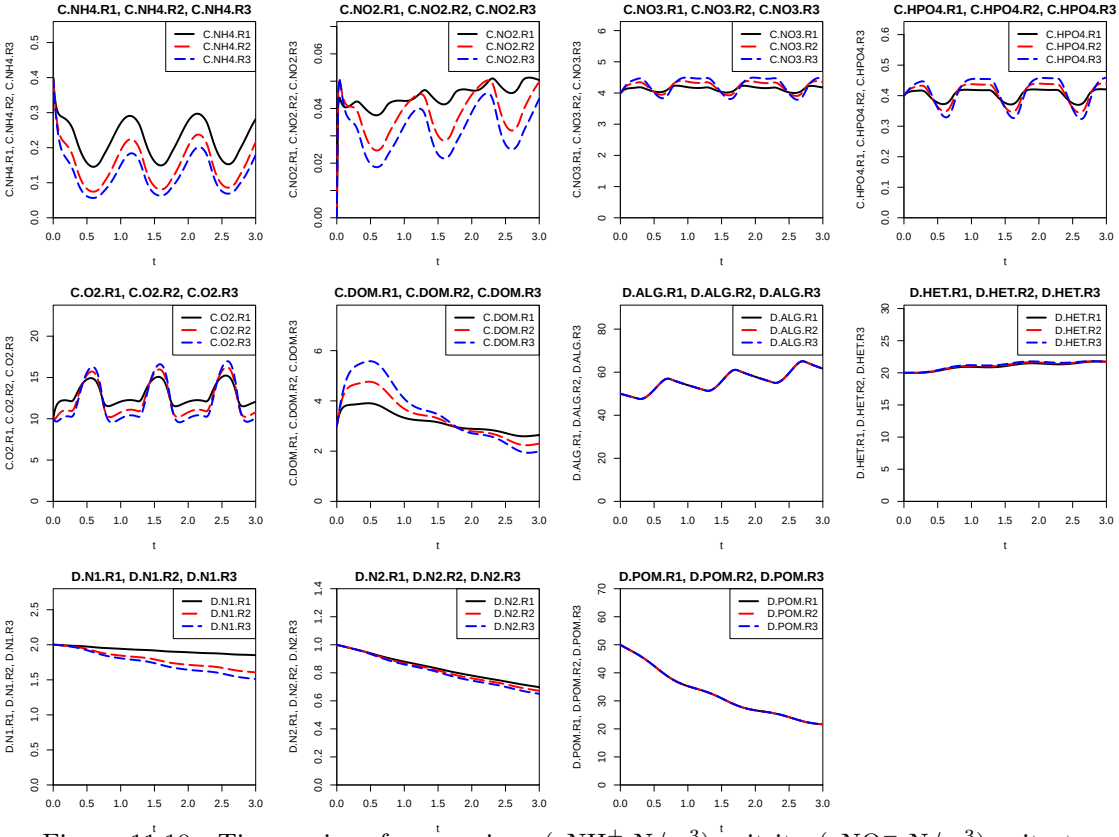

Figure 11.10: Time series of ammonium (gNH_4^+-N/m^3), nitrite (gNO_2^--N/m^3), nitrate (gNO_3^--N/m^3), phosphate ($gHPO_4^{2-}$-P/m^3), dissolved oxygen (gO_2/m^3), and dissolved organic matter (gDOM/m^3), benthic algae (gDM/m^2), benthic heterotrophic bacteria (gDM/m^2), benthic first stage nitrifiers (gDM/m^2), benthic second stage nitrifiers (gDM/m^2), and benthic particulate organic matter (gDM/m^2) in all three river reaches.

the phenomena discussed at the end of section 11.5 with the additional changes of benthic biomass of the different organisms classes. Dissolved organic matter in the water column (DOM) is produced during the process of hydrolysis and consumed by the growth of heterotrophic bacteria. In figure 11.9 with constant bacteria density the diurnal variation in DOM concentration result mainly from variations in ammonium and to a smaller extent from the temperature dependency of hydrolysis and growth of heterotrophic bacteria. In figure 11.10 with modelled density of benthic algae and bacteria the DOM concentrations vary depending on the relation between consumption and production rate. Algae are growing only during the day, because the growth process is limited by the available light. During the night the processes of respiration and death lead to a decrease of the algae density. This leads to the diurnal variation of algae density. In total the algae density increases with time. The density of heterotrophic bacteria increases as well due to the fact that the growth rate exceeds respiration and death. The control of algae and heterotrophic bacteria would be achieved by grazing by higher organisms and/or by detachment due to the shear force of water flow. Nitrifying bacteria densities decrease with time because the increase due to growth is overcompensated by death and respiration processes. The density of organic particles (POM) decreases as well since the rate of hydrolysis is greater than the production by the death processes of algae and bacteria.

11.7 Model Predictions with Stochasticity and Uncertainty

In this section, we add environmental stochasticity and parameter uncertainty, as described in chapter 9 to the models discussed in the sections 11.1 and 11.2. These models are based on the chapters and sections 1, 2, 3.1, 3.2, 4.1, 4.2, 8.1, 8.3, and 8.4. The model descriptions are not reproduced here, please refer to the sections 11.1 and 11.2.

Figure 11.11 shows the results of 10 Monte Carlo simulations of the model described in section 11.1 under constant driving conditions with either parameter uncertainty or environmental stochasticity in the parameters $k_{\mathrm{gro,ALG}}$, $k_{\mathrm{death,ALG}}$ and $K_{\mathrm{HPO_4^{2-},ALG}}$. For

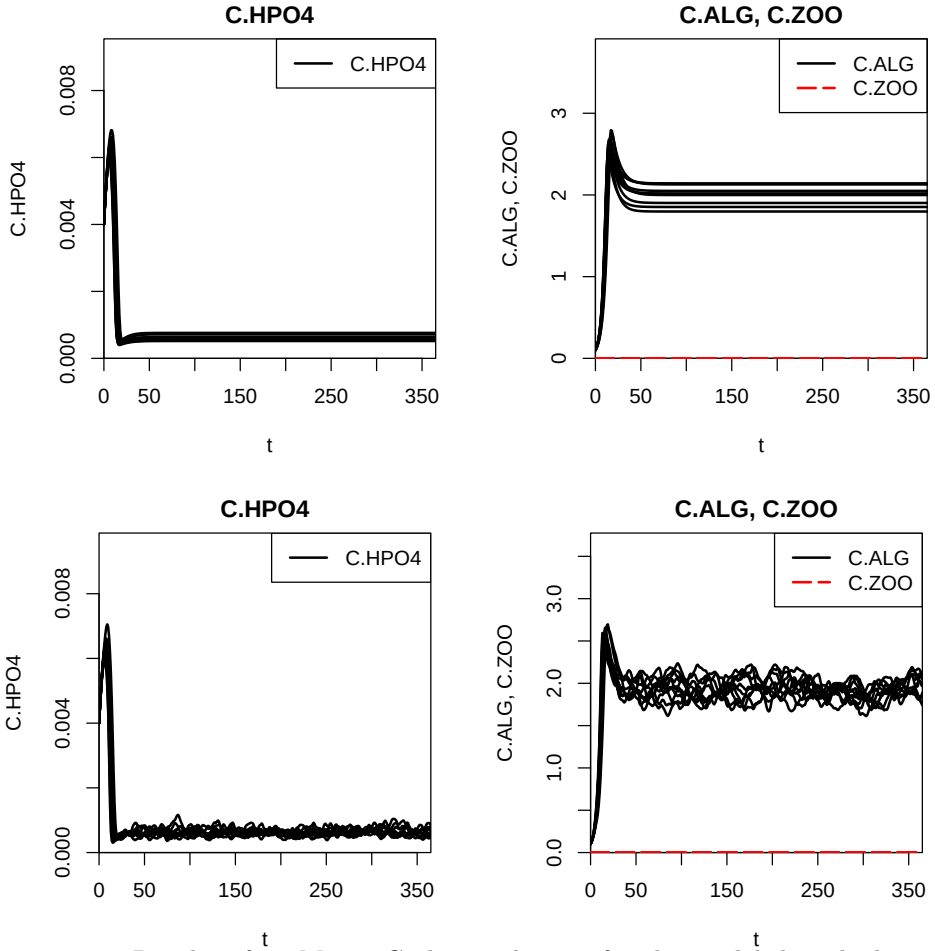

Figure 11.11: Results of 10 Monte Carlo simulations for the model described in section 11.1 under constant driving conditions with parameter uncertainty (top row) and with environmental stochasticity (bottom row). The standard deviation of the parameters is in both cases 10%. (See Fig. 11.2 for the analogous results without uncertainty.)

parameter uncertainty, a sample of 10 draws of parameter values was taken from lognormal distributions with the mean given by the parameter value used in section 11.1 and a standard deviation of 10%. The top row of plots in Fig. 11.11 then shows the corresponding 10 model simulations. Analogously, to consider environmental stochasticity, 10 realizations of Ornstein-Uhlenbeck processes were drawn for the log-parameters with a correlation time of 5 days and parameters such that the mean and standard deviation in the original units are the same as for parameter uncertainty (see section 14.3 for the

required transformations). Then, again, model simulations were done based on these 10 sets of parameter time series. Please note that the 10 Monte Carlo simulations shown in Fig. 11.11 (and Figs. 11.12 to 11.14) give only a rough idea of the order of magnitude of the prediction uncertainty. To get more accurate results, one would perform hundreds or thousands of simulations and use empirical quantiles of the simulation results as approximate prediction quantiles. However, for the didactical purpose of this section, example runs of such a large sample may be more illustrative and take much less simulation time. Figure 11.12 shows the corresponding results under periodic driving conditions as they were used in section 11.1. Please note that the results with environmental stochasticity

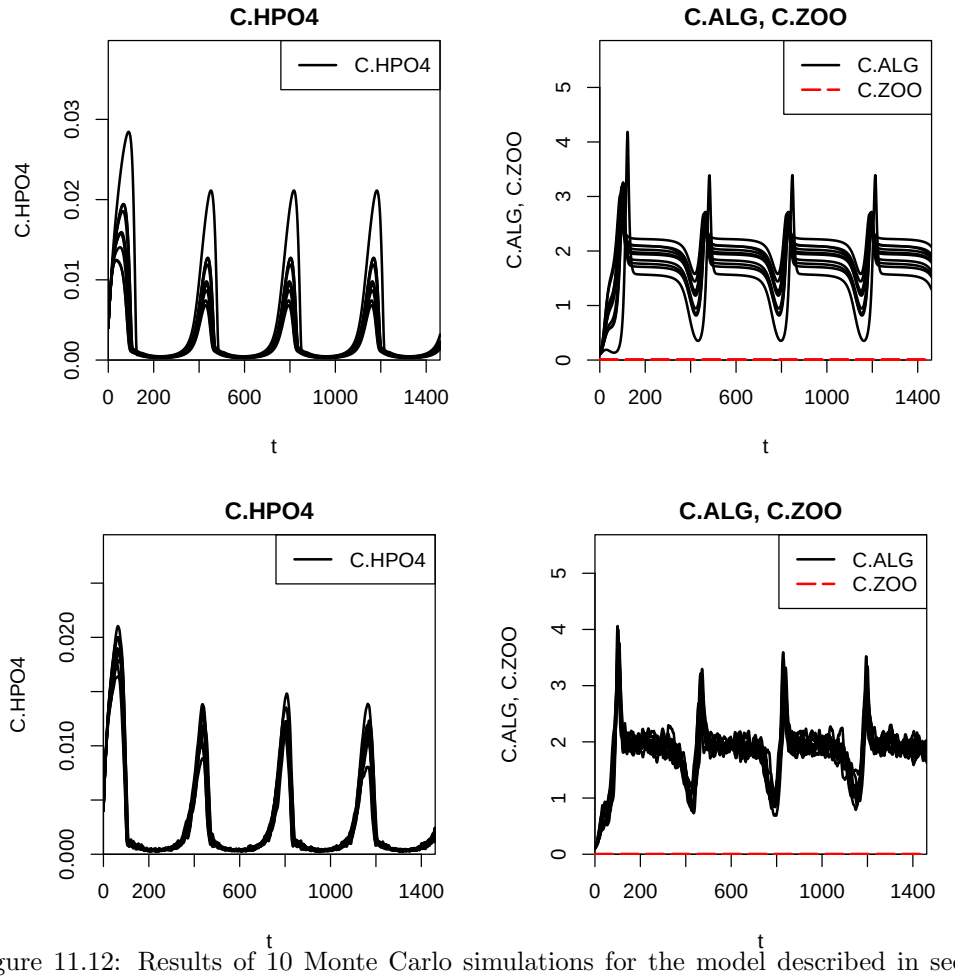

Figure 11.12: Results of 10 Monte Carlo simulations for the model described in section 11.1 under periodic driving conditions with parameter uncertainty (top row) and with environmental stochasticity (bottom row). The standard deviation of the parameters is in both cases 10%. (See Fig. 11.3 for the analogous results without uncertainty.)

tend to be less uncertain than those with parameter uncertainty as the parameters do not stay at the same value during the course of the simulation but it fluctuates around its mean.

Figure 11.13 shows the results of the model described in section 11.2 under constant driving conditions with either parameter uncertainty or environmental stochasticity in the parameters $k_{\text{gro,ALG}}$, $k_{\text{death,ALG}}$, $K_{\text{HPO}_4^{2-},\text{ALG}}$, $k_{\text{gro,ZOO}}$ and $k_{\text{death,ZOO}}$. Figure 11.14 shows the analogous results of the same model under the same periodic driving conditions

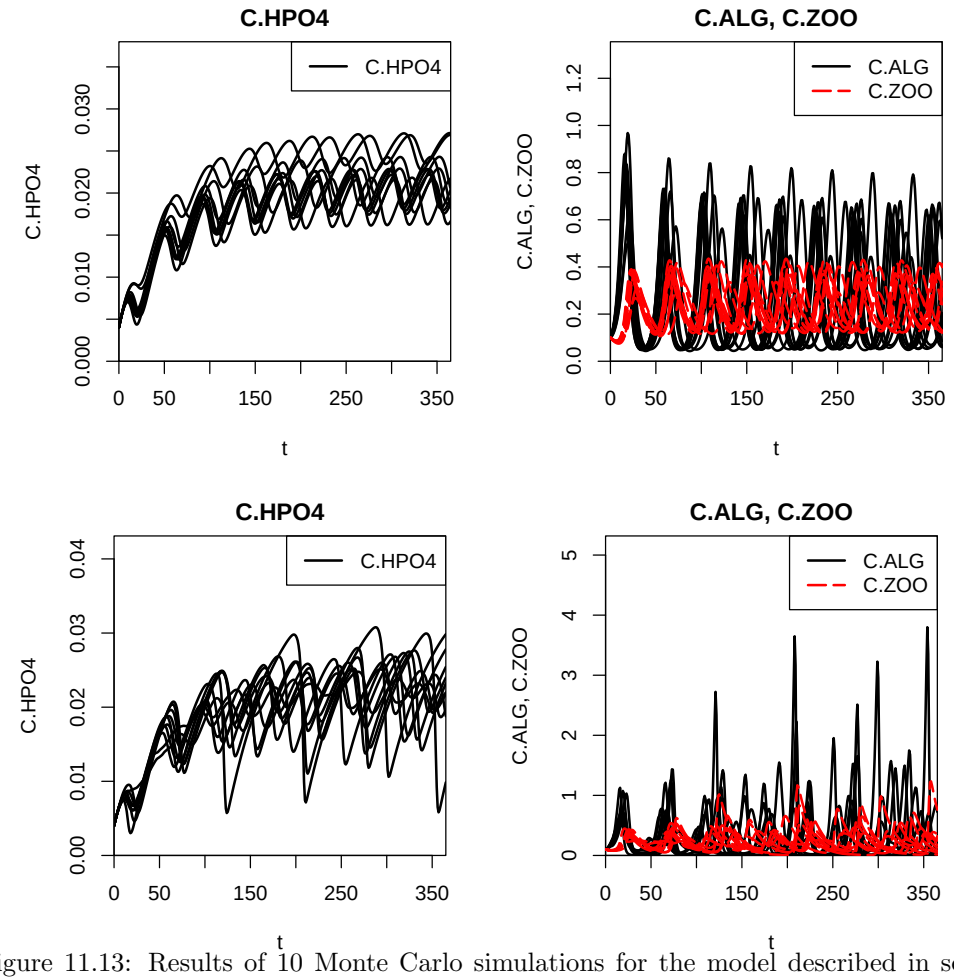

Figure 11.13: Results of 10 Monte Carlo simulations for the model described in section 11.2 under constant driving conditions with parameter uncertainty (top row) and with environmental stochasticity (bottom row). The standard deviation of the parameters is in both cases 10%. (See Fig. 11.4 for the analogous results without uncertainty.)

as they were used in section 11.2. Note that changes in parameters lead to changes in phase, period and amplitude of the oscillatory behaviour of this model. This leads to a much larger uncertainty than in the case of the steady-state solution of the phytoplankton model shown in the Figs. 11.11 and 11.12. Another interesting observation is that in contrast to the results of the phytoplankton model, the prediction uncertainty due to parametric uncertainty is now smaller than that due to environmental stochasticity. This may be caused by amplitude amplifications induced by the stochasticity (McKane and Newman, 2005).

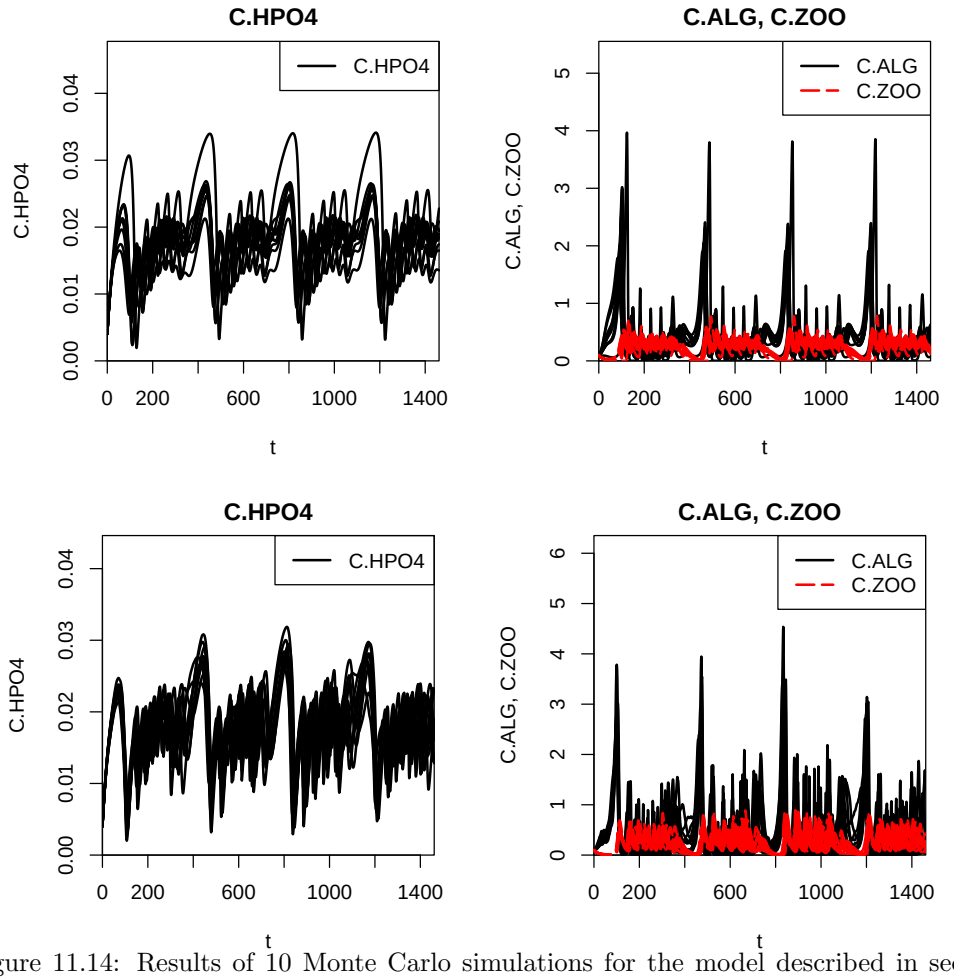

Figure 11.14: Results of 10 Monte Carlo simulations for the model described in section 11.2 under periodic driving conditions with parameter uncertainty (top row) and with environmental stochasticity (bottom row). The standard deviation of the parameters is in both cases 10%. (See Fig. 11.5 for the analogous results without uncertainty.)

Part V

Advanced Aquatic Ecosystem Modelling

Chapter 12

Extensions of Processes and Model Structure

In the preceding chapters of this manuscript we dealt with the formulation of physical, chemical and biological processes relevant in ecosystems, their combination to simple ecosystem process models, and the behaviour of the resulting ecosystem model. With the simple, didactical models, we already reached a significant level of complexity of ecosystem description. However, natural ecosystems are still much more complicated than our models and it remains a difficult decision, for which problem which model complexity is most appropriate.

In this chapter, we first discuss some processes in aquatic ecosystems that are often important enough to be included in ecosystem models and which were not covered in the preceding chapters (sections 12.1 and 12.2). We then describe structural extension to the model structure and alternative model structures that can be useful to get an even better description of reality.

12.1 Mechanistic Description of Physical Processes

In chapter 6 we gave an overview of important physical processes in rivers and lakes and introduced some parameterizations of transport and mixing processes. After sufficient calibration, these parameterizations allow us to describe the physical environment that influences the chemical and biological processes in the ecosystem. This level of description is usually sufficient to investigate the biogeochemical and ecological processes in the system. However, there are two types of cases that require a more detailed, mechanistic physical description. The first type of cases is an ecosystem in which there is a significant feedback from biogeochemical and ecological processes on the physical processes. A particularly important example is chemical stratification. The release of substances from the sediment to the water column can affect its density and lead to reduced diffusion due to chemical stratification. This process cannot be described by a model that decouples the physical sub-model from the biogeochemical sub-model. The second type is prediction under changing physical driving forces. Parameterization of physical processes is rarely universal enough to predict effects of changed physical driving forces. The most important example for this type of problem is the prediction of the effect of climate change. To correctly represent the effects of modified physical driving forces on an aquatic ecosystem, we need a mechanistic physical sub-model in addition to mechanistic biogeochemical and ecological sub-models.

The simplest models for mixing and stratification in reservoirs and lakes are one dimensional models that resolve the depth of the system. Upper mixed layer dynamics is typically modelled by an energy balance model that incorporates the processes of convective overturn due to surface cooling, wind stirring, entrainment at the base of the mixed layer due to seiche-induced shear, and billowing due to shear instability. Mixing in the hypolimnion is usually based on an eddy diffusivity parameterization (Imberger, 1978; Imberger and Patterson, 1981; Patterson et al., 1984; Hamilton and Schladow, 1997; Gal et al., 2003). While these models are quite successful in modelling the upper mixed layer, the description of mixing in the hypolimnion is more critical due to the three dimensional nature of the processes generating turbulence in the hypolimnion (in particular internal seiches). This deficit is often not recognised as the flat temperature profiles in the hypolimnion are insensitive to wrong mixing coefficients.

Three dimensional hydrodynamic modelling could in principle solve this problem. However, due to the high computational requirements and the difficulty of calibrating the corresponding three dimensional biogeochemical and ecological model, three dimensional simulations of reservoirs and lakes are still rare (Romero et al., 2004).

12.2 Important Extensions of Biological Processes

12.2.1 Consideration of Silicon

Diatoms are a very important group of phytoplankton that are dominant in many lakes. An important property of diatoms is that their cell walls consist of a silica frustule encased in an organic coating (Hecky et al., 1972; Martin-Jézéquel et al., 2000). For this reason, diatoms need dissolved silicic acid ($Si(OH)_4$) as a nutrient for growth. This makes silicate an important regulating nutrient for phytoplankton composition (Tilman et al., 1986; Egge and Aksnes, 1992). Figure 12.1 demonstrates this dependence in chemostat experiments (Tilman et al., 1986) at two different temperatures.

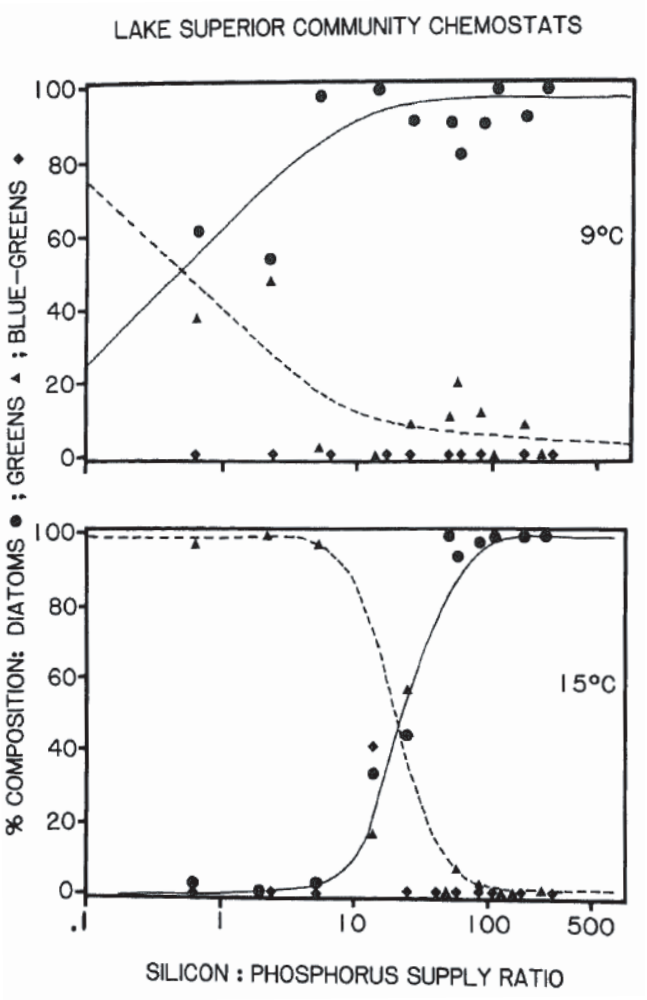

Figure 12.1: Relative proportion of diatoms, green, and bluegreen algae in continuous culture competition experiments at two different temperatures as a function of the ratio at which Si and P were supplied (Tilman et al., 1986). Diatoms are dominant at high Si:P ratios, green and bluegreen algae at low Si:P ratios.

The concepts of deriving process stoichiometry based on mass composition described in section 4.3 can easily be extended to silicon (Si). Only diatoms would have a mass fraction of Si and a corresponding limitation term in their growth rate. This is not relevant

if phytoplankton is aggregated into one model state variable as in this case diatoms will be replaced by other algae within the same state variable if silicate is rate limiting. However, in phytoplankton functional group models as described in section 12.2.5 this becomes relevant for functional groups consisting of diatoms (e.g. small and large diatoms).

12.2.2 Variable Phosphorus Stoichiometry

Investigations of the composition of algae have shown that during periods with strong phosphorus limitation, algae grow with a significantly reduced phosphorus content compared to conditions in which dissolved inorganic phosphorus is easily available. Figure 12.2 shows an example of time series of C:P and C:N ratios in Lake Sempach together with corresponding time series of bioavailable phosphorus species, here measured as soluble reactive phosphorus (SRP) (Hupfer et al., 1995). This figure demonstrates a considerable

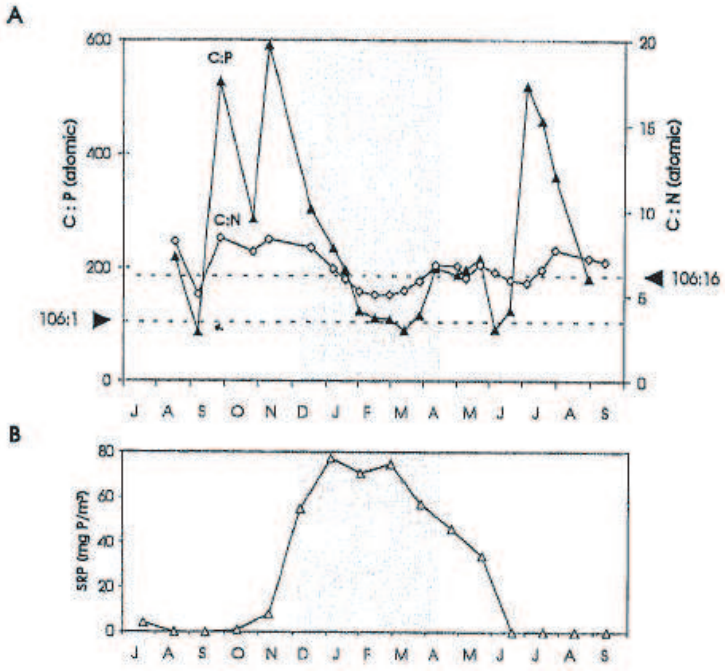

Figure 12.2: Time series of C:P and C:N ratios in Lake Sempach (top) together with corresponding time series of soluble reactive phosphorus (SRP) (bottom) (Hupfer and Gächter, 1995).

variation in particular for C:P.

Modelling variable phosphorus stoichiometry requires an extension of the concepts discussed in section 4.3. The simplest way of dealing with variable composition would be to introduce two types of algae with different phosphorus content and switch growth from one type to the other as a function of dissolved inorganic phosphorus concentration in the water column. An alternative would be to represent the phosphorus content of algae as a separate state variable in the model (Omlin et al., 2001). This will be discussed in more detail in the case study presented in section 13.2.1.

12.2.3 Phosphate Uptake by Organic Particles

Organic particles sedimenting through the hypolimnion during lake stratification have shown to take up inorganic phosphorus (Hupfer et al., 1995). Figure 12.3 shows evidence from sediment traps exposed at different depths of the lake.

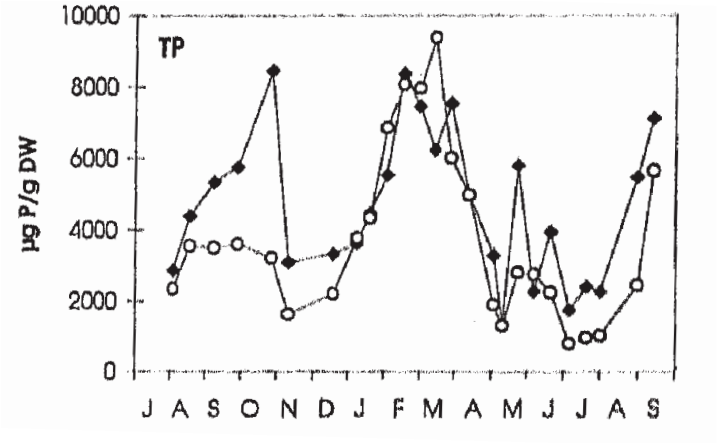

Figure 12.3: Composition of sedimenting particles in 20 m (light dots) and in 80 m (solid dots) as observed in Lake Sempach by Hupfer and Gächter (1995).

Although the mechanism of this process is not completely clear, it may have to be included in an aquatic ecosystem model to make its results more realistic (Omlin et al., 2001). This will be discussed in more detail in the case study presented in section 13.2.1.

12.2.4 Modelling Internal Concentrations

Growth processes were described so far as dependent directly on external nutrient or substrate concentrations in the water. A more detailed look at growth processes reveals that this is a significant simplification of the process consisting of nutrient or substrate uptake into the cell followed by growth on internal nutrient or substrate reservoirs. Growth models can easily be modified to describe growth as such a two step process. This has been quite successfully applied for describing algal growth (Droop, 1973; M., 1980; Droop, 1983; Droop, 2003).

Droop (see references given above) formulated the specific growth rate as a function of "cell quota", Q_{cell}, the concentration of a nutrient or substrate in the cell:

$$\mu = \max\left(\mu'_{\mathrm{m}}\left(1 - \frac{k_Q}{Q_{\mathrm{cell}}}\right), 0\right) \tag{12.1}$$

with the maximum specific growth rate μ'_{m}, and the minimum quota k_Q. The internal concentration, Q_{cell}, increases by uptake (dependent on the external concentration, C_{S}) and decreased due to growth:

$$\frac{\mathrm{d}Q_{\mathrm{cell}}}{\mathrm{d}t} = u_{\mathrm{m}}\frac{C_{\mathrm{S}}}{K_{\mathrm{S}} + C_{\mathrm{S}}} - \mu Q_{\mathrm{cell}} \quad . \tag{12.2}$$

If we use these equations to formulate the mass balances of microorganisms, M (concentration C_{M}), and nutrient or substrate, S (concentration C_{S}), in a mixed reactor without

in- and outflow, and if we interpret Q_{cell} as cell-internal mass of substrate per mass of microorganisms (in the absence of explicitly modelling cells), we get

$$\frac{\mathrm{d}C_{\mathrm{M}}}{\mathrm{d}t} = \mu C_{\mathrm{M}} - bC_{\mathrm{M}} = \max\left(\mu'_{\mathrm{m}}\left(1 - \frac{k_Q}{Q_{\mathrm{cell}}}\right), 0\right) C_{\mathrm{M}} - bC_{\mathrm{M}} \tag{12.3}$$

and

$$\frac{\mathrm{d}C_{\mathrm{S}}}{\mathrm{d}t} = -u_{\mathrm{m}}\frac{C_{\mathrm{S}}}{K_{\mathrm{S}} + C_{\mathrm{S}}}C_{\mathrm{M}} + bQ_{\mathrm{cell}}C_{\mathrm{M}} \quad . \tag{12.4}$$

The mass-balance equation for the cell-internal nutrient or substrate confirms the fulfillment of the overall mass balance:

$$\frac{\mathrm{d}(Q_{\mathrm{cell}}C_{\mathrm{M}})}{\mathrm{d}t} = \frac{\mathrm{d}Q_{\mathrm{cell}}}{\mathrm{d}t}C_{\mathrm{M}} + Q_{\mathrm{cell}}\frac{\mathrm{d}C_{\mathrm{M}}}{\mathrm{d}t} = u_{\mathrm{m}}\frac{C_{\mathrm{S}}}{K_{\mathrm{S}} + C_{\mathrm{S}}}C_{\mathrm{M}} - bQ_{\mathrm{cell}}C_{\mathrm{M}} = -\frac{\mathrm{d}C_{\mathrm{S}}}{\mathrm{d}t} \quad . \tag{12.5}$$

Note that in these equations the quota, Q_{cell}, never drops (again) below k_Q once it was higher than that value. Assuming $Q_{\mathrm{cell}} > k_Q$, we can write the differential equation for Q_{cell} as

$$\frac{\mathrm{d}Q_{\mathrm{cell}}}{\mathrm{d}t} = \mu'_{\mathrm{m}}\big(Q_{\mathrm{eq}}(C_{\mathrm{S}}) - Q_{\mathrm{cell}}\big) \quad . \tag{12.6}$$

This indicates that the cell quota Q_{cell} tends to approximate its (dynamic) equilibrium value Q_{eq} that depends on the external concentration, C_{S}, of the nutrient or substrate:

$$Q_{\mathrm{eq}}(C_{\mathrm{S}}) = k_Q + \frac{u_{\mathrm{m}}}{\mu'_{\mathrm{m}}}\frac{C_{\mathrm{S}}}{K_{\mathrm{S}} + C_{\mathrm{S}}} \quad . \tag{12.7}$$

If the time scale of this relaxation process, $1/\mu'_{\mathrm{m}}$, is much smaller than the time scale of changes in external nutrient or substrate concentration, we can assume that the cell quota is always very close to its equilibrium value, $Q_{\mathrm{eq}}(C_{\mathrm{S}})$. Substituting the equilibrium concentration (12.7) into the equations (12.3) and (12.4) leads then to the limiting case

$$\frac{\mathrm{d}C_{\mathrm{M}}}{\mathrm{d}t} = \mu_{\max}\frac{C_{\mathrm{S}}}{K'_{\mathrm{S}} + C_{\mathrm{S}}}C_{\mathrm{M}} - bC_{\mathrm{M}} \tag{12.8}$$

and

$$\frac{\mathrm{d}C_{\mathrm{S}}}{\mathrm{d}t} = -\mu_{\max}Q_{\mathrm{eq}}(C_{\mathrm{S}})\frac{C_{\mathrm{S}}}{K'_{\mathrm{S}} + C_{\mathrm{S}}}C_{\mathrm{M}} + bQ_{\mathrm{eq}}(C_{\mathrm{S}})C_{\mathrm{M}} \tag{12.9}$$

with

$$\mu_{\max} = \frac{u_{\mathrm{m}}}{k_Q + \dfrac{u_{\mathrm{m}}}{\mu'_{\mathrm{m}}}} \tag{12.10}$$

and

$$K'_{\mathrm{S}} = \frac{k_Q K_{\mathrm{S}}}{k_Q + \dfrac{u_{\mathrm{m}}}{\mu'_{\mathrm{m}}}} \quad . \tag{12.11}$$

This demonstrates that Monod-type growth as mainly used before is the limiting case of the Droop cell-quota model for the case that changes in external nutrient or substrate concentrations are slow. However, under fluctuations of external nutrient concentrations, the behaviour of the Droop model is smoother than the conventional Monod-type model, because the internal nutrient concentrations do not follow the external variations very quickly.

12.2.5 Modelling Functional Groups of Algae, Zooplankton or Invertebrates

There is a very large number of different species of phytoplankton and they show a tremendous diversity in properties relevant for their description by a model. The simple models we dealt with so far, aggregated all of these species into a single model state variable of algae. As the properties of different species can vary considerably, this may not be a realistic description of the ecosystem. To consider this variability without making the model too complex, species with similar properties (traits) can be aggregated to so-called functional groups (for algae the term "functional" does not perfectly apply as all "functional" groups still have the same function of primary production; still this term is often used, as other organisms may be distinguished by their function in the food web). In a functional group model of algae, we could therefore distinguish a (relatively small) number of such functional groups.

Important properties to distinguish phytoplankton functional groups could be (Mieleitner et al., 2008):

- maximum specific growth rate;
- edibility by zooplankton;
- sedimentation velocity;
- light dependence of growth;
- phosphorus dependence of growth;
- nitrogen dependence of growth / capability of fixing nitrogen;
- silicon dependence of growth (see section 12.2.1).

In a similar way functional groups of other organism classes could be distinguished leading to a functional group model with about 4-10 functional groups.

From the model formulation point of view, disaggregation of an aggregated state variable into functional groups is a simple step. All organisms can be described with growth either through primary production (see section 8.1) or through consumption with multiple processes for multiple food sources (see section 8.4 for the formulating consumption on a single food source and section 4.2.5 for formulating preferences among different food sources), respiration (see section 8.2), and death (see section 8.3). The difficulties of formulating a functional group model are the choice of the functional groups and of the parameter values (Anderson, 2005; Mieleitner and Reichert, 2008). Organisms may have a high diversity of traits so that a unique classification into functional groups is difficult and parameter values are not measurable directly, as they represent an average of parameter values for the taxa belonging to the functional group (which may even change its taxonomic composition over time).

12.2.6 Modelling Individual Taxa

Given the difficulties of arranging taxa into functional groups, in particular if ecosystem behaviour should be analyzed under different external pressures (e.g. concentrations of nutrients and toxic substances), and of finding adequate parameter values for functional groups, modelling taxa (species or families) directly can be an alternative strategy. This

strategy avoids the aggregation problem and facilitates the interpretation of parameter values (reflecting properties of taxa rather than averages of taxa within a functional group that may change its taxononmic composition over time).

The problem of a model at the taxonomic level is the very large number of required parameters. A realistic model may contain 30-50 or even more taxa, in particular if more taxa are included that present in the real ecosystem to predict its taxonomic composition. Two strategies may be applied to reduce the number of required parameters:

- The Metabolic Theory of Ecology is a basis for so-called allometric scaling of metabolic parameters of a model based on body mass.
- The use of trait databases may allow a parameterization of deviations from allometric scaling due to external effects such as stream velocity, nutrient or toxicant concentrations, etc.

The metabolic theory of ecology (Brown et al., 2004) starts from the observation that the basal metabolic rate of organisms scales as follows with body mass, m, and temperature, T

$$r_{\text{basal}} = i_0 \left(\frac{M}{M_0}\right)^b \exp\left(-\frac{E_\text{a}}{k_\text{B}}\left(\frac{1}{T} - \frac{1}{T_0}\right)\right) \tag{12.12}$$

In this equation, i_0 is a "universal" constant specifying the basal energy turnover rate of an organism with body mass m_0 at temperature T_0, b is a "universal" scaling exponent typically in the range between 2/3 and 3/4, E_a is an activation energy, and k_B is the Boltzmann constant. The universal scaling according to equation (12.12) has been shown to be approximately valid over about 20 orders of magnitude of individual body mass although individual deviations may be significant (see example in Fig. 12.4).

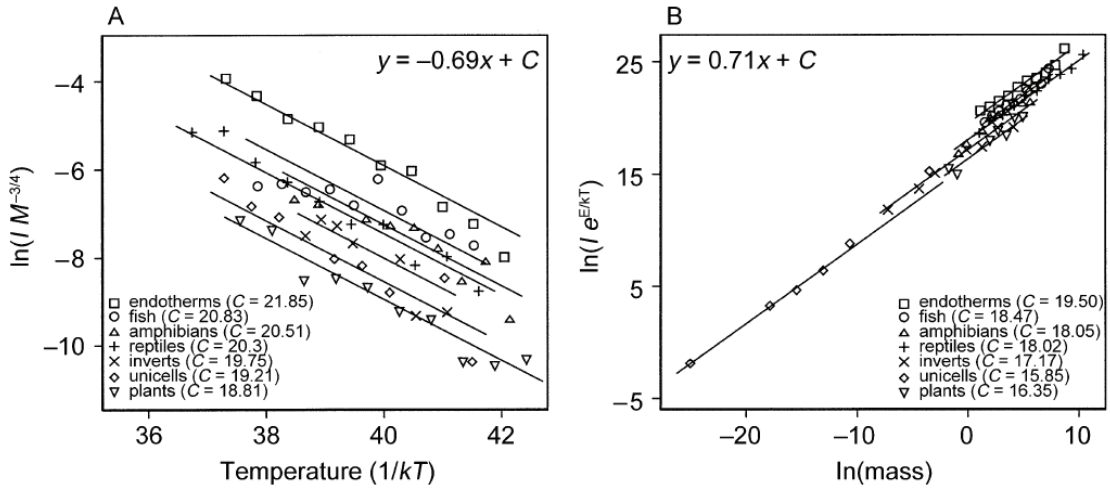

Figure 12.4: Temperature and mass dependence of metabolic rate for several groups of organisms, from unicellular eukaryotes to plants and vertebrates (Brown et al., 2004).

There is a dispute about the correct scaling exponent, b. The theoretical justification for an exponent of 2/3 (Rubner, 1883) is that energy dissipation through the surface of an

organism determines its metabolic rate whereas the mass is determined by the volume. The concept underlying an exponent of 3/4 (Kleiber, 1947; Peters, 1983; Savage et al., 2004) is that essential materials are transported through space-filling fractal networks of branching tubes, that the energy dissipated is minimized and that the terminal tubes do not vary with body size (West et al., 1997). However, none of these theoretical justifications remains valid over the whole range of body masses and individual diversity. Empirical evidence has confirmed that there may not be a single universal exponent (Glazier, 2009; White, 2010). Despite these concerns, models may use empirically fitted relationships of the form (12.12) to formulate basic basal metabolic rates of the model organisms.

The second step of the application of the metabolic theory of ecology is that respiration and growth rates are typically multiples of the basal metabolic rate with a quite constant multiplier. For this reason, these rates follow a similar scaling (see Fig. 12.5).

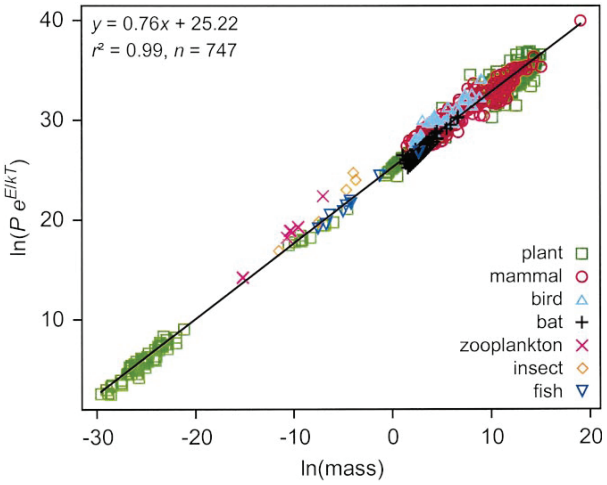

Figure 12.5: The dependence of mass- and temperature corrected biomass production rate, P, shows a power relationship with an exponent close to 3/4 (Brown et al., 2004).

The implications of the metabolic theory of ecology are that body mass may be able to roughly explain quantitative relationships in ecosystems without specific knowledge of life history traits of the involved organisms. As also the rate of molecular evolution scales with the metabolic rate, even patterns of biological diversity across body size may be explained by the metabolic theory of ecology (Gillooly et al., 2005). The approximately universal scaling of basal metabolic rates and the approximately constant multipliers for respiration and growth rates makes it possible to reduce the number of parameters in food web models considerably (Yodzis and Innes, 1992; Brose et al., 2006; Schuwirth and Reichert, 2013).

While the metabolic theory of ecology may be able to explain basic patterns without considering other traits of organisms than the body mass, at a more detailed level of description, an ecosystem model can profit from a modification of the basic patterns by knowledge of traits of individual taxa. Thus, combining a biological model based on the metabolic theory of ecology by modification factors of growth or death rates that consider specific information about the sensitivity of specific taxa to external influence factors can turn a conceptual ecosystem model into a model that describes specific taxa (Schuwirth and Reichert, 2013). The required information about traits of specific taxa can be gathered

from trait databases, such as `http://freshwaterecology.info`. See also case study in section 13.2.3.

12.2.7 Consideration of Rapid Evolution

It was on only recently realized that evolutionary processes can be relevant already on short time scales (Yoshida et al., 2003; Hairston et al., 2005; Carrol et al., 2007; Fussmann et al., 2007; Urban et al., 2008). This can lead to fast adaptation of communities to changing environmental conditions. Current models of such processes concentrate on the selection step and have the same mathematical structure as functional group models (see section 12.2.5). The difference is that the different state variables do not represent different types of organisms but different clones of the same species.

12.3 Important Extensions to the Model Structure

12.3.1 Age-, Size- or Stage-Structured Models

The models discussed so far distinguished functional groups or taxa of organisms but did not resolve their age, size or life-stage. To get a more detailed description and to be able to describe the dependence of the susceptibility to external influence factors on age or life-stage, a model is required that resolves these additional structural elements.

The simplest approach to age or stage-structured models is to distinguish n_{age} discrete age classes or stages and re-formulate growth and death processes as transfer processes from one age class or stage to the next. At a discrete time scale, this leads to the Leslie-Matrix approach of describing age-structured populations (Leslie, 1945; Leslie, 1948). In this approch the vector of the densities of individuals at the different age classes at time $t+1$, $\mathbf{n}_{t+1}$, is derived from the densities of individuals at time t by

$$\mathbf{n}_{t+1} = \mathbf{L}\mathbf{n}_t \tag{12.13}$$

with the "Leslie-Matrix", $\mathbf{L}$, given by

$$\mathbf{L} = \begin{pmatrix} b_1 & b_2 & b_3 & \dots & b_{n_{\text{age}}-1} & b_{n_{\text{age}}} \\ s_1 & 0 & 0 & \dots & 0 & 0 \\ 0 & s_2 & 0 & \dots & 0 & 0 \\ 0 & 0 & s_3 & \dots & 0 & 0 \\ \vdots & \vdots & \vdots & \ddots & 0 & 0 \\ 0 & 0 & 0 & \dots & s_{n_{\text{age}}-1} & 0 \end{pmatrix} \quad . \tag{12.14}$$

In the Leslie-Matrix, the s_i are the fractions of surviving organisms of life-stage or age i to life-stage or age $i+1$ and the b_i are the birth rates from age i. Obviously, the birth rates from ages before maturation are zero. Written without matrix notation, equations (12.13) and (12.14) lead to

$$\begin{aligned} n_{1,t+1} &= \textstyle\sum_{j=1}^{n_{\text{age}}} b_i\, n_{j,t} \\ n_{i,t+1} &= s_{i-1}\, n_{i-1,t} \qquad \text{for } 2 < i < n_{\text{age}} \quad , \end{aligned} \tag{12.15}$$

where the sum in the first equation could be restricted to the ages after reaching maturity.

This model can easily be modified to consider demographic stochasticity. If we introduce a distribution of the clutch size, F, with the mean given by b_i, and interpret s_{i-1} as a survival probability rather than a survival fraction, we get

$$\begin{aligned} n_{1,t+1} &\sim \textstyle\sum_{j=1}^{n_{\text{age}}} n_{j,t} F(b_i) \\ n_{i,t+1} &\sim \text{Binom}(n_{i-1,t}, s_{i-1}) \quad \text{for } 2 < i < n_{\text{age}} \quad . \end{aligned} \tag{12.16}$$

Here, Binom is the binomial distribution. In these equations, the n are all non-negative integers.

A continuous time approach can be based on a continuous formulation of the additional structuring element(s) (age, mass, life-stage). This requires the formulation of the model as a partial differential equation model in which an "advection process" moves the organisms continuously through age, mass or life-stage.

To derive the partial differential equation for a continuous age-structured population model, we apply the theory on one-dimensional mass balance equations outlined in section 3.4.1 to the number of organisms, N, in the system. We replace the spatial dimension, x, by the age, a. Thus, our one-dimensional density, $\hat{\boldsymbol{\rho}}$, is the number of organisms per unit of age, $n(a,t)$ (T^{-1}). The total flux, $\hat{\mathbf{j}}$, is the number of organisms passing a given age per unit of time. As the age and the time dimensions are the same, the density, $n(a,t)$, the number of organisms per unit age at age a and time t is also the number of organisms passing that age at this time: $\hat{\mathbf{j}} = n(a,t)$ (T^{-1}). Finally, the death of the organisms per unit of age, can be parameterized as $\hat{\mathbf{r}} = -k_{\text{death}} n(a,t)$ (T^{-2}), where, in general, k_{death} (T^{-1}) could depend on a, t and n. Given these expressions, the differential form of the one-dimensional mass balance equation (3.26) takes the form of a one-dimensional advection equation (Webb, 1985):

$$\frac{\partial}{\partial t} n(a,t) + \frac{\partial}{\partial a} n(a,t) = -k_{\text{death}}\, n(a,t) \quad . \tag{12.17}$$

Similarly to the first row of the Leslie-Matrix (12.14) that describes birth in the first age class due to all (other) age classes, reproduction takes the form of a boundary condition at age $a = 0$:

$$n(0,t) = \int_0^{a_{\max}} b\big(a, n(a,t), t\big)\, n(a,t)\, \mathrm{d}a \quad . \tag{12.18}$$

Here, b is the reproduction "kernel" and $a_{\max}$ the maximum age of the organisms. Again, $b(a,t)$ is zero for ages less than the maturation age, a_{m}. Figure 12.6 illustrates "advection"

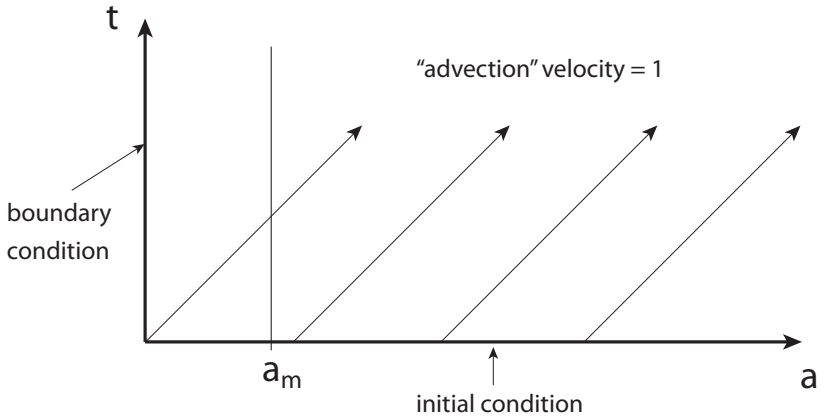

Figure 12.6: Movement of the individual densities of the age-structured model in the age-time diagram.

of the organism density, n in the age-time plane. The density is defined on the lower axis by the initial condition, $n(a,0)$, and on the left axis by the boundary condition, $n(0,t)$, calculated by equation (12.18) from the densities of all ages at the same time point. It is then "advected" with velocity equal to 1 (the age increases by one unit whenever the time increases by one unit) along the arrows in the diagram and decays at the same time with relative decay rate k_{death}. The total number of organisms between the ages a_1 and a_2 at

a particular time is given by

$$N_{[a_1,a_2]}(t) = \int_{a_1}^{a_2} n(a,t)\,\mathrm{d}a \quad . \tag{12.19}$$

If mass-structuring is applied instead of age-structuring, the constant advection term through time must be replaced by a growth term that is no longer constant. $n(m,t)$ denotes now the number of organisms per unit of mass, instead of per unit of age. Again, the one-dimensional density is equal to n: $\hat{\boldsymbol{\rho}} = n(m,t)$ (M^{-1}). However, the flux of organisms through a given mass is now equal to the specific growth rate, k_{gro} (T^{-1}), times the number of organisms per unit of mass, $n(m,t)$: $\hat{\mathbf{j}} = k_{\mathrm{gro}} n(m,t)$. Again, k_{gro} can depend on the mass, m, time, t, and the current density, $n(m,t)$. Given these expressions, the differential form of the one-dimensional mass balance equation (3.26) takes the form of a one-dimensional advection equation

$$\frac{\partial}{\partial t} n(m,t) + \frac{\partial}{\partial m}\big(k_{\mathrm{gro}} n(m,t)\big) = -k_{\mathrm{death}}\, n(m,t) \tag{12.20}$$

with the boundary condition for birth

$$n(m_0,t) = \int_{m_0}^{m_{\max}} b\big(m, n(m,t), t\big)\, n(m,t)\,\mathrm{d}m \quad . \tag{12.21}$$

Here, m_0 is the body mass at birth and $m_{\max}$ the maximum body mass. Figure 12.7 illustrates advection of the organism density, n in the mass-time plane. The density is

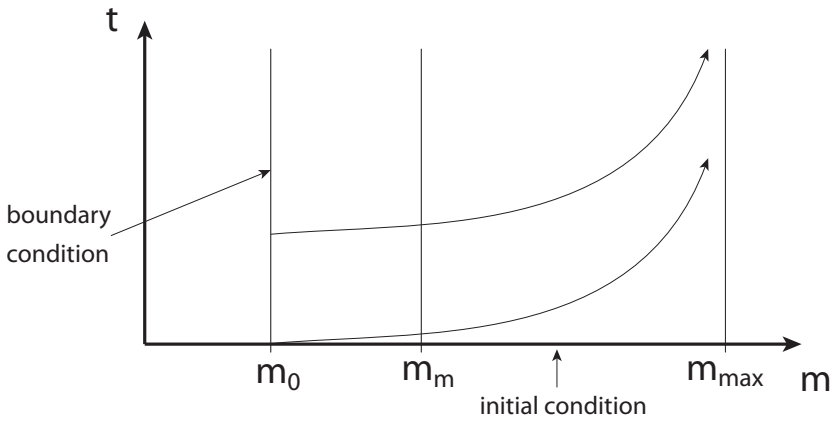

Figure 12.7: Movement of the individual densities of the mass-structured model in the mass-time diagram.

defined on the lower axis by the initial condition, $n(m,0)$, and on the left axis by the boundary condition, $n(m_0,t)$, calculated by equation (12.21) from the densities of all masses at the same time point. It is then "advected" with decreasing "velocity" (the mass does not exceed the maximum mass) along the arrows in the diagram and decays at the same time with relative decay rate k_{death}. Again, the number of organisms with mass

between m_1 and m_2 at a particular time is given by

$$N_{[m_1,m_2]}(t) = \int_{m_1}^{m_2} n(m,t)\,\mathrm{d}m \quad . \tag{12.22}$$

Combining age- and mass-structuring, and now denoting by $n(a,m,t)$ the number of organisms per unit of age and per unit of mass, we get

$$\frac{\partial}{\partial t}n(a,m,t) + \frac{\partial}{\partial a}n(a,m,t) + \frac{\partial}{\partial m}\big(k_{\mathrm{gro}}n(a,m,t)\big) = -k_{\mathrm{death}}\,n(a,m,t) \tag{12.23}$$

with the boundary condition

$$n(0,m,t) = \int_0^{a_{\max}}\int_{m_0}^{m_{\max}} b\big(a,m,n(a,m,t),t\big)\,n(a,m,t)\,\mathrm{d}m\,\mathrm{d}a \quad . \tag{12.24}$$

Again, the number of organisms with age between a_1 and a_2 and mass between m_1 and m_2 is given by

$$N_{[a_1,a_2]\ [m_1,m_2]}(t) = \int_{a_1}^{a_2}\int_{m_1}^{m_2} n(a,m,t)\,\mathrm{d}m\,\mathrm{d}a \tag{12.25}$$

(Tucker and Zimmerman, 1988).

Mass-structured models can be combined with allometric scaling according to the metabolic theory of ecology (see section 12.2.6) to predict mass-spectra of food webs (Hartvig et al., 2011). Figure 12.8 shows an example of a food web mass-spectrum as calculated by such a model.

12.3.2 Discrete Individuals Models

So far, we described populations and communities by organism densities or mass densities of organisms in space. This is a meaningful description as long as the numbers of organisms in the considered volume is large and their properties are similar. If the numbers of organisms becomes small, demographic stochasticity induced by the probabilistic nature of the birth and death processes becomes relevant (see also the discussion in section 9.1.1). As an example, exponential decay of an organism density by a death process leads finally to numbers of individuals in a given volume that are smaller than a single individuum. To adequately deal with this problem, we need discrete individuals models that describe the state of the population by discrete numbers of organisms. As death and reproduction processes can only be described probabilistically, this requires a stochastic model description. In this section, will give a brief introduction to stochastic, discrete individuals models with indistinguishable individuals (of certain classes, such as species, age or stage). In section 12.3.3, we will further extend discrete individuals models to individual-based or agent-based models that additionally consider differences among individuals of the same population (or age or stage class).

In the simplest case, discrete individuals models for a population of identical organisms can be formulated by the transition rates for an increase, $T(N+1 \mid N)$, and a decrease,

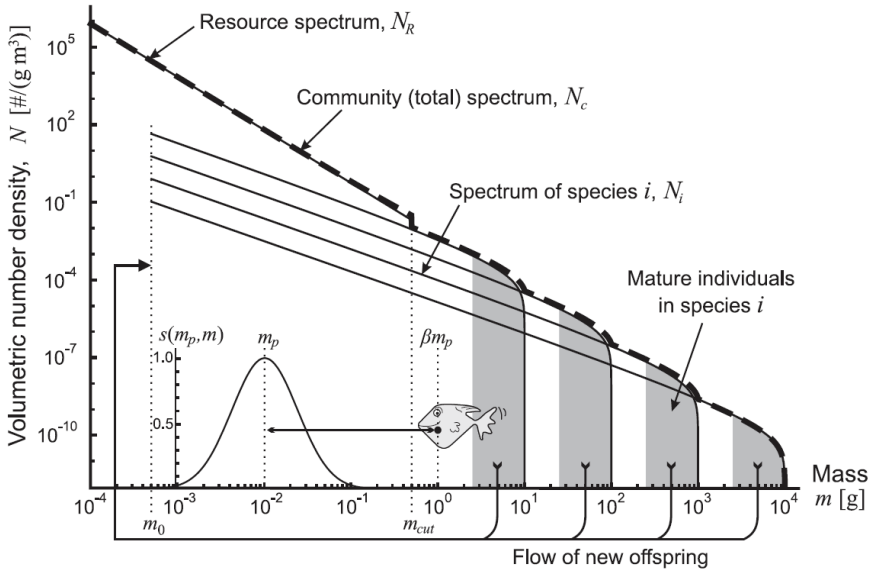

Figure 12.8: Community mass spectrum as calculated by a model consisting of a resource and four species of different mass at maturation (Hartvig et al., 2011).

$T(N-1 \mid N)$, in the number of individuals, N. The so-called master equation for the probability of having N organisms at a given time in the system is then given by (Black and McKane, 2012):

$$\frac{\partial P(N,t)}{\partial t} = T(N \mid N+1)P(N+1,t) + T(N \mid N-1)P(N-1,t) - \big(T(N-1 \mid N) + T(N+1 \mid N)\big)P(N,t) \quad . \quad (12.26)$$

The change in probability for the state with N individuals is composed of four terms: increase due to transition from a state with $N+1$ individuals, increase due to transition from a state with $N-1$ individuals, decrease due to transition to a state with $N-1$ individuals, and decrease due to transition to a state with $N+1$ individuals. This equation can easily be extended from a population to a community model by extending the scalar N to a vector $\mathbf{N}$ of the size of the number of populations building the community.

As an example, we formulate and solve the equations for a simple organism or individual density population model and the corresponding discrete individuals population model. For this purpose, we use a very simple model of a population of organisms with a constant decay rate constant, k_{death}, and without growth in a mixed reactor of fixed volume, V. The deterministic equation of the time-evolution of the (mass-) concentration, C, of the organisms is given as

$$\frac{\mathrm{d}C}{\mathrm{d}t} = -k_{\text{death}}C \quad . \quad (12.27)$$

This equation can be solved analytically to describe the exponential decay of the concentration from its initial concentration C_0:

$$C(t) = C_0 \exp(-k_{\text{death}}t) \quad . \quad (12.28)$$

With the mass, M, of an individual (assuming all individuals to have the same mass), and the total mass of the population, m, we can easily get a continuous approximation for the number of individuals in the reactor

$$N = \frac{m}{M} = \frac{CV}{M} \quad , \tag{12.29}$$

which fulfills the differential equation

$$\frac{\mathrm{d}N}{\mathrm{d}t} = -k_{\mathrm{death}} N \tag{12.30}$$

and is solved by

$$N(t) = N_0 \exp(-k_{\mathrm{death}} t) \quad . \tag{12.31}$$

Note that this equation obviously does no longer make sense as a reasonable approximation to reality if the number of organisms becomes small. Using the right-hand side of equation (12.30) to formulate transition rates for a master equation, we get

$$\begin{aligned} T(N-1 \mid N) &= k_{\mathrm{death}} N \\ T(N+1 \mid N) &= 0 \quad . \end{aligned} \tag{12.32}$$

Growth rates could be formulated similarly for $T(N+1 \mid N)$, but we keep the simple decay model to allow for analytical solution. Substituting these transition rates into the master equation (12.26) we get:

$$\frac{\partial P(N,t)}{\partial t} = k_{\mathrm{death}}(N+1)P(N+1,t) - k_{\mathrm{death}} N P(N,t) \quad . \tag{12.33}$$

This equation can be solved analytically. Starting with an initial population size N_0 ($P(N_0,0) = 1,\ P(N,0) = 0\ \forall N \neq N_0$), we get the analytical solution as a binomial distribution with $p = \exp(-k_{\mathrm{death}} t)$:

$$P(N,t) = \begin{pmatrix} N_0 \\ N \end{pmatrix} \left(1 - \exp(-k_{\mathrm{death}} t)\right)^{N_0 - N} \exp(-k_{\mathrm{death}} t)^N \quad \forall N \leq N_0 \; . \tag{12.34}$$

As the expected value of the binomial distribution is equal to pN_0, we get the expected number of individuals in the population as a function of time as

$$\mathrm{E}[N(t)] = N_0 \exp(-k_{\mathrm{death}} t) \quad . \tag{12.35}$$

For this simple, linear model, the expected value of the population size of the discrete individuals model (12.35) is thus the same as the solution of the deterministic model (12.31). However, with the binomial distribution (12.34), the discrete individuals model describes the demographic fluctuations around this mean. The variance of these fluctuations is given by

$$\mathrm{Var}[N(t)] = N_0 \exp(-k_{\mathrm{death}} t)\big(1 - \exp(-k_{\mathrm{death}} t)\big) \quad . \tag{12.36}$$

Note that for nonlinear models, the expected value of the discrete individuals model will in general no longer be equal to the result of the deterministic model with the same rate expressions as the demographic fluctuations can significantly affect also the mean behaviour of the system.

For realistic models, the master equation (12.26) can usually not be solved analytically. In this case, the population distribution can be numerically approximated by random sampling using the Gillespie algorithm (Gillespie, 1976; Gillespie, 1977).

12.3.3 Individual-Based Models

To describe the properties of and variability among individuals of a population more explicitly, individual-based models represent a population by an assembly of individually modelled organisms (Grimm, 1999). This has three main advantages: First, it derives occurrence pattern of populations from properties of the individual, which are often easier to obtain. Second, such a model makes it much easier to describe life-stages and differences between individuals. This makes such models more realistic. Third, this model formulation considers intrinsically demographic stochasticity which becomes important for populations with small numbers of organisms (see section 9.1.1 and note that this property can already be considered by discrete individuals models as described in section 12.3.2). On the other hand, individual-based models have often many more parameters than the models described so far. This, and their stochastic nature, makes statistical inference of model parameters from observed data much more difficult than with deterministic models combined with an error term that can be evaluated analytically.

Chapter 13

Research Models of Aquatic Ecosystems

In this chapter, we give a short description of selected aquatic ecosystem models published in the literature and their recommended use (section 13.1). Finally, we give a brief overview of selected case studies of model application. The first case demonstrates how we can make a biogeochemical lake model more universal, the second on how we can use Bayesian inference to combine prior knowledge about model parameter values with observed benthic community abundance data to decrease the uncertainty of some of the model parameters in a model that describes functional feeding groups of invertebrates in streams, the third how we can predict the occurrence of invertebrate taxa in streams (section 13.2).

13.1 Examples of Models of Aquatic Ecosystems

In this section we give a brief overview of model structures, calibration strategies, and applications of selected ecological lake and river models (Reichert and Mieleitner, 2008). This overview is far from being complete. Nevertheless, it provides insight into the variety of approaches used in science and management. We will briefly present an aggregated trophic level lake model (BELAMO), two functional group lake models (SALMO and CAEDYM), a dominant species algal community model (PROTECH), two river water quality models (QUAL2K and RWQM1), and two models for benthic communities of rivers (ERIMO and Streambugs).

13.1.1 BELAMO

The **B**iogeochemical-**E**cological **LA**ke **MO**del (BELAMO) (Omlin et al., 2001; Mieleitner and Reichert, 2006; Mieleitner et al., 2008; Mieleitner and Reichert, 2008) represents a relatively simple, aggregated trophic level lake model with emphasis on biogeochemical cycles rather than ecology. A particular feature is the consideration of closure of element cycles by explicit consideration of mineralization processes in the sediment.

Model Overview
BELAMO describes the concentrations of, algae, zooplankton, dissolved oxygen, ammonium, nitrate, phosphate and degradable and inert dead organic particles in the water column and in the sediment. The model considers growth, respiration and death of algae and zooplankton, mineralization, nitrification and phosphate uptake on sinking particles. The model is one dimensional and resolves the depth of the lake. The physical processes vertical mixing, advection, sedimentation, mobility of zooplankton and molecular diffusion in the sediment and across the water sediment interface are considered. Algae can grow with a variable stoichiometry with respect to phosphorus depending on the phosphate concentration in the water column to describe the low phosphorus content of algae growing during phosphate-limited periods in summer.

Calibration strategy
BELAMO applications estimate kinetic parameters of transformation processes with the attempt of finding "universal" values across lakes of different trophic state. As all algal species are aggregated to a single state variable, it is hard to use kinetic parameters measured for selected cultured species in this model. To avoid non-identifiability problems during the parameter estimation, sensitivity and identifiability analysis techniques are used.

13.1.2 SALMO

SALMO (**S**imulation by means of **A**nalytical **L**ake **MO**del) (Benndorf and Recknagel, 1982) represents a functional group lake model. The emphasis is on a very detailed description of the plankton growth dynamics. Recently SALMO was extended to SALMO-HR (high resolution). In this version the ecological model is coupled to a hydro-thermodynamic model of the water column.

Model Overview
SALMO describes ortho-phosphate, dissolved inorganic nitrogen, dissolved oxygen, organic particles, three functional groups of phytoplankton, and zooplankton concentrations

in a lake. The processes growth and mortality of phytoplankton and zooplankton and mineralization are considered. Sedimentation of phytoplankton and migration of zooplankton is also modelled. SALMO was designed to mechanistically describe physical, chemical and biological processes according to a maximum of generality. The model uses only a small number of state variables but more complex process formulations than other models in order to achieve this goal. Each functional group of algae is characterized by an indicator species, the properties of which were measured or compiled from the literature. Fish are considered implicitly by their grazing rate on zooplankton. The nutrient release from the sediment is modelled as an empirical function of oxygen depletion and denitrification. SALMO describes the water body as two mixed reactors representing the epilimnion and the hypolimnion. The depth of the epilimnion has to be specified as a boundary condition. SALMO-HR uses a very detailed hydro-thermodynamic model of the water column.

Calibration strategy
In contrast to most other ecological lake models, the parameters of SALMO are not fitted. Measured values are used for all parameters. The parameter values for phytoplankton growth are determined in the laboratory for key species of each functional group. This strategy not to calibrate the model has the advantage that the parameters are not adapted to a specific lake at a specific time and the parameters are universal for that reason. This improves the prediction quality and the generality of the model.

13.1.3 CAEDYM

The **C**omputational **A**quatic **E**cosystem **DY**namics **M**odel (CAEDYM) (Romero et al., 2004) is an ecological model that can be linked to different hydrodynamic models. In our list of example models, CAEDYM represents a functional group lake model of very high degree of resolution of ecosystem variables and processes. This is a chance for a detailed representation of many processes and mass fluxes, but also a challenge with respect to the number of model parameters and to calibration.

Model Overview
The ecosystem model implemented in CAEDYM is based on a detailed description of the ecosystem. The user can choose between different ecological configuration options and use a different model for each specific application. CAEDYM can be used for freshwater, estuaries or costal waters. The model gives the user a large flexibility in the choice of state variables, processes and process formulations. The state variables that can be used include concentrations of dissolved oxygen, ammonium, nitrate, phosphate, silica, dissolved inorganic carbon, quickly and slowly degradable dissolved and particulate organic matter, up to two groups of inorganic suspended solids, bacteria, up to seven groups of algae, up to five groups of zooplankton, up to five groups of fish, and pathogens in the water column, up to four groups of benthic macroalgae, seagrass, up to 3 groups of benthic invertebrates, and up to seven groups of benthic algae and more. The nonliving components in the water column are also modelled in the sediment. Process descriptions for primary production, secondary production, nutrient and metal cycling, and oxygen dynamics and exchange with the sediment are included in the model. CAEDYM can easily be coupled to zero-, one-, two- and three-dimensional lake hydrodynamics programs. It can easily be coupled to DYRESM (a one-dimensional hydrodynamic model for lakes and reservoirs) or ELCOM (a three-dimensional hydrodynamic model).

Calibration strategy
CAEDYM studies follow the reductionist approach with a detailed, general lake ecosystem model. Model parameters are fitted, but the attempt is made to find "universal" values that do not depend on the particular application. In typical applications, most parameters are held constant, some are fitted jointly for several systems, and some may need site specific calibration.

13.1.4 PROTECH

The **P**hytoplankton **R**esp**O**nse **T**o **E**nvironmental **Ch**ange model (PROTECH) (Reynolds et al., 2001) describes the phytoplankton growth in lakes at the species level. The emphasis of this model is on describing the phytoplankton dynamics in a wide range of different ecosystems.

Model Overview
PROTECH is designed to make simulations of the dynamic changes in the populations of different species of algae within a reservoir or lake environment which may be subject to thermal stratification, periodic destratification, and hydraulic exchange. Chlorophyll a, phosphorus, nitrogen and silica are modelled. The phytoplankton model is very detailed; up to eight species can be selected from a library of 18 phytoplankton species. The effect of zooplankton is described by the death rate of phytoplankton. The maximum growth rate of the different phytoplankton species is calculated using correlations with surface area and volume of the species. Adjustments for temperature dependence, light limitation and nutrient limitation are made. The physical model is one dimensional. It divides the water body into mixed layers.

Calibration strategy
The parameters for the growth of the algal species are not fitted in PROTECH. However, inputs are sometimes adapted to improve the quality of the fit. The experience with PROTEC simulations was that the model results did not correspond well with data at the species level. However, when aggregating data and model simulations to functional groups, there was a good agreement. This led the authors to formulate the hypothesis that a model should resolve one level further down than required for the comparison with data.

13.1.5 QUAL2K

QUAL2K (http://www.epa.gov/ATHENS/wwqtsc/html/qual2k.html) is an extended version of the QUAL2E model that has been used for many years to simulate water quality in rivers. Qual2K describes one-dimensional steady state hydraulics of a river network. It models temperature, dissolved oxygen, slowly and quickly degradable organic matter, organic nitrogen, ammonium, nitrate, organic phosphorus, phosphate, phytoplankton, detritus, pathogens, alkalinity in the water column, and benthic algae.

13.1.6 RWQM1

The **R**iver **W**ater **Q**uality **M**odel No. **1** (Shanahan et al., 2001; Reichert et al., 2001; Vanrolleghem et al., 2001) was developed to bridge the gap between river water quality models and activated sludge sewage treatment process models and to stimulate the development of a sequence of such models similarly to that of activated sludge models (Henze

et al., 1986; Gujer et al., 1995; Henze et al., 1995; Gujer et al., 1999; Henze et al., 1999; Henze et al., 2000).

13.1.7 ERIMO

The mechanistic model **E**cological **RI**ver **MO**del (ERIMO) (Schuwirth et al., 2008; Schuwirth et al., 2011) describes how the main groups of benthic organisms (invertebrates, algae) and the organic matter deposited on the river bed (detritus) vary over time. The invertebrates are grouped according to their feeding types and the algae are differentiated into filamentous and non-filamentous algae. The model describes their growth, death, and loss induced by floods using ordinary differential equations. This model and its calibration using Bayesian inference is described in more detail in the following section.

13.1.8 Streambugs

The mechanistic model Streambugs (http://www.eawag.ch/en/department/siam/projects/streambugs/) combines concepts of theoretical food web modeling, the metabolic theory of ecology, and ecological stoichiometry with the use of functional trait databases to predict the coexistence of invertebrate taxa in streams. The model describes population growth, death, and respiration of different invertebrate taxa and algae to estimate their occurrence or the dynamic development of their populations dependent on various environmental influence factors (Schuwirth and Reichert, 2013). So far, the model was used to assess the effect of multiple stressors and biotic interactions on the presence or absence of invertebrate taxa in the river Glatt (Schuwirth et al., 2016), the effects of a pesticide on invertebrate community dynamics in stream mesocosms (Kattwinkel et al., 2016), the effect of hydropeaking on the temporal dynamics of invertebrates in the river Sihl (Mondy and Schuwirth, 2017), and to predict the effects of river restoration on the occurrence of macroinvertebrate taxa in the rivers Thur and Toess in Switzerland (Paillex et al., 2017). This model is described in more detail in the following section.

13.2 Case Studies of Aquatic Ecosystem Model Application

In this section we discuss two case studies. The focus of the first study is the development of the biogeochemical lake ecosystem model BELAMO and the application of this model to lakes of different trophic state. The second case study uses the model ERIMO, a river benthos community model that describes the dynamic development of algae and functional feeding groups of invertebrates, to demonstrate how we can apply the methodology of Bayesian inference to combine prior knowledge of parameter values with data and analyze what we can learn from the data. The third case study shows an application of the model Streambugs that predicts the occurrence of invertebrate taxa in streams.

13.2.1 Modelling Biogeochemistry and Plankton in Three Lakes of Different Trophic State

This case study illustrates the development of a model for Lake Zurich, Switzerland, and its extension to two additional lakes of different trophic state.

13.2.1.1 Model of Lake Zurich

The model BELAMO extends the didactical model described in section 11.4 (Omlin et al., 2001). Tables 13.1 to 13.3 summarize process stoichiometry and process rates.

No.	Process	S_{NH4} $\left[\frac{gN}{m^3}\right]$	S_{NO3} $\left[\frac{gN}{m^3}\right]$	S_{HPO4} $\left[\frac{gP}{m^3}\right]$	S_{O2} $\left[\frac{gO}{m^3}\right]$	X_{ALG} $\left[\frac{gDM}{m^3}\right]$	$X_{P,ALG}$ $\left[\frac{gP}{m^3}\right]$	X_{PLR} $\left[\frac{gDM}{m^3}\right]$	$X_{P,PLR}$ $\left[\frac{gP}{m^3}\right]$	X_{ZOO} $\left[\frac{gDM}{m^3}\right]$	X_S $\left[\frac{gDM}{m^3}\right]$	$X_{P,S}$ $\left[\frac{gP}{m^3}\right]$	$X_{PI,S}$ $\left[\frac{gP}{m^3}\right]$	X_I $\left[\frac{gDM}{m^3}\right]$	$X_{P,I}$ $\left[\frac{gP}{m^3}\right]$
1	Growth ALG		$-a_N$	$-b_P$	1.2	1	b_P								
2	Growth PLR		$-a_N$	$-b_P$	1.2			1	b_P						
3	Growth ZOO	$\nu_{ZOO,N}$		$\nu_{ZOO,N}$	$-\nu_{ZOO,O}$	$-1/Y_{ZOO}$	$-a_{P,ALG}/Y_{ZOO}$			1	f_e/Y_{ZOO}	0			
4	Resp ALG	a_N		$a_{P,ALG}$	-0.94	-1	$-a_{P,ALG}$								
5	Resp PLR	a_N		$a_{P,PLR}$	-0.94			-1	$-a_{P,PLR}$						
6	Resp ZOO	a_N		$a_{P,red}$	-0.94					-1					
7	Death ALG					-1	$-a_{P,ALG}$				$1-f_p$	$(1-f_p)\ a_{P,ALG}$		f_p	$f_p\ a_{P,ALG}$
8	Death PLR							-1	$-a_{P,PLR}$		$1-f_p$	$(1-f_p)\ a_{P,PLR}$		f_p	$f_p\ a_{P,PLR}$
9	Death ZOO									-1	$1-f_p$	$(1-f_p)\ a_{P,red}$		f_p	$f_p\ a_{P,red}$
10	Aer miner	a_N		$a_{P,S}+a_{PI,S}$	-0.94						-1	$-a_{P,S}$	$-a_{PI,S}$		
11	Anox miner	a_N	-0.33	$a_{P,S}+a_{PI,S}$							-1	$-a_{P,S}$	$-a_{PI,S}$		
12	Nitrification	-1	1		-4.6										
13	P – uptake			-1									1		

Table 13.1: Stoichiometry of the model BELAMO. See Table 13.2 for an explanation of some of the variables.

The main differences to the didactical model described in section 11.4 are the following:

- The model resolves the vertical dimension of the lake continuously. It uses parameterizations of the coefficients of vertical turbulent diffusion calibrated by temperature profiles and, for the deep hypolimnion, by phosphate profiles.
- The model describes mineralization processes in two sediment layers. This leads to a better description of oxic and anoxic mineralization processes than in the didactical model, but this still resolves gradients in the sediment only poorly.
- The model contains two functional groups of alge: plaktothrix rubescens (PLR) and other algae (ALG).
- The model considers variable phosphorus stoichiometry of algal growth (see section 12.2.2 for empirical evidence that this is an important process feature). For this reason, the model contains a separate state variable for phosphorus content of

planktothrix rubescens ($X_{\mathrm{P,PLR}}$), oder algae ($X_{\mathrm{P,ALG}}$), degradable organic particles ($X_{\mathrm{P,S}}$), and inert organic particles ($X_{\mathrm{P,I}}$). The stoichiometry of growth processes assigns a fraction b_{P} of phosphorus to $X_{\mathrm{P,ALG}}$ or $X_{\mathrm{P,PLR}}$, respectively. This fraction, b_{P}, depends on the current phosphate concentration in the water column.

- The model considers an uptake process of phosphate to degradable organic particles (X_{S}). This requires a state variable describing the inorganich phoshorus load of organic particles, $X_{\mathrm{PI,S}}$.

Variable	Algebraic expression
$a_{\mathrm{P,ALG}}$	$\frac{X_{\mathrm{P,ALG}}}{X_{\mathrm{ALG}}}$
$a_{\mathrm{P,PLR}}$	$\frac{X_{\mathrm{P,PLR}}}{X_{\mathrm{PLR}}}$
$a_{\mathrm{P,S}}$	$\frac{X_{\mathrm{P,S}}}{X_{\mathrm{S}}}$
$a_{\mathrm{PI,S}}$	$\frac{X_{\mathrm{PI,S}}}{X_{\mathrm{S}}}$
$a_{\mathrm{P,I}}$	$\frac{X_{\mathrm{P,I}}}{X_{\mathrm{I}}}$
b_{P}	$\frac{b_{\mathrm{P,min}}+b_{\mathrm{P,max}}}{2}+\frac{b_{\mathrm{P,max}}-b_{\mathrm{P,min}}}{2}\cdot\tanh\left(\frac{S_{\mathrm{HPO_4}}-S_{\mathrm{HPO_4,crit}}}{\Delta S_{\mathrm{HPO_4}}}\right)$
Y_{ZOO}	$Y_{\mathrm{ZOO,max}}\min\left(1,\frac{a_{\mathrm{P,ALG}}}{a_{\mathrm{P,red}}}\right)$
F_{e}	$c_{\mathrm{e}}(1-Y_{\mathrm{ZOO}})$
$v_{\mathrm{ZOO,N}}$	$a_{\mathrm{N}}\cdot\frac{1-Y_{\mathrm{ZOO}}-f_{\mathrm{e}}}{Y_{\mathrm{ZOO}}}$
$v_{\mathrm{ZOO,P}}$	$\frac{a_{\mathrm{P,ALG}}}{Y_{\mathrm{ZOO}}}-a_{\mathrm{P,red}}$
$v_{\mathrm{ZOO,O}}$	$0.93\cdot\frac{1-Y_{\mathrm{ZOO}}-f_{\mathrm{e}}}{Y_{\mathrm{ZOO}}}$

Table 13.2: Meaning of stoichiometric variables use in Table 13.1.

Figure 13.1 summarizes the results of the simulations in the year 1990 after calibration of model pararameters during the years 1988 - 1989.

These profiles clearly show mixing of the water column in spring and development of significant concentration gradients during summer stratification. The dissolved oxygen profiles show depletion of oxygen in the hypolimnion during the stratified period due to mineralization of sedimented organic particles. The metalimnic local oxygen minimum is primarily caused by a particularly large sediment surface in this depth (there is a large fraction of the lake that is only about 20 m deep). The phosphate profiles reflect the build-up of phosphate during the stratification period due to release of phosphate by mineralization processes (primarily in the sediment). There is a very strong depletion of phosphate in the epilimnion during stratification due to primary production. The depletion below the epilimnion (between depths of 10 and 20 m) is caused by phosphate uptake of sinking organic particles. The depletion of nitrate in the deep hypolimnion is due to anoxic mineralization (denitrification) in the lower sediment layer. Algae show a spring and a fall peak, but the temporal resolution of the data of one month makes it difficult to analyze

No.	Process	Rate
1	Growth ALG	$k_{\mathrm{gro,ALG},T_0} \cdot \exp(\beta_{\mathrm{ALG}}(\mathrm{T}-\mathrm{T}_0)) \cdot \frac{I(z)}{K_{\mathrm{I,ALG}}+I(z)} \cdot \min\left(\frac{S_{\mathrm{NO_3}}}{K_{\mathrm{NO_3,ALG}}+S_{\mathrm{NO_3}}}, \frac{S_{\mathrm{HPO_4}}}{K_{\mathrm{HPO_4,ALG}}+S_{\mathrm{HPO_4}}}\right) \cdot X_{\mathrm{ALG}}$
2	Growth PLR	$k_{\mathrm{gro,PLR},T_0} \cdot \exp(\beta_{\mathrm{PLR}}(\mathrm{T}-\mathrm{T}_0)) \cdot \frac{I(z)}{K_{\mathrm{I,PLR}}} \exp\left(1-\frac{I(z)}{K_{\mathrm{I,PLR}}}\right) \cdot \min\left(\frac{S_{\mathrm{NO_3}}}{K_{\mathrm{NO_3,ALG}}+S_{\mathrm{NO_3}}}, \frac{S_{\mathrm{HPO_4}}}{K_{\mathrm{HPO_4,ALG}}+S_{\mathrm{HPO_4}}}\right) \cdot X_{\mathrm{PLR}}$
3	Growth ZOO	$k_{\mathrm{gro,ZOO},T_0} \cdot \exp(\beta_{\mathrm{ZOO}}(\mathrm{T}-\mathrm{T}_0)) \cdot \mathrm{X}_{\mathrm{ALG}} \cdot \left(1, \frac{a_{\mathrm{P,ALG}}}{a_{\mathrm{P,red}}}\right) \cdot X_{\mathrm{ZOO}}$
4	Resp ALG	$k_{\mathrm{resp,ALG},T_0} \cdot \exp(\beta_{\mathrm{ALG}}(\mathrm{T}-\mathrm{T}_0)) \cdot \frac{\mathrm{S}_{\mathrm{O_2}}}{K_{\mathrm{O_2resp}}+\mathrm{S}_{\mathrm{O_2}}} \cdot X_{\mathrm{ALG}}$
5	Resp PLR	$k_{\mathrm{resp,PLR},T_0} \cdot \exp(\beta_{\mathrm{PLR}}(\mathrm{T}-\mathrm{T}_0)) \cdot \frac{\mathrm{S}_{\mathrm{O_2}}}{K_{\mathrm{O_2resp}}+\mathrm{S}_{\mathrm{O_2}}} \cdot X_{\mathrm{PLR}}$
6	Resp ZOO	$k_{\mathrm{gro,ZOO},T_0} \cdot \exp(\beta_{\mathrm{ZOO}}(\mathrm{T}-\mathrm{T}_0)) \cdot \frac{\mathrm{S}_{\mathrm{O_2}}}{K_{\mathrm{O_2resp}}+\mathrm{S}_{\mathrm{O_2}}} \cdot X_{\mathrm{ZOO}}$
7	Death ALG	$k_{\mathrm{death,ALG},T_0} \cdot \exp(\beta_{\mathrm{ALG}}(\mathrm{T}-\mathrm{T}_0)) \cdot X_{\mathrm{ALG}}$
8	Death PLR	$k_{\mathrm{death,PLR},T_0} \cdot \exp(\beta_{\mathrm{PLR}}(\mathrm{T}-\mathrm{T}_0)) \cdot X_{\mathrm{PLR}}$
9	Death ZOO	$k_{\mathrm{death,ZOO},T_0} \cdot \exp(\beta_{\mathrm{ZOO}}(\mathrm{T}-\mathrm{T}_0)) \cdot X_{\mathrm{ZOO}}$
10	Aer miner	$k_{\mathrm{miner,aero},T_0} \cdot \exp(\beta_{\mathrm{BAC}}(\mathrm{T}-\mathrm{T}_0)) \cdot \frac{S_{\mathrm{O_2}}}{K_{\mathrm{O_2,miner}}+S_{\mathrm{O_2}}} \cdot X_{\mathrm{S}}$
11	Anox miner	$k_{\mathrm{miner,anox,}\ T_0} \cdot \exp(\beta_{\mathrm{BAC}}(\mathrm{T}-\mathrm{T}_0)) \cdot \frac{S_{\mathrm{NO_3}}}{K_{\mathrm{NO_3,miner}}+S_{\mathrm{NO_3}}} \cdot \left(1-\frac{S_{\mathrm{O_2}}}{K_{\mathrm{O_2,miner}}+S_{\mathrm{O_2}}}\right) \cdot X_{\mathrm{S}}$
12	Nitrification	$k_{\mathrm{nitri},T_0} \cdot \exp(\beta_{\mathrm{BAC}}(\mathrm{T}-\mathrm{T}_0)) \cdot \min\left(\frac{S_{\mathrm{O_2}}}{K_{\mathrm{O_2,nitri}}+S_{\mathrm{O_2}}}, \frac{S_{\mathrm{NH_4}}}{K_{\mathrm{NH_4,nitri}}+S_{\mathrm{NH_4}}}\right)$
13	P-uptake	$k_{\mathrm{upt}} \cdot \frac{1}{A}\left\lvert\frac{\mathrm{d}A}{\mathrm{d}z}\right\rvert \cdot \left(a_{\mathrm{P,max}}-\frac{X_{\mathrm{PLS}}}{X_{\mathrm{S}}}\right) \cdot \frac{S_{\mathrm{O_2}}}{K_{\mathrm{O_2,upt}}+S_{\mathrm{O_2}}} \cdot S_{\mathrm{HPO_4}} \cdot X_{\mathrm{S}}$

Table 13.3: Process rates of the model BELAMO.

plankton dynamics accurately. Planktothrix rubescenc grows at low light intensities in the metalimnion.

Figure 13.2 shows an independent check of the reliability of the simulations. Both flux time series of organic carbon as well as on particulate phosphorus show qualitative agreement with measured profiles taken six years earlier.

Finally, Figure 13.3 shows a comparison of simulations of the full model with models that omit the phosphate uptake process and the variable phosphorus stoichiometry of algal growth. The comparison demonstrate that the phosphate uptake process is necessary to explain the phosphate depletion at between 10 and 20 m depth below the epilimnion where there is no primary production (compare with nitrate profiles). This process is also required to bring enough phosphorus down to the sediment for release to the deep hypolimnion by mineralization. Finally, the variable stoichiometry of primary production is required to model the nitrate depletion in the epilimnion.

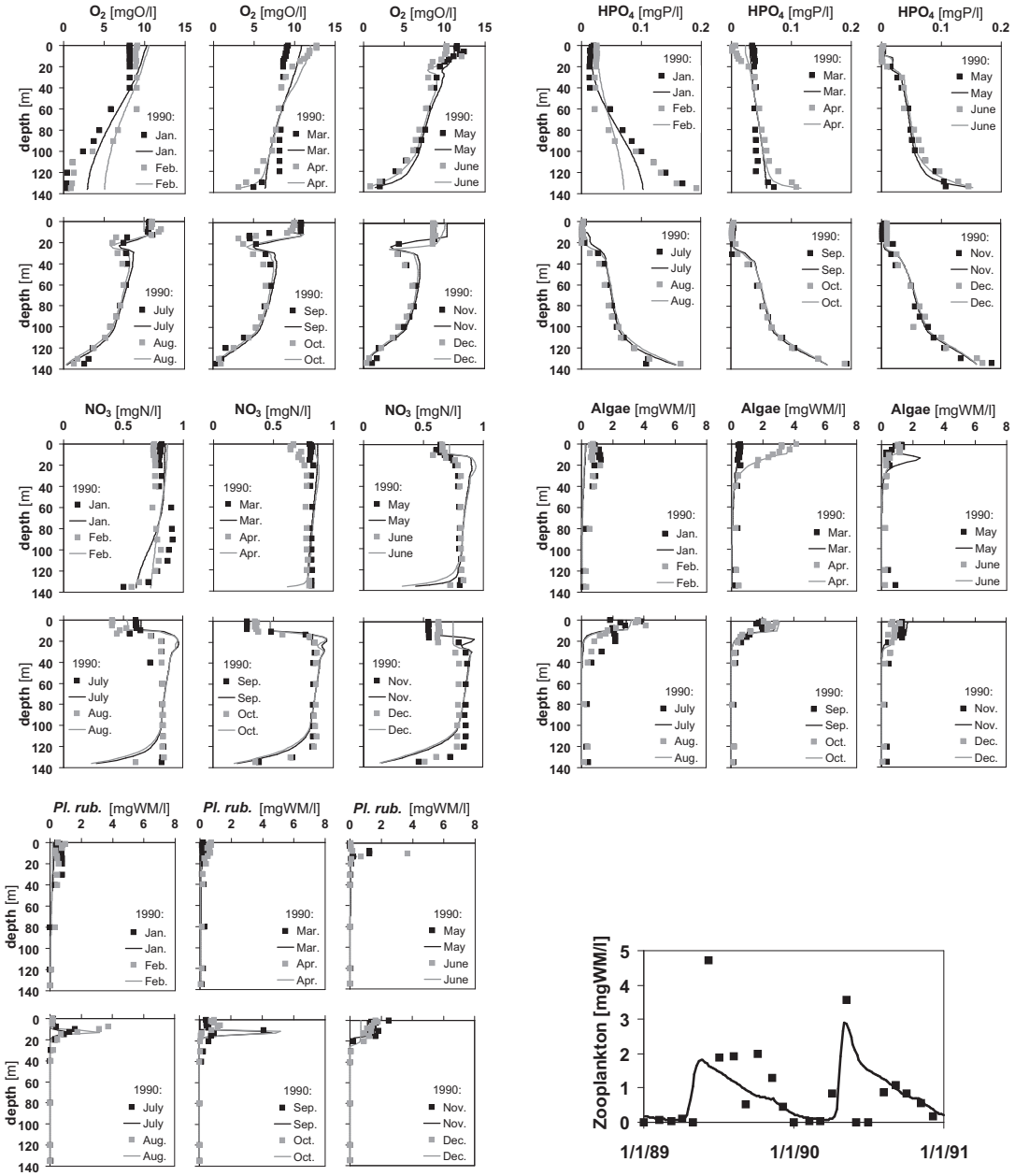

Figure 13.1: Spatial profiles of dissolved oxygen (top left), phosphate (top right), nitrate (middle left), algae without oscillatoria rubescens (middle right), and oscillatoria rubescenc (bottom left) in Lake Zurich in the year 1990 and time series of zooplankton in the epilimnion over the years 1989 and 1990 (bottom right). Lines indicate simulation results, dots measurements (Omlin et al. 2001).

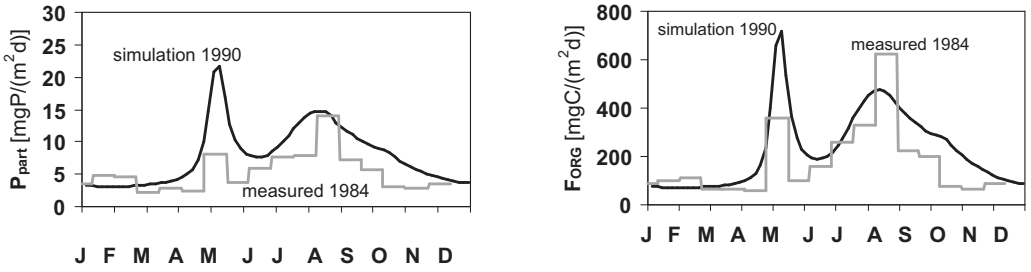

Figure 13.2: Calculated particulate organic carbon flux (left) and particulate phosphorus flux (right) in 130 m depth in Lake Zurich. Lines indicate simulation results for 1990 by Omlin et al. (2001); histograms measurements by Sigg et al. (1987) from 1984.

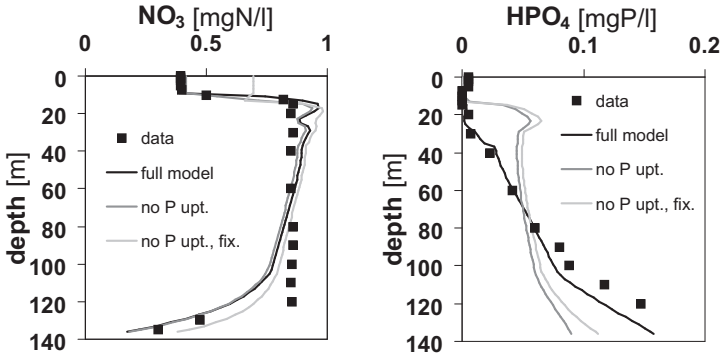

Figure 13.3: Comparison of the resulting phosphate and nitrate profiles in September 1989 for the full model (black lines), for a model with omission of the phosphate uptake process on sinking particles (dark grey lines), and for a model with omission of the phosphate uptake process and with a constant (Redfield) stoichiometry of algal growth (light grey lines). From Omlin et al. (2001).

13.2.1.2 Extension to Three Lakes of Different Trophic State

The model described in the previous subsection was later extended to describe three lakes of different trophic state (Mieleitner and Reichert, 2006). With only minor modifications and only very few lake specific parameter values, the model could be calibrated to the three lakes Walensee (oligotrophic), Lake Zurich (mesotrophic) and Greifensee (eutrophic) shown in Figure 13.4.

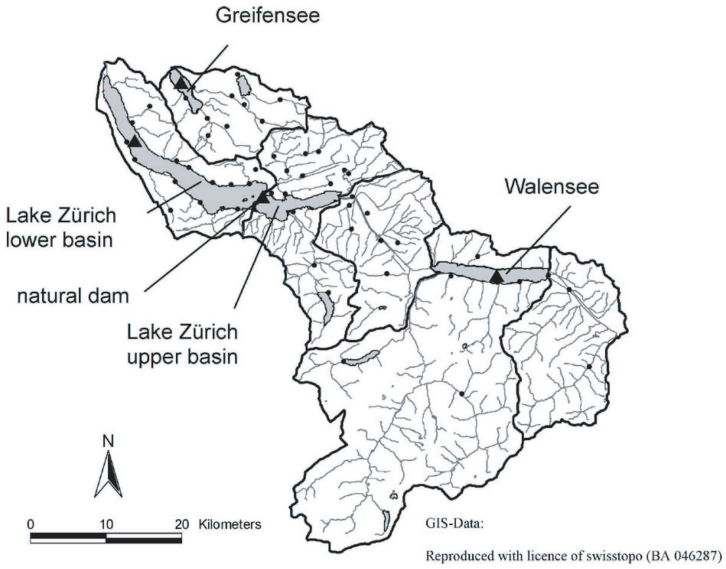

Figure 13.4: Lakes, watersheds, rivers, measurement sites (triangles) and waste water treatment plants (dots).

Figure 13.5 shows some results for all three lakes.

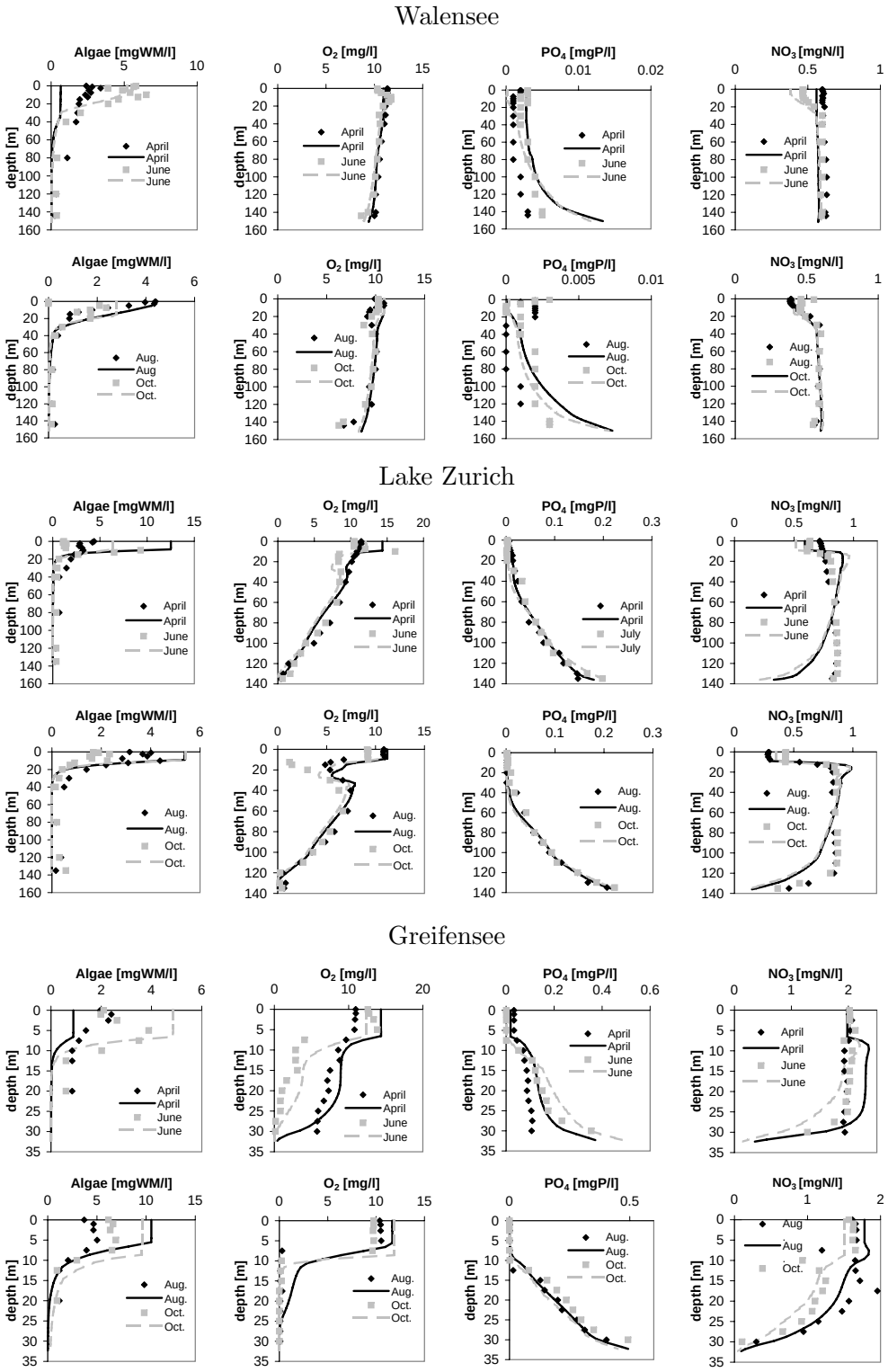

Figure 13.5: Examples of measured (dots) and modelled (lines) profiles for the year 1989 from Walensee (top), Lake Zurich (middle), and Greifensee (bottom). From Mieleitner and Reichert (2006).

13.2.1.3 Long-Term Simulation

It is of particular interest, if a model is able to follow long-term plankton and nutrient dynamics, in particular during a phase of changing inputs to the lakes. The model BELAMO described in the previous sections was used for long-term simulations of the three lakes Lake Zurich, Greifensee and Walensee (Dietzel et al., 2013). Figure 13.6 shows the input loading of bioavailable nitrogen and phosphorus during the simulation period. Only

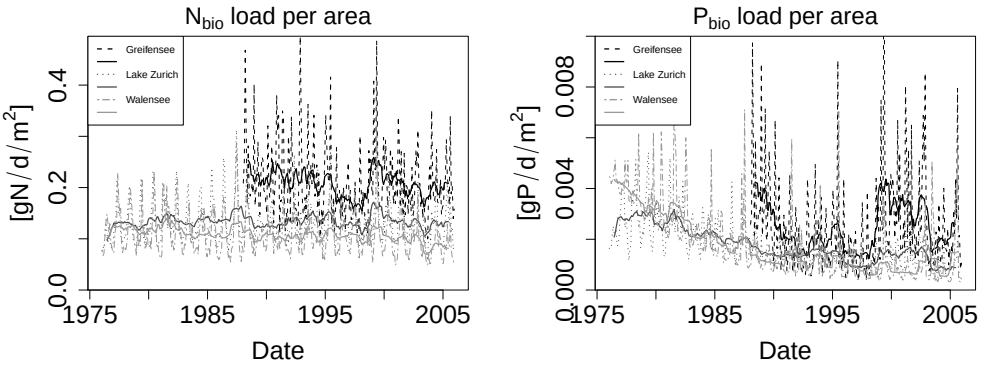

Figure 13.6: Changes in input loding of bioavailable nitrogen and phposphorus into the lakes. Dashed, dotted and dash-dotted lines indicate measured input data, bold lines their moving averages over 12 months. (Dietzel et al., 2013).

observed data up to ten years before the end of the simulations was used for model calibration, data of the last ten years was used for model validation. Figures 13.7, 13.8 and 13.9 show the results of these simulations. The results indicate that the significant reduction in phosphorus turnover did not to the same degree lead to a reduction in phytoplankton concentrations. This demonstrates that it is difficult to learn about nutrient turnover from concentrations. The uncertainty analysis demonstrates that despite the relatively simple model that is constrained through mass balances of the nutrients, prediction uncertainty is very high.

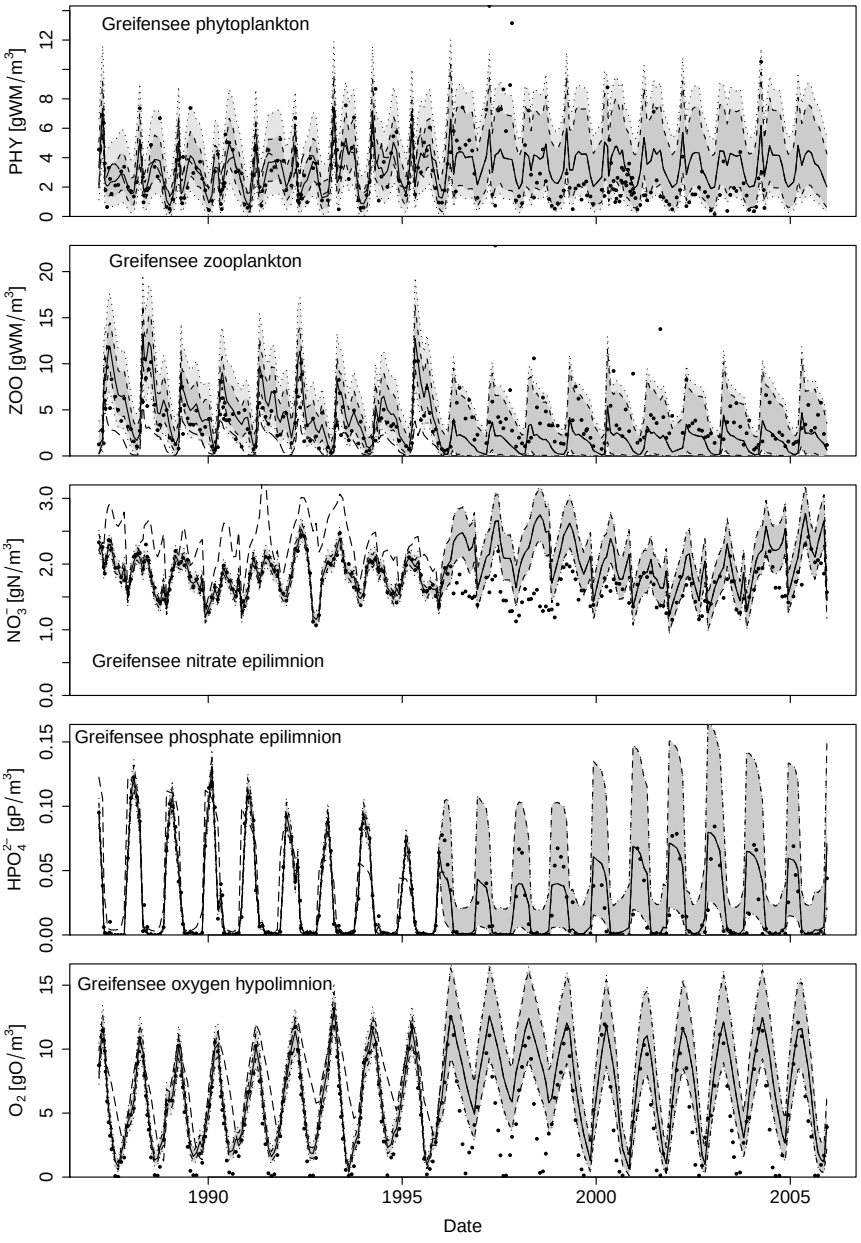

Figure 13.7: Phytoplankton (entire lake), zooplankton (entire lake), nitrate (epilimnion), phosphate (epilimnion) and oxygen (hypolimnion) concentrations in Greifensee. Data points (markers), output of the deterministic model (long-dashed), median (solid) and 95% credibility bounds (dark grey area with dashed boundaries) of bias-corrected output and median (solid; same as for bias-corrected output) and 95% credibility bounds (dark and light grey areas with dotted boundaries) of predictions of new observations (including observation error) (Dietzel et al., 2013).

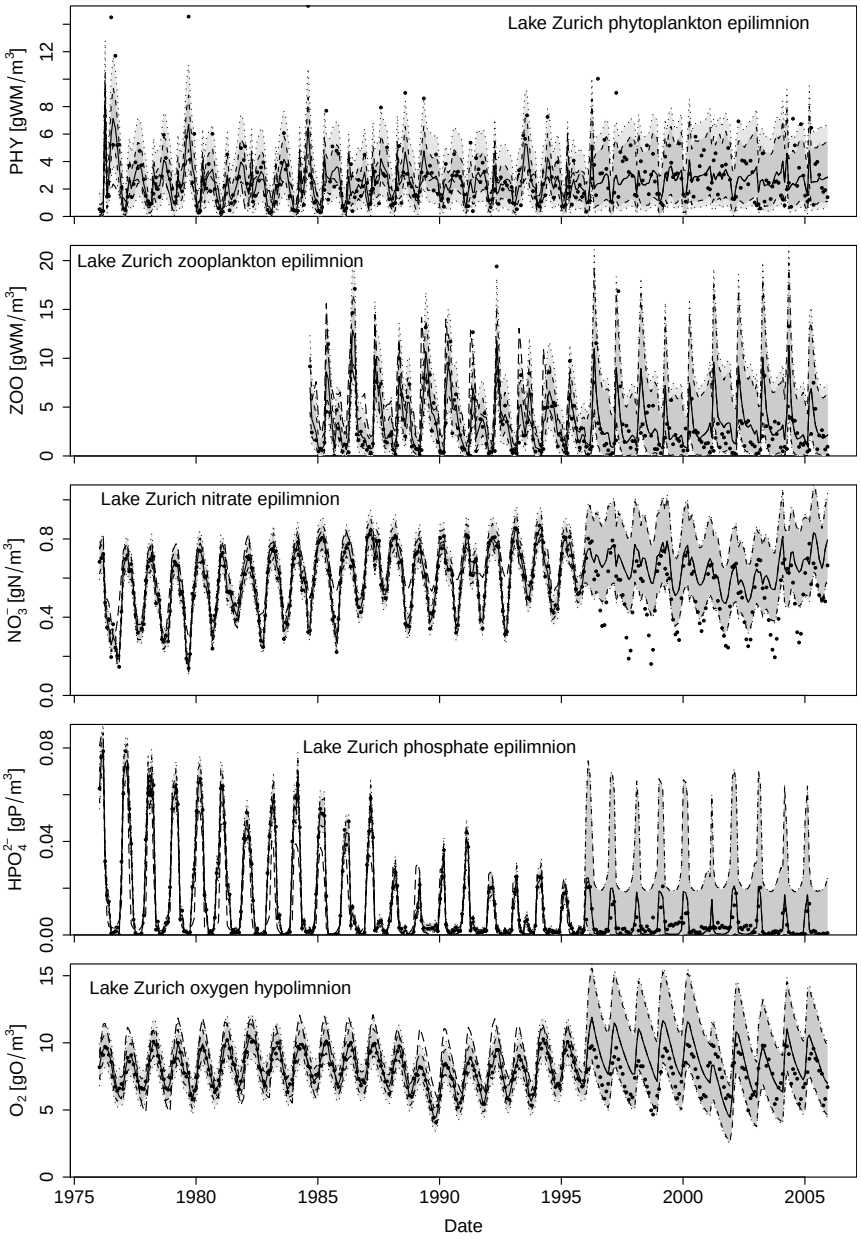

Figure 13.8: Phytoplankton, zooplankton, nitrate and phosphate concentrations in the epilimnion and oxygen concentrations in the hypolimnion of Lake Zurich. Data points (markers), output of the deterministic model (long-dashed), median (solid) and 95% credibility bounds (dark grey area with dashed boundaries) of bias-corrected output and median (solid; same as for bias-corrected output) and 95% credibility bounds (dark and light grey areas with dotted boundaries) of predictions of new observations (including observation error) (Dietzel et al., 2013).

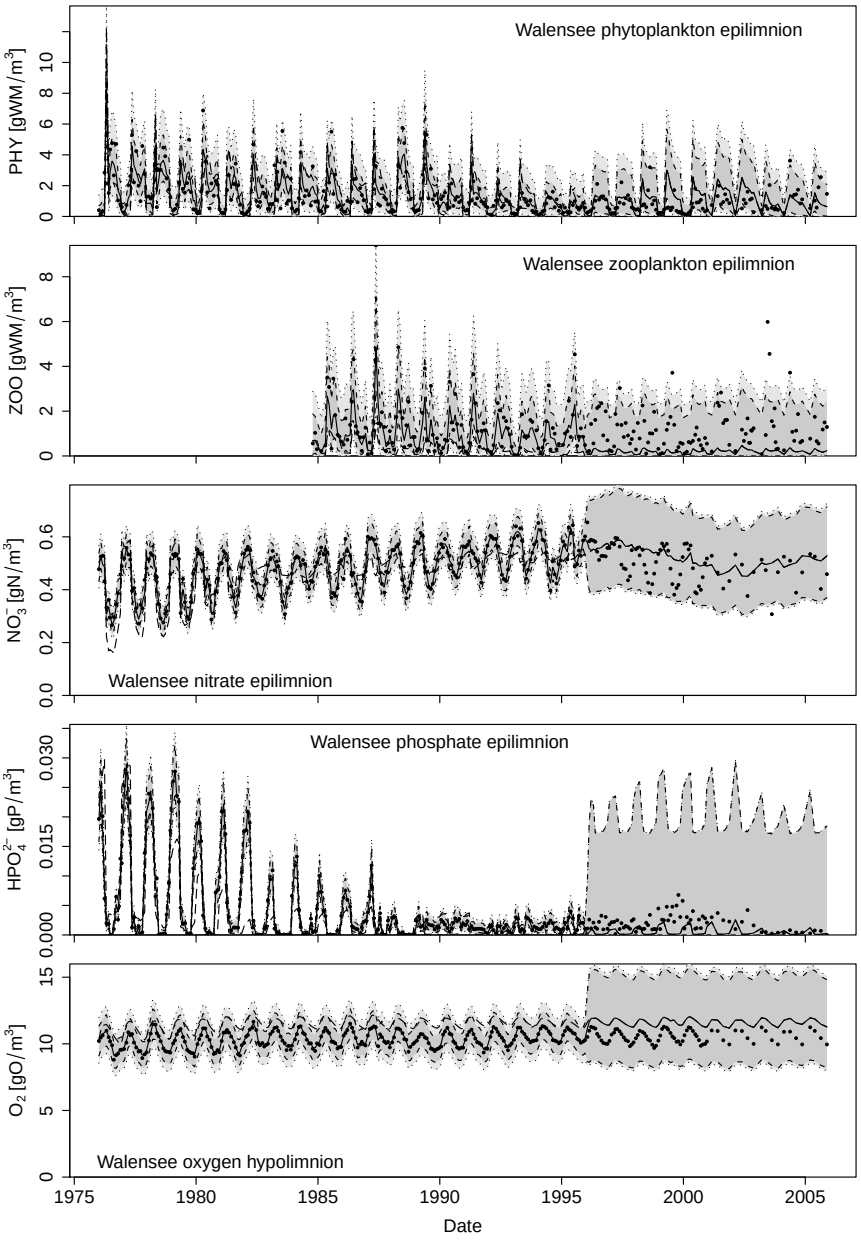

Figure 13.9: Phytoplankton, zooplankton, nitrate and phosphate concentrations in the epilimnion and oxygen concentrations in the hypolimnion of Walensee. Data points (markers), output of the deterministic model (long-dashed), median (solid) and 95% credibility bounds (dark grey area with dashed boundaries) of bias-corrected output and median (solid; same as for bias-corrected output) and 95% credibility bounds (dark and light grey areas with dotted boundaries) of predictions of new observations (including observation error) (Dietzel et al., 2013).

13.2.2 Modelling Benthos Community Dynamics in the River Sihl

The emphasis of this manuscript is on the mathematical formulation of processes in aquatic ecosystems and interpretation of the combined effect of these processes interacting in an ecosystem (model). There was less emphasis on how to use data for model calibration, how to statistically assess model performance, and how to estimate prediction uncertainty (chapter 2 provides a very brief summary). These topics are treated in a separate manuscript as they are not specific to aquatic ecosystem models (Reichert, 2007). Nevertheless, this case study provides the opportunity to demonstrate how Bayesian techniques can be used to update prior knowledge on model parameters based on observed data from the aquatic ecosystem.

Figure 13.10 summarizes the methodology applied in this study (Schuwirth et al., 2008). We start with the **design of the model** according to basic natural scientific

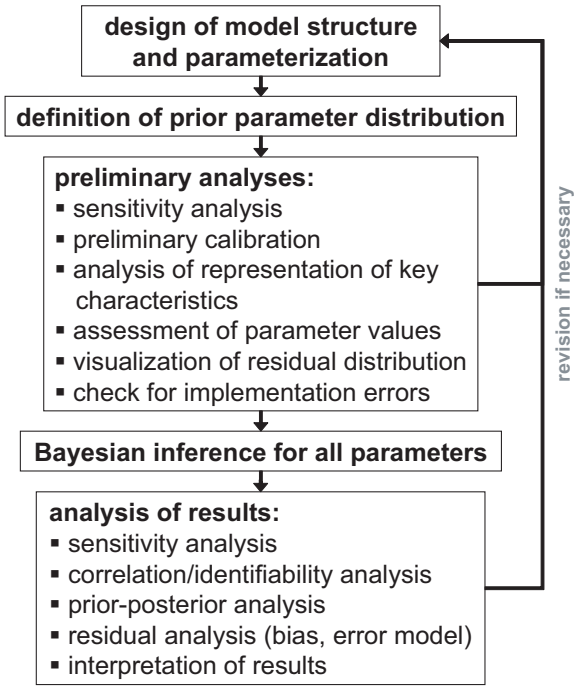

Figure 13.10: Concept of model development applied in Schuwirth et al. 2008.

knowledge. In addition, we summarize prior knowledge about parameter values by the **prior parameter distribution**. Then we perform **preliminary analyses**:

- Sensitivity analysis supports our understanding of the importance of parameters on model results.
- Preliminary calibration either done manually or with empirical loss functions can be used to find adequate model parameter values.
- The analysis of representation of key characteristics of the data by the model makes it possible to obtain a first qualitative assessment of model performance. This has to be done after preliminary calibration to distinguish model deficits from poor choice of parameter values.

- The values of model parameters that have a mechanistic interpretation must be assessed for being within a meaningful range.
- The distribution of residuals can give us hints for the formulation of a probabilistic error model.
- Finally, these preliminary analyses can uncover model implementation errors.

If significant model deficits have been identified during these premliminary analyses, the model structure needs to be revised. Otherwise, the mechanistic model can be combined with an error model that characterizes the measurement process and may also parameterize remaining model deficits. This probabilistic model can then be used for updating the prior parameter distribution with the aid of observed data to a posterior distribution by **Bayesian inference**. This posterior distribution combines prior knowledge with information gained from the data. Finally, an **analysis of the results** with respect to identifiability, gain of information, fulfilment of statistical assumptions, and interpretation of the results helps us assess the reliability of the model.

Figure 13.11 shows the structure of the benthos community model. The model dis-

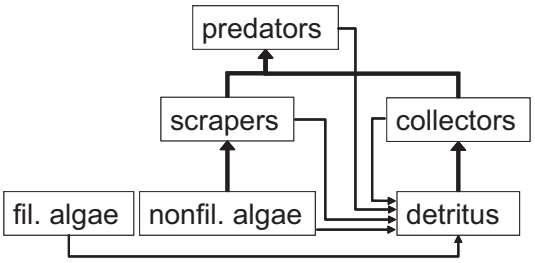

Figure 13.11: Structure of the benthos community dynamics model used by Schuwirth et al. (2008).

tinguishes filamentous and non-filamentous (benthic) algae, three functional groups of benthic invertebrates (scrapers, collectors and predators), and detritus. Tables 13.4 and 13.5 show the stoichiometry and process rates of the model.

Figure 13.12 shows the results of the posterior simulation. The residual plots shown in Figure 13.13 demonstrate the approximate fulfillment of the statistical assumptions made for model formulation. This indicates that we can trust the model results. Figure 13.14 shows a comparison of the marginals of the prior and posterior distributions of the model parameters. This diagram provides an overview of what we could learn about individual parameter values from the data.

	Functional groups of organisms and substances						
Processes	X_{ALGfil}	$X_{\mathrm{ALGnonfil}}$	X_{Scra}	X_{Pred}	X_{Coll}	X_{SedOP}	Rates
Colonization of ALGfil	1						$r_{\mathrm{col\ ALGfil}}$
Colonization of ALGnonfil		1					$r_{\mathrm{col\ ALGnonfil}}$
Colonization of Scra			1				$r_{\mathrm{col\ Scra}}$
Colonization of Pred				1			$r_{\mathrm{col\ Pred}}$
Colonization of Coll					1		$r_{\mathrm{col\ Coll}}$
Growth of ALGfil	1						$r_{\mathrm{gro\ ALGfil}}$
Growth of ALGnonfil		1					$r_{\mathrm{gro\ ALGnonfil}}$
Growth of Scra on ALGnonfil		$-1/Y_{\mathrm{Scra}}$	1				$r_{\mathrm{gro\ Scra}}$
Growth of Pred on Scra			$-1/Y_{\mathrm{Pred}}$	1			$r_{\mathrm{gro\ Pred\ Scra}}$
Growth of Pred on Coll				1	$-1/Y_{\mathrm{Pred}}$		$r_{\mathrm{gro\ Pred\ Coll}}$
Growth of Coll on SedOP					1	$-1/Y_{\mathrm{Coll}}$	$r_{\mathrm{gro\ Coll\ SedOP}}$
Detachment of ALGfil	−1						$r_{\mathrm{det\ ALGfil}}$
Detachment of ALGnonfil		−1					$r_{\mathrm{det\ ALGnonfil}}$
Drift of Scra			−1				$r_{\mathrm{det\ Scra}}$
Drift of Pred				−1			$r_{\mathrm{det\ Pred}}$
Drift of Coll					−1		$r_{\mathrm{det\ Coll}}$
Resuspension of SedOP						−1	$r_{\mathrm{det\ SedOP}}$
Death of ALGfil	−1					1	$r_{\mathrm{death\ ALGfil}}$
Death of ALGnonfil		−1				1	$r_{\mathrm{death\ ALGnonfil}}$
Death of Scra			−1			1	$r_{\mathrm{death\ Scra}}$
Death of Pred				−1		1	$r_{\mathrm{death\ Pred}}$
Death of Coll					−1	1	$r_{\mathrm{death\ Coll}}$

Table 13.4: Process stoichiometry of the benthos community dynamics model by Schuwirth et al. 2008.

Process	Symbol	Rate expression
Growth of filamentous algae	$r_{\mathrm{gro\ ALGfil}}$	$k_{\mathrm{gro\,ALGfil}} \cdot \mathrm{e}^{\beta_{\mathrm{Alg}}(T-T_0)} \cdot \frac{K_{\mathrm{ALGfil\,shadow}}}{K_{\mathrm{ALGfil\,shadow}} + X_{\mathrm{ALGfil}}} \cdot \min\left(\frac{S_{\mathrm{PO_4}}}{K_{\mathrm{gro\,ALG\,P}} + S_{\mathrm{PO_4}}}, \frac{S_{\mathrm{NO_3}} + S_{\mathrm{NH_4}}}{K_{\mathrm{gro\,ALG\,N}} + S_{\mathrm{NO_3}} + S_{\mathrm{NH_4}}}\right) \cdot X_{\mathrm{ALGfil}}$
Growth of non-filamentous algae	$r_{\mathrm{gro\ ALGnonfil}}$	$k_{\mathrm{gro\,ALGnonfil}} \cdot \mathrm{e}^{\beta_{\mathrm{Alg}}(T-T_0)} \cdot \frac{K_{\mathrm{ALGnonfil\,shadow}}}{K_{\mathrm{ALGnonfil\,shadow}} + X_{\mathrm{ALGnonfil}}} \cdot \mathrm{e}^{-k_{\mathrm{ALG\,shadow}} \cdot X_{\mathrm{ALGfil}}} \cdot \min\left(\frac{S_{\mathrm{PO_4}}}{K_{\mathrm{gro\,ALG\,P}} + S_{\mathrm{PO_4}}}, \frac{S_{\mathrm{NO_3}} + S_{\mathrm{NH_4}}}{K_{\mathrm{gro\,ALG\,N}} + S_{\mathrm{NO_3}} + S_{\mathrm{NH_4}}}\right) \cdot X_{\mathrm{ALGnonfil}}$
Growth of invertebrates i on their food source f	$r_{\mathrm{gro}\ i}$	$k_{\mathrm{gro}\ i} \cdot \mathrm{e}^{\beta_i(T-T_0)} \cdot \frac{X_f}{K_{\mathrm{gro}\ i} + X_f} \cdot X_i$ with i: scrapers, collectors, predators with f: non-filamentous algae, sedimented organic particles, scrapers, collectors
Colonization	$r_{\mathrm{col}\ i}$	$c_{\mathrm{col}\ i}$ with i: filamentous algae, non-filamentous algae, scrapers, collectors, predators
Catastrophic loss/resuspension	$r_{\mathrm{det}\ i}$	$\begin{cases} 0 & \text{for } Q < Q_{\mathrm{crit}} \\ c_{\mathrm{det}\ i} \cdot X_i \cdot (Q - Q_{\mathrm{crit}})^2 & \text{for } Q > Q_{\mathrm{crit}} \end{cases}$ with i: filamentous algae, non-filamentous algae, scrapers, collectors, predators, sedimented organic particles
Death	$r_{\mathrm{death}\ i}$	$k_{\mathrm{death}\ i} \cdot X_i$ with i: filamentous algae, non-filamentous algae, scrapers, collectors, predators, sedimented organic particles

Table 13.5: Process rates of the benthos community dynamics model by Schuwirth et al. 2008.

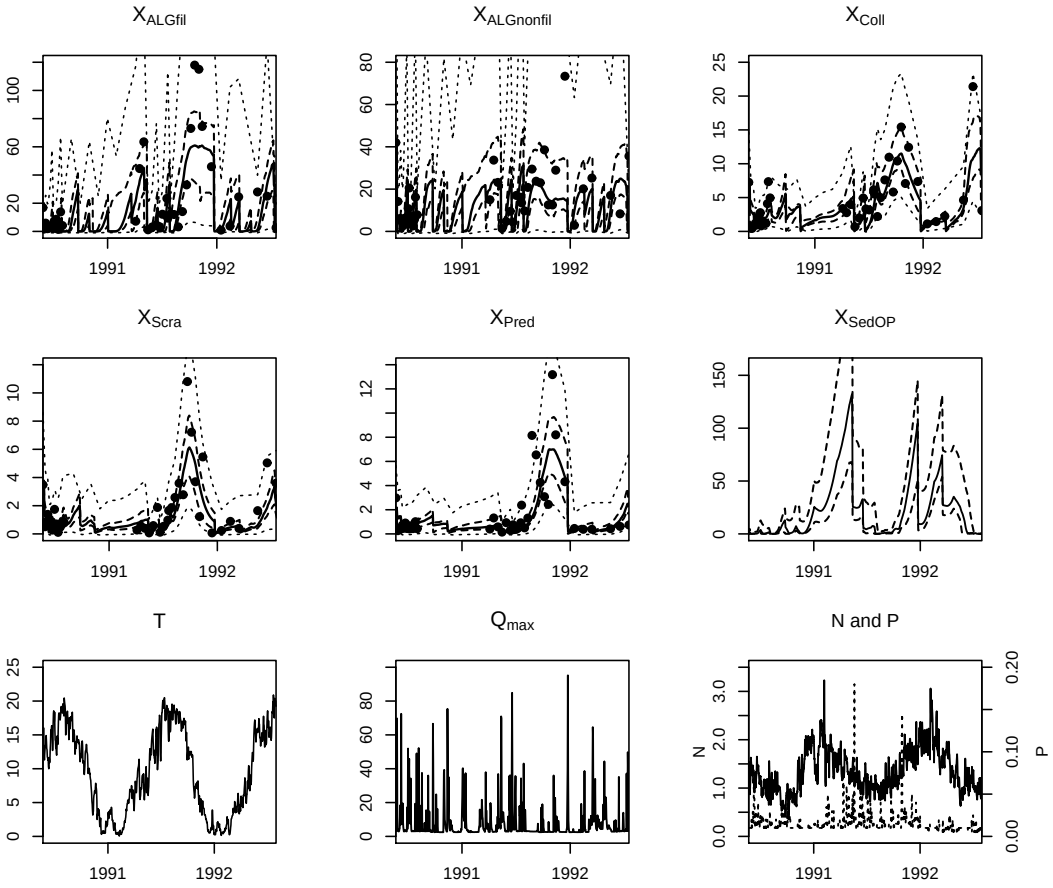

Figure 13.12: Comparison of measured data (markers) and simulation results corresponding to the parameter values at the maximum of the posterior distribution (solid lines) with 2.5% and 97.5% quantiles covering the 95% prediction interval (dashed lines) of all six state variables (in gAFDM/m^2 for algae and gDM/m^2 for invertebrates and sedimented organic particles); the interval bounded by long dashed lines represents the uncertainty in model results due to the uncertainty in the model parameters; the interval bounded by short dashed lines includes model structure uncertainty, input uncertainty and measurement error, too; time series of measured input parameters (water temperature, T, in degC, discharge (instantaneous maximum daily flow), $Q_{\max}$, in m^3/s, and nutrients, N (solid line) in mgN/L and P (dashed line) in mgP/L. From Schuwirth et al. (2008).

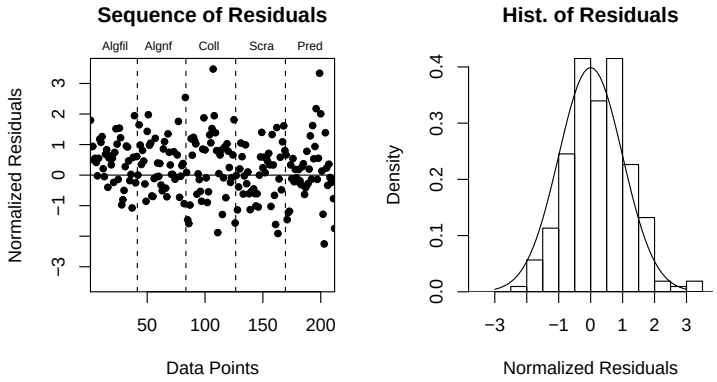

Figure 13.13: Sequence and histogram of the normalized residuals of transformed observations and model results. From Schuwirth et al. (2008).

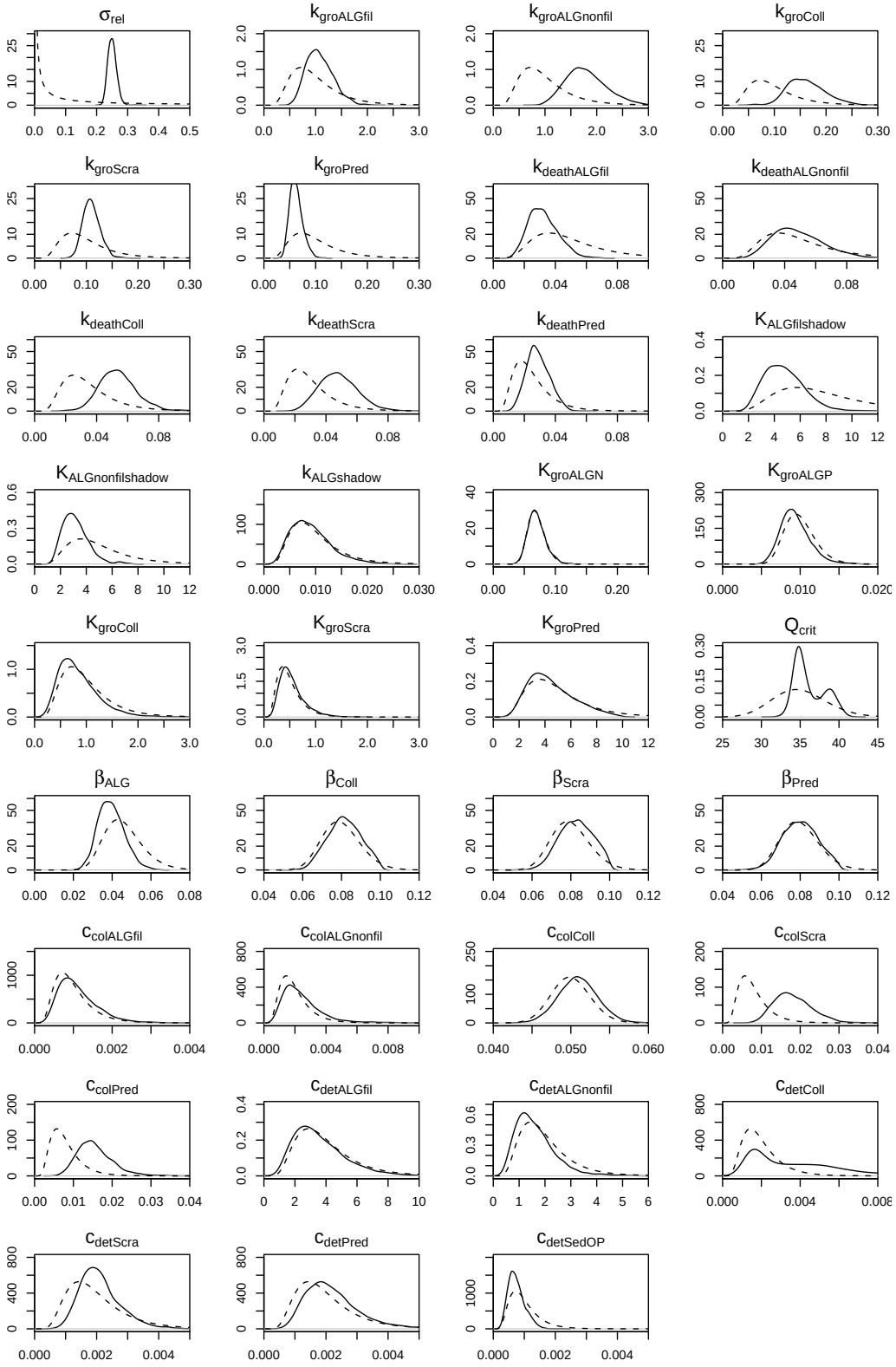

Figure 13.14: Comparison of prior (dashed line) and posterior (solid line) marginal distributions of the parameters. From Schuwirth et al. (2008).

13.2.3 Modelling Taxonomic Composition of Steam Benthos Communities

The model Streambugs combines the concepts of the metabolic theory of ecology (see section 12.2.6) with ecological trait information of potentially occurring taxa to predict occurrence patterns of macroinvertebrate taxa in streams at specific sites. It uses trait information about the susceptibility of taxa to nutrient and micropollutant concentrations and their preferences regarding flow velocity, temperature and substrate conditions. (Schuwirth and Reichert, 2013).

Fig. 13.15 shows the dependence of modelled processes that influence the biomass of each taxon (growth, respiration, death) on taxon requirements (e.g. regarding habitat and water quality conditions), environmental conditions, and biotic interactions (predation and competition for food).

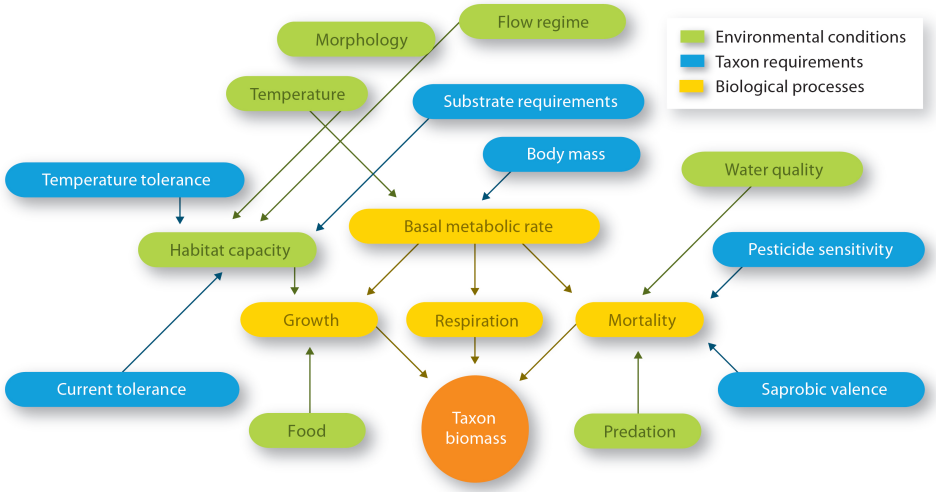

Figure 13.15: Scheme of the model Streambugs (Schuwirth and Reichert, 2012).

Fig. 13.16 shows the occurrence pattern of food webs predicted by this model, and for comparative purposes, the observed taxa. Despite the relatively rough approach that ignors life stages of taxa and individual variablity, the basic features of the observed occurrence pattern could be reproduced by this model.

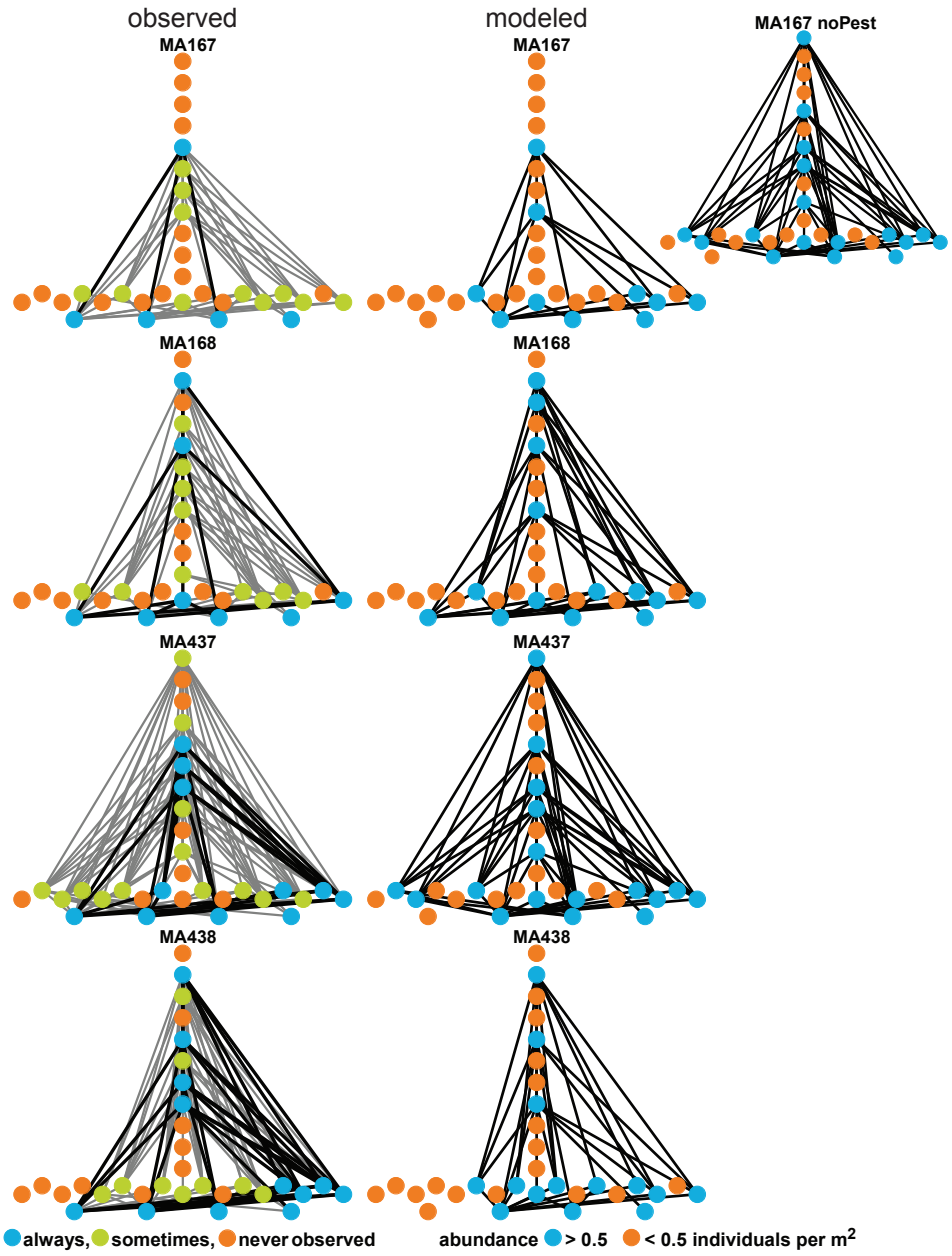

Figure 13.16: Observed taxa and modelled food webs at four sites in the Mönchaltorfer Aa catchment (Schuwirth and Reichert, 2013).

Part VI

Appendix

Chapter 14

Important Univariate Probability Distributions

In this appendix a summary is given of properties and parameters of the univariabe probability distributions most frequently used in environmental modelling. More complete overviews of commonly used probability distributions can be found in the literature (Evans et al., 2000).

14.1 Uniform Distribution

The uniform distribution is often used to describe lack of knowledge about a position variable. It is characterized by its minimum and maximum which bound the range of the distribution. The probability density is constant between minimum and maximum and zero below the minimum and above the maximum. Consequently, the distribution function increases linearly from zero at the minimum to unity at the maximum (see Fig. 14.1).

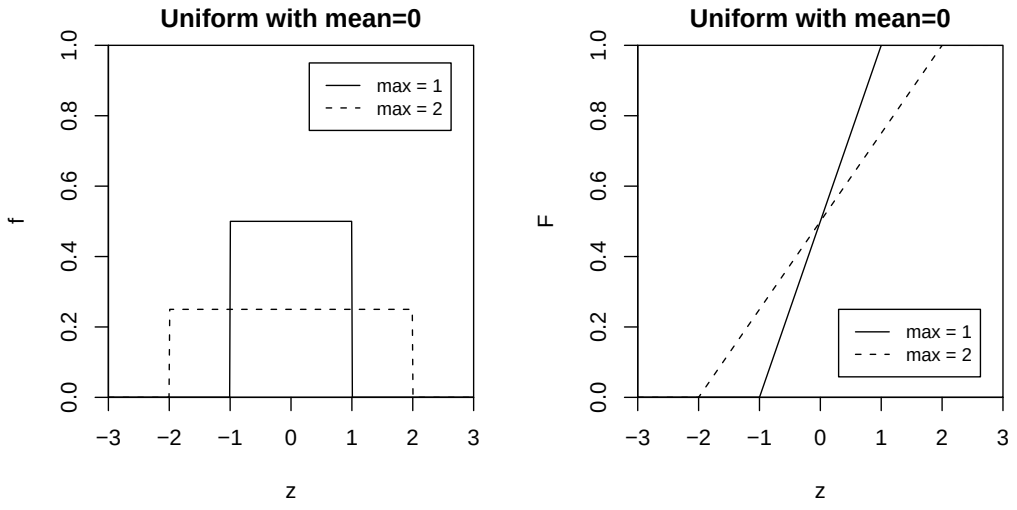

Figure 14.1: Probability densities and distribution functions of univariate uniform distributions.

A uniform random variable

$$Z \sim \mathrm{U}(z_{\min}, z_{\max}) \tag{14.1}$$

is characterized by its minimum, $z_{\min}$, and its maximum, $z_{\max}$, which characterize the range of the distribution. They must fulfill the condition

$$z_{\min} < z_{\max} \quad . \tag{14.2}$$

The probability density of the uniform distribution is given by

$$f_{\mathrm{U}(z_{\min}, z_{\max})}(z) = \begin{cases} \dfrac{1}{z_{\max} - z_{\min}} & \text{for } z \in [z_{\min}, z_{\max}] \\ 0 & \text{otherwise} \end{cases} \quad . \tag{14.3}$$

The expected value, the median and the standard deviation are given by the following expressions, respectively:

$$\mathrm{E}\big[\mathrm{U}(z_{\min}, z_{\max})\big] = \frac{z_{\min} + z_{\max}}{2} \quad , \tag{14.4}$$

$$\mathrm{Med}\big[\mathrm{U}(z_{\min}, z_{\max})\big] = \frac{z_{\min} + z_{\max}}{2} \quad , \tag{14.5}$$

$$\mathrm{SD}\big[\mathrm{U}(z_{\min}, z_{\max})\big] = \frac{z_{\max} - z_{\min}}{2\sqrt{3}} \quad . \tag{14.6}$$

Of special importance is the uniform distribution in the unit interval $[0, 1]$, $\mathrm{U}(0, 1)$, as the random variable with this distribution is the basis for constructing other random variables through transformation.

14.2 Normal Distribution

The central limit theorem of probability theory states that an appropriately scaled sum of any identical and independent random variables with finite variance tends to a normally distributed random variable when the number of terms in the sum tends to infinity. More precisely, if $\{X_i\}$ are independent and identically distributed random variables with mean μ and (finite) standard deviation σ, then

$$\lim_{n \to \infty} \frac{\sum_{i=1}^{n} (X_i - \mu)}{\sqrt{n}\, \sigma} \sim \mathrm{N}(0, 1) \tag{14.7}$$

where $\mathrm{N}(0, 1)$ is the standard Normal distribution (Normal distribution with mean equal to zero and standard deviation equal to unity). This makes the normal distribution to a natural choice for describing quantities that are sums of many additive components. This property and its mathematical convenience is the basis of the importance of the Normal distribution in all fields of statistics. The normal distribution is symmetrical around its mean and extends to infinity in the positive and negative directions (see Fig. 14.2).

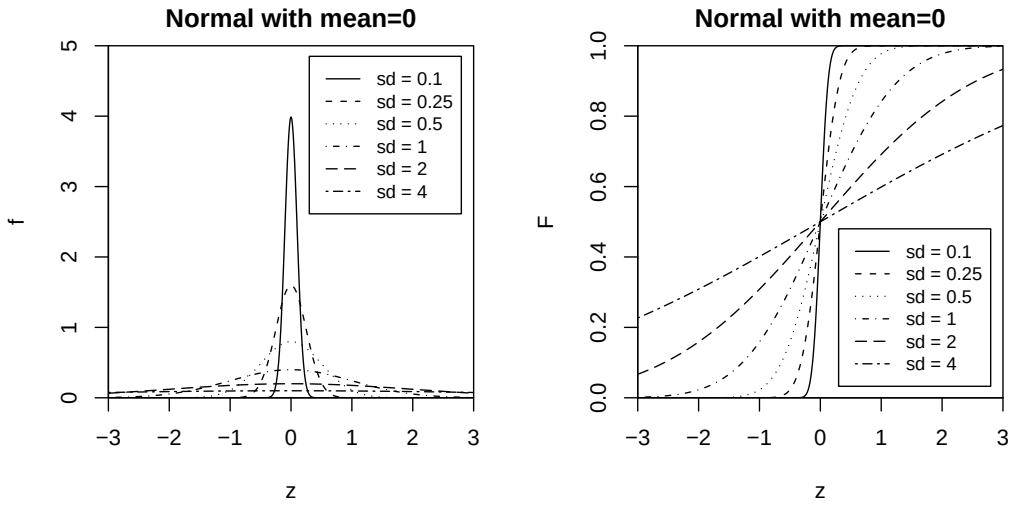

Figure 14.2: Probability densities and distribution functions of univariate normal distributions.

A normally distributed random variable

$$Z \sim \mathrm{N}(\mu, \sigma) \tag{14.8}$$

is characterized by its mean, μ, and its standard deviation, σ. The standard deviation must be positive:

$$\sigma > 0 \quad . \tag{14.9}$$

The probability density of the normal distribution is given by

$$f_{\mathrm{N}(\mu,\sigma)}(z) = \frac{1}{\sqrt{2\pi}} \frac{1}{\sigma} \exp\left(-\frac{1}{2} \frac{(z-\mu)^2}{\sigma^2}\right) \tag{14.10}$$

The expected value, the mode, the median, and the standard deviation are given by the following expressions, respectively:

$$\mathrm{E}\big[\mathrm{N}(\mu, \sigma)\big] = \mu \quad , \tag{14.11}$$

$$\mathrm{Mode}\big[\mathrm{N}(\mu, \sigma)\big] = \mu \quad , \tag{14.12}$$

$$\mathrm{Med}\big[\mathrm{N}(\mu, \sigma)\big] = \mu \quad , \tag{14.13}$$

$$\mathrm{SD}\big[\mathrm{N}(\mu, \sigma)\big] = \sigma \quad . \tag{14.14}$$

Of special importance is the **standard Normal distribution** with mean zero and standard deviation unity, $\mathrm{N}(0, 1)$.

14.3 Lognormal Distribution

If the random variable X is normally distributed, then

$$Z = \exp(X) \quad , \quad X \sim \mathrm{N}(m, s) \tag{14.15}$$

is lognormally distributed. The range of the lognormal distribution is limited to nonnegative numbers. If the standard deviation is not small compared to its expected value, it has a significant asymmetry by extending further to larger than to smaller values than the mean (see Fig. 14.3). These properties make the lognormal distribution in many cases a reasonable description of highly uncertain positive variables for which the normal distribution cannot be used because of the nonzero probability for negative numbers.

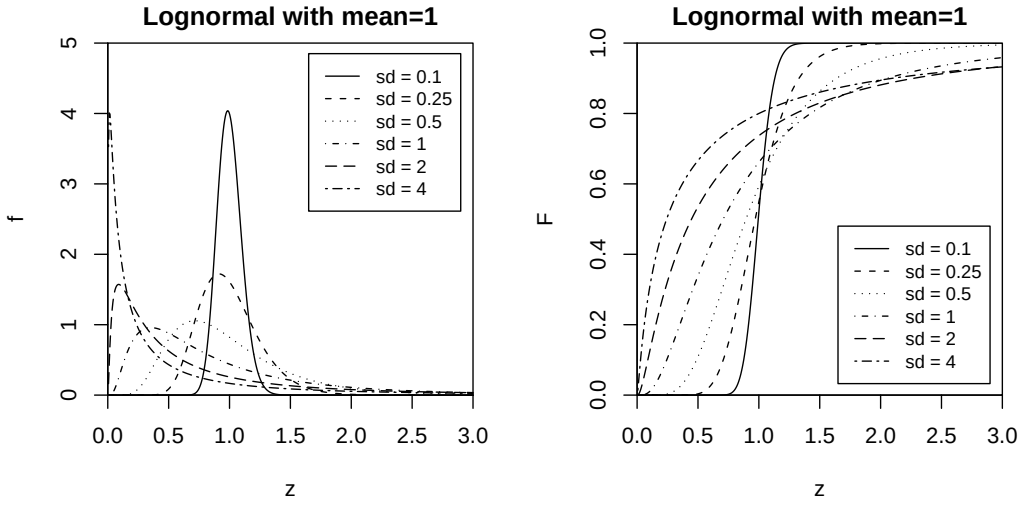

Figure 14.3: Probability densities and distribution functions of univariate lognormal distributions.

A lognormally distributed random variable

$$Z \sim \mathrm{LN}(\mu, \sigma) \tag{14.16}$$

can be characterized by its mean, μ, and its standard deviation, σ. Nevertheless, a lognormally distributed random variabe is often characterized by the mean and standard deviation of its logarithm (variable X in the equation given above). Mean and standard deviation of a lognormally distributed random variable must be positive:

$$\mu > 0 \quad , \quad \sigma > 0 \qquad . \tag{14.17}$$

The probability density of the lognormal distribution is given as

$$f_{\mathrm{LN}(\mu,\sigma)}(z) = \begin{cases} \dfrac{1}{\sqrt{2\pi}} \dfrac{1}{sz} \exp\left(-\dfrac{1}{2} \dfrac{\left(\log\left(\dfrac{z}{\mu} \right) + \dfrac{s^2}{2} \right)^2}{s^2} \right) & \text{for } z > 0 \\ 0 & \text{for } z \leq 0 \end{cases} \tag{14.18}$$

with

$$s = \sqrt{\log\left(1 + \frac{\sigma^2}{\mu^2}\right)} \tag{14.19}$$

This is the preferred representation of the lognormal distribution as it makes evident that the units of the involved variables are consistent. Because the lognormal distribution is often characterized by the mean, m, and the standard deviation, s of the normal distribution $X = \log(Z)$, the following form is often used:

$$f_{\mathrm{LN}(m,s)}(z) = \begin{cases} \dfrac{1}{\sqrt{2\pi}} \dfrac{1}{sz} \exp\left(-\dfrac{1}{2} \dfrac{\big(\log(z) - m\big)^2}{s^2}\right) & \text{for } z > 0 \\ 0 & \text{for } z \leq 0 \end{cases} \tag{14.20}$$

with

$$s = \sqrt{\log\left(1 + \frac{\sigma^2}{\mu^2}\right)} \quad , \quad m = \log(\mu) - \frac{s^2}{2} \quad . \tag{14.21}$$

From the point of view of units of the involved variables, this form is less satisfying, as m is an expression that is not consistent with respect to its units. This inconsistency does not cause a problem, because m is only used in the expression $\log(z) - m = \log(z) - \log(\mu) + s^2/2 = \log(z/\mu) + s^2/2$, which is consistent (all terms of the last expression are non-dimensional).

The expected value, the mode, the median, the standard deviation, and the geometric standard deviation are given by the following expressions, respectively:

$$\mathrm{E}\big[\mathrm{LN}(\mu, \sigma)\big] = \mu \quad , \tag{14.22}$$

$$\mathrm{Mode}\big[\mathrm{LN}(\mu, \sigma)\big] = \frac{\mu}{\left(1 + \dfrac{\sigma^2}{\mu^2}\right)^{\frac{3}{2}}} \quad , \tag{14.23}$$

$$\mathrm{Med}\big[\mathrm{LN}(\mu, \sigma)\big] = \frac{\mu}{\sqrt{1 + \dfrac{\sigma^2}{\mu^2}}} \quad , \tag{14.24}$$

$$\mathrm{SD}\big[\mathrm{LN}(\mu, \sigma)\big] = \sigma \quad , \tag{14.25}$$

$$\mathrm{GeoSD}\big[\mathrm{LN}(\mu, \sigma)\big] = \exp\left(\sqrt{\log\left(1 + \frac{\sigma^2}{\mu^2}\right)}\right) \quad . \tag{14.26}$$

Note, however, that the expressions for the transformation of means are not consistent with respect to the units (see comment above).

Because a lognormal random variable, Z, is often characterized by mean and standard deviation of its normally distributed logarithm, $X = \log(Z)$, $m = \mathrm{E}\big[\log\big(\mathrm{LN}(\mu, \sigma)\big)\big]$, $s = \mathrm{SD}\big[\log\big(\mathrm{LN}(\mu, \sigma)\big)\big]$, we give the conversion formulas between these two parameterizations:

$$\mu = \exp\left(m + \frac{s^2}{2}\right) \quad , \tag{14.27}$$

$$\sigma = \mu\sqrt{\exp\big(s^2\big) - 1} \quad , \tag{14.28}$$

$$m = \log\big(\mu\big) - \frac{s^2}{2} = \log\big(\mu\big) - \frac{1}{2}\log\left(1 + \frac{\sigma^2}{\mu^2}\right) \quad , \tag{14.29}$$

$$s = \sqrt{\log\left(1 + \frac{\sigma^2}{\mu^2}\right)} \quad . \tag{14.30}$$

Chapter 15

Introduction to the R Package `stoichcalc`

15.1 Concepts

R (http://www.r-project.org) is a very powerful publicly available program for data analysis, graphics, and statistics. `stoichcalc` is a (small) R package that implements the general solution of stoichiometric equations described in section 4.3.3 (Reichert and Schuwirth, 2010). The design of the implementation is guided by the criterion of allowing the user a high flexibility with respect to changes in "elementary constituents", substances and processes considered in the model.

15.2 Routines

The `stoichcalc` package consists of three functions. These functions are described in the subsections of this section.

15.2.1 `calc.comp.matrix`

The first routine does not do any calculations, but it provides a convenient way for rebuilding the substance composition matrix $\boldsymbol{\alpha}$ according to equation (4.52) after changes in the set of substances or their composition have been made. When introducing new substances and "elementary constituents" the substance composition matrix, $\boldsymbol{\alpha}$, will change its dimension. In order not to have to redefine substances that have already been defined and do not contain newly introduced "elementary constituents", it is better not to refer to "elementary constituents" in substance composition definitions by indices. Similarly, we should not refer to substances by indices when defining processes. For this reason we define the composition of a substance as a named vector with entries that refer to the names of the "elementary constituents" and the "masses" of the "constituent" contained in one measurement unit of the substance. Then we define a list of substance compositions, `subst.comp`, which contains the substance composition vectors of all substances. As we finally need the composition matrix, we provide the function

```
calc.comp.matrix(subst.comp)                                    (15.1)
```

which takes the list of substance compositions as its argument and returns the composition matrix, $\boldsymbol{\alpha}$, according to equation (4.52).

15.2.2 calc.stoich.basis

The second function is the core routine we need to solve all stoichiometric problems. It calculates the basis of the vector space of stoichiometries that are compatible with a given composition and constraints. To do this, it calculates and returns a basis of the left nullspace of the matrix

$$\mathbf{A} = \begin{pmatrix} \boldsymbol{\alpha} \\ \boldsymbol{\gamma} \end{pmatrix}^{\mathrm{T}} \tag{15.2}$$

where $\boldsymbol{\alpha}$ is a substance composition matrix according to equation (4.52) and $\boldsymbol{\gamma}$ a matrix of coefficients (4.58) of linear constraints (4.57). The call to this function is

```
calc.stoich.basis(alpha,constraints)
```
(15.3)

where `alpha` refers to the composition matrix, $\boldsymbol{\alpha}$, and `constraints` refers to an optional list of linear constraints, $\boldsymbol{\gamma}$.

The composition matrix must contain column names that refer to the names of the substances under consideration. It will usually have been calculated by applying the function `calc.comp.matrix` to a list of substance definitions as described in the previous section. Each constraint in this list of constraints is formulated as a vector which specifies named coefficients of a row of the matrix $\boldsymbol{\gamma}$ according to equation (4.58). Such a vector has only to contain the non-zero elements of the row of $\boldsymbol{\gamma}$. The elements have to be named according to substances specified as column names of the composition matrix $\boldsymbol{\alpha}$. In many cases, a constraint is of the form of a given ratio of two stoichiometric coefficients. In this case, according to equation (4.57), this vector will only have two elements, one being -1 and the other the given ratio of two stoichiometric coefficients. The routine (15.3) constructs a singular value decomposition of the matrix $\tilde{\mathbf{A}}$ which consists of the matrix $\mathbf{A}$ given above made quadratic by extending it by columns containing only elements equal to zero as described in section 4.3.3. The singular value decomposition is then done using the R routine `svd` which is based on the LAPACK routines `DGESVD` and `ZGESVD` (Anderson et al., 1999). The routine (15.3) returns a matrix consisting of all rows of $\tilde{\mathbf{U}}^{\mathrm{T}}$ according to equation (4.62) which correspond to singular values that are zero. This means that the rows of the returned matrix build a basis of the linear space of stoichiometries that are consistent with respect to conservation laws and additional stoichiometric constraints.

15.2.3 calc.stoich.coef

The last routine provides a simpler interface for calculating the unique stoichiometric coefficients of a process once the affected substances, their composition, and the required additional constraints are specified. This function solves equation (4.60)

$$\boldsymbol{\nu}_i \cdot \begin{pmatrix} \boldsymbol{\alpha}_{(i)} \\ \boldsymbol{\gamma}_{(i)} \end{pmatrix}^{\mathrm{T}} = \mathbf{0} \tag{15.4}$$

for the unique row vector $\boldsymbol{\nu}_i$ or returns an error message if this vector is not uniquely defined. In this equation, $\boldsymbol{\alpha}_{(i)}$ is the composition matrix with only the columns corresponding to the substances involved in process i, and $\boldsymbol{\gamma}_{(i)}$ is the matrix of the stoichiometric constraints of process i. The call to this function is

```
calc.stoich.coef(alpha,name,subst,subst.norm,nu.norm,constraints)
```
(15.5)

It requires the following input: `alpha` is the composition matrix, $\boldsymbol{\alpha}$, according to equation (4.52); `name` is the name of the process (used to name the row of returned stoichiometric coefficients to facilitate binding of output rows of different processes to a complete stoichiometric matrix); `subst` is a vector of names of all substances involved in the process (this has to be a subset of the column names of `alpha`), `subst.norm` is the name of the substance that should have a normed stoichiometric coefficient; `nu.norm` is the value of the normed stoichiometric coefficient (usually +1 or -1); and `constraints` is a (possibly empty) list of constraints in the same format as described in section 15.2.2. The routine deletes the columns of the composition matrix of all substances that are not affected by the process, adds the additional stoichiometric constraints, and then calculates the basis of the left nullspace of the matrix $\mathbf{A}$ in equation (4.60). It returns an error message if no consistent process stoichiometry exists (if the left nullspace is empty), the number of additional stoichiometric constraints needed to make the process unique if more than one solution exists (if the dimension of the left nullspace is larger than unity), or the row vector of stoichiometric coefficients of the process if these are unique (if the dimension of the left nullspace is unity). The routine renormalizes the coefficients according to the value specified for one of the coefficients.

15.3 Performing Stoichiometric Calculations with `stoichcalc`

Once installed with the command `install.packages("stoichcalc")`, the package is loaded with the command

```
library(stoichcalc)
```

After execution of this statement, the three functions described in section 15.2 are available.

The following two examples demonstrate the use of the package. Please compare with the description of the applied routines in section 15.2 if statements are unclear.

15.3.1 Simple Model for Growth and Respiration of Algae

This section demonstrates the use of the package `stoichcalc` with the derivation of the stoichiometry of the simple model for growth and respiration of algae with consumption and release of ammonium and phosphate described in section 4.3.2.1. For a more complex example, see the next subsection.

Introducing a vector of important stoichiometric or compositional parameters facilitates later changes. For the current example, we use the relative nitrogen and phosphorus content of algal biomass as parameters:

```
param <- list(a.N.ALG     = 0.06,          # gN/gALG
              a.P.ALG     = 0.01)          # gP/gALG
```

We then construct the composition vectors of ammonium, phosphate and algae that consider their mass fractions of nitrogen and phosphorus, combine them to the list of substance compositions `subst.comp`, use the `stoichcalc` routine `calc.comp.matrix` to get the composition matrix `alpha`, and print this composition matrix to test this intermediate result.

```
NH4    <- c(N      = 1)                # gN/gNH4-N
HPO4   <- c(P      = 1)                # gP/gHPO4-P
ALG    <- c(N      = param$a.N.ALG,    # gN/gALG
            P      = param$a.P.ALG)    # gP/gALG

subst.comp <- list(NH4    = NH4,
                   HPO4   = HPO4,
                   ALG    = ALG)

alpha <- calc.comp.matrix(subst.comp)

print(alpha)
```

Using this composition matrix, we can apply the `stoichcalc` routine `calc.stoich.basis` to calculate the basis of the vector space of stoichiometries that are compatible with the composition matrix. The first statement gets this basis, the next statement prints the matrix and the last statement demonstrates that all these stoichiometries are really compatible with the constraining equation (4.55).

```
nu.basis <- calc.stoich.basis(alpha)

print(nu.basis)

nu.basis %*% t(alpha)
```

As a last step, we use the `stoichcalc` routine `calc.stoich.coef` to calculate the stoichiometric coefficients of the processes of primary production and respiration. For this purpose, we use the composition matrix `alpha` calculated above, define the processes by the list of included processes (in both cases ammonium, phosphate and algae), and by the normed stoichiometric coefficient and its value. The only difference between the definition of these processes is the value of the normed stoichiometric coefficient. For growth of algae, the stoichiometric coefficient of algae is plus unity, for respiration it is minus unity. Finally, we construct the stoichiometric matrix of the process system consisting of these two processes and write composition matrix and stoichiometric matrix to a file.

```
nu.gro.ALG.NH4 <-
   calc.stoich.coef(alpha       = alpha,
                    name        = "gro.ALG.NH4",
                    subst       = c("NH4","HPO4","ALG"),
                    subst.norm  = "ALG",
                    nu.norm     = 1)

nu.resp.ALG <-
   calc.stoich.coef(alpha       = alpha,
                    name        = "resp.ALG",
                    subst       = c("NH4","HPO4","ALG"),
```

```
                    subst.norm  = "ALG",
                    nu.norm     = -1)

nu <- rbind(nu.gro.ALG.NH4,
            nu.resp.ALG)

print(nu)

write.table(alpha,file="prodrespdeath_alpha.dat",sep="\t",col.names=NA)
write.table(nu,file="prodrespdeath_nu.dat",sep="\t",col.names=NA)
```

15.3.2 Model of Growth, Respiration and Death of Algae Based on C, H, O, N and P Conservation

This section illustrates more complex stoichiometric calculations with `stoichcalc` compared to the previous section. It implements the stoichiometry of a model for growth, respiration and death of algae and zooplankton for different composition of organisms and dead organic particles and under consideration of conservation laws for the elements C, H, O, N and P and electrical charge. This example was discussed in section 4.3.2.2.

As in the previous example, we start with defining composition parameters and stoichiometric parameters of the model. We choose the composition parameters to fulfil the constraint given by equation (4.45).

```
param <- list(a.O.ALG     = 0.50,         # gO/gALG
              a.H.ALG     = 0.07,         # gH/gALG
              a.N.ALG     = 0.06,         # gN/gALG
              a.P.ALG     = 0.005,        # gP/gALG
              a.O.ZOO     = 0.50,         # gO/gZOO
              a.H.ZOO     = 0.07,         # gH/gZOO
              a.N.ZOO     = 0.06,         # gN/gZOO
              a.P.ZOO     = 0.01,         # gP/gZOO
              a.O.POM     = 0.40,         # gO/gPOM
              a.H.POM     = 0.07,         # gH/gPOM
              a.N.POM     = 0.04,         # gN/gPOM
              a.P.POM     = 0.007,        # gP/gPOM
              Y.ZOO       = 0.2,          # gZOO/gALG
              f.e         = 0.4)          # gPOM/gALG
# choose carbon fractions to guarantee that the fractions sum to unity:
param$a.C.ALG = 1-(param$a.O.ALG+param$a.H.ALG+param$a.N.ALG+param$a.P.ALG)
param$a.C.ZOO = 1-(param$a.O.ZOO+param$a.H.ZOO+param$a.N.ZOO+param$a.P.ZOO)
param$a.C.POM = 1-(param$a.O.POM+param$a.H.POM+param$a.N.POM+param$a.P.POM)
# choose yield of death to guarantee that no nutrients are required
# (oxygen content of POM was reduced to avoid need of oxygen):
param$Y.ALG.death = min(1,param$a.N.ALG/param$a.N.POM,param$a.P.ALG/param$a.P.POM)
param$Y.ZOO.death = min(1,param$a.N.ZOO/param$a.N.POM,param$a.P.ZOO/param$a.P.POM)
```

There are now many more substances to consider. In contrast to the previous example, we switch to molar mass units for the inorganic compounds because this facilitates the definition of their composition. As before, we collect all composition definitions in the list `subst.comp` and apply the function `calc.comp.matrix` to get the composition matrix.

```
NH4    <- c(H      = 4,                  # molH/molNH4
            N      = 1,                  # molN/molNH4
            charge = 1)                  # chargeunits/molNH4
NO3    <- c(O      = 3,                  # molO/molNO3
            N      = 1,                  # molN/molNO3
            charge = -1)                 # chargeunits/molNO3
HPO4   <- c(O      = 4,                  # molO/molHPO4
            H      = 1,                  # molH/molHPO4
            P      = 1,                  # molP/molHPO4
            charge = -2)                 # chargeunits/molHPO4
HCO3   <- c(C      = 1,                  # molC/molHCO3
            O      = 3,                  # molO/molHCO3
            H      = 1,                  # molH/molHCO3
            charge = -1)                 # chargeunits/molHCO3
O2     <- c(O      = 2)                  # molO/molO2
H      <- c(H      = 1,                  # molH/molH
            charge = 1)                  # chargeunits/molH
H2O    <- c(O      = 1,                  # molO/molH2O
            H      = 2)                  # molH/molH2O
ALG    <- c(C      = param$a.C.ALG/12,   # molC/gALG
            O      = param$a.O.ALG/16,   # molO/gALG
            H      = param$a.H.ALG,      # molH/gALG
            N      = param$a.N.ALG/14,   # molN/gALG
            P      = param$a.P.ALG/31)   # molP/gALG
ZOO    <- c(C      = param$a.C.ZOO/12,   # molC/gZOO
            O      = param$a.O.ZOO/16,   # molO/gZOO
            H      = param$a.H.ZOO,      # molH/gZOO
            N      = param$a.N.ZOO/14,   # molN/gZOO
            P      = param$a.P.ZOO/31)   # molP/gZOO
POM    <- c(C      = param$a.C.POM/12,   # molC/gPOM
            O      = param$a.O.POM/16,   # molO/gPOM
            H      = param$a.H.POM,      # molH/gPOM
            N      = param$a.N.POM/14,   # molN/gPOM
            P      = param$a.P.POM/31)   # molP/gPOM

subst.comp <- list(NH4    = NH4,
                   NO3    = NO3,
                   HPO4   = HPO4,
                   HCO3   = HCO3,
                   O2     = O2,
                   H      = H,
                   H2O    = H2O,
```

```
                    ALG    = ALG,
                    ZOO    = ZOO,
                    POM    = POM)

alpha <- calc.comp.matrix(subst.comp)

print(alpha)
```

As before, we check the compatibility of composition and stoichiometry according to eqation (4.55):

```
nu.basis <- calc.stoich.basis(alpha)

print(nu.basis)

nu.basis %*% t(alpha)
```

Finally, we calculate the stoichiometric coefficients of all processes, bind these vectors by rows to get the stoichiometric matrix and print the matrix. Please note how the stoichiometric contraints are implemented. For death of algae the condition

$$Y_{\text{ALG,death}} = -\frac{\nu_{\text{death,ALG POM}}}{\nu_{\text{death,ALG ALG}}}$$

is written in the form of equation (4.57) or (4.59)

$$\nu_{\text{death,ALG POM}} \cdot 1 + \nu_{\text{death,ALG ALG}} \cdot Y_{\text{ALG,death}} = 0$$

The constraints

$$Y_{\text{ZOO,death}} = -\frac{\nu_{\text{death,ZOO POM}}}{\nu_{\text{death,ZOO ALG}}}$$

$$Y_{\text{ZOO}} = -\frac{\nu_{\text{gro,ZOO ZOO}}}{\nu_{\text{gro,ZOO ALG}}}$$

$$f_{\text{e}} = -\frac{\nu_{\text{gro,ZOO POM}}}{\nu_{\text{gro,ZOO ALG}}}$$

are implemented analogously.

```
nu.gro.ALG.NH4 <-
   calc.stoich.coef(alpha       = alpha,
                    name        = "gro.ALG.NH4",
                    subst       = c("NH4","HPO4","HCO3","O2","H","H2O","ALG"),
                    subst.norm  = "ALG",
                    nu.norm     = 1)

nu.gro.ALG.NO3 <-
   calc.stoich.coef(alpha       = alpha,
                    name        = "gro.ALG.NO3",
                    subst       = c("NO3","HPO4","HCO3","O2","H","H2O","ALG"),
```

```
                    subst.norm  = "ALG",
                    nu.norm     = 1)

nu.resp.ALG <-
   calc.stoich.coef(alpha       = alpha,
                    name        = "resp.ALG",
                    subst       = c("NH4","HPO4","HCO3","O2","H","H2O","ALG"),
                    subst.norm  = "ALG",
                    nu.norm     = -1)

nu.death.ALG <-
   calc.stoich.coef(alpha       = alpha,
                    name        = "death.ALG",
                    subst       = c("NH4","HPO4","HCO3","O2","H","H2O","ALG","POM"),
                    subst.norm  = "ALG",
                    nu.norm     = -1,
                    constraints = list(c("ALG" = param$Y.ALG.death,
                                         "POM" = 1)))

nu.gro.ZOO <-
   calc.stoich.coef(alpha       = alpha,
                    name        = "groZOO",
                    subst       = c("NH4","HPO4","HCO3","O2","H","H2O","ALG","ZOO","POM"),
                    subst.norm  = "ZOO",
                    nu.norm     = 1,
                    constraints = list(c("ZOO" = 1,
                                         "ALG" = param$Y.ZOO),
                                       c("POM" = 1,
                                         "ALG" = param$f.e)))

nu.resp.ZOO <-
   calc.stoich.coef(alpha       = alpha,
                    name        = "resp.ZOO",
                    subst       = c("NH4","HPO4","HCO3","O2","H","H2O","ZOO"),
                    subst.norm  = "ZOO",
                    nu.norm     = -1)

nu.death.ZOO <-
   calc.stoich.coef(alpha       = alpha,
                    name        = "death.ZOO",
                    subst       = c("NH4","HPO4","HCO3","O2","H","H2O","ZOO","POM"),
                    subst.norm  = "ZOO",
                    nu.norm     = -1,
                    constraints = list(c("ZOO" = param$Y.ZOO.death,
                                         "POM" = 1)))

nu <- rbind(nu.gro.ALG.NH4,
            nu.gro.ALG.NO3,
```

```
            nu.resp.ALG,
            nu.death.ALG,
            nu.gro.ZOO,
            nu.resp.ZOO,
            nu.death.ZOO)

print(nu)
write.table(alpha,file="prodrespdeath_alpha.dat",sep="\t",col.names=NA)
write.table(nu,file="prodrespdeath_nu.dat",sep="\t",col.names=NA)
```

Chapter 16

Introduction to the R Package `ecosim`

16.1 Concepts

R (http://www.r-project.org) is a very powerful publicly available program for data analysis, graphics, and statistics. `ecosim` is a package of R classes that allows its users to define a model consisting of mixed reactors connected by advective and/or diffusive links and with arbitrary inputs and transformation processes. For this model, dynamic simulations can be performed and results can be plotted. Through the functionality of R, it is easy to extend the functionality of `ecosim` and to apply systems analytical techniques, such as parameter estimation, sensitivity analysis or Monte Carlo simulation to models implemented with the `ecosim` package.

Figure 16.1 gives an overview of the classes of `ecosim` and how they are linked to a model system. Usually, implementation of a model starts with setting up processes.

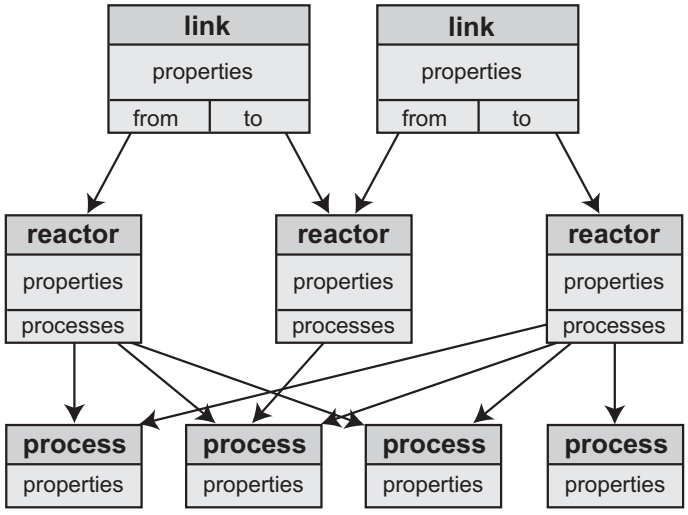

Figure 16.1: Overview of an `ecosim` system consisting of reactors, processes, and advective and diffusive links.

Processes are defined by a common process rate and substance-specific stoichiometric coefficients as described in section 4.1. As a next step, mixed reactors are defined. This

requires the definition of inflow, substance and/or organism concentrations in the inflow, outflow, substance and/or organism input not related to inflow, initial conditions, environmental conditions to which the reactor is exposed, and a list of processes that are active in the reactor. If the system consists of several interlinked reactors, the next step is to define the required advective and/or diffusive links between the reactors. Finally, the system definition consists of the list of reactors, the lists of advective and diffusive links, the global environmental conditions, model parameters, and definitions of output and integration. The method `calcres` then allows the user to perform simulations that can be plotted with the function `plotres`.

16.2 Class Definitions

16.2.1 Class "process"

Table 16.1 shows the elements of the class "`process`" that is used to define a transformation process. Each process has a unique name which should give a minimum explanation

Elements of class "`process`"

Name	Type	Meaning
`name`	string	Name of process.
`rate`	expression	Expression for the dependence of the process rate on substance concentrations, model parameters, and external influence factors.
`stoich`	list	List of numbers or expressions for stoichiometric coefficients. Substances are identified by their names.
`pervol`	logical	Type of process rate: mass per volume and time (TRUE) or per area and time (FALSE).

Table 16.1: Definition of a transformation process in `ecosim`.

of the physical, chemical or biological process represented by the object realizing the class "`process`". This name is specified using the entry "`name`" of the class definition. The entry "`rate`" is a mathematical expression describing the dependence or the process rate, ρ_i, (see Table 4.1) on substance or organism concentrations, model parameters, environmental conditions, and time. The entry "`stoich`" is a list of numbers or mathematical expressions describing the stoichiometric coeficients, ν_{ij} of the process i. Note that this list must contain the names of the substances to allow the program to uniquely identify the stoichiometric coefficients (the order in which the coefficients are provided is irrelevant; they are identified by their names). Finally, the logical entry "`pervol`" must be set to "TRUE" if the rate is formulated as mass per volume (for suspended or dissolved substances or floating organims), or to "FALSE" if it is formulated as mass per surface area (for attached substances or sessile organisms). Note that the process stoichiometry does not have to care with conversions of substances that are attached (measured as mass per area) and substances that are suspended or dissolved (measured as mass per volume); this conversion is done automatically.

16.2.2 Class "reactor"

Table 16.2 shows the elements of the class "reactor" that is used to define a mixed reactor. Each reactor has a unique name which should give a minimum explanation of the part of

Elements of class "reactor"

Name	Type	Meaning
name	string	Name of reactor.
volume.ini	expression	Initial volume of reactor.
area	expression	Surface area available for sessile organisms or attached (sedimented, adsorbed, etc.) substances.
conc.pervol.ini	list	Initial concentrations (mass per volume) of substances or organisms suspended or dissolved in the water column. Each substance to be calculated in the reactor must be initialized here.
conc.perarea.ini	list	Initial concentrations (mass per area) of substances or organisms attached to a surface. Each substance to be calculated in the reactor must be initialized here.
input	list	Input (mass per time) of substances to the reactor not associated with inflow.
inflow	expression	Inflow into the reactor (volume per time)
inflow.conc	list	Concentration of substances in the inflow.
outflow	expression	Outflow of the reactor (volume per time)
cond	list	Environmental conditions to which the reactor is exposed.
processes	list	Processes active in the reactor.

Table 16.2: Definition of a mixed reactor in ecosim.

the aquatic ecosystem represented by the object realizing the class "reactor". This name is specified using the entry "name" of the class definition. The entry "volume.ini" is a mathematical expression specifying the initial volume of the reactor. Later on, changes in volume are calculated according to equation (3.12) with inflow and outflow defined by the entries "inflow" and "outflow" and by advective links. The entry "area" specifies the surface area available for sessile organisms or attached (sedimented, adsorbed, etc.) substances in the reactor. The entry "conc.pervol.ini" is used to specify initial concentrations (mass per volume) of substances suspended or dissolved in the water column and of floating organisms. These substances and/or organisms are transported with in- and outflow. Note that each dissolved or suspended substance to be calculated in the reactor must be initialized here. Similarly to the processes, the substances are identified by their names. The user is responsible for keeping the same name for the same substance here and in the process and link definitions. The entry "conc.perarea.ini" is used to specify initial concentrations (mass per surface area) of substances or organisms attached to a surface in the reactor. These attached substances are not transported with in- and outflow. Note that each attached substance to be calculated in the reactor must be initialized here. Similarly to the processes, the substances are identified by their names.

The user is responsible for keeping the same name for the same substance here and in the process and link definitions. The entry "input" represents a vector of expressions defining substance input to, or when negative, output from the reactor that is not associated with in- and outflow. It represents the term interface fluxes, $\mathbf{J}_{\text{int}}$, in equation (3.12). The entry "inflow" is used to define inflow to the reactor according to the term Q_{in} in the equations (3.12) and (3.12). The entry "inflow.conc" is a list of numbers or expressions used to define concentrations of suspended or dissolved substances in the inflow. This corresponds to the term $\mathbf{C}_{\text{in}}^{k}$ in equation (3.12). The entry "cond" is used to define "environmental conditions". These are any reactor-specific influence factors on process rates in the reactor. Finally, the entry "processes" is used to specify a list of processes that are active in the reactor. This list must consist of objects of the class "process" described above.

16.2.3 Class "link"

Table 16.3 shows the elements of the class "link" that is used to define a link between mixed reactors. Each advective link has a unique name which should give a minimum

Elements of class "link"

Name	Type	Meaning
name	character	Name of advective link.
from	character	Name of reactor from which the link starts.
to	character	Name of reactor at which the link ends.
flow	expression	Flow from one rector to the other (volume per time)
qadv.gen	expression	General (applies to all dissolved or suspended substances) advective transfer coefficient.
qadv.spec	list	Substance-specific advective transfer coefficients.
qdiff.gen	expression	General (applies to all dissolved or suspended substances) diffusive exchange coefficient.
qdiff.spec	list	Substance-specific diffusive exchange coefficients.

Table 16.3: Definition of a link in ecosim.

explanation of the physical significance of the object realizing the class "link". This name is specified using the entry "name" of the class definition. The entries "from" and "to" are used to specify the names of the reactors that should be connected by the advective link. The entry "flow" is used to specify an expression describing the flow from one reactor to the other (positive means from "from" to "to"). The entry "qadv.gen" is used to specify a general advective transfer coefficient that applies to all dissolved or suspended substances. See section 3.3 for a more detailed explanation of its meaning. The entry "qadv.spec" is used to specify a list of substance-specific advective transfer coefficients. The entry "qdiff.gen" is used to specify a general diffusive exchange coefficient that applies to all dissolved or suspended substances. See section 3.3 for a more detailed explanation of its meaning. The entry "qdiff.spec" is used to specify a list of substance-specific diffusive exchange coefficients.

16.2.4 Class "system"

Table 16.4 shows the elements of the class "system" that is used to define the model representing the system to be analyzed. Each system has a unique name. This name

Elements of class "system"

Name	Type	Meaning
name	string	Name of system.
reactors	list	List of the reactors in the system.
links	list	List of advective links between reactors of the system.
cond	list	List of global environmental conditions to which all reactors are exposed.
param	list	List of model parameters in the form of numerical values or lists of vectors for x and y values describing a realization of a time-dependent parameter.
t.out	vector	Vector of points in time at which output should be calculated when dynamically solving the differential equations.

Important methods of class "system"

Name	Arguments	Meaning
calcres	system	Function for calculating dynamic solutions for the system given as the argument. The function returns a matrix with columns for the volumes and substance concentrations in all reactors and rows for all points of time requested for output. A quick overview plot of all substances can be produced with the function plotres.
calcsens	system param.sens scaling.factors	Function for calculating sensitivity analyses for given model parameters. The function returns a list of lists of matrices as produced by calcres where the outer list represents sensitivity calculations for different parameters, whereas the inner list represents results for different values of a single parameter. A quick overview plot of all analyses can be produced with the function plotres.

Table 16.4: Definition of a system of mixed reactors in ecosim.

is specified using the entry "name" of the class definition. The entries "reactors" and "links" are used to specify lists of mixed reactors and links that represent the system to be modelled (see also Figure 16.1). The entry "cond" represents a list of numbers or expressions for global environmental conditions to which all reactors are exposed. The entry "param" is used for specifying model parameters. Please note that all variables used for formulating process rates and stoichiometric coefficients must be defined either by global or local (reactor-specific) environmental conditions, model parameters and initial concentrations of the reactor. Inflows, outflows, inputs, exchange coefficients, etc. can depend on global environmental conditions or model parameters.

The only exception of a variable that has not to be defined by the user is the name "t" for time. This variable can be used in all expressions. The entry "t.out" is used to define a vector of output times at which model results should be returned. The first of these values is used as start time of the simulation.

The method "calcres" is used with the ecosim system as the only argument to perform a simulation. The function returns a matrix with columns for the volumes and substance concentrations in all reactors and rows for all points of time requested for output. The time corresponding to each row is given as the row name. A quick overview plot of all integrated variables can be obtained by calling "plotres" with the returned matrix from "calcres" as the only argument (see Table 16.5). The algorithm used for

Global function associated with class "system"

Name	Arguments	Meaning
plotres	res colnames file ...	Function for plotting columns of a matrix against the values provided as row names. This function is convenient to plot results of the method calcres of the class "system". res is then the result of calcres, colnames can be used to select column names (list of vectors of column names), file can be used to specify a pdf output file, and ... are arguments passed to the pdf driver. If a list of result matrices is provided, multiple simulations for all list elements will be plotted.

Table 16.5: Global function plotres to visulize results.

numerically integrating the system of ordinary differential equations can be chosen by the optional argument method of the function calcres. Numerical integration is done using the R package deSolve and all integration methods of this package are available. See details on the argument method of the function ode that serves as a wrapper of all integration techniques in the package deSolve and further literature on the underlying algorithms (Soetaert et al., 2010; Soetaert et al., 2012).

In order to propagate environmental stochasticity implemented as fluctuating parameter values and uncertainty implemented as probability distributions of parameters to the results by Monte Carlo simulation, two global functions are provided to draw from Normal and Lognormal distributions and Ornstein-Uhlenbeck processes (Table 16.6).

Global functions for realizations of Normal dist. and Ornstein-Uhlenbeck processes

Name	Arguments	Meaning

`randnorm`	`mean`
	`sd`
	`log`
	`n`
		Function for drawing a random sample of size `n` from a Normal or a Lognormal distribution (`log=TRUE`) with given mean (`mean`) and standard deviation (`sd`). Please note that also the Lognormal distribution is parameterized by mean and standard deviation on the original scale.

`randou`	`mean`
	`sd`
	`tau`
	`y0`
	`t`
	`log`
		Function for drawing a realization from an Ornstein-Uhlenbeck process with given mean (`mean`), standard deviation (`sd`), correlation time (`tau`), and initial value (`y0`; `NA` indicates the initial value to be drawn randomly) at given points in time. For `log=TRUE` the log of the variable is an Ornstein-Uhlenbeck process, but mean and standard deviations are in original units.

Table 16.6: Global functions `randnorm` and `randou` to draw from Normal distributions and Ornstein-Uhlenbeck processes.

16.3 Defining and Using a Model with ecosim

Once installed with the command `install.packages("ecosim")`, the package is loaded with the command

```
library(ecosim)
```

Objects are then generated with the command

```
new(Class=...)
```

where the class name has to be given in quotes after the identifier "`Class`" and the equal sign. This statement is followed by a comma-separated list of identifier = value pairs, where "identifier" represents one of the names given in Tables 16.1 to 16.4.

As an example of how this works we demonstrate the implementation of the simple aquatic ecosystem model discussed in section 11.2.

Implementation of the processes according to Tables 11.4 and 11.5:

```
gro.ALG <-
   new(Class  = "process",
       name   = "Growth of algae",
       rate   = expression(k.gro.ALG
                           *C.HPO4/(K.HPO4+C.HPO4)
                           *C.ALG),
       stoich = list(C.ALG  = 1,
                     C.HPO4 = expression(-alpha.P.ALG)))

death.ALG <-
   new(Class  = "process",
       name   = "Death of algae",
       rate   = expression(k.death.ALG*C.ALG),
       stoich = list(C.ALG  = -1))

gro.ZOO <-
   new(Class  = "process",
       name   = "Growth of zooplankton",
       rate   = expression(k.gro.ZOO
                           *C.ALG
                           *C.ZOO),
       stoich = list(C.ZOO = 1,
                     C.ALG = expression(-1/Y.ZOO)))

death.ZOO <-
   new(Class  = "process",
       name   = "Death of zooplankton",
       rate   = expression(k.death.ZOO*C.ZOO),
       stoich = list(C.ZOO  = -1))
```

Definition of a mixed reactor for the epilimnion of a lake with initial conditions, boundary conditions, reactor-specific environmental conditions, and the list of active processes:

```
epilimnion <-
   new(Class            = "reactor",
       name             = "Epilimnion",
       volume.ini       = expression(A*h.epi),
       conc.pervol.ini  = list(C.HPO4 = expression(C.HPO4.ini),
                               C.ALG  = expression(C.ALG.ini),
                               C.ZOO  = expression(C.ZOO.ini)),
       inflow           = expression(Q.in*86400),
       inflow.conc      = list(C.HPO4 = expression(C.HPO4.in),
                               C.ALG  = 0,
                               C.ZOO  = 0),
       outflow          = expression(Q.in*86400),
       processes        = list(gro.ALG,death.ALG,gro.ZOO,death.ZOO))
```

Definition of model parameters:

```
param1 <- list(k.gro.ALG   = 0.5,      # 1/d
               k.gro.ZOO   = 0.4,      # m3/gDM/d
               k.death.ALG = 0.1,      # 1/d
               k.death.ZOO = 0.05,     # 1/d
               K.HPO4      = 0.002,    # gP/m3
               Y.ZOO       = 0.2,      # gDM/gDM
               alpha.P.ALG = 0.003,    # gP/gDM
               A           = 5e+006,   # m2
               h.epi       = 5,        # m
               Q.in        = 5,        # m3/s
               C.HPO4.in   = 0.04,     # gP/m3
               C.ALG.ini   = 0.1,      # gDM/m3
               C.ZOO.ini   = 0.1,      # gDM/m3
               C.HPO4.ini  = 0.04)     # gP/m3
```

Finally, the model system has to be defined. Combining the definitions given above into the class "`system`" leads to the following object definition:

```
lake <- new(Class    = "system",
            name     = "Lake",
            reactors = list(epilimnion),
            param    = param1,
            t.out    = seq(0,730,by=1))
```

This completes the definition of the simple lake model. Simulations and plotting of results can then be done with the commands:

```
res1 <- calcres(lake)

plotres(res=res1)                              # plot to screen
plotres(res=res1,colnames=c("C.ALG","C.ZOO"))
```

```
plotres(res=res1,colnames=list("C.HPO4",c("C.ALG","C.ZOO")))
plotres(res=res1[1:365,],colnames=list("C.HPO4",c("C.ALG","C.ZOO")))
plotres(res      = res1,                      # plot to pdf file
        colnames = list("C.HPO4",c("C.ALG","C.ZOO")),
        file     = "didacticmodel_lakeplankton_1.pdf",
        width    = 8,
        height   = 4)
```

The first of these commands executes the simulation and returns a matrix of results to the variable "`res1`". The results stored in this matrix are then plotted to the screen with the following commands and to the pdf file "`didacticmodel_lakeplankton_1.pdf`" with the last command. This file is shown in Figure 16.2. For the chosen parameter values there is a natural damped oscillation of algae, zooplankton and phosphate concentrations.

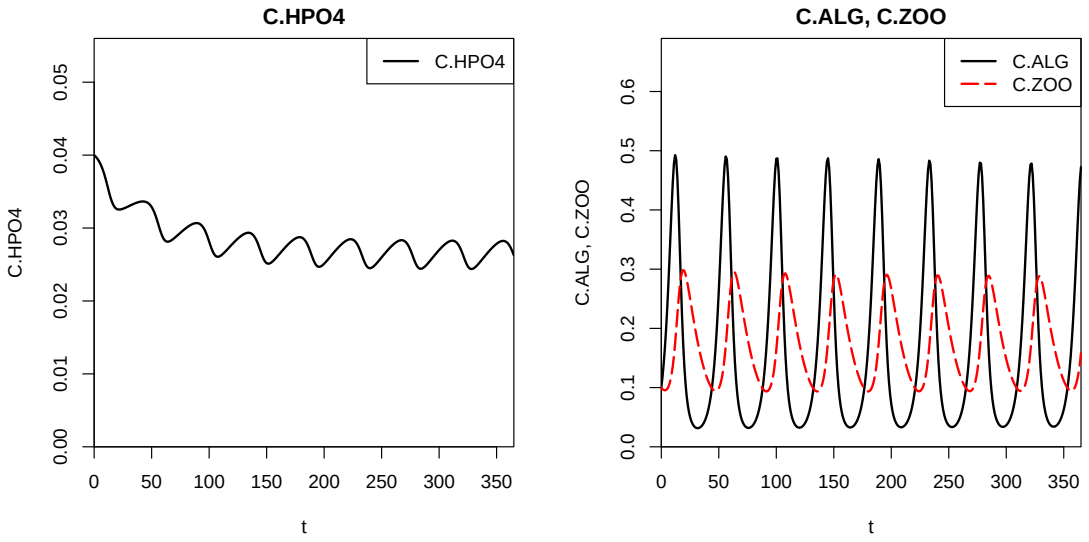

Figure 16.2: Results of a simulation of the simple ecosystem model discussed in section 11.2 with parameter values defined in the text. Phosphate concentrations are in gP/m^3, algae and zooplankton concentrations in gDM/m^3, and time in days.

It is interesting to compare these results with results for periodic (seasonal) instead of constant environmental conditions for temperature and light. To do this, we first have to replace the rates given in Table 11.5 by those given in Table 11.6:

```
gro.ALG.ext <-
   new(Class  = "process",
       name   = "Growth of algae",
       rate   = expression(k.gro.ALG
                           *exp(beta.ALG*(T-T0))
                           *C.HPO4/(K.HPO4+C.HPO4)
                           *log((K.I+I0)/
                           (K.I+I0*
                           exp(-(lambda.1+lambda.2*C.ALG)*h.epi)))/
```

```
                          ((lambda.1+lambda.2*C.ALG)*h.epi)
                          *C.ALG),
       stoich = list(C.ALG  = 1,
                     C.HPO4 = expression(-alpha.P.ALG)))

gro.ZOO.ext <-
   new(Class  = "process",
       name   = "Growth of zooplankton",
       rate   = expression(k.gro.ZOO
                          *exp(beta.ZOO*(T-T0))
                          *C.ALG
                          *C.ZOO),
       stoich = list(C.ZOO = 1,
                     C.ALG = expression(-1/Y.ZOO)))


epilimnion@processes <- list(gro.ALG.ext,death.ALG,
                             gro.ZOO.ext,death.ZOO)
```

We then modify and extend the list of model parameters:

```
param2 <- list(k.gro.ALG   = 0.8,      # 1/d
               k.gro.ZOO   = 0.4,      # m3/gDM/d
               k.death.ALG = 0.1,      # 1/d
               k.death.ZOO = 0.05,     # 1/d
               K.HPO4      = 0.002,    # gP/m3
               Y.ZOO       = 0.2,      # gDM/gDM
               alpha.P.ALG = 0.002,    # gP/gDM
               A           = 5e+006,   # m2
               h.epi       = 5,        # m
               Q.in        = 5,        # m3/s
               C.HPO4.in   = 0.04,     # gP/m3
               C.ALG.ini   = 0.1,      # gDM/m3
               C.ZOO.ini   = 0.1,      # gDM/m3
               C.HPO4.ini  = 0.04,     # gP/m3
               beta.ALG    = 0.046,    # 1/degC
               beta.ZOO    = 0.08,     # 1/degC
               T0          = 20,       # degC
               K.I         = 30,       # W/m2
               lambda.1    = 0.10,     # 1/m
               lambda.2    = 0.10,     # m2/gDM
               t.max       = 230,      # d
               I0.min      = 25,       # W/m2
               I0.max      = 225,      # W/m2
               T.min       = 5,        # degC
               T.max       = 25)       # degC
```

The new parameter list can be copied to the compartment with the following command:

```
lake@param <- param2
```

The seasonal variation of light intensity and temperature in the epilimnion are specified:

```
epilimnion@cond <-
   list(I0 = expression(0.5*(I0.min+I0.max)+
                        0.5*(I0.max-I0.min)*
                        cos(2*pi/365.25*(t-t.max))),   # W/m2
        T  = expression(0.5*(T.min+T.max)+
                        0.5*(T.max-T.min)*
                        cos(2*pi/365.25*(t-t.max))))   # degC
```

added to the epilimnion and copied to the lake compartment:

```
lake@reactors <- list(epilimnion)
```

Finally, we extend the duration of the simulation to several years:

```
t.out <- seq(0,1461,by=1)
lake@t.out <- t.out
```

Now, we can redo the simulation and plot the results:

```
res2 <- calcres(lake)

plotres(res=res2)                              # plot to screen
plotres(res=res2,colnames=c("C.ALG","C.ZOO"))
plotres(res=res2,colnames=list("C.HPO4",c("C.ALG","C.ZOO")))
plotres(res=res2[1:365,],colnames=list("C.HPO4",c("C.ALG","C.ZOO")))
plotres(res      = res2,                       # plot to pdf file
        colnames = list("C.HPO4",c("C.ALG","C.ZOO")),
        file     = "didacticmodel_lakeplankton_2.pdf",
        width    = 8,
        height   = 4)
```

The first of these commands executes the simulation and returns a matrix of results to the variable "res2". The results stored in this matrix is then plotted to the screen with the following commands and to the pdf file "didacticmodel_lakeplankton_2.pdf" with the last command. Figure 16.3 shows the results. The damped oscillations are now triggered by the external changes in environmental conditions.

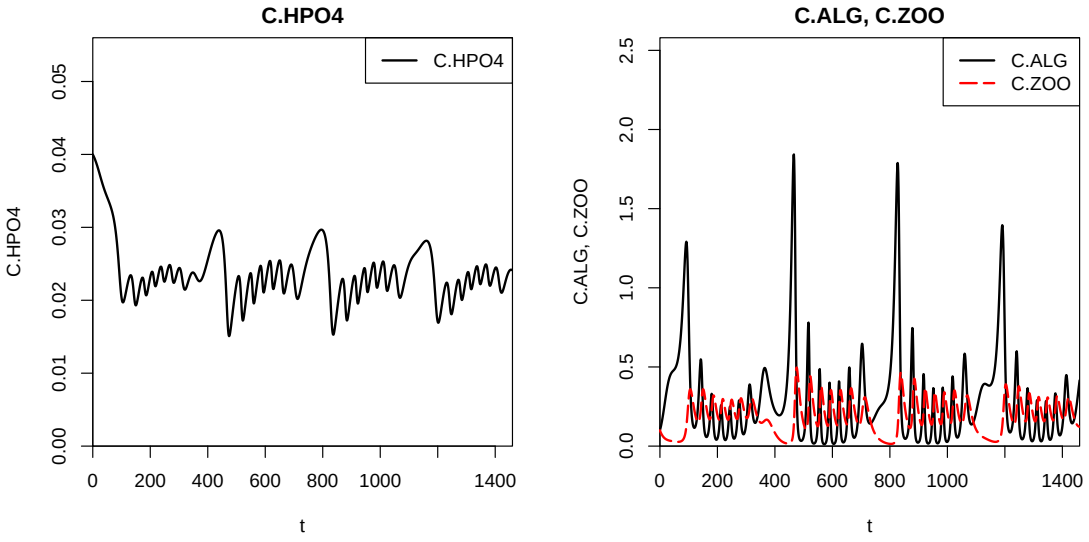

Figure 16.3: Results of a simulation of the simple ecosystem model discussed in section 11.2 with periodic driving conditions for temperature and light (compare with Figure 16.2 for a simulation with constant driving conditions). Phosphate concentrations are in gP/m^3, algae and zooplankton concentrations in gDM/m^3, and time in days.

Chapter 17

Notation

Substances and Organisms

ALG	phytoplankton.
DOM	dissolved organic matter.
HPO_4^{2-}	soluble reactive phosphorus; for the derivation of stoichiometric coefficients assumed to be phosphate.
NH_4^+	ammonium.
NO_2^-	nitrite.
NO_3^-	nitrate.
POM	dead particulate organic matter.
POMD	degradable dead particulate organic matter.
POMI	inert dead particulate organic matter.
SALG	periphyton.
SHET	heterotrophic bacteria in the sediment.
SPOM	dead particulate organic matter in the sediment.
SPOMD	dead degradable particulate organic matter in the sediment.
SPOMI	dead inert particulate organic matter in the sediment.
ZOO	zooplankton.

Variables

A	surface area (L^2).
$\mathrm{d}\vec{A}$	surface element multiplied by a outward directed vector of unit length (L^2).
A^k	surface area in reactor k available for colonization or adsorption (L^2).
C	concentration of a substances or organism (ML^{-3}).
$\mathbf{C}$	vector of concentrations of substances or organisms (ML^{-3}).
$\mathbf{C}^k$	vector of concentrations of substances or organisms in reactor k (ML^{-3}).
C_j	concentration of substance or organism j (ML^{-3}).
$\mathbf{C}_{\mathrm{in}}$	vector of concentrations of substances or organisms in the inflow (ML^{-3}).
$\mathbf{C}_{\mathrm{in}}^k$	vector of concentrations of substances or organisms in the inflow of reactor k (ML^{-3}).

$C_{\mathrm{in},j}$	concentration of substance or organism j in the inflow (ML^{-3}).
$\mathrm{d}\vec{A}$	surface element multiplied by a outward directed vector of unit length (L^2).
d_p	particle diameter (L).
div	divergence: the divergence of a vector field $\vec{v}$, represented by div, is a scalar field that quantifies the volume density of the outward flux of a vector field at each point in space; in cartesian coordinates, it is given by $\operatorname{div}\vec{v} = \partial v_x/\partial x + \partial v_y/\partial y + \partial v_z/\partial z$.
$\mathbf{D}$	vector of surface densities of substances or organisms (ML^{-2}).
$\mathbf{D}^k$	vector of surface densities of substances or organisms in reactor k (ML^{-2}).
D_j	surface density of substance or organism j (ML^{-2}).
D_j	molecular diffusion coefficient of substance j ($\mathrm{L}^2\mathrm{T}^{-1}$).
e_y	coefficient of lateral dispersion ($\mathrm{L}^2\mathrm{T}^{-1}$).
E_x	coefficient of longitudinal dispersion ($\mathrm{L}^2\mathrm{T}^{-1}$).
f_e	fraction of algal biomass converted to dead organic particles due to excretion and sloppy feeding by zooplankton.
f_I	fraction of biomass of dead organic particles in death process that are inert.
f_r	fraction of algal biomass that is respired during feeding of zooplankton.
f_st	shape factor for calculation of sedimentation velocity.
g	gravitational acceleration (LT^{-2}).
$\overrightarrow{\mathrm{grad}}$	gradient: the gradient of a scalar field s is a vector field that represents its steepest ascent direction and magnitude (slope); in cartesiann coordinates, it is given by $\overrightarrow{\mathrm{grad}}(s) = (\partial s/\partial x, \partial s/\partial y, \partial s/\partial z)^\mathrm{T}$ [T transposes the row vector to a column vector]).
h	height or thickness of (part of) a water body (L).
h_epi	height or thickness of the epilimnion of a lake or reservoir (L).
h_meta	height or thickness of the metalimnion of a lake or reservoir (L).
h_hypo	height or thickness of the hypolimnion of a lake or reservoir (L).
H	non-dimensional Henry's law coefficient.
I	light intensity (MT^{-3}).
I_0	light intensity at the surface of the water body (MT^{-3}).
I_opt	optimum light intensity of light limitation factor of algal growth (MT^{-3}).
$\hat{\mathbf{j}}$	vector of total fluxes ("mass" per unit of time) of the quantities for which balance equations should be formulated ($[\mathbf{m}]T^{-1}$).
$\vec{\mathbf{j}}$	vector of fluxes ("mass" per unit of time and cross-sectional area) of the quantities for which balance equations should be formulated $\mathbf{m}$ ($[\mathbf{m}]L^{-2}T^{-1}$).
$\mathbf{j}_x$	x-component of vector of total fluxes $\vec{\mathbf{j}}$ ($[\mathbf{m}]L^{-2}T^{-1}$).
$\mathbf{j}_y$	y-component of vector of total fluxes $\vec{\mathbf{j}}$ ($[\mathbf{m}]L^{-2}T^{-1}$).
$\mathbf{j}_z$	z-component of vector of total fluxes $\vec{\mathbf{j}}$ ($[\mathbf{m}]L^{-2}T^{-1}$).

$\mathbf{J}$	vector of total (net) input fluxes of the masses, $\mathbf{m}$, to the given region per unit of time ($[\mathbf{m}]\mathrm{T}^{-1}$).
$\mathbf{J}_l$	vector of mass fluxes of link l that are not associated with water flow ($[\mathbf{m}]\mathrm{T}^{-1}$).
$\mathbf{J}_{\mathrm{int}}$	vector of fluxes of substances or organisms across the interface to a compartment (e.g. a mixed reactor) (MT^{-1}).
$J_{\mathrm{int},j}$	flux of substance or organism j across the interface to a compartment (e.g. a mixed reactor) (MT^{-1}).
$J_{l,j}^{\mathrm{adv}}$	advective flux of substance or organism j in link l (MT^{-1}).
$J_{l,j}^{\mathrm{diff}}$	diffusive flux of substance or organism j in link l (MT^{-1}).
k_l^{from}	index of reactor at which the link l starts.
k_l^{to}	index of reactor at which the link l ends.
$k_{\mathrm{death,ALG}}$	specific death rate of algae (T^{-1}).
$k_{\mathrm{death,HET}}$	specific death rate of heterotrophic bacteria (T^{-1}).
$k_{\mathrm{death,N1}}$	specific death rate of first stage nitrifiers (T^{-1}).
$k_{\mathrm{death,N2}}$	specific death rate of second stage nitrifiers (T^{-1}).
$k_{\mathrm{death,ZOO}}$	specific death rate of zooplankton (T^{-1}).
$k_{\mathrm{gro,ALG},T_0}$	specific maximum growth rate of algae (under non-limited conditions with respect to light and nutrients) at the standard temperature, T_0 (T^{-1}).
$k_{\mathrm{gro,HET,ox},T_0}$	specific maximum growth rate of heterotrophic bacteria under oxic conditions at the standard temperature, T_0 (T^{-1}).
$k_{\mathrm{gro,HET,anox},T_0}$	specific maximum growth rate of heterotrophic bacteria under anoxic conditions at the standard temperature, T_0 (T^{-1}).
$k_{\mathrm{gro,N1},T_0}$	specific maximum growth rate of first stage nitrifiers at the standard temperature, T_0 (T^{-1}).
$k_{\mathrm{gro,N2},T_0}$	specific maximum growth rate of second stage nitrifiers at the standard temperature, T_0 (T^{-1}).
$k_{\mathrm{gro,ZOO},T_0}$	rate coefficient for growth of zooplankton at reference temperature ($\mathrm{M}^{-1}\mathrm{L}^3\mathrm{T}^{-1}$).
$k_{\mathrm{hyd,POM},T_0}$	specific hydrolysis rate at the standard temperature, T_0 (T^{-1}).
$k_{\mathrm{miner,anox,POM},T_0}$	specific maximum anoxic mineralization rate at the standard temperature, T_0 (T^{-1}).
$k_{\mathrm{miner,ox,POM},T_0}$	specific maximum oxic mineralization rate at the standard temperature, T_0 (T^{-1}).
k_{nitri,T_0}	maximum nitrification rate at the standard temperature, T_0 ($\mathrm{ML}^{-3}\mathrm{T}^{-1}$).
k_{nitri1,T_0}	maximum rate of first step nitrification at the standard temperature, T_0 ($\mathrm{ML}^{-3}\mathrm{T}^{-1}$).
k_{nitri2,T_0}	maximum rate of second step nitrification at the standard temperature, T_0 ($\mathrm{ML}^{-3}\mathrm{T}^{-1}$).
$k_{\mathrm{resp,ALG},T_0}$	specific maximum respiration rate of algae at the standard temperature, T_0 (T^{-1}).
$k_{\mathrm{resp,HET},T_0}$	specific maximum respiration rate of heterotrophic bacteria at the

	standard temperature, T_0 (T^{-1}).
$k_{\mathrm{resp,N1},T_0}$	specific maximum respiration rate of first stage nitrifiers at the standard temperature, T_0 (T^{-1}).
$k_{\mathrm{resp,N2},T_0}$	specific maximum respiration rate of second stage nitrifiers at the standard temperature, T_0 (T^{-1}).
$k_{\mathrm{resp,ZOO},T_0}$	specific maximum respiration rate of zooplankton at the standard temperature, T_0 (T^{-1}).
K	coefficient of turbulent diffusion ($\mathrm{L}^2\mathrm{T}^{-1}$).
K_{xy}	coefficient of horizontal turbulent diffusion ($\mathrm{L}^2\mathrm{T}^{-1}$).
K_z	coefficient of vertical turbulent diffusion ($\mathrm{L}^2\mathrm{T}^{-1}$).
K_{st}	friction coefficient according to Strickler ($\mathrm{L}^{1/3}\mathrm{T}^{-1}$).
K_I	half-saturation light intensity of light limitation factor of algal growth (MT^{-3}).
$K_{\mathrm{HPO}_4^{2-},\mathrm{ALG}}$	half-saturation concentration of algae with respect to phosphate (ML^{-3}).
$K_{\mathrm{HPO}_4^{2-},\mathrm{HET}}$	half-saturation concentration of heterotrophic bacteria with respect to phosphate (ML^{-3}).
$K_{\mathrm{N,ALG}}$	half-saturation concentration of algae with respect to nitrogen (ML^{-3}).
K_{N}	half-saturation concentration with respect to the unspecified nutrient N or with respect to nitrogen (ammonium plus nitrate) (ML^{-3}).
$K_{\mathrm{N,ALG}}$	half-saturation concentration of algae with respect to nitrogen (ammonium plus nitrate) (ML^{-3}).
$K_{\mathrm{N,HET}}$	half-saturation concentration of heterotrophic bacteria with respect to nitrogen (ammonium plus nitrate) (ML^{-3}).
$K_{\mathrm{NH}_4^+,\mathrm{nitri}}$	half-saturation concentration of nitrification with respect to ammonium (ML^{-3}).
$K_{\mathrm{NO}_3^-,\mathrm{miner}}$	half-saturation concentration of mineralization with respect to nitrate (ML^{-3}).
$K_{\mathrm{NO}_3^-,\mathrm{HET}}$	half-saturation concentration of anoxic growth of heterotrophic bacteria with respect to nitrate (ML^{-3}).
$K_{\mathrm{NO}_2^-,\mathrm{nitri}}$	half-saturation concentration of nitrification with respect to nitrite (ML^{-3}).
$K_{\mathrm{O_2,ALG}}$	half-saturation concentration of algae with respect to oxygen (ML^{-3}).
$K_{\mathrm{O_2,miner}}$	half-saturation concentration of mineralization with respect to oxygen (ML^{-3}).
$K_{\mathrm{O_2,HET}}$	half-saturation concentration of heterotrophic bacteria with respect to oxygen (ML^{-3}).
$K_{\mathrm{O_2,nitri}}$	half-saturation concentration of nitrification with respect to oxygen (ML^{-3}).
$K_{\mathrm{O_2,ZOO}}$	half-saturation concentration of zooplankton with respect to oxygen (ML^{-3}).
$K_{\mathrm{DOM,HET}}$	half-saturation concentration of heterotrophic bacteria with respect to dissolved organic matter (ML^{-3}).

$K_{\mathrm{SPOM,det}}$	half-saturation concentration of detachment with respect to particulate organic matter in the sediment (ML^{-2}).
L	dimension of length.
$\mathrm{L}_{\mathrm{diff}}$	diffusion distance.
M	dimension of mass.
$\mathbf{m}$	vector of "masses" (quantities of substances, physical variables or properties) in a given region for which balance equations are to be formulated ($[\mathbf{m}]$).
n	friction coefficient according to Manning ($\mathrm{L}^{-1/3}\mathrm{T}$).
n	organism density (L^{-3}).
$\mathbf{n}$	Vector of organism densities for different species or age or stage classes. ($\mathrm{L}^{-1/3}\mathrm{T}$).
n_{a}	number of substances attached to a surface.
n_{age}	number of age classes.
n_{e}	number of "elementary constituents".
n_{p}	number of processes.
n_{s}	number of substances.
n_{v}	number of dissolved or suspended substances.
N	Number of organisms. ($\mathrm{L}^{-1/3}\mathrm{T}$).
$\mathbf{N}$	Vector of numbers of organisms for different species or age or stage classes. ($\mathrm{L}^{-1/3}\mathrm{T}$).
$p_{\mathrm{NH}_4^+,\mathrm{ALG}}$	preference factor of phytoplankton for ammonium rather than nitrate as their nitrogen source.
$p_{\mathrm{NH}_4^+,\mathrm{HET}}$	preference factor of heterotrophic bacteria for ammonium rather than nitrate as their nitrogen source; only active if organic food does not contain sufficient nitrogen.
P	wetted perimeter (L).
$q_{l,j}^{\mathrm{adv}}$	transfer coefficient of advective flux of substance or organism j in link l ($\mathrm{L}^3\mathrm{T}^{-1}$).
$q_{l,j}^{\mathrm{diff}}$	transfer coefficient of diffusive flux of substance or organism j in link l ($\mathrm{L}^3\mathrm{T}^{-1}$).
Q	discharge ($\mathrm{L}^3\mathrm{T}^{-1}$).
Q_l	discharge of link l ($\mathrm{L}^3\mathrm{T}^{-1}$).
Q_{in}	discharge of inflow ($\mathrm{L}^3\mathrm{T}^{-1}$).
Q_{in}^k	discharge of inflow to reactor k ($\mathrm{L}^3\mathrm{T}^{-1}$).
Q_{out}	discharge of outflow ($\mathrm{L}^3\mathrm{T}^{-1}$).
Q_{out}^k	discharge of outflow of reactor k ($\mathrm{L}^3\mathrm{T}^{-1}$).
$\hat{\mathbf{r}}$	vector of "mass" per unit length and time of net production of the quantities for which balance equations should be formulated ($[\mathbf{m}]L^{-1}T^{-1}$).
$\mathbf{r}$	vector of net production rates ("mass" per unit volume and time) of the quantities for which balance equations should be formulated ($[\mathbf{m}]L^{-3}T^{-1}$).

$\mathbf{r}_\mathrm{C}$	vector of production rates of substances or organisms per unit volume ($\mathrm{ML^{-3}T^{-1}}$).
$\mathbf{r}_\mathrm{D}$	vector of production rates of substances or organisms per unit surface area ($\mathrm{ML^{-2}T^{-1}}$).
r_{C_j}	production rate of substance or organism j per unit volume ($\mathrm{ML^{-3}T^{-1}}$).
$r^k_{C_j}$	production rate of substance or organism j per unit volume in reactor k ($\mathrm{ML^{-3}T^{-1}}$).
r_{D_j}	production rate of substance or organism j per unit surface area ($\mathrm{ML^{-2}T^{-1}}$).
$r^k_{D_j}$	production rate of substance or organism j per unit surface area in reactor k ($\mathrm{ML^{-2}T^{-1}}$).
$\mathbf{R}$	vector of total (net) production of the masses, $\mathbf{m}$, in a given region per unit of time ($[\mathbf{m}]\mathrm{T^{-1}}$).
R	hydraulic radius ($= A/P$) (L).
S_0	slope of river bed.
S_f	friction slope of river.
t	time (T).
t_end	end time (T).
t_ini	initial time (T).
T	dimension of time.
T	temperature (θ).
T_0	standard or reference time (T).
v	velocity ($\mathrm{LT^{-1}}$).
$\vec{v}$	velocity vector ($\mathrm{LT^{-1}}$).
v_ex	gas exchange velocity ($\mathrm{LT^{-1}}$).
v_sed	sedimentation velocity ($\mathrm{LT^{-1}}$).
$v_{\mathrm{sed},j}$	sedimentation velocity of substance or organism j ($\mathrm{LT^{-1}}$).
v_x	x-component of velocity vector ($\mathrm{LT^{-1}}$).
v_y	y-component of velocity vector ($\mathrm{LT^{-1}}$).
v_z	z-component of velocity vector ($\mathrm{LT^{-1}}$).
V	volume ($\mathrm{L^3}$).
V^k	volume of reactor k ($\mathrm{L^3}$).
x	horizontal coordinate (L).
$\vec{x}$	vector of spatial coordinates (L).
y	horizontal coordinate (L).
Y_HET	yield of heterotrophic bacteria.
Y_N1	biomass production of first stage nitrifiers per unit of consumed ammonium-nitrogen.
Y_N2	biomass production of second stage nitrifiers per unit of consumed nitrite-nitrogen.
Y_ZOO	yield of zooplankton.
$Y_\mathrm{ALG,death}$	yield of death process of algae.

$Y_{\mathrm{ZOO,death}}$	yield of death process of zooplankton.
z	vertical coordinate (L).
z_{b}	vertical coordinate of the sole of the river. (L).
$\boldsymbol{\alpha}$	matrix mass fraction of elemental constituents on substances or organisms.
$\alpha_{k,j}$	mass fraction of elemental constituent k on mass of substance or organism j.
$\alpha_{\mathrm{C},j}$	mass fraction of carbon on mass of substance or organism j.
$\alpha_{\mathrm{H},j}$	mass fraction of hydrogen on mass of substance or organism j.
$\alpha_{\mathrm{N},j}$	mass fraction of nitrogen on mass of substance or organism j.
$\alpha_{\mathrm{O},j}$	mass fraction of oxygen on mass of substance or organism j.
$\alpha_{\mathrm{P},j}$	mass fraction of phosphorus on mass of substance or organism j.
β	coefficient of temperature dependence (θ^{-1}).
β_{ALG}	coefficient of temperature dependence of algae (θ^{-1}).
β_{BAC}	coefficient of temperature dependence of bacteria (θ^{-1}).
β_{HET}	coefficient of temperature dependence of heterotrophic microorganisms (θ^{-1}).
β_{hyd}	coefficient of temperature dependence of hydrolysis (θ^{-1}).
β_{N1}	coefficient of temperature dependence of first stage nitrifiers (θ^{-1}).
β_{N2}	coefficient of temperature dependence of second stage nitrifiers (θ^{-1}).
β_{ZOO}	coefficient of temperature dependence of zooplankton (θ^{-1}).
$\boldsymbol{\gamma}_{(i)}$	matrix of equations constraining the stoichiometry of process i.
λ	light extinction coefficient. (L^{-1}).
μ	dynamic viscosity ($\mathrm{ML}^{-1}\mathrm{T}^{-1}$).
$\boldsymbol{\nu}$	matrix of stoichiometric coefficients.
$\boldsymbol{\nu}_i$	row vector of stoichiometric coefficients of process i.
$\nu_{i,j}$	stoichiometric coefficient of process i with respect to substance or organism j.
$\boldsymbol{\rho}$	vector of densities ("mass" per unit volume) of the quantities for which balance equations should be formulated ($[\mathbf{m}]L^{-3}$).
$\hat{\boldsymbol{\rho}}$	vector of one-dimensional densities ("mass" per unit length) of the quantities for which balance equations should be formulated ($[\mathbf{m}]L^{-1}$).
ρ	density (ML^{-3}).
ρ_{p}	density of particle (ML^{-3}).
ρ_{w}	density of water (ML^{-3}).
ρ_i	process rate of process i ($\mathrm{ML}^{-3}\mathrm{T}^{-1}$).
τ	shear stress ($ML^{-1}T^{-1}$).
τ_0	bottom shear stress ($ML^{-1}T^{-1}$).
θ	dimension of temperature.
θ	non-dimensional bottom shear stress.

Bibliography

Andersen, T. (1997). *Pelagic Nutrient Cycles*. Springer, Berlin.

Anderson, E., Bai, Z., Bischof, C., Blackford, S., Demmel, J., Dongarra, J., Du Croz, J., Greenbaum, A., Mammarling, S., McKenney, A., and Sorensen, D. (1999). *LAPACK User's Guide*. SIAM, third edition. http://www.netlib.org/lapack/lug/lapack_lug.html.

Anderson, T. R. (2005). Plankton functional type modelling: running before we can walk? *Journal of Plankton Research*, 27(11):1073–1081.

Anderson, T. R., Hessen, D. O., Elser, J. J., and Urabe, J. (2005). Metabolic stoichiometry and the fate of excess carbon and nutrients in consumers. *The American Naturalist*, 165(1):1–15.

Appelo, C. A. J. and Postma, D. (2005). *Geochemistry, Groundwater and Pollution*. A.A. Balkema, Leiden, second edition.

Benndorf, J. and Recknagel, F. (1982). Problems of application of the ecological model SALMO to lakes and reservoirs having various trophic states. *Ecological Modelling*, 17:129–145.

Black, A. J. and McKane, A. J. (2012). Stochastic formulation of ecologial models and their applications. *Trends in Ecology and Evolution*, 27(6):337–345.

Bosse, T. and Kleiser, L. (2005). Small particles in homogeneous turbulence: settling velocity enhancement by two-way coupling. *Physics of Fluids*, 18. Art. No. 027102.

Brenan, K. E., Campbell, S. L., and Petzold, L. R. (1989). *Numerical Solution of Initial-Value Problems in Differential Algebraic Equations*. North Holland, New York.

Brooks, S. P. and Roberts, G. O. (1998). Convergence assessment techniques for Markov chain Monte Carlo. *Statistics and Computing*, 8:319–335.

Brose, U., Williams, R. J., and Martinez, N. D. (2006). Allometric scaling enhances stability in complex food webs. *Ecology Letters*, 9:1228–1236.

Brown, J. H., Gillooly, J. F., Allen, A. P., Savage, V. M., and West, G. B. (2004). Toward a metabolic theory of ecology. *Ecology*, 85:1771–1789.

Bührer, H. and Ambühl, H. (1975). Die Einleitung von gereinigtem Abwasser in Seen. *Schweizerische Zeitschrift für Hydrologie*, 37:347–369.

Carrol, S. P., Hendry, A. P., Reznick, D. N., and Fox, C. W. (2007). Evolution on ecological time-scales. *Functional Ecology*, 21:387–393.

Clarke, A. (1987). Temperature, latitude and reproductive effort. *Marine Ecology Progress Series*, 38:89–99.

Clemen, R. T. (1996). *Making Hard Decisions*. PWS-Kent, Boston, second edition.

Cowan, W. L. (1956). Estimating hydraulic roghness coefficients. *Agricult. Eng.*, 37:473–475.

Cowles, M. K. and Carlin, B. P. (1996). Markov chain Monte Carlo convergence diagnostics: A comparative review. *Journal of the American Statistical Association*, 92:883–904.

Cox, R. T. (1946). Probability, frequency and reasonable expectation. *American Journal of Physics*, 14(1):1–13.

Dabes, J. M., Finn, R. K., and Wilke, C. R. (1973). Equations of substrate-limited growth: The case for Blackman kinetics. *Biotechnology & Bioengineering*, 15:1159–1177.

Danckwerts, P. V. (1951). Significance of liquid-film coefficients in gas absorption. *Ind. Eng. Chem.*, 43:1460–1467.

DeMott, W. R., Gulati, R. D., and Siewertsen, K. (1998). Effects of phosphorus-deficient diet on the carbon and phosphorus balance of Daphnia magna. *Limnology & Oceanography*, 43:1147–1161.

Dietzel, A., Mieleitner, J., Kardaetz, S., and Reichert, P. (2013). Effects of changes in the driving forces on water quality and plankton dynamics in three Swiss lakes - long-term simulations with BELAMO. *Freshwater Biology*, 58:10–35.

Dodds, W. K. (2002). *Freshwater ecology: concepts and environmental applications*. Academic Press, San Diego.

Droop, M. (1973). Some thoughts on nutrient limitation in algae. *Journal of Phycology*, 9:264–272.

Droop, M. (1983). 25 years of algal growth kinetics. *Botanica Marina*, XXVI:99–112.

Droop, M. (2003). Comment: In defence of the cell quota model of micro-algal growth. *Journal of Plankton Research*, 25(1):103–107.

Egge, J. K. and Aksnes, D. L. (1992). Silicate as regulating nutrient in phytoplankton competion. *Marine Ecology Progress Series*, 83:281–289.

Eisenführ, F. and Weber, M. (1999). *Rationales Entscheiden*. Springer, Berlin, 3. edition.

Elser, J. J. (2006). Biological stoichiometry: A chemical bridge between ecosystem ecology and evolutionary biology. *The American Naturalist*, 168:S25–S35.

Elser, J. J., Sterner, R. W., Gorokhova, E., Fagan, W. F., Markow, T. A., Cotner, J. B., Harrison, J. F., Hobbie, S. E., Odell, G. M., and Weider, L. J. (2000). Biological stoichiometry from genes to ecosystems. *Ecology Letters*, 3:540–550.

Evans, M., Hastings, N., and Peacock, B. (2000). *Statistical Distributions*. John Wiley & Sons, New York, third edition.

Fischer, H. B. (1967). The mechanics of dispersion in natural streams. *Journal of the Hydraulics Division, ASCE*, 93(HY6):187–216.

Fischer, H. B., List, E. J., Koh, C. Y., Imberger, J., and Brooks, N. H. (1979). *Mixing in Inland and Coastal Waters*. Academic Press, New York.

French, R. H. (1985). *Open-channel hydraulics*. McGraw-Hill, Stuttgart. New York.

Fussmann, G. F., Loreau, M., and Abrams, P. A. (2007). Eco-evolutionary dynamics of communities and ecosystems. *Functional Ecology*, 21:465–477.

Gal, G., Imberger, J., Zohary, T., Antenucci, J., Anis, A., and Rosenberg, T. (2003). Simulating the thermal dynamics of Lake Kinneret. *Ecological Modelling*, 162:69–86.

Gamerman, D. (1997). *Markov Chain Monte Carlo - Statistical Simulation for Bayesian Inference*. Chapman & Hall, London.

Gear, C. W. (1971a). Algorithm 407, DIFSUB for solution of ordinary differential equations. *Communications ACM*, 14(3):185–190.

Gear, C. W. (1971b). The automatic integration of ordinary differential equations. *Communications ACM*, 14(3):176–179.

Gear, C. W. (1971c). *Numerical initial value problems in ordinary differential equations*. Prentice Hall, Stuttgart. Englewood Cliffs, N.J.

Gelman, A., Carlin, J. B., Stern, H. S., and Rubin, D. B. (1995). *Bayesian Data Analysis*. Chapman & Hall, London.

Gillespie, D. T. (1976). A general method for numerically simulating the stochastic time evolution of coupled chemical reactions. *Journal of Computational Physics*, 22:403–434.

Gillespie, D. T. (1977). Exact stochastic simulation of coupled chemical reactions. *Journal of Physical Chemistry*, 81(25):2340–2361.

Gillies, D. (1991). Intersubjective probability and confirmation theory. *The British Journal for the Philosophy of Science*, 42:513–533.

Gillooly, J. F., Allen, A. P., West, G. B., and Brown, J. H. (2005). The rate of DNA evolution: Effects of body size and temperature on the molecular clock. *Proceedings of the National Academy of Sciences of the United States of America*, 102(1):140–145.

Glazier, D. S. (2009). Metabolic level and size scaling of rates of respiration and growth in unicellular organisms. *Functional Ecology*, 23:963–968.

Golub, G. H. and Loan, C. F. (1996). *Matrix Computations*. Johns Hopkins University Press, Baltimore, USA, third edition.

Grimm, V. (1999). Ten years of individual-based modelling in ecology: what have we learned and what could we learn in the future? *Ecological Modelling*, 115:129–148.

Gujer, W. and Henze, M. (1991). Activated sludge modelling and simulation. *Water Science and Technology*, 23:1011–1023.

Gujer, W., Henze, M., Mino, T., Matsuo, T., Wentzel, M. C., and Marais, G. v. R. (1995). The Activated Sludge Model No. 2: Biological phosphorus removal. *Water Science and Technology*, 31(2):1–11.

Gujer, W., Henze, M., Mino, T., and van Loosdrecht, M. (1999). Activated Sludge Model No. 3. *Water Science and Technology*, 39(1):183–193.

Gujer, W. and Larsen, T. A. (1995). The implementation of biokinetics and conservation principles in ASIM. *Water Science and Technology*, 31(2):257–266.

Hairston, N. G., J., Ellner, S. P., Gerber, M. A., Yoshida, T., and Fox, J. A. (2005). Rapid evolution and the convergence of ecological and evolutionary time. *Ecology Letters*, 8:1114–1127.

Hamilton, D. P. and Schladow, S. G. (1997). Prediction of water quality in lakes and reservoirs. Part i - Model description. *Ecological Modelling*, 96:91–110.

Hartvig, M., Andersen, K. H., and Beyer, J. E. (2011). Food web framework for size-structured populations. *Journal of Theoretical Biology*, 272:113–122.

Hecky, R. E., Mopper, K., Kilham, P., and Degens, E. T. (1972). The amino acid and sugar composition of diatom cell-walls. *Marine Biology*, 19:323–331.

Heitzer, A., Kohler, H.-P., E., Reichert, P., and Hamer, G. (1991). Utility of phenomenological models for describing temperature dependence of bacterial growth. *Applied Environmental Microbiology*, 57(9):2656–2665.

Henze, M., Grady, C. P. L., Gujer, W., Marais, G. v. R., and Matsuo, T. (1986). Activated Sludge Model No. 1. Scientific and Technical Report 1, IAWPRC Task Group on Mathematical Modelling for Design and Operation of Biological Wastewater Treatment Processes, IAWPRC, London.

Henze, M., Gujer, W., Mino, T., Matsuo, T., Wentzel, M. C., and Marais, G. v. R. (1995). Activated Sludge Model No. 2. Scientific and Technical Report 3, IAWPRC Task Group on Mathematical Modelling for Design and Operation of Biological Wastewater Treatment Processes, IAWPRC, London.

Henze, M., Gujer, W., Mino, T., Matsuo, T., Wentzel, M. C., Marais, G. v. R., and Van Loosdrecht, M. C. M. (1999). Activated Sludge Model no. 2d, ASM2d. *Water Science and Technology*, 39(1):165–182.

Henze, M., Gujer, W., Mino, T., and van Loosdrecht, M. (2000). Activated Sludge Models asm1, asm2, asm2d and asm3. Scientific and Technical Report 9, IWA Task Group on Mathematical Modelling for Design and Operation of Biological Wastewater Treatment, IWA Publishing, London.

Hessen, D. O., Faerovig, P. J., and Andersen, T. (2002). Light, nutrients and P:C ratios in algae: grazer performance related to food quality and quantity. *Ecology*, 83(7):1886–1898.

Higbie, R. (1935). The rate of absorption of a pure gas into a still liquid during short periods of exposure. *Trans. Am. Inst. Chem. Engrs.*, 31:365–389.

Hindmarsh, A. C. (1983). ODEPACK. a systematized collection of ODE solvers. In Stepleman, R., editor, *Scientific Computing*, pages 55–64. IMACS / North-Holland.

Holling, C. S. (1959). The components of predation as revealed by a study of small-mammal predation of the european pine sawfly. *The Canadian Entomologist*, 91:292–320.

Howson, C. and Urbach, P. (1989). *Scientific Reasoning: The Bayesian Approach*. Open Court, La Salle, Illinois, USA.

Hupfer, M., Gächter, R., and Giovanoli, R. (1995). Transformation of phosphorus species in settling seston and during early sediment diagenesis. *Aquatic Sciences*, 57:305–324.

Huppert, A., Blasius, B., Olinky, R., and Stone, L. (2005). A model for seasonal phytoplankton blooms. *Journal of Theoretical Biology*, 236:276–290.

Imberger, J. (1978). Dynamics of reservoirs of medium size. *Journal of the Hydraulics Division, ASCE*, 104(5):725–743.

Imberger, J. and Patterson, J. C. (1981). A dynamic reservoir simulation model - DYRESM. In Fischer, H. B., editor, *Transport models for inland and coastal waters*, pages 310–361. Academic Press, New York.

Imboden, D. M. and Koch, S. (2003). *Systemanalyse - Einführung in die mathematische Modellierung natürlicher Systeme*. Springer, Berlin.

Kattwinkel, M., Reichert, P., Rüegg, J., Liess, M., and Schuwirth, N. (2016). Modeling macroinvertebrate community dynamics in stream mesocosms contaminated with a pesticide. *Environmental Science & Technology*, 50(6):3165–3173.

Kay, A. D., Ashton, I. W., Gorokhova, E., Kerkhoff, A. J., Liess, A., and Litchman, E. (2005). Toward a stoichiometric framework for evoltionary biology. *Oikos*, 109:6–17.

Kleiber, M. (1947). Body size and metabolic rate. *Physiological Reviews*, 27:511–541.

Kontopoulos, D., Sentis, A., Daufresne, M., Glazman, N., Dell, A., and Pawar, S. (2024). No universal mathematical model for thermal performance curves across traits and taxonomic groups. *Nature Communications*, 15:8855.

Lampert, W. and Sommer, U. (1997). *Limnoecology*. Oxford University Press.

Leibundgut, C., Petermann, J., and Schudel, B. (1988). *Markierversuch Rhein Albbruck-Basel*. Geographisches Institut der Universität Bern, Bern.

Lenton, T. M. and Watson, A. J. (2000a). Redfield revisited - 1. Regulation of nitrate, phosphate, and oxygen in the ocean. *Global Biogeochemical Cycles*, 14(1):225–248.

Lenton, T. M. and Watson, A. J. (2000b). Redfield revisited - 2. What regulates the oxygen content of the atmosphere? *Global Biogeochemical Cycles*, 14(1):249–268.

Leslie, P. H. (1945). On the use of matrices in certain population mathematics. *Biometrika*, 33(3):183–212.

Leslie, P. H. (1948). Some further notes on the use of matrices in population mathematics. *Biometrika*, 35(3-4):213–245.

Lorenz, E. N. (1963). Deterministic nonperiodic flow. *Journal of the Athmospheric Sciences*, 20:130–141.

Lucas, A. (1996). *Bioenergetics of aquatic animals*. Taylor & Francis Ltd., London.

M., D. D. (1980). Applicability of cellular equilibrium and Monod theory to phytoplankton growth kinetics. *Ecological Modelling*, 8:201–218.

Martin-Jézéquel, V., Hildebrand, M., and Brzezinski, M. A. (2000). Silicon metabolism in diatoms: implications for growth. *Journal of Phycology*, 36:821–840.

McCarty, P. L. (1975). Stoichiometry of biological reations. *Progress in Water Technology*, 7(1):157–172.

McKane, A. J. and Newman, T. J. (2005). Predator-prey cycles from resonant amplification of demographic stochasticity. *Physical Review Letters*, 94:218102:1–4.

Metropolis, N., Rosenbluth, A. W., Rosenbluth, M. N., Teller, A. H., and Teller, E. (1953). Equations of state calculations by fast computing machines. *Journal of Chemical Physics*, 21(6):1087–1092.

Michaelis, M. and Menten, M. L. (1913). Die Kinetik der Invertinwirkung. *Biochem. Z.*, 43:333–369.

Mieleitner, J., Borsuk, M., Bürgi, H.-R., and Reichert, P. (2008). Identifying functional groups of phytoplankton using data from three lakes of different trophic state. *Aquatic Sciences*, 70:30–46.

Mieleitner, J. and Reichert, P. (2006). Analysis of the transferability of a biogeochemical lake model to lakes of different trophic state. *Ecological Modelling*, 194:49–61.

Mieleitner, J. and Reichert, P. (2008). Modelling functional groups of phytoplankton in three lakes of different trophic state. *Ecological Modelling*, 211:279–291.

Mondy, C. P. and Schuwirth, N. (2017). Integrating ecological theories and traits in process-based modeling of macroinvertebrate community dynamics in streams. *Ecological Applications*, 27(4):1365–1377.

Monod, J. (1942). *Recherches sur la croissance des cultures bacteriennes*. Hermann et Cie., Paris.

Mortimer, C. H. (1981). The oxygen content of air-saturated fresh waters over ranges of temperature and atmospheric presure of limnological interest. *Mitteilungen Internationale Vereinigung für theoretische und angewandte Limnologie*, 22:1–23.

Omlin, M., Reichert, P., and Forster, R. (2001). Biogeochemical model of Lake Zürich: Model equations and results. *Ecological Modelling*, 141:77–103.

Paillex, A., Reichert, P., Lorenz, A. W., and Schuwirth, N. (2017). Mechanistic modelling for predicting the effects of restoration, invasion and pollution on benthic macroinvertebrate communities in rivers. *Freshwater Biology*, 62(6):1083–1093.

Patterson, J. C., Hamblin, P. F., and Imberger, J. (1984). Classification and dynamic simulation of the vertical density structure of lakes. *Limnology & Oceanography*, 36:845–861.

Peeters, F., Wüest, A., Piepke, G., and Imboden, D. M. (1996). Horizontal mixing in lakes. *J. Geophys. Res.*, 101(C8):18361–18375.

Peters, R. H. (1983). *The Ecological Implications of Body Size*. Cambridge University Press, Cambridge, UK.

Petzold, L. (1983). A description of DASSL: A differential/algebraic system solver. In Stepleman, R. e., editor, *Scientific Computing*, pages 65–68. IMACS / North-Holland, Amsterdam.

Press, W. H., Teukolsky, S. A., Vetterling, W. T., and Flannery, B. P. (1992a). *Numerical Recipes in C - The Art of Scientific Computing*. Cambridge University Press, Cambridge, UK, second edition.

Press, W. H., Teukolsky, S. A., Vetterling, W. T., and Flannery, B. P. (1992b). *Numerical Recipes in Fortran 77 - The Art of Scientifc Computing*. Cambridge University Press, Cambridge, UK, second edition.

Press, W. H., Teukolsky, S. A., Vetterling, W. T., and Flannery, B. P. (2002). *Numerical Recipes in C++ - The Art of Scientific Computing*. Cambridge University Press, Cambridge, UK.

Ratkowsky, D. A., Olley, J., McMeein, T. A., and Ball, A. (1982). Relationship btween temperature and growth rate of bacterial cultures. *Journal of Bacteriology*, 149:1–5.

Redfield, A. C. (1958). The biological control of chemical factors in the environment. *American Scientist*, 46:205–222.

Reichert, P. (2001). River Water Quality Model No. 1 (RWQM1): Case study II. Oxygen and nitrogen conversion processes in the River Glatt. *Water Science and Technology*, 43(5):51–60.

Reichert, P. (2007). Environmental systems analysis. Technical report, Course Manuscript ETH Zurich, Switzerland.

Reichert, P., Borchardt, D., Henze, M., Rauch, W., Shanahan, P., Somlyódy, L., and Vanrolleghem, P. (2001). River Water Quality Model No. 1 (RWQM1): II. Biochemical process equations. *Water Science and Technology*, 43(5):11–30.

Reichert, P., Langhans, S. D., Lienert, J., and Schuwirth, N. (2015). The conceptual foundation of environmental decision support. *Journal of Environmental Management*. In Press.

Reichert, P. and Mieleitner, J. (2008). Lake models. In Jorgensen, S. E. and Fath, B. D., editors, *Encyclopedia of Ecology*, volume 3. Elsevier, Oxford.

Reichert, P. and Schuwirth, N. (2010). A generic framework for deriving process stoichiometry in environmental models. *Environmental Modelling and Software*, 25:1241–1251.

Reynolds, C. S., Irish, A. E., and Elliott, J. A. (2001). The ecological basis for simulating phytoplankton responses to environmental change (PROTECH). *Ecological Modelling*, 140:271–291.

Romero, J. R., Antenucci, J. P., and Imberger, J. (2004). One- and three-dimensional biogeochemical simulations of two differing reservoirs. *Ecological Modelling*, 174:143–160.

Rubner, M. (1883). Über den Einfluss der Körpergrösse auf stoff- und kraftwechsel. *Zeitschrift für Biologie*, 19:536–562.

Ruiz, J., Macias, D., and Pters, F. (2005). Turbulence increases average settling velocity of phytoplankton cells. *Proceedings of the National Academy of Sciences of the United States of America*, 101(51):17720–17724.

Rutherford, J. C. (1994). *River mixing*. John Wiley & Sons, Chichester.

Savage, V. M., Gillooly, J. F., Woodruff, W. H., West, G. B., Allen, A. P., Enquist, B. J., and Brown, J. H. (2004). The predominance of quarter-power scaling in biology. *Functional Ecology*, 18:257–282.

Scheidegger, A. (1992). Sauerstoffhaushalt im Hallwilersee: Eine Untersuchung des Einflusses der internen Massnahmen zur Seesanierung. Diploma thesis, EAWAG/ETH, Dübendorf/Zürich.

Schuwirth, N., Acuña, V., and Reichert, P. (2011). Development of a mechanistic model (erimo-i) for analyzing the temporal dynamics of the benthic community of an intermittent Mediterranean stream. *Ecological Modelling*, 222(1):91–104.

Schuwirth, N., Dietzel, A., and Reichert, P. (2016). The importance of biotic interactions for the prediction of macroinvertebrate communities under multiple stressors. *Functional Ecology*, 30(6):974–984.

Schuwirth, N., Kühni, M., Schweizer, S., Uehlinger, U., and Reichert, P. (2008). A mechanistic model of benthos community dynamics in the River Sihl, Switzerland. *Freshwater Biology*, 53:1372–1392.

Schuwirth, N. and Reichert, P. (2012). Predicting the occurrence of macroinvertebrates. *Eawag News*, 72:14–17.

Schuwirth, N. and Reichert, P. (2013). Bridging the gap between theoretical ecology and real ecosystems: modeling invertebrate community composition in streams. *Ecology*, 94(2):368–379.

Schwarzenbach, R. P., Gschwend, P. M., and Imboden, D. M. (2003). *Environmental Organic Chemistry*. John Wiley, New York, second edition.

Shampine, L. F. (1994). *Numerical solution of ordinary differential equations*. Chapman & Hall, New York.

Shanahan, P., Borchardt, D., Henze, M., Rauch, W., Reichert, P., Somlyódy, L., and Vanrolleghem, P. (2001). River Water Quality Model No. 1 (RWQM1): I. Modelling approach. *Water Science and Technology*, 43(5):1–10.

Smith, E. L. (1936). Photosynthesis in relation to light and carbon dioxide. *Proc. Natl. Acad. Sci.*, 22:504–511.

Soetaert, K., Cash, J., and Mazzia, F. (2012). *Solving Differential Equations in R.* Springer, Heidelberg, Germany.

Soetaert, K., Petzoldt, T., and Woodrow Setzer, R. (2010). Solving differential equations in R: Package deSolve. *Journal of Statistical Software*, 33(9).

Steele, J. (1962). Environmental control of photosynthesis in the sea. *Limnology & Oceanography*, 7:137–150.

Sterner, R. W. and Elser, J. J. (2002). *Ecological stoichiometry: the biology of elements from molecules to the biosphere.* Princeton University Press, Princeton, HJ, USA.

Stumm, W. and Morgan, J. J. (1981). *Aquatic Chemistry.* John Wiley, New York.

Teschl, G. (2012). *Ordinary Differential Equations and Dynamical Systems.* American Mathematical Society: Graduate Studies in Mathematics 140, Providence, RI, USA.

Tierney, L. (1994). Markov chains for exploring posterior distributions. *The Annals of Statistics*, 22(4):1701–1762.

Tilman, D., Kiesling, R., Sterner, R., Kilham, S. S., and Johnson, F. A. (1986). Green, bluegreen and diatom algae: Taxonomic differences in competitive ability for phosphorus, silicon and nitrogen. *Archiv für Hydrobiologie*, 106(4):473–485.

Tucker, S. L. and Zimmerman, S. O. (1988). A nonlinear model of population dynamics containing an arbitrary number of continuous structure variables. *SIAM Journal of Applied Mathematics*, 48(3):549–591.

Urban, M. C., Leibold, M. A., Amarasekare, P., De Meester, L., Gomulkiewicz, R., Hochberg, M. E., Klausmeier, C. A., Loeuille, N., de Mazancourt, C., Norberg, J., Pantel, J. H., Strauss, S. Y., Vellend, M., and Wade, M. J. (2008). The evolutionary ecology of metacommunities. *Trends in Ecology and Evolution*, 23(6):311–317.

Vanrolleghem, P., Borchardt, D., Henze, M., Rauch, W., Reichert, P., Shanahan, P., and Somlyódy, L. (2001). River Water Quality Model No. 1 (RWQM1): III. Biochemical submodel selection. *Water Science and Technology*, 43(5):31–40.

Webb, G. (1985). *Theory of Nonlinear Age-Dependent Population Dynamics.* Marcel Dekker, New York.

West, G. B., Brown, J. H., and Enquist, B. J. (1997). A general model for the origin of allometric scaling laws in biology. *Science*, 276:122–126.

White, C. R. (2010). There is no single p. *Nature*, 464:691–693.

Whitman, W. G. (1923). The two-film theory of gas absorption. *Chemical and Metallurgical Engineering*, 29(4):146–148.

Wüest, A., Imboden, D. M., and Schurter, M. (1988). Origin and size of hypolimnic mixing in urnersee, the southern basin of vierwaldstättersee (lake lucerne). *Schweiz. Z. Hydrol.*, 50:40–70.

Yodzis, P. and Innes, S. (1992). Body size and consumer-resource dynamics. *The American Naturalist*, 139:1151–1175.

Yoshida, T., Jones, L. E., Ellner, S. P., Fussmann, G. F., and Hairston, N. G. J. (2003). Rapid evolution drives ecological dynamics in a predator-prey system. *Nature*, 424:303–306.